05-4506832 pustaka.upsi.edu.my Perpustakaan Tuanku Bainun Kampus Sultan Abdul Jalil Shah PustakaTBainun ptbupsi

SURFACE PRESSURE-AREA ISOTHERM, OPTICAL AND ELECTRICAL PROPERTIES OF P3HT/NANOPARTICLES THIN FILMS BY MODIFIED LANGMUIR-BLODGETT TECHNIQUE

FATIN HANA BINTI NANING @ ZIN

05-4506832 pustaka.upsi.edu.my Perpustakaan Tuanku Bainun Kampus Sultan Abdul Jalil Shah PustakaTBainun ptbupsi

THESIS SUBMITTED IN FULFILLMENT OF THE REQUIREMENT FOR THE DEGREE OF DOCTOR OF PHILOSOPHY (PHYSICS)

FACULTY OF SCIENCE AND MATHEMATICS
SULTAN IDRIS EDUCATION UNIVERSITY

2017

05-4506832 pustaka.upsi.edu.my Perpustakaan Tuanku Bainun Kampus Sultan Abdul Jalil Shah PustakaTBainun ptbupsi

05-4506832 pustaka.upsi.edu.my Perpustakaan Tuanku Bainun Kampus Sultan Abdul Jalil Shah PustakaTBainun ptbupsi

ABSTRACT

Hybrid organic-inorganic nanocomposite materials have emerged as one of the most potential alternative candidate to silicon as future optoelectronic material due to their unique optical and electrical characteristics. However, current fabrication process involving synthesizing the pre-made nanoparticles inside the polymer matrices is tediously complex, costly and time consuming. In this research, two approaches in preparing nanocomposite thin films, *in situ* hybridization and *ex situ* hybridization, were studied and the results were compared. *In situ* hybridization, a novel method, where the nanoparticles were grown directly in the Poly(3-hexylthiophene) (P3HT) mixed with stearic acid layers by exposing the films to either H_2S or H_2Se gas. *Ex situ* hybridization were done by mixing pre-made CdS or CdSe quantum dots into P3HT solution. For both approaches, depositions of thin films on the solid substrate were done by employing modified Langmuir-Blodgett technique. Studies on Langmuir layer found that the film is very sensitive towards its environment where the amount of solutions, the weight percentage, and the subphase affecting the gas-liquid-solid transformation. Absorbance spectra show higher polymer crystallization for thin films exposed to H_2S or H_2Se gas. The peak shifting and depreciation of absorption intensity indicates the quantum confinement effect of nanoparticles formed. Photoluminescence intensity decreased with the increment of gas exposure time and quantum dots' weight percentage. The current density-voltage measurement revealed open circuit voltage for *in situ* hybrid thin film nucleating CdS and CdSe is 0.56 V and 0.72 V respectively. Thin films fabricated by *ex situ* method possess lower Johnson noise than that of *in situ*. Overall, *in situ* hybridization has shown a better performance as compared to hybrid nanocomposite thin films fabricated using *ex situ* approach. These findings have given a promising future for gas exposure method to be further studied in the fabrication of hybrid organic-inorganic nanocomposite thin films for optoelectronics application.

05-4506832 pustaka.upsi.edu.my Perpustakaan Tuanku Bainun Kampus Sultan Abdul Jalil Shah PustakaTBainun ptbupsi

05-4506832 pustaka.upsi.edu.my Perpustakaan Tuanku Bainun Kampus Sultan Abdul Jalil Shah PustakaTBainun ptbupsi

PENCIRIAN ISOTERM TEKANAN PERMUKAAN-LUAS, OPTIK DAN ELEKTRIK BAGI FILEM TIPIS P3HT/NANOPARTIKEL MENGGUNAKAN KAEDAH UBAH SUAI LANGMUIR-BLODGETT

ABSTRAK

Bahan komposit nano hibrid organik-tak organik telah menjadi salah satu calon alternatif kepada silikon sebagai bahan optoelektronik disebabkan oleh ciri-ciri optik dan elektrik yang unik. Walau bagaimanapun, proses fabrikasi masakini melibatkan sintesis pra-hasil nanopartikel di dalam matriks polimer adalah rumit, mahal dan memakan masa. Di dalam kajian ini, dua pendekatan dalam penyediaan filem tipis komposit nano, penghibridan *in situ* dan penghibridan *ex situ*, telah dikaji dan keputusannya dibandingkan.Penghibridan *in situ* ialah kaedah novel di mana nanopartikel ditumbuhkan secara langsung dalam lapisan Poly(3-hexylthiophene) (P3HT) yang dicampur dengan asid stearik, dengan mendedahkan filem tipis dengan gas H_2S atau H_2Se. Penghibridan *ex situ* dilakukan dengan mencapurkan titik kuantum CdS atau CdSe ke dalam larutan P3HT. Untuk kedua-dua pendekatan ini, filem tipis didepositkan ke atas substrat dengan menggunakan kaedah ubahsuai Langmuir-Blodgett. Kajian terhadap lapisan Langmuir mendapati bahawa filem tersebut sangat sensitif kepada perubahan sekeliling, di mana jumlah larutan, peratusan berat dan sub-fasa memberi kesan terhadap transformasi gas-cecair-pepejal. Serapan spektrum menunjukkan filem tipis yang didedahkan kepada gas H_2S atau H_2Se mengalami penghabluran polimer yang lebih tinggi. Anjakan puncak dan penurunan keamatan serapan menandakan kesan kekangan kuantum oleh nanopartikel yang terbentuk. Keamatan PL menurun dengan kenaikan masa dedahan dan peratusan berat titik kuantum. Pengukuran ketumpatan arus-voltan menunjukkan bahawa nilai voltan litar terbuka bagi filem tipis hibrid *in situ* menghasilkan CdS dan CdSe ialah 0.56 V dan 0.72 V. Filem tipis yang difabrikasi secara *ex situ* mempunyai ciri hingar Johnson yang lebih rendah berbanding fiem tipis yang dihasilkan secara *in situ*. Secara keseluruhan, hibrid filem tipis yang terhasil dari proses *in situ* mempunyai prestasi yang lebih baik berbanding dengan komposit nano hibrid filem tipis yang difabrikasi menggunakan pendekatan *ex situ*. Keputusan-keputusan ini memberikan masa depan yang cerah untuk kaedah pendedahan gas dikaji dengan lebih lanjut untuk fabrikasi hibrid filem nipis organik–tak organik bagi aplikasi optoelektronik.

05-4506832 pustaka.upsi.edu.my Perpustakaan Tuanku Bainun Kampus Sultan Abdul Jalil Shah PustakaTBainun ptbupsi

05-4506832 pustaka.upsi.edu.my Perpustakaan Tuanku Bainun Kampus Sultan Abdul Jalil Shah PustakaTBainun ptbupsi

TABLE OF CONTENTS

		Pages
DECLARATION		ii
ACKNOWLEDGEMENT		iii
ABSTRACT		iv
ABSTRAK		v
TABLES OF CONTENT		vi
LIST OF TABLES		x
LIST OF FIGURES		xi
LIST OF ABBREVIATIONS AND SYMBOLS		xvi
CHAPTER 1	**INTRODUCTION**	1
1.1	Research Background	1
1.2	Physical Vapor Deposition (PVD)	5
1.3	Chemical Vapor Deposition (CVD)	7
1.4	Wet Chemical Deposition	9
1.4.1	Sol-gel	10
1.4.2	Spin Coating	12
1.4.3	Spray Pyrolisis	14
1.4.4	Electrodeposition	16
1.4.5	Langmuir-Blodgett (LB)	18
1.5	Motivation	19

05-4506832 pustaka.upsi.edu.my Perpustakaan Tuanku Bainun Kampus Sultan Abdul Jalil Shah PustakaTBainun ptbupsi

05-4506832 pustaka.upsi.edu.my Perpustakaan Tuanku Bainun Kampus Sultan Abdul Jalil Shah PustakaTBainun ptbupsi

1.6 Research Objectives 21

1.7 Scope of Study 22

1.8 Limitation of Study 24

1.9 Contribution of Knowledge 24

1.10 Thesis Organization 25

1.11 Conclusion 26

CHAPTER 2 THEORETICAL BACKGROUND AND LITERATURE REVIEW 27

2.1 Introduction 27

2.2 Langmuir Film 28

2.3 Langmuir Film Formation 29

2.4 Langmuir Film Preparation 37

2.5 Transfer of Langmuir Film onto Solid Substrate 39

2.5.1 Langmuir-Blodgett (LB) Thin Films Deposition 40

2.5.2 Langmuir-Schaefer (LS) Thin Films Deposition 44

2.6 Hybrid Nanocomposite Thin Films 45

2.7 Inorganic Nanoparticles-Polymer Blend 47

2.7.1 Hybrid II-VI group: Polymer 48

2.7.2 Hybrid III-V group: Polymer 52

2.7.3 Hybrid Metal Oxide (MeO_x): Polymer 53

2.7.4 Hybrid Quantum Dots: Polymer 55

2.8 Conclusion 57

CHAPTER 3 MATERIALS AND METHOD 58

3.1 Introduction 58

05-4506832 pustaka.upsi.edu.my Perpustakaan Tuanku Bainun Kampus Sultan Abdul Jalil Shah PustakaTBainun ptbupsi

05-4506832 pustaka.upsi.edu.my Perpustakaan Tuanku Bainun Kampus Sultan Abdul Jalil Shah PustakaTBainun ptbupsi

05-4506832 pustaka.upsi.edu.my Perpustakaan Tuanku Bainun Kampus Sultan Abdul Jalil Shah PustakaTBainun ptbupsi

3.2 Research Design 59

3.3 Materials Selection 61

3.3.1 Poly(3-hexylthiophene) (P3HT) 62

3.3.2 Stearic Acid 63

3.3.3 Cadmium (II) Chloride 64

3.3.4 Quantum Dots 65

3.3.5 PEDOT:PSS 66

3.3.6 Indium Tin Oxide (ITO) Coated Glass 67

3.37 Quartz 68

3.4 Strategy of Nanocomposite Preparation 68

3.4.1 *In situ* Hybridization 69

3.4.2 *Ex situ* Hybridization 74

3.5 Aluminum Thermal Evaporation 77

3.6 Characterization Methods 78

3.6.1 Surface Pressure-Area (Π-A) Isotherm 78

3.6.2 UV-Vis Spectroscopy 80

3.6.3 Photoluminescence (PL) Measurement 82

3.6.4 Current Density-Voltage (J-V) Measurement 83

3.6.5 Johnson Noise Measurement 86

3.7 Conclusion 88

CHAPTER 4 RESULTS AND DISCUSSION 89

4.1 Introduction 89

4.2 Surface Pressure-Area (Π-A) Isotherm 90

05-4506832 pustaka.upsi.edu.my Perpustakaan Tuanku Bainun Kampus Sultan Abdul Jalil Shah PustakaTBainun ptbupsi

05-4506832 pustaka.upsi.edu.my Perpustakaan Tuanku Bainun Kampus Sultan Abdul Jalil Shah PustakaTBainun ptbupsi

4.2.1 *In situ* Hybridization 90

4.2.2 *Ex situ* Hybridization 99

4.3 UV-Vis Spectroscopy 101

4.3.1 *In situ* Hybridization 101

4.3.2 *Ex situ* Hybridization 108

4.4 Photoluminescence (PL) Measurement 110

4.4.1 *In situ* Hybridization 110

4.4.2 *Ex situ* Hybridization 113

4.5 Current Density-Voltage (J-V) Measurement 115

4.5.1 *In situ* Hybridization 115

4.5.2 *Ex situ* Hybridization 124

4.6 Johnson Noise Measurement 129

4.6.1 *In situ* Hybridization 132

4.6.2 *Ex situ* Hybridization 134

4.7 Conclusion 136

CHAPTER 5 CONCLUSION AND SUGGESTIONS FOR FUTURE WORK 137

5.1 Introduction 137

5.2 Conclusion 138

5.3 Suggestions for Future Work 141

REFERENCES 142

APPENDIX A 166

APPENDIX B 167

LIST OF PUBLICATIONS 168

05-4506832 pustaka.upsi.edu.my Perpustakaan Tuanku Bainun Kampus Sultan Abdul Jalil Shah PustakaTBainun ptbupsi

05-4506832 pustaka.upsi.edu.my Perpustakaan Tuanku Bainun Kampus Sultan Abdul Jalil Shah PustakaTBainun ptbupsi

LIST OF TABLES

Table No.		Page
1.1	Comparison of thin film deposition techniques	19
2.1	Examples of amphiphilic molecules and its structure	31
2.2	Some elements on periodic table	49
4.1	Mean molecular area (Mma) of P3HT and stearic acid on DI water subphase	93
4.2	Phase transformation of P3HT:Stearic acid (P3HT:SA) at different spreading volume ratio	96
4.3	Summary of gas–liquid–solid phase transformation	98
4.4	The electrical properties of thin films exposed to H_2S and H_2Se gas at different exposure time	124
4.5	The electrical properties of P3HT:QDs thin films at different weight percentage	128
4.6	The maximum direct current and noise current for every gain setting of 5182 preamplifier	130

05-4506832 pustaka.upsi.edu.my Perpustakaan Tuanku Bainun Kampus Sultan Abdul Jalil Shah PustakaTBainun ptbupsi

05-4506832 pustaka.upsi.edu.my Perpustakaan Tuanku Bainun Kampus Sultan Abdul Jalil Shah PustakaTBainun ptbupsi

LIST OF FIGURES

Figure No.		Page
1.1	Electron beam physical vapor deposition (EB-PVD)	6
1.2	Illustration of typical chemical vapor deposition reactor	8
1.3	Formation of thin film through sol-gel method	11
1.4	Stages of thin film formation through spin coating technique	13
1.5	Instrumentation set up for spray pyrolysis	15
1.6	Set-up of electrodeposition	17
1.7	Scope of study. Two approaches used in preparing the hybrid nanocomposite thin film: *in situ* and *ex situ* hybridization	23
2.1	Surface pressure-area (Π-A) isotherm of Langmuir monolayer, where A_o is denoted as the area occupied by a molecule	35
2.2	Spreading of polymeric solution on subphase (adapted from Hagtig, 1999)	36
2.3	Schematic diagrams of Langmuir trough used in this project. The barrier movement and Wilhelmy plate that monitors the surface pressure are controlled by the computer through an interfacing process	38
2.4	Schematic representations of LB-deposition methods (a) Y-type, (b) X-type, (c) Z-type	41
2.5	Schematic presentation of L thin film method	44
3.1	Experimental designs for *in situ* and *ex situ* hybridization approaches	60
3.2	Chemical structure of Poly(3-hexylthiophene) (P3HT)	62
3.3	Stearic acid skeletal structure, where COOH is the hydrophilic part, and the tail, $CH_3(CH_2)_{16}$ is the hydrophobic part	64

05-4506832 pustaka.upsi.edu.my Perpustakaan Tuanku Bainun Kampus Sultan Abdul Jalil Shah PustakaTBainun ptbupsi

05-4506832 pustaka.upsi.edu.my Perpustakaan Tuanku Bainun Kampus Sultan Abdul Jalil Shah PustakaTBainun ptbupsi

05-4506832 pustaka.upsi.edu.my Perpustakaan Tuanku Bainun Kampus Sultan Abdul Jalil Shah PustakaTBainun ptbupsi

3.4	Skeletal molecular structure of cadmium stearate	64
3.5	Chemical structure of Poly(3,4-ethylenedioxythiophene), and polyelectrolyte, poly(styrenesulfonate), merged as PEDOT:PSS. The “dot’’ and “plus’’ represent the unpaired electron and positive charge on the PEDOT chain, respectively	67
3.6	In-house Langmuir KSV 2002 System 2 apparatus (1) Computer (2) Interface unit (3) Movable barrier (4)Trough (5) Pressure sensor (6) Dipping mechanism	70
3.7	Schematic illustration of modified LB technique	72
3.8	Lack of material region of Langmuir film of P3HT at solid phase after first deposition. Insert is the thin films deposited on substrate	73
3.9	Samples are exposed to H2S or H2Se gas in a sealed reaction vessel	74
3.10	The ligand removing process: (a) 432 µl of QDs in toluene was added into 6 ml hexanoic acid in hot oil bath. (b) Hot solution before centrifuge. The yellowish liquid contains CdS QDs while the maroon liquid contains CdSe QDs. (c) Centrifuge at 3000 rpm. (d) Precipitated QDs after centrifuging process	76
3.11	(a) Vacuum thermal evaporator used for aluminum coating. (b) Aluminum fingers on thin films deposited on ITO coated glass	78
3.12	Illustration of absorption when light passes through a sample	80
3.13	In-house UV-Vis spectrophotometer	82
3.14	Fluorescence Spectroscopy for photoluminescence analysis	83
3.15	In-house computerized J-V measurement equipment consists of (a) four-point probe, (b) solar simulator, (c) Keithley 2636A source measure unit	84
3.16	Electrical connection schematic of thin film for current J-V measurement where ITO acts as anode and Aluminum layer acts as cathode	85
3.17	LFeNM experimental setup and the schematic diagram	88

05-4506832 pustaka.upsi.edu.my Perpustakaan Tuanku Bainun Kampus Sultan Abdul Jalil Shah PustakaTBainun ptbupsi

05-4506832 pustaka.upsi.edu.my Perpustakaan Tuanku Bainun Kampus Sultan Abdul Jalil Shah PustakaTBainun ptbupsi

4.1	Surface pressure versus area (Π-A) isotherm graph displays the phase transformation of pristine stearic acid with different spreading volume, where (i) gas phase, (ii) liquid phase, (iii) solid phase, (iv) collapse phase	91
4.2	Surface pressure versus area (Π-A) isotherm of pristine P3HT at 400 µl	92
4.3	Surface pressure versus area (Π-A) isotherms of P3HT mixed with stearic acid (SA) at different volume ratio	94
4.4	The surface pressure versus area (Π-A) isotherm graphs of (a) 400 µl P3HT, (b) 600 µl stearic acid, (c) 400 µl P3HT: 100 µl stearic acid, on different subphases	97
4.5	The surface pressure versus area (Π-A) isotherm graphs of (a) CdS QDs incorporated into P3HT, (b) CdSe QDs incorporated into P3HT, at different weight percentage	100
4.6	UV-Vis absorption spectra of pristine stearic acid, pristine P3HT and P3HT:SA:Cd^{2+} thin films	102
4.7	UV-Vis absorption spectra of P3HT:SA:Cd^{2+} thin films exposed to H_2S gas	104
4.8	UV-Vis absorption spectra of P3HT:SA:Cd^{2+} thin films exposed to H_2Se gas	106
4.9	The nucleation process of nanoparticles in between the P3HT/SA matrix: (a) $CdSt_2$ after deposition (b) Gas exposure (c) Nucleation of nanoparticles (d) Further nanoparticles formation (e) Aggregation of larger nanoparticles cluster	107
4.10	UV-Vis absorption spectra of P3HT mixed with CdS quantum dots	109
4.11	UV-Vis-absorption spectra of P3HT mixed with CdSe quantum dots	109
4.12	Photoluminescence spectra for thin films exposed to H_2S gas	111
4.13	Photoluminescence spectra for thin films exposed to H_2Se gas	111
4.14	Photoluminescence spectra for hybrid P3HT:CdS QDs thin films	114

05-4506832 pustaka.upsi.edu.my Perpustakaan Tuanku Bainun Kampus Sultan Abdul Jalil Shah PustakaTBainun ptbupsi

05-4506832 pustaka.upsi.edu.my Perpustakaan Tuanku Bainun Kampus Sultan Abdul Jalil Shah PustakaTBainun ptbupsi

4.15	Photoluminescence spectra for hybrid P3HT:CdSe QDs thin films	114
4.16	Current density versus voltage (J-V) graphs for samples under dark and under illumination of a solar simulator. The thin films were exposed to H_2S gas for (a) 0 hour, (b) 2 hours, (c) 4 hours, (d) 6 hours	116
4.17	The fourth quadrant of current density versus voltage (J-V) curve for thin films exposed to H_2S gas at varying time	118
4.18	Evaluation of open-circuit voltage (V_{oc}), short-circuit current density (J_{sc}), fill factor (FF) and maximum power output (P_{max}) at different H_2S gas exposure time	119
4.19	Current density versus voltage (J-V) graphs for sample exposed to H_2Se gas for (a) 0 hour, (b) 2 hours, (c) 4 hours, and (d) 6 hours	121
4.20	The fourth quadrant of current density versus voltage (J-V) curve for thin films exposed to H_2Se gas at varying time	122
4.21	Evaluation of open-circuit voltage (V_{oc}), short-circuit current density (J_{sc}), fill factor (FF) and maximum power output (P_{max}) at different H_2Se gas exposure time	123
4.22	Current density versus voltage (J-V) graphs for (a) P3HT:CdS quantum dots thin films, (b) P3HT:CdSe quantum dots thin films	125
4.23	The fourth quadrant of current density versus voltage (J-V) curve for thin films fabricated by physically mixing P3HT with quantum dots at different weight percentage	126
4.24	Measurement parameters for P3HT:CdS and P3HT:CdSe thin films made from different quantum dots loading amounts	127
4.25	Johnson noise of low-noise (LN) current preamplifier 5182 with different gain setting	130
4.26	Validation of measurement set up using 5 MΩ resistor	132
4.27	Johnson noise current spectral density of thin films exposed to H_2S gas at varying time	133

05-4506832 pustaka.upsi.edu.my Perpustakaan Tuanku Bainun Kampus Sultan Abdul Jalil Shah PustakaTBainun ptbupsi

05-4506832 pustaka.upsi.edu.my Perpustakaan Tuanku Bainun Kampus Sultan Abdul Jalil Shah PustakaTBainun ptbupsi

4.28	Johnson noise current spectral density of thin films exposed to H_2Se gas at varying time	134
4.29	Johnson noise current spectral density of P3HT mixed with CdS quantum dot thin films	135
4.30	Johnson noise current spectral density of P3HT mixed with CdSe quantum dot thin films	135

05-4506832 pustaka.upsi.edu.my Perpustakaan Tuanku Bainun Kampus Sultan Abdul Jalil Shah PustakaTBainun ptbupsi

05-4506832 pustaka.upsi.edu.my Perpustakaan Tuanku Bainun Kampus Sultan Abdul Jalil Shah PustakaTBainun ptbupsi

05-4506832 pustaka.upsi.edu.my Perpustakaan Tuanku Bainun Kampus Sultan Abdul Jalil Shah PustakaTBainun ptbupsi

LIST OF ABBREVIATIONS AND SYMBOLS

µA	microampere
2D	Two-dimension
3D	Three-dimension
A	Area per molecule
Å	Armstrong
A_i	Lift off area
Al	(Aluminum)
AM 1G	Air Mass 1 Global
A_o	Molecular area
APCVD	Atmospheric pressure chemical vapor deposition
ASTM	American Standard for Testing and Materials
c	velocity of light
Cd^{2+}	Cadmium ion
$CdCl_2$	Cadmium chloride
CdS	Cadmium sulfide
CdSe	Cadmium selenide
CVD	Chemical vapor deposition
D/A	Donor/Acceptor
DC	Direct current
DFT	Density functional theory

05-4506832 pustaka.upsi.edu.my Perpustakaan Tuanku Bainun Kampus Sultan Abdul Jalil Shah PustakaTBainun ptbupsi

05-4506832 pustaka.upsi.edu.my Perpustakaan Tuanku Bainun Kampus Sultan Abdul Jalil Shah PustakaTBainun ptbupsi

DI	De-ionized
DSA	Dynamic signal analyzer
DUT	Device under test
E	Energy
EB-PVD	Electron beam physical vapor deposition
EDX	Energy Dispersive X-ray
emf	Electromotive force
FACVD	Flame assisted chemical vapor deposition
FESEM	Field Emission Scanning Microscopy
FF	Fill factor
h	Planck's contant
H_2S	Hydrogen sulfide
H_2Se	Hydrogen selenide
HOMO	Highest occupied molecular orbital
Hz	Hertz
ITO	Indium Tin Oxide
J_{MPP}	Current density at maximum power point
J_{sc}	Short-circuit current density
J-V	Current density-Voltage
k	Boltzmann constant
kHz	kilohertz
LB	Langmuir-Blodgett
LED	Light-emitting diode

05-4506832 pustaka.upsi.edu.my Perpustakaan Tuanku Bainun Kampus Sultan Abdul Jalil Shah PustakaTBainun ptbupsi

05-4506832 pustaka.upsi.edu.my Perpustakaan Tuanku Bainun Kampus Sultan Abdul Jalil Shah PustakaTBainun ptbupsi

LFeNM	Low frequency electrical noise measurement
LN	Low noise
LPCVD	Low pressure chemical vapor deposition
LS	Langmuir-Schaefer
LUMO	Lowest occupied molecular orbital
Mma	Mean molecular area
M_w	Molecular weight
N(f,T)	Planck number
N_A	Avogadro's number
OLED	Organic light-emitting diode
P3HT	Poly(3-hexylthiophene)
PCE	Power conversion efficiency
PECVD	Plasma enhanced chemical vapor deposition
PL	Photoluminescence
PLD	Pulsed laser deposition
P_{max}	Maximum power output
PSD	Power spectral density
PVD	Physical vapor deposition
QD	Quantum dot
R	Resistance
rpm	Rotation per minute
SA	Stearic acid
$S_I(f)$	Current noise

05-4506832 pustaka.upsi.edu.my Perpustakaan Tuanku Bainun Kampus Sultan Abdul Jalil Shah PustakaTBainun ptbupsi

05-4506832 pustaka.upsi.edu.my Perpustakaan Tuanku Bainun Kampus Sultan Abdul Jalil Shah PustakaTBainun ptbupsi

SMU	Source measure unit
$S_v(f)$	Voltage noise
T	Temperature
UV-Vis	Ultraviolet-visible
V_{MPP}	Voltage at maximum power point
V_{oc}	Open-circuit voltage
wt%	Weight percentage
γ	Surface tension of water covered by film
γ_o	Surface tension of pure water
λ	Wavelength
ν	Frequency
Π	Surface pressure

05-4506832 pustaka.upsi.edu.my Perpustakaan Tuanku Bainun Kampus Sultan Abdul Jalil Shah PustakaTBainun ptbupsi

05-4506832 pustaka.upsi.edu.my Perpustakaan Tuanku Bainun Kampus Sultan Abdul Jalil Shah PustakaTBainun ptbupsi

05-4506832 pustaka.upsi.edu.my Perpustakaan Tuanku Bainun Kampus Sultan Abdul Jalil Shah PustakaTBainun ptbupsi

CHAPTER 1

INTRODUCTION

05-4506832 pustaka.upsi.edu.my Perpustakaan Tuanku Bainun Kampus Sultan Abdul Jalil Shah PustakaTBainun ptbupsi

1.1 Research Background

Semiconductor materials have been an important catalyst in tremendous progress of electronic and microelectronic devices. Semiconductor is a group of materials whose conductivity lies between conductor and insulator, ranging from 10^{5} S/cm – 10^{-8} S/cm (Czichos, Saito & Smith, 2007). It exhibits an energy bandgap, where the states below the gap are fully occupied by electrons whilst the upper state is empty. At absolute zero, the semiconductor carries no net current hence acts like an insulator.

05-4506832 pustaka.upsi.edu.my Perpustakaan Tuanku Bainun Kampus Sultan Abdul Jalil Shah PustakaTBainun ptbupsi

05-4506832 pustaka.upsi.edu.my Perpustakaan Tuanku Bainun Kampus Sultan Abdul Jalil Shah PustakaTBainun ptbupsi

The most dominant material for semiconductor devices is silicon, a single-element from group IV, which is abundantly and cheaply available all around the world. One main advantage of silicon general properties is its ability to be doped to tune the types of conductivity in order to fabricate high quality substrates. Silicon semiconductor industry is a matured technology that began in 1947 when silicon-based transistors were invented in Bell Laboratories (Zekry, 2014). The rapid progress in silicon technology enabled Bell Lab to invent photovoltaic device with efficiency around 6% in 1954 (Chapin, Fuller & Pearson, 1954). However, the substrate fabrication is very expensive as compared to the cost of overall device. For example, in order to fabricate photovoltaic panel, around 50% of overall fabrication cost is due to cost of silicon substrate production (Aberle & Widenborg, 2011). Thinner wafers are produced to lower the cost, but it causes the wafer to break easily at minimum achievable thickness. Thinner substrates also lead to fractional loss due to sawing damage. Thus, among possible approach to address this issue are by using alternative semiconducting materials, thin film technology, or the combination of both.

The most popular choice of alternative semiconducting material is conjugated polymer, owing to its relatively lower cost as compared to silicon (Gaudiana & Brabec, 2008). While semiconducting properties of silicon depending on its crystal structure, conjugated polymer semiconductivity depends on its chemical structure. Conjugation in polymer is due to alternating single and double bonds between the carbon atoms on its backbone. Single bond comprises of strong covalent bond called sigma (σ) bond only, whilst double bond is constructed by both σ bond and a pi (π) bond. The π bond is due to

05-4506832 pustaka.upsi.edu.my Perpustakaan Tuanku Bainun Kampus Sultan Abdul Jalil Shah PustakaTBainun ptbupsi

05-4506832 pustaka.upsi.edu.my Perpustakaan Tuanku Bainun Kampus Sultan Abdul Jalil Shah PustakaTBainun ptbupsi

weak overlapping of unhybridized p-orbital electron. Electrons in π bond are known as π electrons, delocalized along carbon backbone. Atomic orbitals overlapping also creating occupied π-bond and unoccupied π*-anti-bond molecular orbital. The filled π band is called the highest occupied molecular orbital (HOMO) and the empty π* band is called the lowest unoccupied molecular orbital (LUMO). This is analogous to silicon band gap, where HOMO is equivalent to valence band and LUMO is called conduction band.

Among interesting characteristic of conjugated polymer are it has strong absorption and high quantum yield in the solid state that make it a promising material for optoelectronic devices (Brandão, Viana, Bucknall & Bernardo, 2014), exhibits molecular wire properties and highly fluorescent (Y. Liu, Lam & Tang, 2015) and it can be easily processed (Gaudiana & Brabec, 2008) and deposited on a wide range of substrates (Levell, Giardini & Samuel, 2010). The deposition of conjugated polymer is generally done by means of thin film technology.

Thin film technology henceforth became the basis in the development of solid state electronics, in which the properties of functional materials are significantly different when analyzed in the form of thin films as compared to their bulk materials. Thin film is a solid layer of a material, adhered to a substrate that possesses different properties of the said film, with the thickness ranging from tenths of nanometers to micrometers. The processing of materials into thin film allows easy integration into many types of applications in various industries (West, 2003).

05-4506832 pustaka.upsi.edu.my Perpustakaan Tuanku Bainun Kampus Sultan Abdul Jalil Shah PustakaTBainun ptbupsi

05-4506832 pustaka.upsi.edu.my Perpustakaan Tuanku Bainun Kampus Sultan Abdul Jalil Shah PustakaTBainun ptbupsi

The major application of thin film is in microelectronic field (Lazar, Tadvani, Tung, Lopez, & Daoud, 2010), with growing applications in other areas like optoelectronics, magnetic devices, electrochemistry, and protective and decorative coatings. Studies on thin films have advanced and combined many new area of research, particularly in solid state physics, chemistry and biophysics. One of the leading reasons behind thin film advancement is the miniaturization of electronic devices towards cheaper and faster gadget but with lower power consumption and higher efficiency.

The manufacturing technique plays important role in determining thin films' properties (Vilarinho, 2005). There are varieties of thin film deposition techniques available and in use today which originate from purely physical or chemical processes. However, recently many studies combined different well developed process to get more defined control and properties of the thin films. Generally, the deposition technique affects the morphology, adhesion, crystallinity, and growth rate of thin film, in which necessitate direct control of materials on molecular and atomic scale (Mallik & Ray, 2011). Hence the appropriate deposition method selection is vital in order to control the properties of the resultant film.

Thin films deposition can be categorized into one of three approaches: physical vapor deposition, chemical vapor deposition and wet chemical deposition. Each of the categories and several common techniques are described in the next subtopics.

05-4506832 pustaka.upsi.edu.my Perpustakaan Tuanku Bainun Kampus Sultan Abdul Jalil Shah PustakaTBainun ptbupsi

05-4506832 pustaka.upsi.edu.my Perpustakaan Tuanku Bainun Kampus Sultan Abdul Jalil Shah PustakaTBainun ptbupsi

1.2 Physical Vapor Deposition (PVD)

Physical vapor deposition (PVD) methods are a range of techniques used to fabricate thin films using purely physical process. The technique involves the condensation of a solid or liquid source material that is vaporized under vacuum, onto a substrate (Pulker, 1999). The evaporation of the source either by evaporation, or sublimation of ions impinge on a target, depending on the technique to excite the source atoms to the vapor phase. The main PVD techniques are vacuum thermal evaporation, sputter deposition, cathodic arc deposition and pulse laser deposition.

The first system called vacuum thermal evaporation is the easiest system among PVD technique. Due to its low cost and maintenance, most university research laboratories use this system in work of materials science and related field (Stagon, 2013). The evaporation of material occurs inside a vacuum chamber, in which a conductive heating element used to vaporize the materials, and allowed to deposit onto a substrate. This technique generally is performed in high to ultra-high vacuum condition because the vapor atom will not leave the liquid melt if the minimum required pressure is not met (Stagon, 2013).

A method that is categorized under thermal evaporation is electron beam evaporation (EB-PVD), in which a high energy electron beam bombards the source material causing local vaporization (Singh & Wolfe, 2005). The system is as illustrated in

05-4506832 pustaka.upsi.edu.my Perpustakaan Tuanku Bainun Kampus Sultan Abdul Jalil Shah PustakaTBainun ptbupsi

05-4506832 pustaka.upsi.edu.my Perpustakaan Tuanku Bainun Kampus Sultan Abdul Jalil Shah PustakaTBainun ptbupsi

Figure 1.1. With a proper pumping and slow outgassing of the source, high purity film can be achieved. This technique allows a wide range of materials to be deposited.

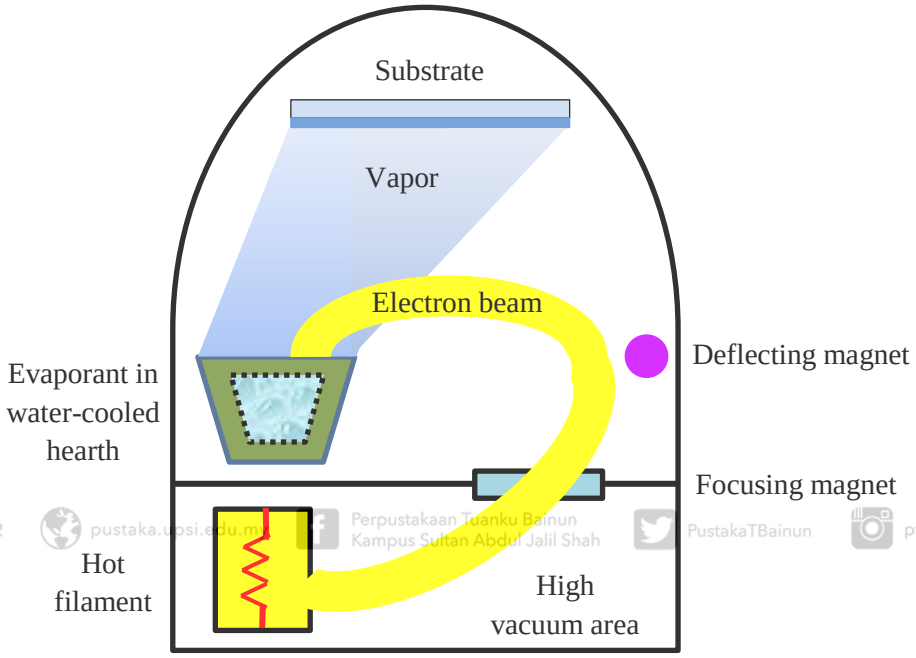


Figure 1.1. Electron beam physical vapor deposition (EB-PVD)

The second PVD technique is sputter deposition, where surface atoms are ejected from source materials by momentum transfer from energetic bombarding particles and then freed into a vacuum chamber. Since the energetic particles are usually gaseous ions accelerated from plasma, it is quite challenging to control the bombardment rate. Another setback of this method is random bombardment angle complicate the process of masking and shadowing that is usually implemented in microelectronic industry.

05-4506832 pustaka.upsi.edu.my Perpustakaan Tuanku Bainun Kampus Sultan Abdul Jalil Shah PustakaTBainun ptbupsi

05-4506832 pustaka.upsi.edu.my Perpustakaan Tuanku Bainun Kampus Sultan Abdul Jalil Shah PustakaTBainun ptbupsi

Cathodic arc deposition is the third system where cathodic electrode was vaporized on anodic electrode using high current, low-voltage arc. The arc beam is only a few microns in size and rapidly heats the area causing the source to evaporate and highly ionized. The ions are then accelerated to a biased substrate resulting a very hard thin film coating. Other deposition system generates a less hard coating even using the same materials because the temperature and velocity of the vapor is lower.

The fourth physical vapor technique is pulsed laser deposition (PLD) where a target is hit with a high energy laser in regular intervals causes evaporation of the source material (Park, Ikegami, Ebihara & Shin, 2006). The interaction of laser and the source not just heats the area, but also generates phonon, excites electrons, and ejects ions, molecules, and melted cluster. Hence this system is quite complicated and it is quite hard to control the deposition rate.

1.3 Chemical Vapor Deposition (CVD)

Chemical vapor deposition (CVD) is a process of formation of a thin film on a substrate by reacting chemical precursors in vapor phase. The precursors are evaporated via heating and transported into the reaction chamber. The product of the reaction is a solid material in thin film form, condenses on the surface inside the chamber. Figure 1.2 depicted the typical CVD reactor.

05-4506832 pustaka.upsi.edu.my Perpustakaan Tuanku Bainun Kampus Sultan Abdul Jalil Shah PustakaTBainun ptbupsi

05-4506832 pustaka.upsi.edu.my Perpustakaan Tuanku Bainun Kampus Sultan Abdul Jalil Shah PustakaTBainun ptbupsi

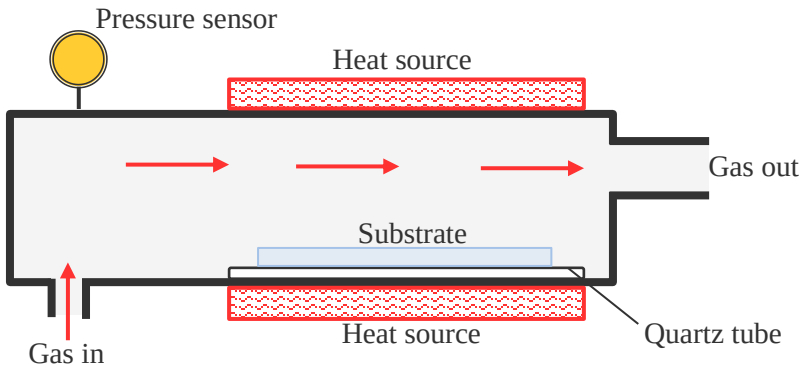


Figure 1.2. Illustration of typical chemical vapor deposition reactor

Main advantage of CVD technique is uniform thickness of thin film even on elaborate shape pieces (Huang et al., 2014). The crystal structure and the morphology of thin film can also be controlled by selection of process parameters such as deposition rate (Choy, 2003). Additionally, CVD method produces highly dense and pure phase thin film, and can easily refabricate (Knapp, 2010).

There are several CVD systems exist. Common types are Atmospheric Pressure CVD (APCVD), Low Pressure CVD (LPCVD), Plasma Enhanced CVD (PECVD) and Flame Assisted CVD (FACVD). The differences of the processes lie on the support and transport of the precursors. In APCVD, the precursor is heat up to generate vapor pressure and transport it to reaction chamber using carrier gas flow at atmospheric pressure. As contrast, LPCVD uses low vapor pressure to aid transport to heated substrate. Meanwhile, PECVD uses the same principle as APCVD, where plasma is produced to escalate the

05-4506832 pustaka.upsi.edu.my Perpustakaan Tuanku Bainun Kampus Sultan Abdul Jalil Shah PustakaTBainun ptbupsi

05-4506832 pustaka.upsi.edu.my Perpustakaan Tuanku Bainun Kampus Sultan Abdul Jalil Shah PustakaTBainun ptbupsi

reaction of the precursors. In FACVD process, activation of the precursor was done by injecting aerosol of the precursor solution into a flame. Usually, the thin film is synthesized in the reaction chamber, where the substrate is put on a heated piece called a susceptor.

The reaction of these processes however, might lead to carbon contamination from metal organic precursors in the film. Another drawback of the process is temperature limitation of the substrate since the CVD process take place at elevated temperature. The chemical reaction in the chamber is strongly temperature dependent. The high temperature also leads to stresses in films deposited on substrate with different thermal coefficient, consequently causes mechanical instability in the deposited films (Bicelli, Bozzini, Mele & D'Urzo, 2008).

05-4506832 pustaka.upsi.edu.my Perpustakaan Tuanku Bainun Kampus Sultan Abdul Jalil Shah PustakaTBainun ptbupsi

1.4 Wet Chemical Deposition

Wet chemical deposition usually requires at least one of the precursors or the material to be deposited is in liquid phase. This technique is a simple and inexpensive alternative as compared to chemical or physical vapor deposition technique. The brief description principles and salient features of the five selected wet chemical deposition technique are discussed below.

05-4506832 pustaka.upsi.edu.my Perpustakaan Tuanku Bainun Kampus Sultan Abdul Jalil Shah PustakaTBainun ptbupsi

05-4506832 pustaka.upsi.edu.my Perpustakaan Tuanku Bainun Kampus Sultan Abdul Jalil Shah PustakaTBainun ptbupsi

1.4.1 Sol-gel

The development of sol-gel method stem from ceramic fabrication at room temperature. Later, this method was used to process a wide variety of materials such as thin film, microporous inorganic membranes and aerogel material (Pier, 1998). It has also been used in preparing pure oxides, for example, ZnO, CuO and TiO_2 for various applications like photovoltaic devices (F. Li et al., 2014) and gas sensing (Gaspera, Gulgielmi & Martucci, 2015; Morsi, Nasser, Ali, Hassan & Kashyout, 2015).

This technique gained much interest in the field of thin film deposition due to its ability to produce homogenous films over large area and due to its simplicity. Generally, sol-gel technique involves spontaneous formation of a dual phase material (gel) through hydrolysis, from the precursor solution (sol), followed by polycondensation reaction that resulting in formation of three-dimensional network of particles (Hector, 2007). Typical precursors are metal chlorides and metal alkoxides. The pictorial process of sol-gel is shown in Figure 1.3. The reaction scheme and its example as explained by (Brinker & Scherer, 1990) are summarized below:

(1) Hydrolysis

$$\text{M-O-R} + H_2O \rightarrow \text{M-OH} + \text{R-OH} \qquad (1.1)$$

$$\equiv \text{Si-OR} + H_2O \rightarrow \equiv \text{Si-OH} + \text{ROH}$$

(2) Water condensation

$$\text{M-OH} + \text{HO-M} \rightarrow \text{M-O-M} + H_2O \qquad (1.2)$$

05-4506832 pustaka.upsi.edu.my Perpustakaan Tuanku Bainun Kampus Sultan Abdul Jalil Shah PustakaTBainun ptbupsi

05-4506832 pustaka.upsi.edu.my Perpustakaan Tuanku Bainun Kampus Sultan Abdul Jalil Shah PustakaTBainun ptbupsi

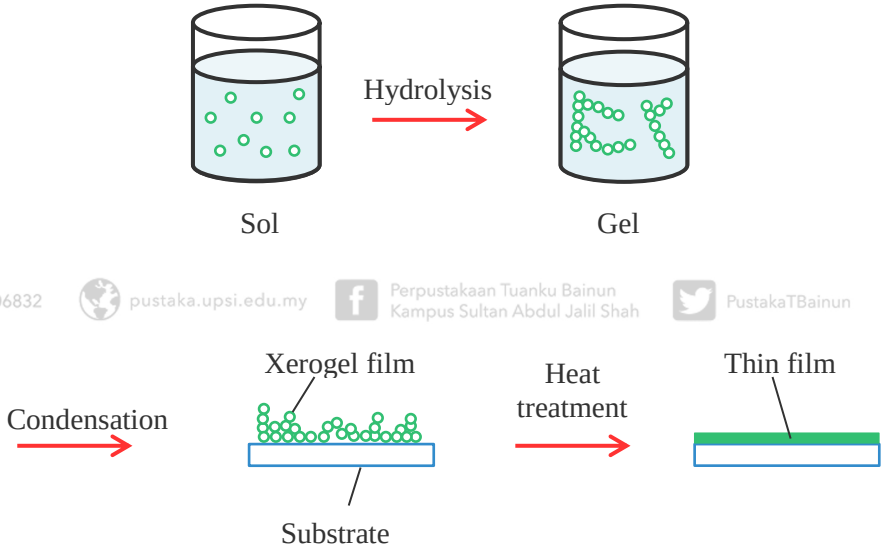
$$\equiv Si\text{-}OH + \equiv SiOH \rightarrow \equiv Si\text{-}O\text{-}Si \equiv + H_2O$$

(3) Alcohol condensation

$$M\text{-}O\text{-}R + HO\text{-}M \rightarrow M\text{-}O\text{-}M + R\text{-}OH \quad (1.3)$$

$$\equiv Si\text{-}OR + \equiv Si\text{-}OH \rightarrow \equiv Si\text{-}O\text{-}Si \equiv + ROH$$

Where M is metal type, OR is chloride or alkoxide groups and OH is hydroxy groups.



05-4506832 pustaka.upsi.edu.my Perpustakaan Tuanku Bainun Kampus Sultan Abdul Jalil Shah PustakaTBainun ptbupsi

Figure 1.3. Formation of thin film through sol-gel method

The attentiveness towards this method stem from its ability to achieve nanocrystalline or nanoporousity materials with controlled shape and size, and pores connectivity (Gaspera & Martucci, 2015). The technique can easily be transferred to industrial scale, and the cost to deposit thin film using this technique is low as the usage of

05-4506832 pustaka.upsi.edu.my Perpustakaan Tuanku Bainun Kampus Sultan Abdul Jalil Shah PustakaTBainun ptbupsi

05-4506832 pustaka.upsi.edu.my Perpustakaan Tuanku Bainun Kampus Sultan Abdul Jalil Shah PustakaTBainun ptbupsi

precursor can be minimized. However, sol gel thin films formation is accompanied by vigorous drying that often induces mechanical stress (Kappert et al., 2015).

1.4.2 Spin Coating

Spin coating is a common technique used in the application of thin films due to its ability to deposit a variety of film thickness by controlling the spin speed (K. R. Lee et al. 2014). The technique was first documented by Emslie, Bonner and Peek (l958) who described the equation of flow of a Newtonian liquid on a rotating disk with constant angular velocity. They showed that centrifugation of a fluid layer does not disturb the uniformity as the thickness of the layer is reduced.

05-4506832 pustaka.upsi.edu.my Perpustakaan Tuanku Bainun Kampus Sultan Abdul Jalil Shah PustakaTBainun ptbupsi

Generally, spin coating process has three stages. The first stage is deposition, where a solution is dispensed onto a stationary or slowly spinning substrate. The substrate is then accelerated, in which it enters the second stage called spin-up. During spin-up process, rotational force created, causing wave front that pushes the fluid to flow to the substrate's edge, consequently producing a fairly uniform layer of film. The final stage is spin-off, where excess solvent is continually removed from substrate surfaces and the wet film is thinned by centrifugal force. Throughout the process, the fluid's solvent evaporates, in which it becomes the primary means of film thinning once fluid flow ceases. The stages of coating are depicted in Figure 1.4.

05-4506832 pustaka.upsi.edu.my Perpustakaan Tuanku Bainun Kampus Sultan Abdul Jalil Shah PustakaTBainun ptbupsi

05-4506832 pustaka.upsi.edu.my Perpustakaan Tuanku Bainun Kampus Sultan Abdul Jalil Shah PustakaTBainun ptbupsi

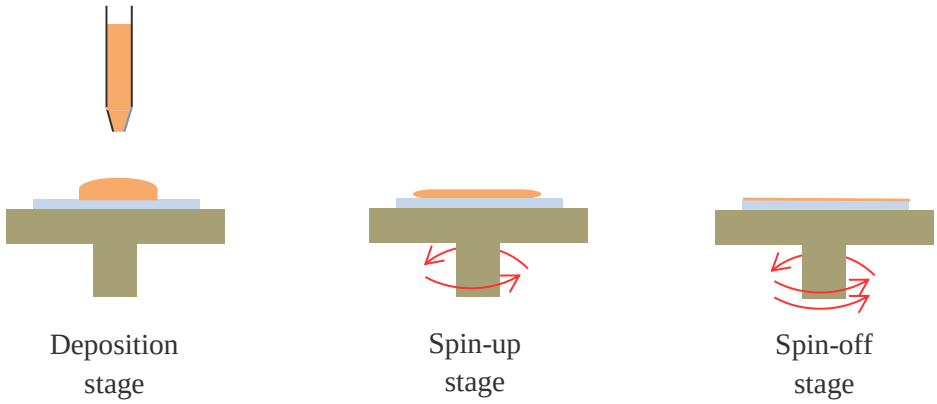


Figure 1.4. Stages of thin film formation through spin coating technique

This method has been widely used in thin film application such as photovoltaic devices (Patel, Mighri, Ajji, Tiwari & Chaudhuri, 2014), anti-reflection coating (Watanabe, Eguchi, Yamada & Saito, 2015) and sensors (Alhreb, Almasri & Alhariri, 2014). Despite of its easy implemented technique that makes it a popular route to prepare thin films, spin coating technique has few drawbacks. Among the most crucial consideration in choosing this method is the size of the substrate. Large substrates size has lower capacity to be coated uniformly and sufficiently (Sahu, Parija & Panigrahi, 2009). Material waste during spinning is very high where only 2-5% of the materials dispensed onto the substrate are useful, while the rest flung off to coating chamber and disposal bowl. However, its fast and straightforward process causing this method still becomes a prevalent technique to deposit thin films.

05-4506832 pustaka.upsi.edu.my Perpustakaan Tuanku Bainun Kampus Sultan Abdul Jalil Shah PustakaTBainun ptbupsi

05-4506832 pustaka.upsi.edu.my Perpustakaan Tuanku Bainun Kampus Sultan Abdul Jalil Shah PustakaTBainun ptbupsi

1.4.3 Spray Pyrolysis

Spray pyrolysis is a method of spraying aqueous solution on the heated substrates to form a solid film. This technique is relatively simple and cost effective because it does not require comprehensive equipment, high quality substrate or chemicals.

The deposition process involves dissolving metal salts in organic solvent, and the solution is atomized towards a hot substrate. Once the solution is sprayed, aerodynamic breakdown of the droplets occurs, followed by internal precipitation and pressurization, and droplets break-up. The atomized droplets impact the substrate to form lamella and undergo a thermal decomposition (Pawlowski, 2014). Nevertheless, process variables of this technique such as temperature, pressure, flow rate and input concentration, are very challenging to control. The most critical parameter is temperature of substrate surface since it influences film roughness, cracking, crystallinity (Perednis & Gauckler, 2005). The composition of the solid product can only be determined after deposition. However, the vapor phase must be determined *in situ* during the reaction to ensure the species do not disappear at high temperature or change during cooling process to room temperature. The quality of thin film obtain through this method is relatively poor as compared to other deposition technique (Muhibbullah, 2011).

Various types of thin films have been studied using this method. For example, Sn_xS_y films have been fabricated by varying molar ratio and growth temperature to study its influence (Polivtseva et al., 2014). The result shows higher content of thiourea (S) yield

05-4506832 pustaka.upsi.edu.my Perpustakaan Tuanku Bainun Kampus Sultan Abdul Jalil Shah PustakaTBainun ptbupsi

05-4506832 pustaka.upsi.edu.my Perpustakaan Tuanku Bainun Kampus Sultan Abdul Jalil Shah PustakaTBainun ptbupsi

thicker film and larger Sn_xS_y crystallites. However, the crystallites' size decreases as oxygen content increase with deposition temperature. The effect of precursor solution's pH towards structural, morphological, electrical and optical properties of SnS film has also been investigated (Sajeesh, Cherian, Kartha & Vijayakumar, 2012). They observed the optimum pH to obtain good device quality is 2. Solar cells active layer is another popular application of spray pyrolysis. A photovoltaic device has been prepared entirely by chemical spray pyrolysis in order to investigate optimal locations within the solar cell to deposit gold nanoparticles (Kärber et al. (2014). The cell consists of a planar ZnO covered by an extremely thin $In_2S_3/CuInS_2$ buffer/absorber layer. They found by placing gold nanoparticles layer on top of $CuInS_2$, absorption ability, short-circuit current and the conversion efficiency increased. Figure 1.5 shows the general spraying process.

05-4506832 pustaka.upsi.edu.my Perpustakaan Tuanku Bainun Kampus Sultan Abdul Jalil Shah PustakaTBainun ptbupsi

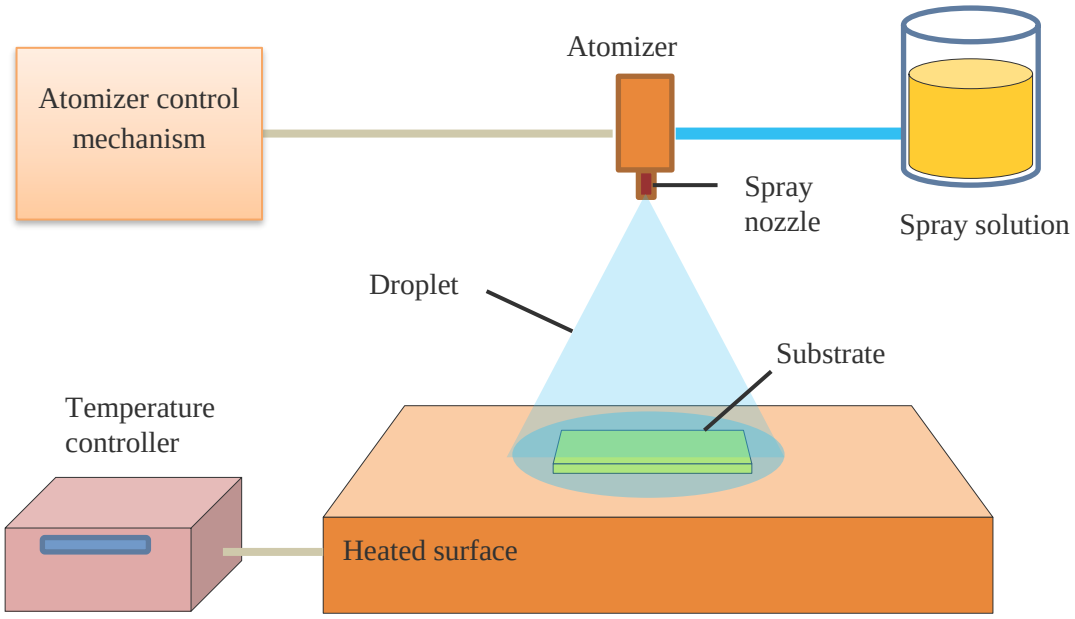


Figure 1.5. Instrumentation set up for spray pyrolysis

05-4506832 pustaka.upsi.edu.my Perpustakaan Tuanku Bainun Kampus Sultan Abdul Jalil Shah PustakaTBainun ptbupsi

05-4506832 pustaka.upsi.edu.my Perpustakaan Tuanku Bainun Kampus Sultan Abdul Jalil Shah PustakaTBainun ptbupsi

1.4.4 Electrodeposition

Electrodeposition is a process of depositing a metal from its salt solution onto another metal by applying an electric potential between two electrodes. However, the nomenclature is somewhat confused with electrochemical deposition. The electrochemical deposition is a general term that also referring to a process in which the compounds reduced in the solution by oxidation process supplying the electrons needed for metal ion reduction (Zangari, 2015).

Thin film deposition process occurs when the supplied direct current is transferred in the solution by means of ions. The cations travel toward cathodes and plating the substrate, whilst the anions travel towards anode. The cathode reactions are characterized as reduction reactions since the electrons are consumed.

Brugnatelli invented electrodeposition method in 1803 with the first materials to be deposited were gold and argentum. Initially, this technique was limited to decorative purposes. The procedures were later improved and used to harden steel parts and machining tools (Hunt, 1973). Nowadays, electrodeposition technique is further developed to comprehend fundamental process at the atomic scale and to precisely control functional properties. It has been applied to improve the performance of microelectronic such as electrical connection within semiconductor chips (Moffat & Josell, 2010), and energy conversion devices such as nanostructures for photovoltaics (Atwater & Polman, 2010; Vukmirovic, Bliznakov, Sasaki, Wang & Adzic, 2011). This method also suit for formation

05-4506832 pustaka.upsi.edu.my Perpustakaan Tuanku Bainun Kampus Sultan Abdul Jalil Shah PustakaTBainun ptbupsi

05-4506832 pustaka.upsi.edu.my Perpustakaan Tuanku Bainun Kampus Sultan Abdul Jalil Shah PustakaTBainun ptbupsi

of thin film on complicated shapes and impregnation of porous substrate (Chattopadhyay & Banerjee, 2009).

Among advantages of electrodeposition method is the simplicity of reactor designs lead to possibility of production in large scale as illustrated in Figure 1.6. The processing can take place at room temperature, and the properties of thin film can be controlled very precisely and quickly (Staikov & Milchev, 2007). The thin film thickness can be controlled by monitoring the consume charge and deposition rate of several microns per hour can be routinely achieved (Bicelli et al., 2008).

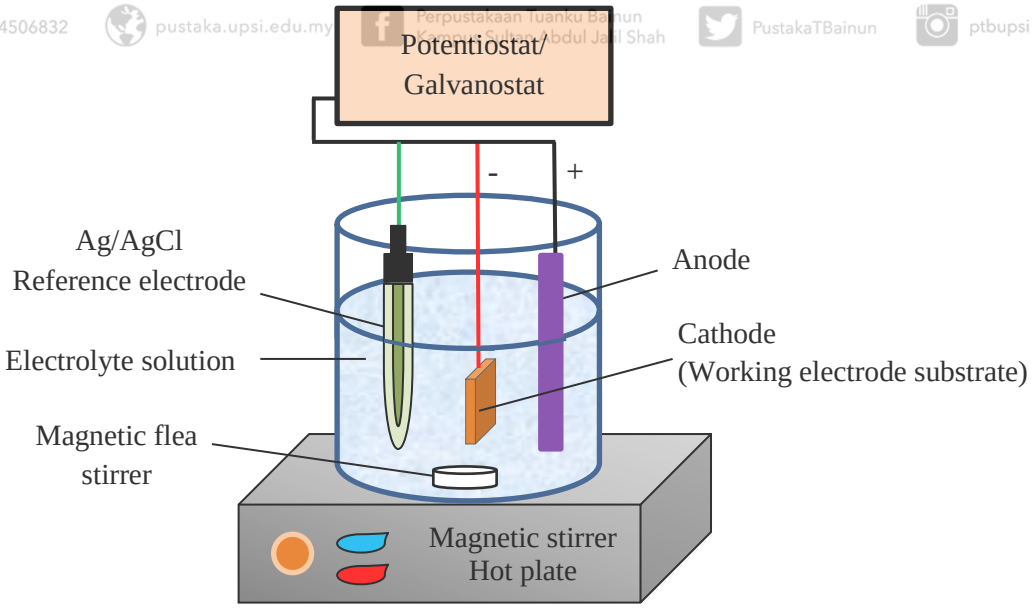


Figure 1.6. Set-up of electrodeposition

05-4506832 pustaka.upsi.edu.my Perpustakaan Tuanku Bainun Kampus Sultan Abdul Jalil Shah PustakaTBainun ptbupsi

05-4506832 pustaka.upsi.edu.my Perpustakaan Tuanku Bainun Kampus Sultan Abdul Jalil Shah PustakaTBainun ptbupsi

1.4.5 Langmuir–Blodgett (LB) Thin Films

Langmuir–Blodgett thin films technique is used to deposit a monolayer or multilayer of floating molecules on a liquid, onto a solid substrate (Blodgett & Langmuir, 1937). Initially, Langmuir–Blodgett studies were inclined towards the interfacial phenomena, but the latest trend is shifted to functional films for optical application and biological membranes. Low molecular weight compounds like stearic acid have been utilized to prepare thin film using this method. In search of better chemical, thermal and mechanical stability, polymeric materials have been used to fabricate thin film (Onah, 2006; Swalen et al., 1987). This technique will be discussed in details in Chapter 2.

The techniques of film formation described above have their own advantages and disadvantages. Different materials and coating applications requires different fabrication technique. Table 1.1 compares the deposition methods that guided the selection of technique used for this research. In order to fabricate thin film for this study, LB thin film deposition method was chosen and some modification in deposition mode was made. The ability of LB thin film technique to produce high quality layer-by-layer thin film as compared to other methods is a budding prospective in developing many electronic devices.

05-4506832 pustaka.upsi.edu.my Perpustakaan Tuanku Bainun Kampus Sultan Abdul Jalil Shah PustakaTBainun ptbupsi

05-4506832 pustaka.upsi.edu.my Perpustakaan Tuanku Bainun Kampus Sultan Abdul Jalil Shah PustakaTBainun ptbupsi

Table 1.1

Comparison of thin film deposition techniques

Deposition Technique	Thickness Precision	Level of Ordering	Cost	References
PVD	Very high	Amorphous	High	Shahidi, Moazzenchi & Ghoranneviss (2015)
CVD	Very high	Amorphous	High	Kawaharamura (2014)
Electro-deposition	Rather poor	Polycrystalline	Low	Al-Bat'hi (2015)
Sol-gel	Rather poor	Amorphous or Polycrystalline	Low	Schubert (2015)
Spin coating	Rather poor	Amorphous or Polycrystalline	Low	Pichumani et al. (2013)
LB Thin Film	Very high	High order of layer-by-layer at molecular level	Low	Cea, Ballesteros & Martín (2014)

05-4506832 pustaka.upsi.edu.my Perpustakaan Tuanku Bainun Kampus Sultan Abdul Jalil Shah PustakaTBainun ptbupsi

1.5 Motivation

Hybrid nanocomposite thin films have emerged as promising materials for optoelectronic device applications due to their ability to be fabricated in variety of ways in order for them to have specific properties (Guzelturk & Demir, 2015). The exploitation of unique properties of the polymer and nanoparticles allows the hybrid nanocomposite thin films to be utilized in optoelectronic (Osuntokun & Ajibade, 2016; X. Liu et al., 2012) and magneto-optic (S. Li et al., 2009). However, as discussed in previous subtopic, the present

05-4506832 pustaka.upsi.edu.my Perpustakaan Tuanku Bainun Kampus Sultan Abdul Jalil Shah PustakaTBainun ptbupsi

05-4506832 pustaka.upsi.edu.my Perpustakaan Tuanku Bainun Kampus Sultan Abdul Jalil Shah PustakaTBainun ptbupsi

way of fabricating plain thin film is complex resulting in higher production cost. In order to fabricate hybrid nanocomposite thin films, extra steps and materials needed are needed. Consequently, it adds the complication to the process.

Langmuir-Blodgett technique offers a conspicuous solution where the structure of thin film yielded from this method is highly organized (Nabok, 2005). Hence it passes excellent platform to explore fabrication of multilayers, influence of surface density toward thin film electrical properties and different molecule-electrode interface (Cea et al., 2014). The high precision of layer-by-layer films has been proven for small molecules such as stearic acid (Kumar, Wang, Siretanu, Duits & Mugele, 2013), arachidic acid (Roy, Das & Gupta, 2013), and behenic acid (Zhavnerko, Agabekov, Gallyamov, Yaminsky & Rogach, 2002). This method also provides a unique environment for supramolecules thin films such as calixarenes (Gonzalez-Delgado, Giner-Casares, Brezesinski, Regnouf-de-Vains & Camacho, 2012) and rotaxanes (Durola, Sauvage & Wenger, 2010).

Nevertheless, this method has some drawbacks when the material used to form the thin film is polymer. Polymer usually form unstable stacked polymer on the air/water interface and highly rigid, causing it extremely difficult to transfer the film onto solid substrate by LB thin film technique. The challenges increase in order to fabricate hybrid nanocomposite thin film, where nanoparticles are embedded in between the polymer matrix. Hence, an alternative method was developed by coining LB thin film principles to address issues stated above.

05-4506832 pustaka.upsi.edu.my Perpustakaan Tuanku Bainun Kampus Sultan Abdul Jalil Shah PustakaTBainun ptbupsi

05-4506832 pustaka.upsi.edu.my Perpustakaan Tuanku Bainun Kampus Sultan Abdul Jalil Shah PustakaTBainun ptbupsi

This method requires investigation on Langmuir monolayer in order to understand the phase changes before depositing the thin film on substrate, and to impregnate the nanoparticles in the thin film. The study of the profile can be done by analyzing its surface pressure-area isotherm graph. The formation of nanoparticles and its effect need to be examined before the thin film can be considered for electronic application. One of possible tool that can be used to check the formation of nanoparticles is by characterizing the films' optical properties, whilst electrical study on the thin films allows us to recognize the effect of nanoparticles synthesized. This study is thus motivated by the demand in fabricating high quality hybrid nanocomposite thin film with minimal work stages.

1.6 Research Objectives

05-4506832 pustaka.upsi.edu.my Perpustakaan Tuanku Bainun Kampus Sultan Abdul Jalil Shah PustakaTBainun ptbupsi

The primary objectives of this work is to study the potential of hybrid nanocomposite thin films for application in optoelectronic devices. This requires the fabrication of hybrid organic/inorganic thin film through modified Langmuir-Blodgett (LB) thin film technique. Hence, the research objectives are:

i) To study the surface pressure – area (Π-A) isotherm profile of the Langmuir films by varying the concentration of the cadmium ions in the subphase.

ii) To investigate cadmium compound (cadmium sulfide and cadmium selenide) nanoparticles formation in thin films when exposed to H_2S or H_2Se gas, and by

05-4506832 pustaka.upsi.edu.my Perpustakaan Tuanku Bainun Kampus Sultan Abdul Jalil Shah PustakaTBainun ptbupsi

05-4506832 pustaka.upsi.edu.my Perpustakaan Tuanku Bainun Kampus Sultan Abdul Jalil Shah PustakaTBainun ptbupsi

means of physical mixing; through its optical properties using UV-Vis spectrophotometer and photoluminescence (PL) spectroscopy.

iii) To investigate the effect of the nanoparticles formation in the thin films towards its current density–voltage (J-V), and Johnson noise characteristics.

With these objectives in mind, the thin film deposition based on a modified LB thin film technique was first studied and then optimized. Extensive work involving the calibration of the LB trough was carried out to understand the effects of various deposition conditions on the films.

1.7 Scope of Study

05-4506832 pustaka.upsi.edu.my Perpustakaan Tuanku Bainun Kampus Sultan Abdul Jalil Shah PustakaTBainun ptbupsi

In this study, two types of thin films have been fabricated. The thin films are categorized according to nanoparticles formation procedure. The first type is *in situ* hybridization, where the nanoparticles are impregnated in thin film matrix by exposing the thin film to hydrogen sulfide (H_2S) or hydrogen selenide (H_2Se) gas. The gas determines the types of nanoparticles nucleated, either cadmium sulfide or cadmium selenide nanoparticles. The second type is an *ex situ* hybridization, where organic/inorganic nanocomposite thin films are fabricated by physically mixing commercially pre-made quantum dots into polymer solution. Quantum dots used were cadmium sulfide and cadmium selenide. The categories of thin film and its varying parameters are show schematically in Figure 1.7.

05-4506832 pustaka.upsi.edu.my Perpustakaan Tuanku Bainun Kampus Sultan Abdul Jalil Shah PustakaTBainun ptbupsi

05-4506832 pustaka.upsi.edu.my Perpustakaan Tuanku Bainun Kampus Sultan Abdul Jalil Shah PustakaTBainun ptbupsi

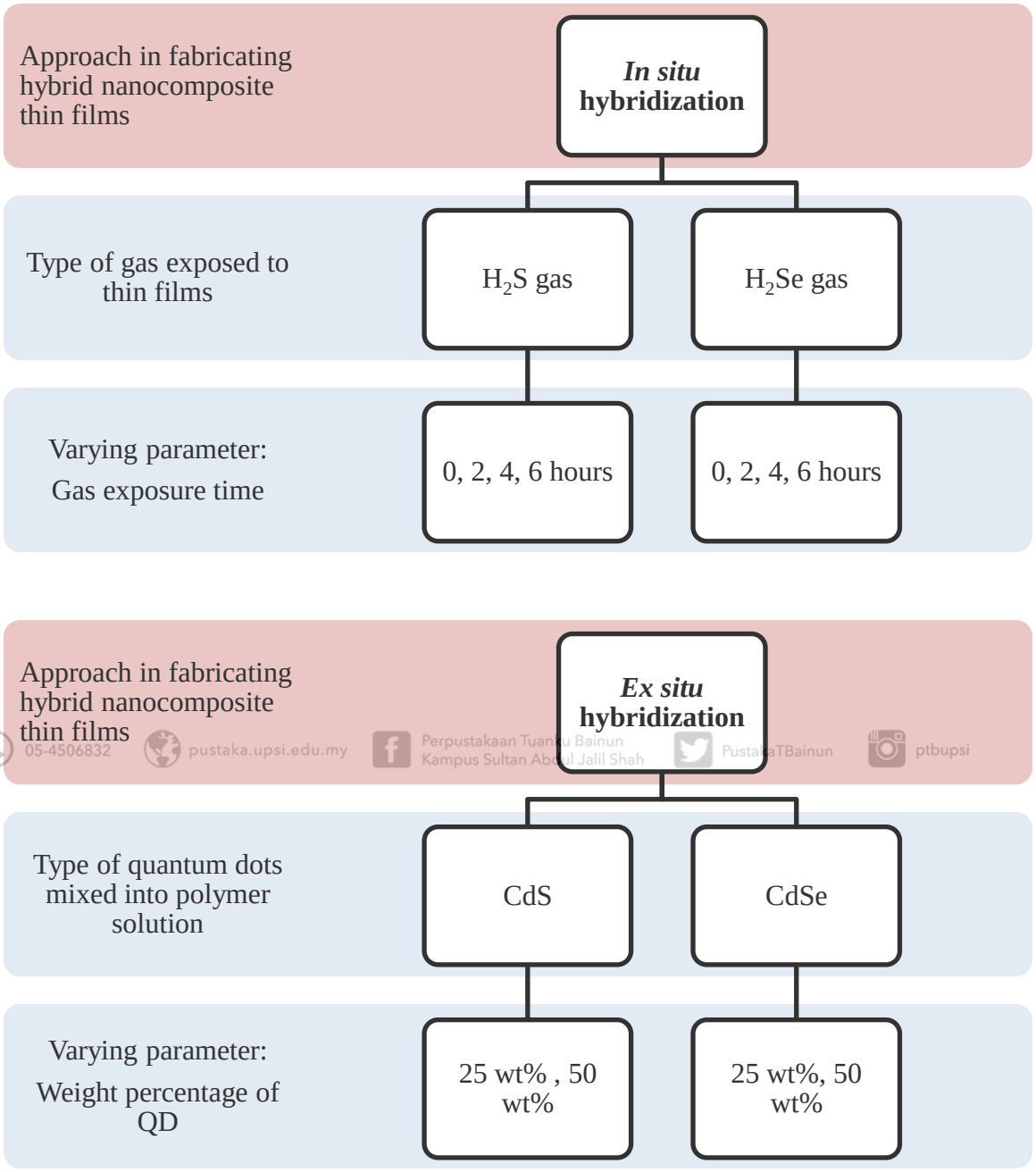


Figure 1.7. Scope of study. Two approaches used in preparing the hybrid nanocomposite thin film: *in situ* and *ex situ* hybridization

These films were then characterized to study their optical absorbance and luminescence. Electrical analysis was conducted by means of current density-voltage

05-4506832 pustaka.upsi.edu.my Perpustakaan Tuanku Bainun Kampus Sultan Abdul Jalil Shah PustakaTBainun ptbupsi

05-4506832 pustaka.upsi.edu.my Perpustakaan Tuanku Bainun Kampus Sultan Abdul Jalil Shah PustakaTBainun ptbupsi

measurement at room temperature by sweeping voltage from -1.5 V to 1.5 V to measure current. The Johnson noise of the thin films was measured using Low Frequency electrical Noise Measurement (LFeNM) setup.

1.8 Limitation of Study

The study does not cover the morphology and the magnetism of the thin films. Nevertheless, few images generated from Field Emission Scanning Electron Microscope (FESEM) will be shown as to consolidate the optical results. The same samples were used for both optical and FESEM characterization.

05-4506832 pustaka.upsi.edu.my Perpustakaan Tuanku Bainun Kampus Sultan Abdul Jalil Shah PustakaTBainun ptbupsi

1.9 Contribution of Knowledge

The study of thin film fabrication through modified Langmuir-Blodgett technique provides new insight in constructing hybrid nanocomposite thin film that is uncomplicated and cost effective. This is relevant because fabrication of plain thin films through common methods is already a complex process. Hybridizing the thin film with nanoparticles will add extra steps and equipment.

The technique of preparing hybrid nanocomposite thin films in this study enables the nanoparticles to be impregnated in the polymer matrix through simple gas exposure. The approach minimizes fabrication procedures and materials usage. The findings from

05-4506832 pustaka.upsi.edu.my Perpustakaan Tuanku Bainun Kampus Sultan Abdul Jalil Shah PustakaTBainun ptbupsi

05-4506832 pustaka.upsi.edu.my Perpustakaan Tuanku Bainun Kampus Sultan Abdul Jalil Shah PustakaTBainun ptbupsi

this study can be used for future development of hybrid nanocomposite using different types of polymer and nanoparticles.

1.10 Thesis Organization

This thesis focuses on fabrication of organic/inorganic nanocomposite thin films using modified Langmuir-Blodgett technique. Two different approaches were presented: (a) *in situ* hybridization, and (b) *ex situ* hybridization. *In situ* hybridization is a novel research of nanoparticles formation, where a simple gas exposure method was exploited to embed cadmium sulfide (CdS) or cadmium selenide (CdSe) nanoparticles in poly(3-hexylthiophene):stearic acid thin films. On the other hand, in *ex situ* hybridization technique, commercially pre-made quantum dots (CdS and CdSe) were physically mixed into the polymer solution and cast into thin films using modified Langmuir Blodgett technique. Both types of fabricated thin films were studied and reported in this thesis. The thesis is organized into five chapters.

Chapter 1 gives a general introduction on semiconducting materials, thin films, and thin films fabrication techniques. It also covers problem statements, objectives, scope, limitation and contribution of the study. Chapter 2 provides the theory and review of Langmuir film, Langmuir-Blodgett and Langmuir-Schaeffer techniques. Several types of hybrid nanocomposites thin films are also presented.

05-4506832 pustaka.upsi.edu.my Perpustakaan Tuanku Bainun Kampus Sultan Abdul Jalil Shah PustakaTBainun ptbupsi

05-4506832 pustaka.upsi.edu.my Perpustakaan Tuanku Bainun Kampus Sultan Abdul Jalil Shah PustakaTBainun ptbupsi

Chapter 3 describes the materials used, the techniques and procedures in fabricating the thin films. It also consists of characterization methods. Chapter 4 reports and discusses the results of thin films physical, optical and electrical characterizations. The results are presented according to objectives. Results for *in situ* hybridization thin film will be discussed preceding *ex situ* hybridization thin films. Finally, Chapter 5 concludes the study and suggests the area to be further investigated in the future.

1.11 Conclusion

Variety of techniques that can be utilized in order to fabricate thin films has been presented. Each of the methods offers different thin film properties as to cater different needs. While physical vapor deposition and chemical vapor deposition technique has been used extensively in industry, wet chemistry deposition technique holds a bright future to be implemented in large-scale. This research focuses in one of its branches, Langmuir-Blodgett thin films. The high quality layer-by-layer thin films that can be yielded from LB thin film technique motivate this study.

05-4506832 pustaka.upsi.edu.my Perpustakaan Tuanku Bainun Kampus Sultan Abdul Jalil Shah PustakaTBainun ptbupsi

05-4506832 pustaka.upsi.edu.my Perpustakaan Tuanku Bainun Kampus Sultan Abdul Jalil Shah PustakaTBainun ptbupsi

CHAPTER 2

THEORETICAL BACKGROUND AND LITERATURE REVIEW

05-4506832 pustaka.upsi.edu.my Perpustakaan Tuanku Bainun Kampus Sultan Abdul Jalil Shah PustakaTBainun ptbupsi

2.1 Introduction

This chapter reviews the theory of Langmuir film and its deposition techniques. Studies by others employing Langmuir-Blodgett or Langmuir-Schaeffer method will be presented too. The chapter also covers topic relating to hybrid nanocomposites thin films focusing on inorganic nanomaterials as the fillers for the polymer matrices. It includes scientific principles, processing and fabrication, and general characteristics of hybrid nanocomposites. Their applications mainly in relation to optical properties are discussed as well.

05-4506832 pustaka.upsi.edu.my Perpustakaan Tuanku Bainun Kampus Sultan Abdul Jalil Shah PustakaTBainun ptbupsi

05-4506832 pustaka.upsi.edu.my Perpustakaan Tuanku Bainun Kampus Sultan Abdul Jalil Shah PustakaTBainun ptbupsi

2.2 Langmuir Film

Benjamin Franklin performed few experiments on wave damping effect by depositing 2 cm^2 of oil on the surface of a large pond and noticed the damping effect of the oil film covering the water surface (Franklin, 1774). Franklin however, did not realize he was actually witnessing the creation of an oil monolayer. If he had calculated the thickness of oil spread over 2000 m^2, he would have found the layer was around 1 nm thick.

In 1890, Lord Rayleigh calculated the film thickness of 0.81 mg olive oil (triolein) that covered an area of 555 cm^2 on a surface of clean water. He also did not realize the film thickness of 16 Å was the length of triolein molecules forming a monomolecular layer. At about the same time, Agnes Pockels invented a shallow container equipped with movable strips that can be used to sweep the surface clean from any impurities prior to an experiment and to compress or relax any oil film while maintaining the amount of material constant and introduced a method to measure surface tension (Pockels, 1891). Lord Rayleigh replicated her apparatus and used it to determine molecular magnitudes. He however, did not consider the molecule shape.

It was Irving Langmuir who found molecules pack with identical orientation at the air-interface, due to amphiphilicity of the molecules (Langmuir, 1920). His student, Katharine Blodgett carried out the study on sequential vertical deposition of multilayers onto a solid substrate that is now termed as Langmuir-Blodgett (LB) method (Blodgett, 1935; Blodgett & Langmuir, 1937). Later, Langmuir collaborated with Vincent Schaefer

05-4506832 pustaka.upsi.edu.my Perpustakaan Tuanku Bainun Kampus Sultan Abdul Jalil Shah PustakaTBainun ptbupsi

05-4506832 pustaka.upsi.edu.my Perpustakaan Tuanku Bainun Kampus Sultan Abdul Jalil Shah PustakaTBainun ptbupsi

and reported depositing thin film horizontally, which led to equally good result as vertical deposition. This technique is known as Langmuir-Schaefer (LS) deposition (Langmuir & Schaefer, 1938).

2.3 Langmuir Film Formation

Langmuir film is the amphiphilic molecules on a liquid (subphase) surface. The formation of Langmuir film is highly dependent on surface pressure of the film, in which it determines either the film is monolayer or multilayers. The typical subphase employed in Langmuir film studies is water, although other substances such as mercury and glycerol have been used as substitutes (Barraud, Leloup & Lesieur, 1985; Kraack, Deutsch, Ocko & Pershan, 2003).

The quality of the Langmuir films is highly dependent on cleanliness of the subphase. The contaminant in the water, such as the presence of Na^+ or K^+ ions, may change the subphase pH, consequently affecting the dissociation of COOH fatty acidheads. Nonetheless, the bivalent metal salts ions (e.g.: Cd^{2+}, Cu^{2+}) is a beneficial factor for the monolayer stabilization. Dust contaminant on the surface of the subphase can also hamper the quality of the film. It could cause spontaneous reduction on the surface pressure causing collapse of the monolayer (Nabok, 2005).

05-4506832 pustaka.upsi.edu.my Perpustakaan Tuanku Bainun Kampus Sultan Abdul Jalil Shah PustakaTBainun ptbupsi

05-4506832 pustaka.upsi.edu.my Perpustakaan Tuanku Bainun Kampus Sultan Abdul Jalil Shah PustakaTBainun ptbupsi

Formation of Langmuir films is usually achieved by utilizing amphiphilic compound dissolved in an evaporating solvent such as chloroform and dichloromethane, spread on the subphase in the Langmuir trough. Examples of amphiphilic materials are long-chain fatty acids such as stearic acid and arachidic acid, esters, and phospholipids. Amphiphilic materials consist of a polar head group that attach to the subphase, and at least one long hydrophobic tail group that prevents dissolution of the molecule into the subphase. Hence, a layer of film at the air/subphase interface can be formed (Petty, 1996).

As the hydrophobicity of the hydrocarbon tails increases, the solubility of amphiphilic molecules decreases. Nonetheless, varieties of amphiphilic polymeric materials such as poly(dimethylsiloxane) (PDMS) (Z. Liao, Hsieh, Baumgart & Dmochowski, 2013), poly(tert-butyl acrylate) (PtBA) (Maestro et al., 2011), and poly(methyl methacrylate) (PMMA) (I. Çapan , Uzunoğlu, Tarımcı & Tanrısever, 2008) may also form stable Langmuir films. Likewise, studies exploiting fullerene derivatives (Zhu et al., 1996), organometallic compounds (Pearson, Gibson, Petty, Moore & Bryce, 1993), and branched polymers (Taniguchi, Yokoyama, Miyashita, 1997) have also been reported. Table 2.1 shows the typical amphiphilic molecular structure.

Apart from above mentioned materials, studies have been done on non-amphiphilic materials such as nanoparticles and quantum dots. Tao et al. (2003) have assembled monolayers of silver nanowires that are closed-packed and parallel to each other, even at the initial phase the nanowires are randomly oriented. A study by Xu et al. (2006) on CdSe and Cd-Se-Zn-S quantum dots shows stable formation of Langmuir films on water

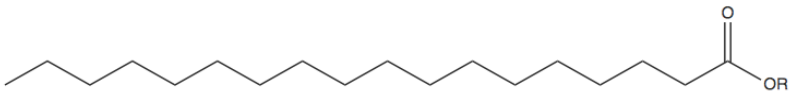
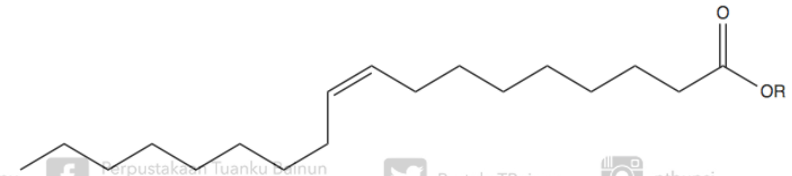
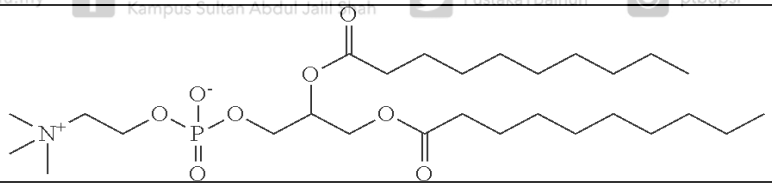
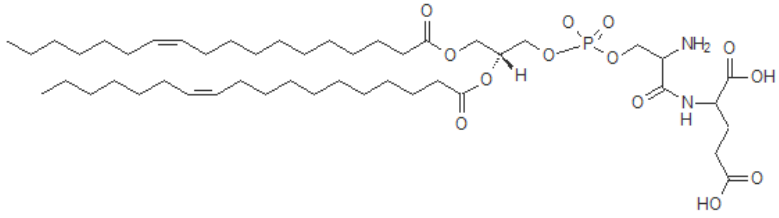
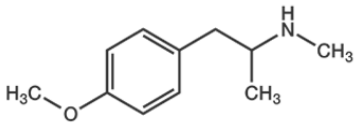
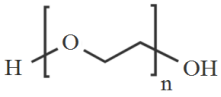
05-4506832 pustaka.upsi.edu.my Perpustakaan Tuanku Bainun Kampus Sultan Abdul Jalil Shah PustakaTBainun ptbupsi

05-4506832 pustaka.upsi.edu.my Perpustakaan Tuanku Bainun Kampus Sultan Abdul Jalil Shah PustakaTBainun ptbupsi

subphase. Similar results have been observed when Langmuir monolayer was formed using PbSe and PbS quantum dots (Justo, Moreels, Lambert & Hens, 2010).

Table 2.1

Examples of amphiphilic molecules and its structure

Amphiphilic type	**Molecule name**	**Molecular structure**
Fatty acid	Stearic acid	
	Oleic acid	
Phospholipid	Lechitin	
	Glycolipid	
Polymer	PMMA	
	Poly (ethylene oxide)	

05-4506832 pustaka.upsi.edu.my Perpustakaan Tuanku Bainun Kampus Sultan Abdul Jalil Shah PustakaTBainun ptbupsi

05-4506832 pustaka.upsi.edu.my Perpustakaan Tuanku Bainun Kampus Sultan Abdul Jalil Shah PustakaTBainun ptbupsi

Langmuir monolayer also provides a unique environment to study molecular interaction, the fundamental aspect of supramolecular chemistry. The molecular recognition on interface is important because biological system mostly occurs at the media of different phase such as internal surfaces of enzyme pockets, and cell membrane surface. Conventional studies were done on homogenous solution phases. Turina, Clop and Perillo (2015) investigated the effect of molecular arrangement on the flunitrazepam (FNZ) receptiveness to the binding sites at the $GABA_A$ receptor ($GABA_A$-R) by using LB film as model membranes. Synaptosomal membranes from bovine brain cortex were spread on the water surface before transferring it to hydrophobic substrate. The Langmuir layer acts as sensor for $GABA_A$-R ligand binding as well as $GABA_A$-R activity modulation. A study regarding the metal ion coordination when a monolayers of 4-{10-[4-(3,5-bis-benzyloxy)-phenyl]-anthracen-9-yl}-benzoic acid ([G1-An]-CO(2)H, G1) and 4-(10-{4-[3,5-bis-(3,5-bis-benzyloxy)-benzyloxy]-phenyl}-anthracen-9-yl)-benzoic acid ([G2-An]-CO(2)H, G2) is spread the air-water interface has been conducted by Yang J. et al. (2011). The results show that G1 and G2 have different limiting areas when Al^{3+} or Eu^{3+} is added in the subphase.

Langmuir films can be exploited to study intermolecular interactions, monolayer/subphase interactions, as well as model systems for biological membranes. This is due to the capability of Langmuir layers of mimicking the biological membrane structure, for example phospholipid monolayers can be viewed as halve of a phospholipid bilayer in a cell. Langmuir films studies are also eminent in fabricating high quality LB-films with controlled orientation and thickness (Sorokin, Bai, Ducharme & Poulsen, 2002).

05-4506832 pustaka.upsi.edu.my Perpustakaan Tuanku Bainun Kampus Sultan Abdul Jalil Shah PustakaTBainun ptbupsi

05-4506832 pustaka.upsi.edu.my Perpustakaan Tuanku Bainun Kampus Sultan Abdul Jalil Shah PustakaTBainun ptbupsi

Preparation of Langmuir film starts with dissolving amphiphilic substance in an appropriate solvent such as chloroform and spread onto the subphase. The solvent is allowed to evaporate for 10 – 15 minutes prior to starting the movable barriers, to reduce the area of floating film. Once the barriers start to move towards each other, the monolayer at the interface will be correspondingly compressed causing the film to undergo different thermodynamic phase transitions (Karabıyık, 2003). This allows for the surface pressure (Π) to be measured by determining the surface tension of a suspended Wilhelmy plate that immersed partially in the subphase. The surface pressure of the film can be mathematically defined as:

$$\Pi = \gamma_o - \gamma \qquad (2.1)$$

where γ_o is the surface tension of pure water and γ is the surface tension of water covered by a film. The surface tension of air/pure water interface at room temperature is equal to 72.8 mN/m. This value is exceptionally high as compared to other liquid making it a popular choice for subphase in studying surface of materials (Kraack et al., 2004).

The Langmuir film can be characterized by computing its surface pressure as a function of surface area available to the molecules of the interface. The measurement is performed during constant area reduction at a constant temperature to obtain a curve called surface pressure – area (Π-A) isotherm.

The shape of the Π-A isotherm graph varies depending on the nature of the materials spread on the subphase (Ariga, Yamauchi, Mori & Hill, 2013). The idealized surface pressure transition of a low molecular amphiphilic compound discloses three

05-4506832 pustaka.upsi.edu.my Perpustakaan Tuanku Bainun Kampus Sultan Abdul Jalil Shah PustakaTBainun ptbupsi

05-4506832 pustaka.upsi.edu.my Perpustakaan Tuanku Bainun Kampus Sultan Abdul Jalil Shah PustakaTBainun ptbupsi

distinct regions in an isotherm curve. At the beginning of the compression process the monolayer is deemed to be in a “gaseous phase” because the molecules are still far apart without any interaction between them, hence the surface pressure asymptotically approaches zero. In gaseous phase, the area occupied by a molecule is enormous as compared to the molecular dimensions of the spread molecules. Thus, the molecules encompass an extremely small surface vapor pressure that makes the experimental study of gaseous phase very challenging (Crisp, 1946).

As the compression increases, the molecules start to come closer together thereby exerting a repulsive force on each other. The area per molecule decreases whilst the surface pressure increases. At this stage the monolayer is considered to be in “liquid phase” which is still compressible. However, when the compression reaches a critical value, monolayer turns into a “solid phase” where now the molecules are arranged in their closest possible packing. This is indicated by a sharp discontinuity in the slope of the isotherm graph. The extrapolation of this steepest part of the graph to intercept the x-axis gives a molecule’s area occupancy value in the condensed state, A_o. This value is presumed to retain the same value once the monolayer is transferred to solid substrate (Nabok, 2005).

When the surface pressure continues to increase with decreasing surface area, a “collapse” phenomena occurs due to mechanical instability at very high surface pressures known as collapse pressure. At this stage the molecules possess high energy and forced out of the interfacial film resulting in disordered multilayers which minimizes the energy resulting from close packing of molecules. The collapse pressure gives information about

05-4506832 pustaka.upsi.edu.my Perpustakaan Tuanku Bainun Kampus Sultan Abdul Jalil Shah PustakaTBainun ptbupsi

05-4506832 pustaka.upsi.edu.my Perpustakaan Tuanku Bainun Kampus Sultan Abdul Jalil Shah PustakaTBainun ptbupsi

the compressibility and intermolecular forces of the substance (Hagting, 1999). These events can be discerned from the surface pressure-mean molecular area isotherm graph as shown in Figure 2.1. The isotherm graph allows us to determine the optimum pressure for LB or LS deposition.

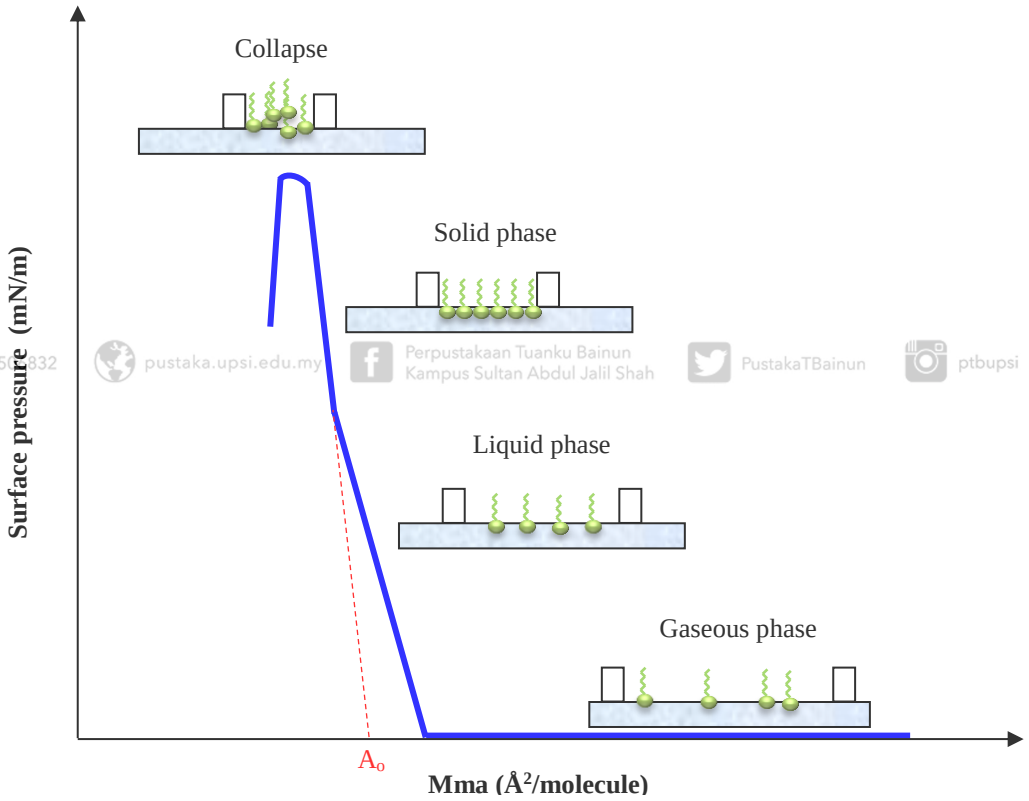


Figure 2.1. Surface pressure-area (Π-A) isotherm of Langmuir monolayer, where A_o is denoted as the area occupied by a molecule.

Amphiphilic polymers layer shows simpler Π-A isotherms compared to small molecules monolayer. The absence of long hydrophobic tails in polymer causing it to have

05-4506832 pustaka.upsi.edu.my Perpustakaan Tuanku Bainun Kampus Sultan Abdul Jalil Shah PustakaTBainun ptbupsi

05-4506832 pustaka.upsi.edu.my Perpustakaan Tuanku Bainun Kampus Sultan Abdul Jalil Shah PustakaTBainun ptbupsi

a simple gas phase, a liquid-like phase, or a solid-like phase. Once the polymer solution is spread on the air/water subphase, they either take on a three-dimensional conformation, or are able to obtain a random two-dimensional conformation. The 2D configuration is a result of maximum material's contact with water, consequently causing a very thin polymeric monolayer to form as depicted in Figure 2.2.

Polymeric Langmuir monolayers phase can be categorized into expanded and condensed stages (Schreiber, 2000). Expanded monolayer is 2D "dissolved" state that depends on hydration forces with the subphase, whilst condensed monolayer is 2D "collapsed" state (Ulman, 1991). Analogous to that of small molecules isotherm graph, slow rise in surface pressure can be observed in expanded polymer monolayer stage, whereas a sharper slope on a Π-A isotherm occurs at condensed state.

05-4506832 pustaka.upsi.edu.my Perpustakaan Tuanku Bainun Kampus Sultan Abdul Jalil Shah PustakaTBainun ptbupsi

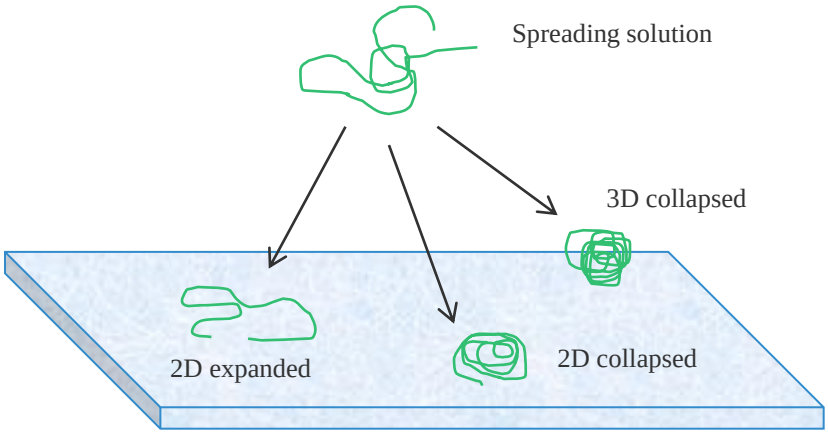


Figure 2.2. Spreading of polymeric solution on subphase (adapted from Hagtig, 1999)

05-4506832 pustaka.upsi.edu.my Perpustakaan Tuanku Bainun Kampus Sultan Abdul Jalil Shah PustakaTBainun ptbupsi

05-4506832 pustaka.upsi.edu.my Perpustakaan Tuanku Bainun Kampus Sultan Abdul Jalil Shah PustakaTBainun ptbupsi

2.4 Langmuir Film Preparation

The preparation of Langmuir films employed a hydrophobic Langmuir-Blodgett (LB) trough, that is made from Teflon or poly(tetrafluoroethylene) (PTFE). The Teflon's hydrophobicity ensure the formation of meniscus when trough filled with water, consequently reduces the formation of collapses and film aggregation during compression to form monolayer (Hagtig, 1999).

One or two movable barriers are affixed to the troughs to alter the surface area occupied by dissolved amphiphilic compound. A Wilhelmy plate is attached to LB trough acts as surface pressure sensor, either used to check cleanliness of the subphase or to measure the change in surface tension during compression. The plate could be platinum, chromatography paper or filter paper. The measurement is based on forces acting on the plate when it is partially immersed into subphase.

Trough is first cleaned by wiping it with chloroform using low-lint soft tissue and then rinsed with ultrapure de-ionized (DI) water. The trough is wiped again with ethanol, and water was subsequently added into trough and then removed. Water rinsing process is repeated for three times in order to eliminate any remaining solvent. The same process is done to clean the trough barriers. Then, ultrapure DI water was poured into the trough and barriers were compressed to the maximum using computer interfacing unit. Throughout barriers closure, water surface is suctioned to ensure the subphase cleanliness.

05-4506832 pustaka.upsi.edu.my Perpustakaan Tuanku Bainun Kampus Sultan Abdul Jalil Shah PustakaTBainun ptbupsi

05-4506832 pustaka.upsi.edu.my Perpustakaan Tuanku Bainun Kampus Sultan Abdul Jalil Shah PustakaTBainun ptbupsi

Once the barriers are fully compressed, the surface pressure is reset to zero before the barriers are fully expanded again. Surface pressure of the DI water is recorded. If the surface pressure is more than 0.2 mN/m, the trough needs to be cleaned again. Surface pressure below 0.2 mN/m indicates trough's cleanliness is satisfactory. The value of surface pressure 0.2 mN/m is the standard set by KSV-Nima for the LB trough under its provision. Figure 2.3 illustrated the Langmuir trough set up for this study.

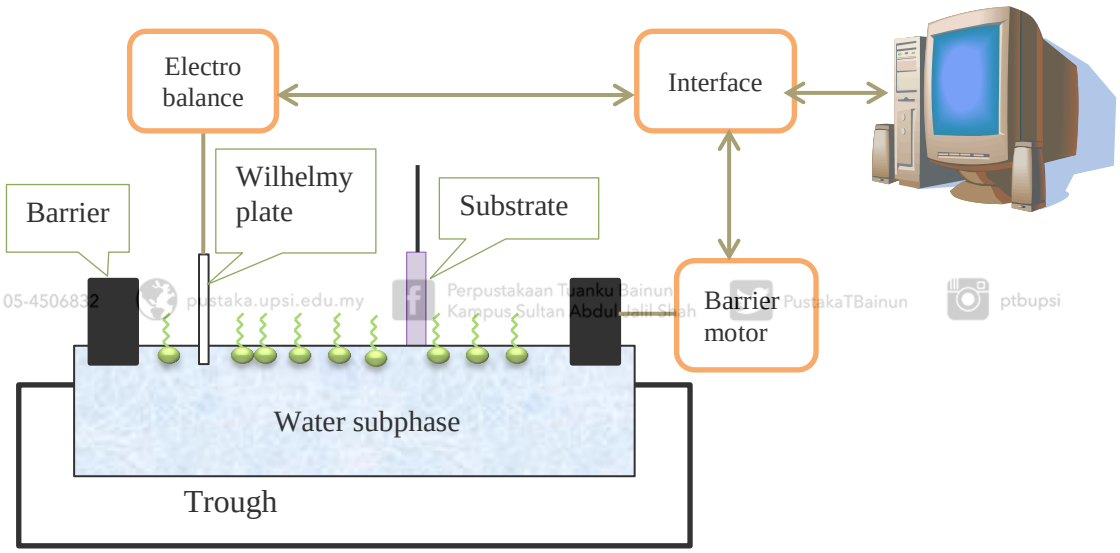


Figure 2.3. Schematic diagrams of Langmuir trough used in this project. The barrier movement and Wilhelmy plate that monitors the surface pressure are controlled by the computer through an interfacing process

After the trough has been clean thoroughly, it is filled with subphase. Then, an amphiphilic dissolved solution is gently placed on the subphase surface by using a glass micro-syringe. The solvent, usually chloroform, is allowed to evaporated before closing the barrier. The remain is floating amphipilic materials, where it will rearrange its position

05-4506832 pustaka.upsi.edu.my Perpustakaan Tuanku Bainun Kampus Sultan Abdul Jalil Shah PustakaTBainun ptbupsi

05-4506832 pustaka.upsi.edu.my Perpustakaan Tuanku Bainun Kampus Sultan Abdul Jalil Shah PustakaTBainun ptbupsi

and becoming more dense and more order as the barriers closed. The packing of the materials will cause the phase changes from gaseous to liquid and then solid phase. The solid phase of the floating monolayer is the Langmuir layer

2.5 Transfer of Langmuir Film onto Solid Substrate

Considerable attention has been shown on the extremely thin and highly organized organic films assembled on solid substrate over the last few decades due to its wide potential application in catalyst, sensors (Erdogan, Özbek, R. Çapan & Yagci, 2012; Bilewicz & Majda, 1991), modified electrodes (Eloul, Batchelor-McAuley & Compton, 2014) and photovoltaic devices (Roh, Jo, Chang, Han & Jang, 2015).

05-4506832 pustaka.upsi.edu.my Perpustakaan Tuanku Bainun Kampus Sultan Abdul Jalil Shah PustakaTBainun ptbupsi

Langmuir monolayer was usually transferred onto solid substrate by two different practices. The first is vertical dipping (90^o) or also known as Langmuir-Blodgett (LB), and the second is horizontal touching (180^o) methods or called Langmuir-Schaefer (LS) technique. The transfer process is done at a constant surface pressure once the monolayer is condensed.

2.5.1 Langmuir-Blodgett (LB) Thin Films Deposition

Langmuir monolayers can be transferred onto a solid substrate by vertical dipping method, which was demonstrated first by Blodgett and Langmuir (1937). Generally, the transferring

05-4506832 pustaka.upsi.edu.my Perpustakaan Tuanku Bainun Kampus Sultan Abdul Jalil Shah PustakaTBainun ptbupsi

05-4506832 pustaka.upsi.edu.my Perpustakaan Tuanku Bainun Kampus Sultan Abdul Jalil Shah PustakaTBainun ptbupsi

process occurs when molecules are at their closest packing in solid phase. The transfer that is done right before collapse phase can yield a high quality film with zero defects (Dynarowicz-Latka, Dhanabalan, & Oliveira, 2001).

In LB thin films deposition technique, the Langmuir film is transferred onto hydrophilic or hydrophobic solid substrate by displacing of the vertical substrate in the upward or downward directions. The surface pressure is kept constant during deposition process.

There are several vertical LB thin films deposition patterns, called X, Y, and Z-type transfers. The deposition sequences are schematically shown in Figure 2.4. Y-type deposition is the most common type of transfer employing a hydrophobic substrate. The substrate is dipped vertically through the Langmuir layer, where the substrate picks up the tails of the amphiphilic molecules. The substrate is then raised; causing another monolayer to be transferred. During transferring process, polar head groups of the amphiphiles on the subphase are attracted to the polar head groups of the already transferred monolayer. The layers are allowed to completely dry in air before the next downstroke. The process is repeated until desired numbers of layers are deposited. The idealized transfer of Y-type are depicted in Figure 2.4 (a).

Notwithstanding, X-type and Z-type deposition can be achieved by depositing the amphiphiles only on downstroke or upstroke, respectively. The transfer results in the same orientation in all layers, as shown in Figure 2.4 (b) and 2.5 (c).

05-4506832 pustaka.upsi.edu.my Perpustakaan Tuanku Bainun Kampus Sultan Abdul Jalil Shah PustakaTBainun ptbupsi

05-4506832 pustaka.upsi.edu.my Perpustakaan Tuanku Bainun Kampus Sultan Abdul Jalil Shah PustakaTBainun ptbupsi

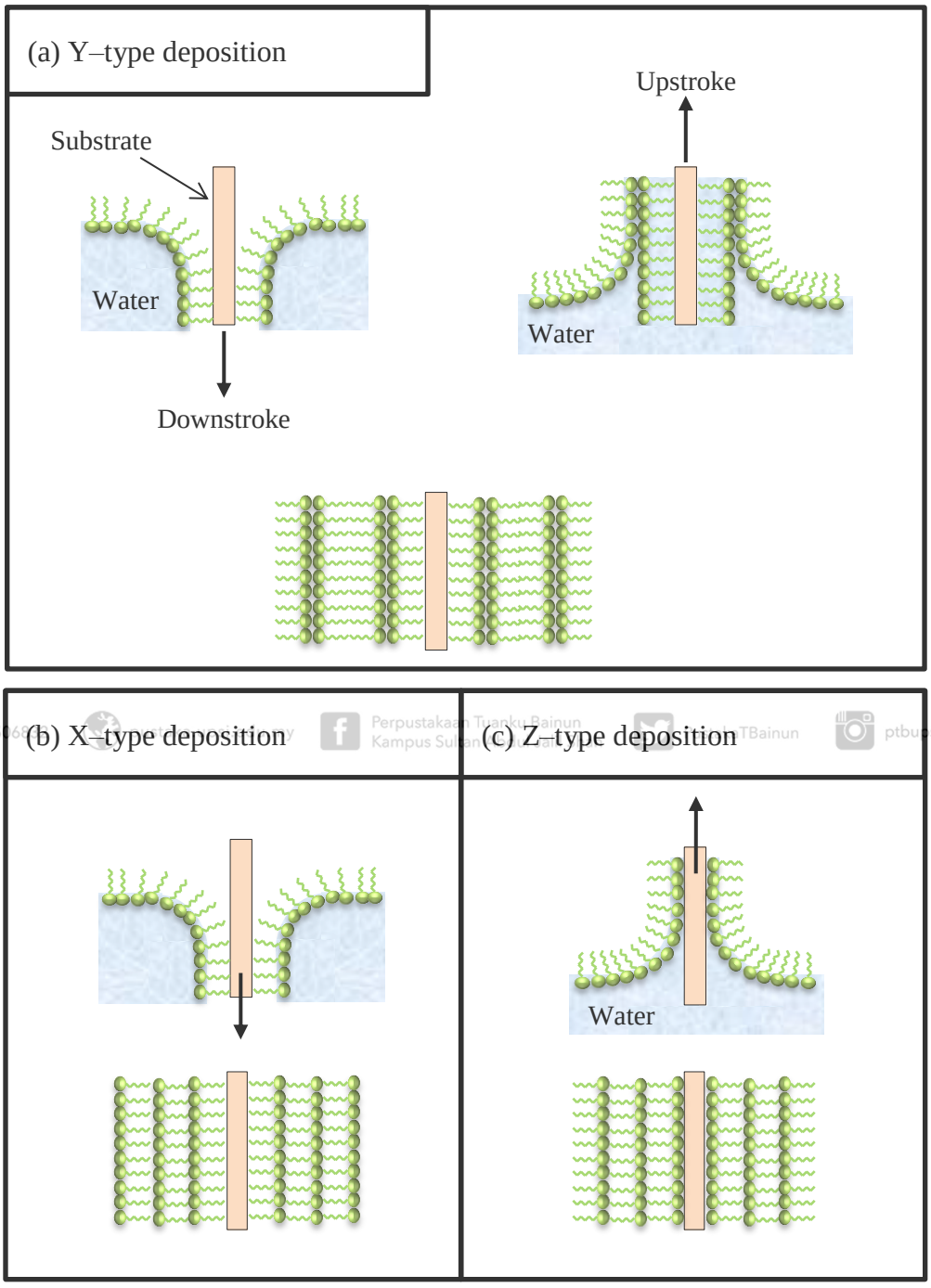


Figure 2.4. Schematic representations of LB thin films deposition methods (a) Y-type, (b) X-type, (c) Z-type

05-4506832 pustaka.upsi.edu.my Perpustakaan Tuanku Bainun Kampus Sultan Abdul Jalil Shah PustakaTBainun ptbupsi

05-4506832 pustaka.upsi.edu.my Perpustakaan Tuanku Bainun Kampus Sultan Abdul Jalil Shah PustakaTBainun ptbupsi

Apart from low-weight amphiphilic molecules, LB method has also being used to fabricate thin films using other compounds that have capability forming monolayer structures on water subphase. Among most researched materials is polymer because the polymer structure organization from this technique is expected to yield superior mechanical and thermal stability (Aminuzzaman, Mitsuishi & Miyashita, 2010).

A study on polyisocyanide thin film showed long polymer chains were packed in the two-dimensional film without any piling chain. They propose that persistence length of the polymers in the two-dimensional films is subject to its three-dimensional chains in solution (Kumaki, Kajitani, Nagai, Okoshi & Yashima, 2010).

Martín-García and co-workers investigated the effect of morphology toward the photoluminescence (PL) of cadmium selenide quantum dots (CdSe QDs):styrene/maleic anhydride copolymer thin film (Martín-García, Paulo, Costa & Velázquez, 2013). They found the photoluminescence dynamics are greatly depended on excitation energy migration between close-packed or small clusters of aggregated quantum dots. The small cluster size reflects the lower density of energy trap. Accordingly, the larger QD aggregation region causing the films to display lesser PL intensities and rapid energy decays.

LB technique also useful in growing various organic and inorganic films on diverse substrates. For example, lamellar multilayer of zinc sulfide–cadmium selenide QDs has been deposited and further modified the thin film using poly(maleic anhydride-alt-1-

05-4506832 pustaka.upsi.edu.my Perpustakaan Tuanku Bainun Kampus Sultan Abdul Jalil Shah PustakaTBainun ptbupsi

05-4506832 pustaka.upsi.edu.my Perpustakaan Tuanku Bainun Kampus Sultan Abdul Jalil Shah PustakaTBainun ptbupsi

tetradecene) (PMA) (Gole, Jana, Selvan & Ying 2008). Hydrophobicity of the QDs and amphipilicity of the PMA drove the self-assembly process.

Whilst another group fabricated stable, transparent and antibacterial graphene oxide (GO) sheets on a PET substrate using LB method (Mangadlao et al., 2015). They observed the antibacterial activity of the GO films is directly influenced by the number of layers deposited. Graphene oxide thin film by LB method can also be hybridized with poly(3,4-ethylenedioxythiophene) (PEDOT) by reducing the thin film and coat it by means of a vapor phase polymerization procedure. The reduced GO/PEDOT nanocomposite shows exceptional electrical conductivity, high specific capacitance and displays improved capacitance retention rate than pure PEDOT. This owing to GO flexible nature, in which sheet's folding and wrinkling can be substantially minimized as compared to conventional method such as spin casting.

LB technique also allows easy films transfer on any substrate to be integrated with microelectronic devices (Wen, Jiang, Y. Yang & S. Li, 2014). Baschir et al. (2014) deposited five layers of 5,10,15, 20-tetrakis(3,4-dimethoxyphenyl)-porphyrin Fe(III) chloride on ceramic substrate to study its sensitivity towards UV radiation. The study on this topic is very broad, and only few recent examples are discussed above. More intensive review on the LB films has been described elsewhere (Ariga et al., 2013; Foest, Schmidt & Gargouri, 2014).

05-4506832 pustaka.upsi.edu.my Perpustakaan Tuanku Bainun Kampus Sultan Abdul Jalil Shah PustakaTBainun ptbupsi

05-4506832 pustaka.upsi.edu.my Perpustakaan Tuanku Bainun Kampus Sultan Abdul Jalil Shah PustakaTBainun ptbupsi

2.5.2 Langmuir-Schaefer (LS) Thin Films Deposition

Langmuir-Schaefer (LS) thin film method is another way of building multilayer structures on solid substrate as introduced by Langmuir and Schaefer (1938). As contrast to LB method, the LS thin films technique requires for the substrate to be positioned horizontally on the Langmuir film. When the substrate is lowered until it touches the floating layer, the hydrophobic tails attracted and hook up to a hydrophobic substrate. The substrate is then lifted and detached from the subphase, consequently transferring the monolayer. The schematic illusion of LS thin films method is presented in Figure 2.5.

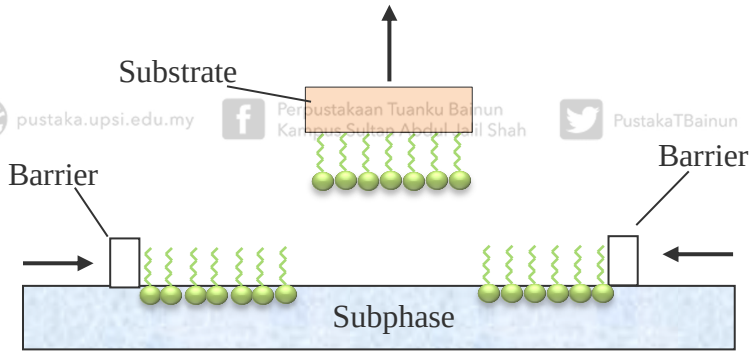


Figure 2.5. Schematic presentation of LS thin film method

Just like LB technique, various materials have been used to fabricate thin films using LS method. Investigation on bis(zinc octaethylporphyrin) (ZnPP) was done by transferring the Langmuir layer using LS thin films method (Giancane, Borovkov, Inoue, Conoci & Valli, 2013). The observation shows interaction of aromatic amines with ZnPP

05-4506832 pustaka.upsi.edu.my Perpustakaan Tuanku Bainun Kampus Sultan Abdul Jalil Shah PustakaTBainun ptbupsi

05-4506832 pustaka.upsi.edu.my Perpustakaan Tuanku Bainun Kampus Sultan Abdul Jalil Shah PustakaTBainun ptbupsi

was sustained even after the transfer process. Hence it makes it possible to selectively detect aromatic amines at concentrations as low as 20 ppb.

Pandey's group studied the ramification of localized silver metal surface plasmons on spectral and charge transport features of poly (3,3‴-dialkylquarterthiophene) [PQT-12] deposited using LS technique (Pandey, Yadav, Upadhyay, Prakash & Mishra, 2015). Smooth PQT-12 films over silver nanostructure island films [SNIF] were observed. Generally, organic molecule excitons coupling with metal nanostructure surface plasmons increase optoelectronic devices performance. Another interesting study is construction of nanodisks with uniform height and tunable diameter without any lithographic processes (Mori et al., 2012). A weak amphiphilic triimide module and water soluble macrocyclic oligoamine were utilized to get better control of domain size. The Langmuir layer was transferred onto mica using LS technique. By varying the surface pressure, the diameter of the disk can be tuned. However, the height of the disks was maintained. The example of studies presented indicates the versatility of the technique, showing the technique is not limited to amphiphilic molecules only.

2.6 Hybrid Nanocomposite Thin Films

Advancements in nanomaterials have resulted in development of hybrid nanocomposites, which are used in various applications such as solar cells (H. C. Liao, Chantarat, Chen & Peng, 2011; Gosnell, Schreuder, Rosenthal & Weiss, 2007), drug delivery system (Fang,

05-4506832 pustaka.upsi.edu.my Perpustakaan Tuanku Bainun Kampus Sultan Abdul Jalil Shah PustakaTBainun ptbupsi

05-4506832 pustaka.upsi.edu.my Perpustakaan Tuanku Bainun Kampus Sultan Abdul Jalil Shah PustakaTBainun ptbupsi

X. C. Wang, H. C. Wu & C. Z. Zhao, 2011), water membrane (Lai, Groth, Gray & Duke, 2014), and automotive components (Sachse et al., 2013). Nanomaterials can be defined as materials with at least one of its dimension is less than 100 nm. The addition of specific types of nanomaterials into matrices such as polymer and clay enhance the composite materials physical, electrical and chemical properties (Buthainah et al., 2013)

Among most studied nanomaterials are inorganic nanoparticles (Cha, Bae & Lee, 2015), ceramic nanoparticles such as titania (Mark, 1996) and carbon (Swain & Jena, 2010). However, the final product does not necessarily have to be in nanoscale, but can be micro- or macroscopic in size (Hussain, Hojjati, Okamoto & Gorga, 2006). Hybrid nanocomposites in this thesis are focusing on mixtures of inorganic nanomaterials in polymer matrices. The main idea of developing hybrid nanocomposite is to manipulate of the best properties of each element that form the hybrid, and at the same time trying to reduce or eradicate their drawbacks (Gomez-Romero, 2001). The polymers are usually chosen by considering their behavior in electrical, optical, mechanical, or chemical stability for intended application. Another attractive feature offered by polymers is easy shaping that allows better processing steps of the composite materials (Jeon & Baek, 2010).

In general, the introduction of nanomaterials into polymer matrices causes the modification in the polymers' properties even at low weight percentage of nanomaterials. This phenomenon is a result of very large surface area to volume ratio of nanoparticles (Luo & Daniel, 2003), and consequently increases forces between atoms/molecules such as electrostatic forces and van der Waals. Mechanical properties of polymer, for example

05-4506832 pustaka.upsi.edu.my Perpustakaan Tuanku Bainun Kampus Sultan Abdul Jalil Shah PustakaTBainun ptbupsi

05-4506832 pustaka.upsi.edu.my Perpustakaan Tuanku Bainun Kampus Sultan Abdul Jalil Shah PustakaTBainun ptbupsi

polypropylene can be tailored according to desired usage by controlling the nanoparticles properties (Wu, Zhang, Rong & Friedrich, 2002). Optical properties of the polymer can also be significantly changed (Haridas, Srivastava & Basu, 2008). Apart from the size of the nanomaterials, the degree of the materials mixing greatly influences the properties of the polymer nanocomposites. If the nanomaterials are poorly dispersed, the mechanical properties of the composites may degrade (Gorga & Cohen, 2004).

Typical nanomaterials can be classified into three classes: particles, fibrous and layered (Thostenson, C. Li & Chou, 2005). Inorganic nanoparticles such as cadmium sulfide and zinc oxide, carbon black and silica nanoparticles are the example for nanomaterials in particles category. Carbon nanotube and nanofibers are the fibrous materials, whilst the layered nanomaterials such as organosilicate that has nanometers in thickness and a high aspect ratio with plate-like structure (Hussain et al., 2006). This study focuses on polymer matrix based nanocomposites with inorganic nanoparticles being one of the key modifications. The optical and electrical properties of the hybrid nanocomposites thin films are the primary area of interest. The next subsections discuss several different types of polymer nanocomposites.

2.7 Inorganic Nanoparticles – Polymer Blend

High surface area to volume ratio and quantum effects is the basis to the improvements in polymer properties when inorganic nanomaterials are incorporated. Consequently, some

05-4506832 pustaka.upsi.edu.my Perpustakaan Tuanku Bainun Kampus Sultan Abdul Jalil Shah PustakaTBainun ptbupsi

05-4506832 pustaka.upsi.edu.my Perpustakaan Tuanku Bainun Kampus Sultan Abdul Jalil Shah PustakaTBainun ptbupsi

hybrid nanocomposites exhibit properties predominated by interfacial reaction while others associated to nanodimensional structures (Christopher & Lerner, 2001). The hybrid nanocomposites can be prepared by various methods including physical adsorption, ligand-metal interaction, or by blending nanoparticless with the desired polymers. Several types of hybrid nanocomposites and its nature of fabrication will be discussed in the following section.

2.7.1 Hybrid II-VI group: Polymer

Materials of group II-VI are semiconductors that composed of element from the second group (M = Zn, Cd, Hg) and sixth group (X = O, S, Se, Te) in the periodic table. The nanoparticles II-VI semiconductors, MX, such as ZnO, ZnS, CdS, CdTe, CdSe and HgSe, have many applications in optoelectronics industry due to their optical and electrical properties. It has wide, direct band gap that is useful for both light emitters and light detectors (J. Wang & Isshiki, 2007).

The II-VI materials can also be tailored into ternaries alloy semiconductors such as cadmium zinc telluride (CdZnTe or CZT) and mercury cadmium telluride (HgCdTe). While cadmium sulfide (CdS) and cadmium selenide (CdSe) nanoparticles will be the focus of this dissertation, other types of II-VI will also be discussed as well. The fragment of periodic table showing the elements from group II and group IV as well as other related group is shown in Table 2.2.

05-4506832 pustaka.upsi.edu.my Perpustakaan Tuanku Bainun Kampus Sultan Abdul Jalil Shah PustakaTBainun ptbupsi

05-4506832 pustaka.upsi.edu.my Perpustakaan Tuanku Bainun Kampus Sultan Abdul Jalil Shah PustakaTBainun ptbupsi

Table 2.2

Some elements on periodic table

Ia	IIa		IIb	IIIa	IVa	Va	VIa	VIIa	VIIIa
Li	Be			B	C	N	O	F	Ne
Na	Mg			Al	Si	P	S	Cl	Ar
K	Ca		Zn	Ga	Ge	As	Se	Br	Kr
Rb	Sr		Cd	In	Sn	Sb	Te	I	Xe
Cs	Ba		Hg	Tl	Pb	Bi	Po	At	Rn

Solid cadmium sulfide nanoparticles is yellow in color due to its band gap of 2.42 eV at 300 K (Kittel, 1995) and absorption peak at 515nm (Dumbrava, Badea, Prodan & Ciupina, 2010; Bhattacharya & Saha, 2008). The CdS nanoparticles show distinct physical, chemical and structural properties from the bulk where its characteristics are affected by size (El-Bially et al., 2012; Banerjee, Jayakrishnan & Ayyub, 2000; Rao & Cheetham, 2006). Likewise, cadmium selenide nanoparticles also demonstrate strong size dependency on their properties (Norris, Sacra, Murray & Bawendi, 1994; Tolbert & Alivisatos, 1994). CdSe nanoparticles optical absorption and emission properties are easily controlled throughout the entire visible wavelength range (Norris, Efros, Rosen, & Bawendi, 1996; Norris & Bawendi, 1996).

Group II-VI nanomaterials can be mixed with polymers to create hybrid nanocomposite thin films to enhance the properties of the nanoparticles or the polymer through synergistic interaction between two molecules. For example, a study has been done

05-4506832 pustaka.upsi.edu.my Perpustakaan Tuanku Bainun Kampus Sultan Abdul Jalil Shah PustakaTBainun ptbupsi

05-4506832 pustaka.upsi.edu.my Perpustakaan Tuanku Bainun Kampus Sultan Abdul Jalil Shah PustakaTBainun ptbupsi

on the mixture of CdSe with Poly[2,6–(4,4–bis–(2–ethylhexyl)–4*H*–cyclopenta[2,1–*b*;3,4–*b'*]dithiophene)–*alt*–4,7(2,1,3-benzothiadiazole)] (PCPDTBT) as the active layer for solar cell (Dayal, Kopidakis, Olson, Ginley and Rumbles (2010). The group reported power conversion efficiency (PCE) as much as 3.13%.

Comparable results have been reported when CdSe nanoparticles were dispersed into Poly(3-hexylthiophene-2,5-diyl) (P3HT), where the performance of solar cells increased with the increment of weight percentage of CdSe (J. Liu, Tanaka, Sivula, Alivisatos & Fréchet, 2004) . Similar trends have been observed when the weight ratio of CdSe : MEH-PPV (poly(2-methoxy-5-(2-ethylhexyloxy)-1,4-phenylene vinylene) increased from 1 : 2 to 9 : 1 (Zhou et al., 2006). However, when the weight ratio further increased from 9 : 1 to 20 : 1, the efficiency then decreased from 1.13 to 0.16%. They suggested that increasing CdSe content in the polymer matrix generates more percolation pathways and promotes the transport of electrons, thereby increasing the photocurrent. Conversely, further increasing nanoparticles in the active layer decreases the contribution of polymer to the light absorption, hence destroys the pathway for holes transport, causing the efficiency to decrease accordingly.

Another interesting feature that affecting the properties of hybrid nanocomposite thin film is the morphology and size of the nanoparticles used. The effect of morphology of branched-shape CdSe and nanorods-shape CdSe nanoprticles in the conjugated polymer towards the power conversion efficiency of solar cells has been compared (B. Sun, Marx & Greenham, 2003). The photovoltaic performance was significantly improved when

05-4506832 pustaka.upsi.edu.my Perpustakaan Tuanku Bainun Kampus Sultan Abdul Jalil Shah PustakaTBainun ptbupsi

05-4506832 pustaka.upsi.edu.my Perpustakaan Tuanku Bainun Kampus Sultan Abdul Jalil Shah PustakaTBainun ptbupsi

branched nanoparticles were used due to the promotion of electron transport perpendicular to the plane of the film.

Further study has been done to compare the morphology of nanoparticles – spherical, and blends of nanorod CdSe and tetrapods CdSe into poly(3-hexylthiophene) (P3HT): [6,6]-phenyl-C61-butyric acid methyl ester (PCBM) matrix. They reported the efficiency of tetrapods/nanorods CdSe samples were higher. The concentrations of nanoparticles were also varied from 10 to 175 wt%, and they found similar results as Zhou et al. (2006), where both short-circuit current density, J_{sc} and efficiency decreased starting from 100 to 175 wt%. The length of tetrapods arms also crucial in determining the efficiency of photovoltaic device. Longer arms aid in better spatial connectivity, decreasing charge hopping events, which lead to better charge transport (K. S. Lee, I. Kim, Gullapalli, Wong & Jabbour, 2011).

Hybrid nanocomposites thin film also found it usage as light emitter. The first hybrid nanocomposite light emitting diodes (LED) were based on CdSe: poly(p-phenylenevinylene) (PPV) (Colvin, Schlamp & Alivisatos, 1994). Since then, tremendous progress has been made where many researches focus on increment of the quality of the color emmision and to attain higher luminescence efficiency. Good emission color can be obtained by mixing different nanoparticles into the polymer matrix (W. Chung, Park, Yu, H. J. Kim and B. Kim, 2010). They managed to get a white emission by mixing various sizes of CdSe incorporated in poly(methyl methacrylate) (PMMA).

05-4506832 pustaka.upsi.edu.my Perpustakaan Tuanku Bainun Kampus Sultan Abdul Jalil Shah PustakaTBainun ptbupsi

05-4506832 pustaka.upsi.edu.my Perpustakaan Tuanku Bainun Kampus Sultan Abdul Jalil Shah PustakaTBainun ptbupsi

Improvement of the overall luminescence efficiency has been achieved by mixing CdSe nanoparticles into poly[(9,9-dioctyl-2,7-divinylenefluorenylene)-alto-co-(2-methoxy-5-(2-ethylhexyloxy)-1,4-phenylene) (PFPV) (H. Yu, W. Chung & S. H. Kim, 2010). They reported luminescence efficiency of 44.2 lm/W for a white light LED. The mechanical improvement of polymer via reinforcement mechanism has been studied, where the modulus and the tensile strength of the hybrid nanocomposites increase as the wt% of ZnS in the hybrid nanocomposites increases (X. Lu, N. Lu, Gao, Jin & C. Lu, 2007).

2.7.2 Hybrid III-V group: Polymer

Compound III-V semiconductors composed of an element from column III, and another from column V, of the periodic table, so that the outer orbitals are filled with exactly eight electrons. Whilst there are twelve possible combinations, many researches focusing on GaAs, InP, GaP and GaN. These semiconductors have direct band gap, hence they are optically active and possess great potential to be used in optoelectronic and photonic devices (Amin, 2011). In addition, they also have high absorption coefficients and tend to radiate light efficiently (Bosi & Pelosi, 2007).

Solar cells fabricated from galium nitride (GaN) nanoparticles and poly(3-hexylthiophene) has been studied and the results show that the device performance is greatly enhanced with addition of GaN nanoparticles (Qian et al., 2014). The potential of this type of hybrid nanocomposite thin films in photovoltaic application was further studied

05-4506832 pustaka.upsi.edu.my Perpustakaan Tuanku Bainun Kampus Sultan Abdul Jalil Shah PustakaTBainun ptbupsi

05-4506832 pustaka.upsi.edu.my Perpustakaan Tuanku Bainun Kampus Sultan Abdul Jalil Shah PustakaTBainun ptbupsi

by investigating how charges are separated and transferred at the interface between GaAs and P3HT (Panahandeh-Fard et al., 2014). Hence, studies using spectroscopy measurements and density functional theory (DFT) to comprehend charge-carrier photogeneration and photoinduced interfacial charge transfer were done. They found the coexistence of electrons and holes transfer at the GaAs/P3HT interface leads to the generation of long-lived species causing higher power conversion efficiency.

2.7.3 Hybrid Metal Oxide (MeO_x): Polymer

Metal oxide (MeO_x) nanostructures are widely used in many areas such as transducer, sensors, photovoltaic and electro-chromic devices. The ability of metal oxide to be processed to form vertically aligned nanostructures or also known as nanowire causing higher interfacial area between nanomaterials and the polymer hence providing efficient conduction pathways (Wright & Uddin, 2012). Other advantages of MeO_x are high optical transparency and sufficient electrical conductivity (Litzov & Brabec, 2013).

Various MeO_x like ZnO, TiO_2, In_2O_3, MoO_3, WO_3 or ZrO_2 have been employed as photodetectors. Among the above-mentioned MeO_x nanostructures, ZnO and TiO_2 are of particular interest owing to its potential in electronics and medical application.

Zinc oxide (ZnO) is an *n*-type and non-toxic semiconductor nanoparticles with a wide-band-gap of 3.37 eV at 300K (Wuu, Wu & Horng, 2013). It can be directly used for

05-4506832 pustaka.upsi.edu.my Perpustakaan Tuanku Bainun Kampus Sultan Abdul Jalil Shah PustakaTBainun ptbupsi

05-4506832 pustaka.upsi.edu.my Perpustakaan Tuanku Bainun Kampus Sultan Abdul Jalil Shah PustakaTBainun ptbupsi

biomedical applications without coatings (Anita, Ramachandran, Koushik, Rajendran, & Mahalakshmi, 2010). The electrical conductivity of ZnO:polystyrene resin has also been investigated (Ma, Chen & Kuan (2006). The hybrid nanocomposites were prepared by melt-blending technique and the amount of ZnO whiskers or spherical nanoparticles were increased to study its resistivity. The whiskers ZnO showed higher surface resistivity reduction as compared to spherical ZnO showing the shape of the embedded nanoparticles plays important role in the electrical properties. This result is in parallel with the study done with II-VI as discussed in earlier subtopic. Another implication of the study is the increment of ZnO in the polymer matrix can gradually increase the conductivity network.

Titanium oxide or titania, TiO_2 is another non-toxic material that extensively used in optoelectronic application owing to its chemical stability and strong photocatalytic activity. Su and Kuramoto (2000) has prepared polyaniline (PANi):TiO_2 nanocomposite trough *in situ* polymerization to study the film conductivity, and found that the conductivity of the film can be improved by post annealing the film. Another research of the same type hybrid nanocomposites has been carried out (Mo, Wang, Chen & Yeh, 2008). They found the increment of TiO_2 quantity leads to increment in conductivity and dielectric constant.

Study also showed that at the presence of aluminum oxide (Al_2O_3) in the polycarbonate (PC) nanoparticles lessened the overall light transmittance of the nanocomposite (Chandra, Turng, Gopalan, Rowell & Gong, 2008). Magnetic properties of MeO_x polymer nanocomposite were investigated by several groups. A study done on Fe_3O_4:PANi nanocomposites showed magnetization saturation as high as 3.2 emu/g at 300

05-4506832 pustaka.upsi.edu.my Perpustakaan Tuanku Bainun Kampus Sultan Abdul Jalil Shah PustakaTBainun ptbupsi

05-4506832 pustaka.upsi.edu.my Perpustakaan Tuanku Bainun Kampus Sultan Abdul Jalil Shah PustakaTBainun ptbupsi

K, suggesting a super paramagnetic characteristic (Alam, Riaz, Ahmad, 2007). On the other hand, undoped PANi exhibits lower magnetization saturation than that of Fe_3O_4@Au:PANi nanocomposites (27.35×10^{-3} emu/g) has been reported (Q. Yu, Shi, Cheng, Wang & Chen, 2008)

2.7.4 Hybrid Quantum Dots: Polymer

Quantum dots (QDs) are semiconductor inorganic nanocrystals with the diameters are in the range of 1-20 nm (Foubert et all., 2016). Due to its dimensions that are smaller than the exciton Bohr radius, QDs display discrete energy levels (Chan, Maxwell, Gao, Bailey & Han, 2002). Another interesting aspect of QDs is by changing the its size, the band gap can be tuned (Klimov, 2007; H. J. Lee et al., 2008). These characteristics allowing the QDs to absorb wide spectra of light and later reemit a specific color reliant on the band gap (Somesree, Diercks, Mills, Hynds, & Ghosh, 2011; Bakalova, Ohba & Zhelev, 2004).

Quantum dot consists of a semiconductor core that is coated by a shell that is manipulated according to application. A significant amount of research has been done on QDs and QDs/polymer nanocomposite such as photovoltaic devices, LEDs and biological markers. Behaviour of quantum dots incorporated in a polymer matrix of MEH-PPV as active layer has been investigated (Greenham, Peng & Alivisatos, 1997). They found that the surface of the quantum dot governs the charge transfer from the polymer matrix to the quantum dots. Quantum dots are commonly shielded by 11 Å thick organic ligands like

05-4506832 pustaka.upsi.edu.my Perpustakaan Tuanku Bainun Kampus Sultan Abdul Jalil Shah PustakaTBainun ptbupsi

05-4506832 pustaka.upsi.edu.my Perpustakaan Tuanku Bainun Kampus Sultan Abdul Jalil Shah PustakaTBainun ptbupsi

trioctylphosphineoxide (TOPO) or trioctylphosphine (TOP) that form barriers for charge transport (Günes, Neugebauer & Sariciftci, 2007; Lane & Kafafi, 2005).

Usually, in order to ensure intimate electrical contact, these barriers have to be removed (Günes et al., 2007). Haridas et al. (2008) showed there is a significant change in optical properties even for very small fraction of the QDs. Solar cells based on poly (3-hexylthiophene) (P3HT) and CdSe prepared by Hyun, Dittmer and Alivisatos (2002) show increment in charge transfer rate and extended spectrum absorption up to 700 nm. Another research group also reported that by integrating $CuInS_2$ QDs into organic photoactive layers, the corresponding power conversion efficiency was 13% higher than the undoped solar cells (Nam, S. Lee, Park, Kim & K. K. Lee, 2011)

05-4506832 pustaka.upsi.edu.my Perpustakaan Tuanku Bainun Kampus Sultan Abdul Jalil Shah PustakaTBainun ptbupsi

One of the challenges in organic/quantum dots blend is the mixed layer morphology since it has a profound effect on materials' electrical properties. The mixed layer must produce sufficient interface with high separation force for excitons dissociation and for effective electrons and holes transportation (Cai, Gong & Cao, 2010). Many researches reveal that by improving the crystalline nature of films (X. N. Yang et al., 2005) by means of annealing (H. C. Liao et al., 2011; G. Li et al. 2007; Ho et al., 2011), by adding processing additive (Peet et al., 2007), or different solvent (W. Li, Guo, Sun & Zhou, 2010; L. Wang, Liu, Jiang, Qin & Cao, 2007; Kekuda et al., 2011); light absorption and overall performance can be enhanced. Investigations also show that when a polymer active layer is deposited onto the substrate, the resulting morphology is strongly affected by the

05-4506832 pustaka.upsi.edu.my Perpustakaan Tuanku Bainun Kampus Sultan Abdul Jalil Shah PustakaTBainun ptbupsi

05-4506832 pustaka.upsi.edu.my Perpustakaan Tuanku Bainun Kampus Sultan Abdul Jalil Shah PustakaTBainun ptbupsi

polymer's interaction with substrate and deposition parameters (Müller-Buschbaum, Gutmann & Stamm, 2000; Halls et al., 2000).

2.8 Conclusion

The theory and studies that have been conducted on Langmuir layer, Langmuir Blodgett, Langmuir Schaefer, and hybrid nanocomposites thin films were presented in this chapter. The fundamental researches and applications of thin films mainly regarding optical and electrical characteristics were reviewed. The next chapter will focus on experimental preparation of this study to produce Langmuir film and hybrid nanocomposite thin films through modification of Langmuir-Blodgett technique.

05-4506832 pustaka.upsi.edu.my Perpustakaan Tuanku Bainun Kampus Sultan Abdul Jalil Shah PustakaTBainun ptbupsi

05-4506832 pustaka.upsi.edu.my Perpustakaan Tuanku Bainun Kampus Sultan Abdul Jalil Shah PustakaTBainun ptbupsi

CHAPTER 3

MATERIALS AND METHOD

05-4506832 pustaka.upsi.edu.my Perpustakaan Tuanku Bainun Kampus Sultan Abdul Jalil Shah PustakaTBainun ptbupsi

3.1 Introduction

This chapter outlines description of materials selection, the sequence of devices fabrications and characterization methods that have been performed. It begins with an overview of the research design, followed by the list of main chemicals used, their preparation, and the formulations of the thin film. The next subsection discusses the steps of thin films fabrications. Finally, the characterization methods and their basic theory are explained.

05-4506832 pustaka.upsi.edu.my Perpustakaan Tuanku Bainun Kampus Sultan Abdul Jalil Shah PustakaTBainun ptbupsi

05-4506832 pustaka.upsi.edu.my Perpustakaan Tuanku Bainun Kampus Sultan Abdul Jalil Shah PustakaTBainun ptbupsi

3.2 Research Design

This study used experimentation method for data gathering and analysis. The experimental work started by selecting materials for the thin film, followed by thin films fabrication and characterization. Two approaches were devised as to fabricate the thin films: (a) *in situ* hybridization, and (b) *ex situ* hybridization. Thin film deposition technique in this research is a modification from Langmuir-Blodgett technique. The alteration was made as to ensure the polymer layers strongly adhere on substrate, and to initiate the polymerization during the deposition process.

In situ hybridization is the focus of the research in which the hybrid nanocomposites thin films were fabricated through modified Langmuir-Blodgett technique coupled with gas exposure. The novelty of this method is the nanoparticles were impregnated in the polymeric thin film without having to prepare the nanoparticles in separate work. On the contrary, *ex situ* hybridization was based on physical mixing of polymer and the quantum dots to produce hybrid nanocomposite thin films. This is a common approach done by many research groups using various deposition techniques like spin coating, where it requires the quantum dots to be prepared separately before it was mixed into polymer. The *ex situ* method is generally tedious and expensive.

The properties of all thin films were then characterized for its optical properties using UV-Vis-NIR and photoluminescence spectrophotometers, electrical properties and Johnson noise analyses. Figure 3.1 summarized the overall experimental framework.

05-4506832 pustaka.upsi.edu.my Perpustakaan Tuanku Bainun Kampus Sultan Abdul Jalil Shah PustakaTBainun ptbupsi

05-4506832 pustaka.upsi.edu.my Perpustakaan Tuanku Bainun Kampus Sultan Abdul Jalil Shah PustakaTBainun ptbupsi

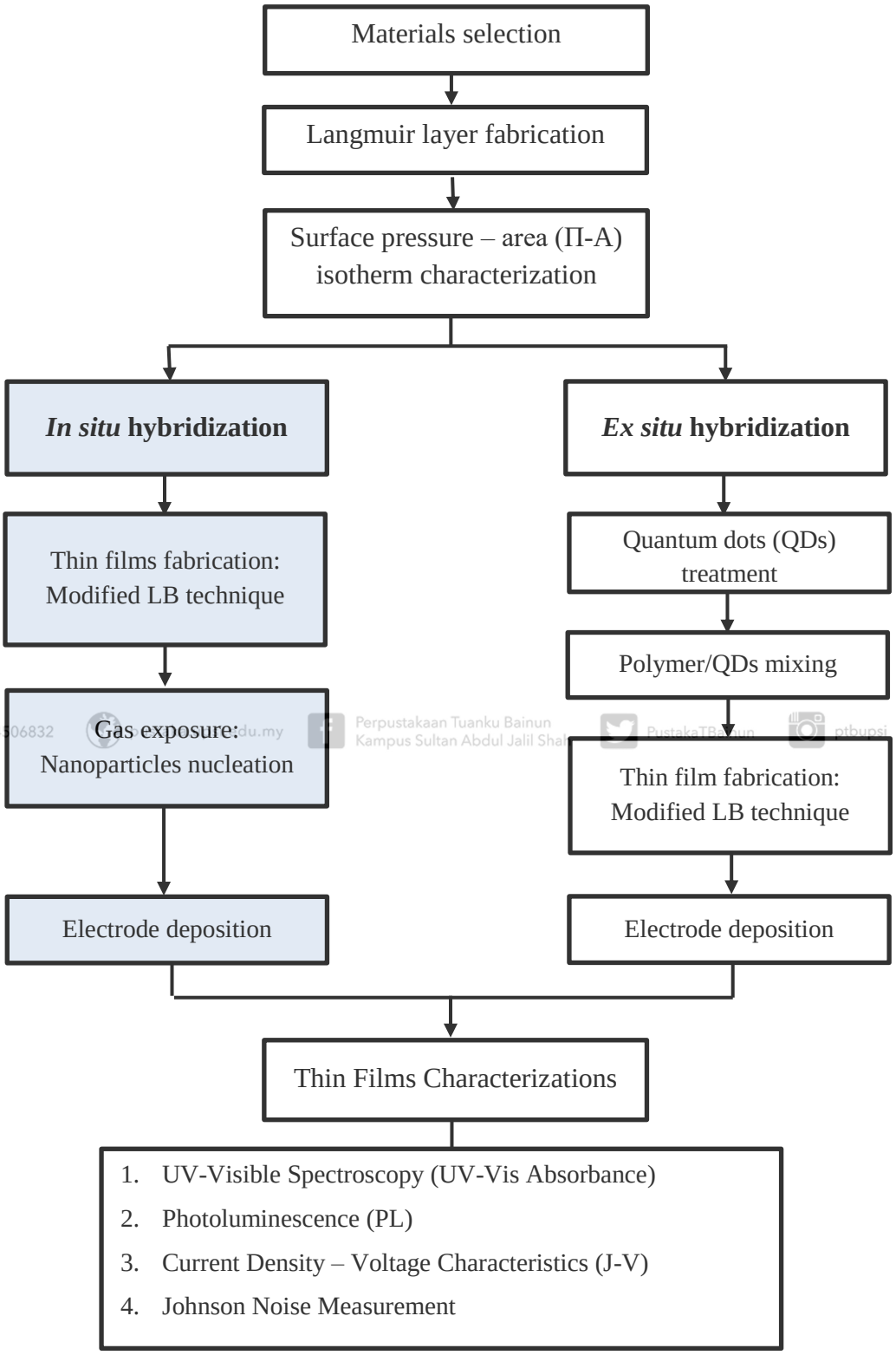


Figure 3.1. Experimental designs for *in situ* and *ex situ* hybridization approaches

05-4506832 pustaka.upsi.edu.my Perpustakaan Tuanku Bainun Kampus Sultan Abdul Jalil Shah PustakaTBainun ptbupsi

05-4506832 pustaka.upsi.edu.my Perpustakaan Tuanku Bainun Kampus Sultan Abdul Jalil Shah PustakaTBainun ptbupsi

3.3 Materials Selection

The most important substance in this study is conjugated polymer that serves as the electrons donor for the nanoparticles. The first consideration of material selection for the conjugated polymer is its optical properties to tailor its intended application as light absorber or light emitter. Poly(3-hyexylthiophene) (P3HT) was chosen because it possesses low energy band gap and relatively strong absorption coefficient, consequently high absorption even in very thin films (Hoppe, 2004). P3HT also has higher hole mobility as compared to poly(phenylene vinylene) (PPV), another material that widely used for solar cells and LED (Hou & Guo, 2012).

Another key material for the thin film fabrication is the nanoparticles. The CdS and CdSe were chosen because of they possess lower Highest Occupied Molecular Orbital (HOMO) and Lowest Unoccupied Molecular Orbital (LUMO) than that of poly(3-hexylthiophene) (Zhou, Eck & Krüger, 2011).

The substrate chosen for this study is Indium Tin Oxide (ITO) coated glass that also acts as an electrode for electrical characterization. Quartz was also used as substrate for optical characterization owing to its low optical noise properties. Detail discussions of all materials used in the study are presented in the following subtopics.

05-4506832 pustaka.upsi.edu.my Perpustakaan Tuanku Bainun Kampus Sultan Abdul Jalil Shah PustakaTBainun ptbupsi

05-4506832 pustaka.upsi.edu.my Perpustakaan Tuanku Bainun Kampus Sultan Abdul Jalil Shah PustakaTBainun ptbupsi

3.3.1. Poly(3-hexylthiphene) (P3HT)

Poly(3-hexylthiophene) or P3HT is a conjugated polymer based on thiophene rings (four carbon atoms and one sulfur) and highly soluble in common organic solvents. Figure 3.2 shows the chemical structure of P3HT. In this study, regioregular P3HT (rr-P3HT) instead of regiorandom P3HT (rra-P3HT) were used since rr-P3HT has higher degree of polymer chain ordering (Tang, Zhao & Zhang, 2011). Moreover, the electrical conductivity of rr-P3HT is greater than rra-P3HT (Sako et al., 2005).

P3HT has high charge-carrier mobility (typical holes mobility, 10^{-4} – 10^{-1}cm^{-2}/Vs), low band-gap energy (1.9 eV) and good self-organization capability (H. J. Wang, Chen & Jeng, 2014). It also has broad absorption spectrum with a maximum around 550 nm. The mobility of P3HT is dependent on orientation of the polymer chains, crystallinity and molecular weight. As compared to other types of conjugated polymer, it has higher environmental stability and structural versatility (Jayaraman, 2012). P3HT (MW: 34,000) purchased from Sigma Aldrich as polymer matrix materials used throughout the research.

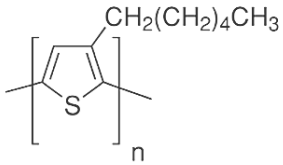


Figure 3.2. Chemical structure of Poly(3-hexylthiophene) (P3HT)

05-4506832 pustaka.upsi.edu.my Perpustakaan Tuanku Bainun Kampus Sultan Abdul Jalil Shah PustakaTBainun ptbupsi

05-4506832 pustaka.upsi.edu.my Perpustakaan Tuanku Bainun Kampus Sultan Abdul Jalil Shah PustakaTBainun ptbupsi

3.3.2 Stearic Acid

Stearic acid is a type of saturated fatty acid that occurs abundantly in natural fat. It is insoluble in water but fairly soluble in chloroform with solubility of 0.5 g/ml and melts at 69.6 ^{o}C (Li & Wu, 2014). Stearic acid is most widely used fatty acid for filler coating. Generally, fatty acids were introduced in the thermoplastic industry as coating agent to improve the melt viscosity, modulus and impact properties of the composite (Petiraksakul, 2000). For the purpose of filler coating, the purity of stearic acid more than 95 % is needed (Markley, 1960).

In this study, stearic acid of 99.9 % purity from Sigma Aldrich was used. Stearic acid possess amphipihilic properties, hence it acts as stabilizer to P3HT because P3HT is a non-amphiphilic material, thus not suitable for LB deposition. Stearic acid mixture will lessen the domination of the hydrophobic part of P3HT, improve the stability and reduce the likelihood of supermonolayer structures formation (Nabok, 2005). It also functioned as caping agent of divalent cation, cadmium ion, into its headgroup structure (COOH). Stearic acid molecular formula is $CH_3(CH_2)_{16}COOH$ and its molecular structure is shown in Figure 3.3.

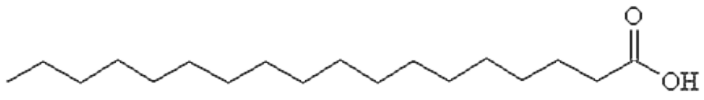


Figure 3.3. Stearic acid skeletal structure, where COOH is the hydrophilic part, and the tail, $CH_3(CH_2)_{16}$ is the hydrophobic part.

05-4506832 pustaka.upsi.edu.my Perpustakaan Tuanku Bainun Kampus Sultan Abdul Jalil Shah PustakaTBainun ptbupsi

05-4506832 pustaka.upsi.edu.my Perpustakaan Tuanku Bainun Kampus Sultan Abdul Jalil Shah PustakaTBainun ptbupsi

3.3.3 Cadmium (II) Chloride

Cadmium is a heavy metal that belongs to group IIb in the periodic table that is silver-white in color. Whilst elemental cadmium is insoluble in water, cadmium chloride ($CdCl_2$) is quite soluble. In water, cadmium can exist as free ions and its mobility is enhanced by low pH, low salinity and high redox potential (Kippler, 2009).

Throughout the experimental work, anhydrous cadmium chloride 99.9 % from Sigma Aldrich has been used. Its molecular weight is 183.32 g/mol. The concentrations used for this study were 0.5 mM and 1.0 mM of $CdCl_2$ in 1.4*l* deionized (DI) water, or 0.1283 g and 0.2566 g respectively. When $CdCl_2$ is mixed into the DI water subphase, it will dissociate into cadmium ion (Cd^{2+}) and chlorine ion (Cl^-). Once stearic acid is dispersed on air/water interface of the subphase, the Cd^{2+} will incorporate with stearic acid's headgroup structure to form cadmium stearate, as shown in following reaction:

$$Cd^{2+} + 2(CH_3(CH_2)_{16}COOH) \rightarrow (CH_3(CH_2)_{16}COO)_2Cd + 2H \qquad (3.1)$$

where, $CH_3(CH_2)_{16}COOH$ is stearic acid and $(CH_3(CH_2)_{16}COO)_2Cd$ is cadmium stearate. Cadmium stearate can also be written as $CdSt_2$. Cadmium stearate will be transferred onto substrate during monolayer deposition. The molecular structure of cadmium stearate is shown in Figure 3.4.

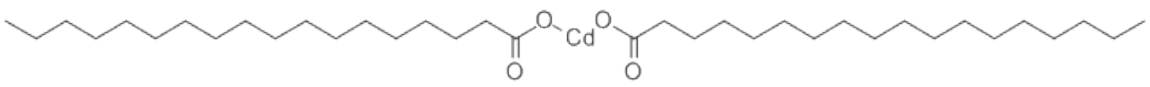


Figure 3.4. Skeletal molecular structure of cadmium stearate (Nabok, 2005)

05-4506832 pustaka.upsi.edu.my Perpustakaan Tuanku Bainun Kampus Sultan Abdul Jalil Shah PustakaTBainun ptbupsi

05-4506832 pustaka.upsi.edu.my Perpustakaan Tuanku Bainun Kampus Sultan Abdul Jalil Shah PustakaTBainun ptbupsi

3.3.4 Quantum Dots

Two types of quantum dots – cadmium sulfide (CdS) and cadmium selenide (CdSe), were employed in this study. Quantum dots (QDs) are artificial nano-structures of semiconductors wherein the charge carriers are confined in all three spatial dimensions (Walther, 2014). Hence it exhibits unique electrical and optical properties, where by simply changing QDs size, its band gap, emission color and absorption spectrum can be tuned (Pisanic, Zhang & T. H. Wang, 2014) making QDs as a potential candidate in wide range of applications such as light-emitting diodes, solar cells and fluorescent tags for biological imaging (Ratnesh & Mehata, 2015).

This research used colloidal QDs, in which CdS and CdSe are held in a liquid suspension (Sigma Aldrich). The size for both types is 5 nm. Before these QDs are incorporated into P3HT, they were treated with hexanoic to remove trioctylphosphine oxide (TOPO) that capped the QDs. TOPO acts as insulating interfacial layers between QDs and polymer and significantly reduce the photocurrent (de Freitas, 2010). The ligands were washed several times with methanol and refluxing them for 15 minutes in hexanoic acid at 115 ^{o}C. The full treatment of the quantum dots are discussed in subsection 3.4.2.

05-4506832 pustaka.upsi.edu.my Perpustakaan Tuanku Bainun Kampus Sultan Abdul Jalil Shah PustakaTBainun ptbupsi

05-4506832 pustaka.upsi.edu.my Perpustakaan Tuanku Bainun Kampus Sultan Abdul Jalil Shah PustakaTBainun ptbupsi

3.3.5 PEDOT:PSS

Poly(3,4-ethylenedioxythiophene):poly(styrenesulfonate) (PEDOT:PSS) is a conducting polymer blend that is commercially available in aqueous dispersions form. PEDOT is a polycation that oxidizes rapidly in air and is insoluble in many common solvents. However, when it is mixed with PSS, PEDOT form colloidal particles that enable it to dissolve in water easily and has excellent stability. The PSS facilitate charge compensation and act as a dispersing agent in the water. Chemical structure of PEDOT:PSS is shown in Figure 3.5. PEDOT:PSS colloid has high electrical conductivity (0.05-10 $S \cdot cm^{-1}$), high visible light transmissivity and good film formation properties (Yoo, J. Kim & J. H. Kim, 2014).

In this research, a thin layer of PEDOT:PSS were spun on the substrate preceding hybrid nanocomposite thin films deposition. The substrates used in this research were indium tin oxide (ITO) coated glass, and quartz for optical spectroscopy purpose. PEDOT:PSS layer helps smoothen the ITO coated glass surface. It also keeps the ITO from diffusing into the deposited thin film, which can lead to creation of trap sites. For optoelectronic device such as photovoltaic, PEDOT:PSS serves as holes transport, to significantly increase its open circuit voltage (Y. Kim, Ballantyne, Nelson & Bradley, 2009). Throughout this study, PEDOT:PSS from Sigma Aldrich (MW: 11,293) has been used. The dispersion was filtered to ensure the solution's concentration consistency.

05-4506832 pustaka.upsi.edu.my Perpustakaan Tuanku Bainun Kampus Sultan Abdul Jalil Shah PustakaTBainun ptbupsi

05-4506832 pustaka.upsi.edu.my Perpustakaan Tuanku Bainun Kampus Sultan Abdul Jalil Shah PustakaTBainun ptbupsi

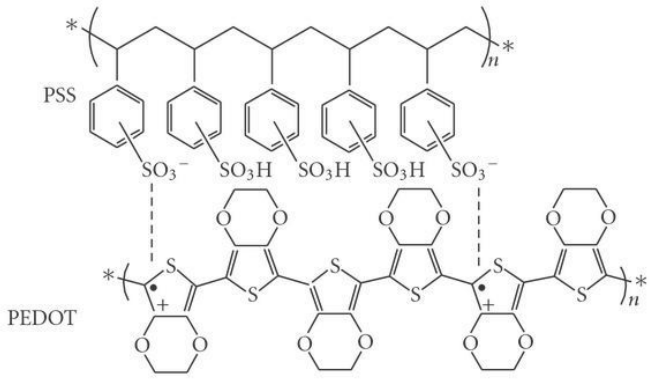


Figure 3.5. Chemical structure of Poly(3,4-ethylenedioxythiophene), and polyelectrolyte, poly(styrenesulfonate), merged as PEDOT:PSS. The "dot'' and "plus'' represent the unpaired electron and positive charge on the PEDOT chain, respectively.

3.3.6 Indium Tin Oxide (ITO) Coated Glass

05-4506832 pustaka.upsi.edu.my Perpustakaan Tuanku Bainun Kampus Sultan Abdul Jalil Shah PustakaTBainun ptbupsi

Indium tin oxide (ITO) is widely used as an anode material, owing to its high electrical conductivity and high transparency. ITO coated glass from Nanocs with a sheet resistance of 5 Ω/sq was employed as substrate. Sequential ultrasonic treatment using chloroform, acetone and propanol was performed to clean the ITO coated glasses. Then, the glasses were rinsed copiously with de-ionized (DI) water. Finally, they were nitrogen dried and kept in vacuumed desiccator and remain clean for few weeks. Generally, ITO films have direct optical bandgap greater than 3.75 eV (Füchsel, Schulz, Kaiser & Tünnermann, 2008).

05-4506832 pustaka.upsi.edu.my Perpustakaan Tuanku Bainun Kampus Sultan Abdul Jalil Shah PustakaTBainun ptbupsi

05-4506832 pustaka.upsi.edu.my Perpustakaan Tuanku Bainun Kampus Sultan Abdul Jalil Shah PustakaTBainun ptbupsi

3.3.7 Quartz

For absorption and luminescence characterization purposes, thin films were also deposited on quartz. The quartz was first cleaned manually by rubbing in water-bath with dishwashing detergent using Nitrile glove and rinsed with de-ionized water. It was then leave overnight in a piranha solution – a mixture of hydrogen peroxide (H_2O_2) and sulfuric acid (H_2SO_4), before rinsed with ultra-pure water supplied by Millipore-RO coupled to a Milli-Q system (resistivity 18.2 MΩ cm) and dried with nitrogen gas.

3.4 Strategy of Nanocomposite Preparation

05-4506832 pustaka.upsi.edu.my Perpustakaan Tuanku Bainun Kampus Sultan Abdul Jalil Shah PustakaTBainun ptbupsi

The first step in hybrid nanocomposite thin film fabrication is substrate preparation. Once the substrates, either ITO coated glass or quartz, has been cleansed as in steps mentioned in subtopics 3.36 and 3.37, PEDOT:PSS solution was spun onto the substrate. Spin coating technique was chosen to coat the substrate because PEDOT:PSS is in aqueous suspension form, hence LB or modified LB thin film deposition technique is not suitable. PEDOT:PSS was filtered using 0.45 µl PVDF filter and then dropped onto the substrates. Spinning were set at 500 rpm (10 s), 1000 rpm (20 s), 4000 rpm (20 s), 2000 rpm (15 s). The film is then annealed for 10 minutes at 120 ^{o}C. The treated substrates were kept in a dark vacuum chamber.

05-4506832 pustaka.upsi.edu.my Perpustakaan Tuanku Bainun Kampus Sultan Abdul Jalil Shah PustakaTBainun ptbupsi

05-4506832 pustaka.upsi.edu.my Perpustakaan Tuanku Bainun Kampus Sultan Abdul Jalil Shah PustakaTBainun ptbupsi

In this research, two approaches were employed to fabricate the hybrid nanocomposite thin film. The first approach is *in situ* hybridization, where nanoparticles are embedded in polymer matrix thin film using gas exposure method. The second approach is *ex situ* hybridization, where ready-made quantum dots and polymer were physically mixed to produce hybrid nanocomposite thin films. The main focus of this research is on *in situ* hybridization, where to the best of our knowledge, it has yet been done elsewhere.

3.4.1 *In situ* Hybridization

In situ hybridization is the main focus of this study, in which nanoparticles were nucleated in the matrix of polymer thin film. Fabrication of hybrid nanocomposite thin films started by preparing Langmuir film on a KSV 2002 System 2 (Helsinki, Finland) trough as shown in Figure 3.6.

The trough was cleaned by wiping it with chloroform, methanol and copious of deionized (DI) water before filling it with DI water (Milli-Q system, resistivity 18.2 MΩ at 25^{o}C) as the subphase. Next, anhydrous cadmium chloride ($CdCl_2$) was added into the sub-phase as a source of Cd^{2+} ion. Two concentrations of $CdCl_2$ 0.5 mM and 1.0 mM were investigated to comprehend its effect towards the phase transformation of Langmuir layer. The ultrapure DI-water as subphase was used as control.

05-4506832 pustaka.upsi.edu.my Perpustakaan Tuanku Bainun Kampus Sultan Abdul Jalil Shah PustakaTBainun ptbupsi

05-4506832 pustaka.upsi.edu.my Perpustakaan Tuanku Bainun Kampus Sultan Abdul Jalil Shah PustakaTBainun ptbupsi

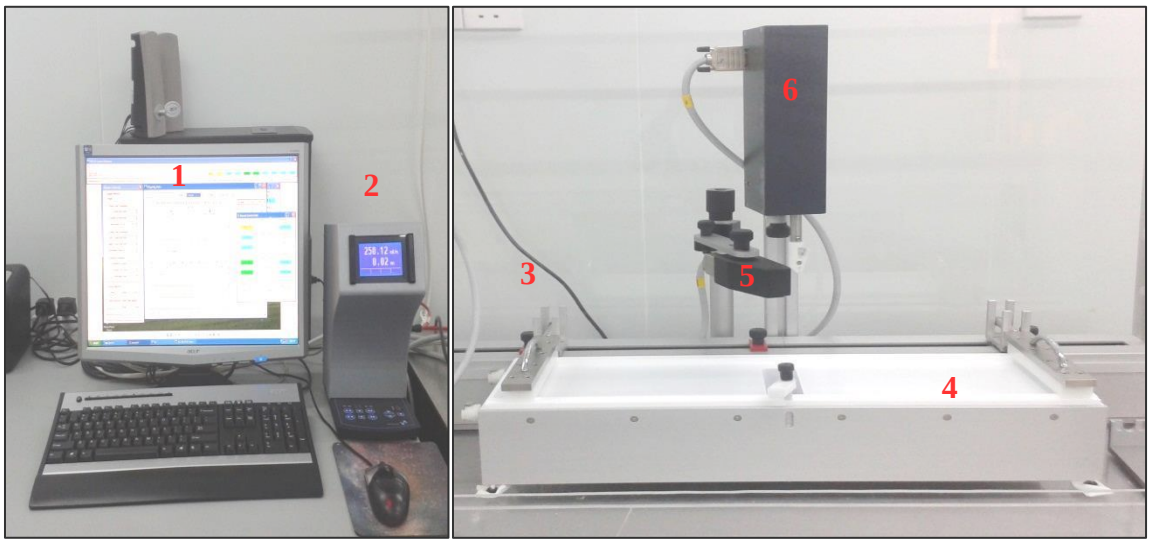


Figure 3.6. In house Langmuir KSV 2002 System 2 apparatus (1) Computer (2) Interface unit (3) Movable barrier (4) Trough (5) Pressure sensor (6) Dipping mechanism

05-4506832 pustaka.upsi.edu.my Perpustakaan Tuanku Bainun Kampus Sultan Abdul Jalil Shah PustakaTBainun ptbupsi

Three types of Langmuir layer were formed. The first was P3HT layer, where 400µl P3HT in chloroform were dispensed on the subphase and compressed. The concentration of P3HT solution was 0.2 mg/ml. The second was stearic acid layer with concentration of 0.14 mg/ml. Two different volumes, 100 µl and 600 µl were dispensed as to compare their isotherm graphs. The third was by dispensing P3HT solution and stearic acid solution on the same subphase. The volume of stearic acid was fixed at 100 µl, whilst the volumes of P3HT were varied at 100 µl, 200 µl, 300 µl or 400 µl. The P3HT:stearic acid layers were compressed on the water subphase only, except for 400 µl P3HT mixed with 100 µl stearic acid, where the layers were also tested on $CdCl_2$ contained subphases.

Chloroform was chosen as solvent for both P3HT and stearic acid due to its volatility characteristic, relatively unreactive, and miscibility with most organic liquid.

05-4506832 pustaka.upsi.edu.my Perpustakaan Tuanku Bainun Kampus Sultan Abdul Jalil Shah PustakaTBainun ptbupsi

05-4506832 pustaka.upsi.edu.my Perpustakaan Tuanku Bainun Kampus Sultan Abdul Jalil Shah PustakaTBainun ptbupsi

After the solutions were spread, the chloroform was allowed to evaporate for 15 minutes prior to barrier compression. Then, the film area was compressed with one barrier at speed 10 mm/min.

The surface pressure changes during compression were recorded by a computer connected to a sensor attached to a chromatography paper. The Langmuir layer profiles were portrayed by isotherm graphs. The new deposition method known as modified Langmuir-Blodgett has been employed to deposit the Langmuir layer. This technique is different from traditional LB and LS, in which modified LB method utilized angle in depositing thin films onto substrate. Another striking different is after every depositions, heat treatment is performed to initialize the polymerization of the film. This approach overcomes the problem imposed by the high molecular weight of the long-chain polymer when using the common LB or LS method.

The films were deposited by carefully touching one edge of substrate onto floating film surface at an angle of 45^{o}, and slowly dropping it on the solid monolayer before lifting the substrate again by raising it the same manner it was dropped. The deposition was done at a constant surface pressure, 27 mN/m. The transferred layers were then dried by hot air ($50^{o}C$) for 15 s to ensure it is completely dry and to induce polymerization before the next layer is deposited. For all samples, thirteen layers of film were deposited. The modified LB technique allows us to construct large-area polymeric thin films, and at the same time control the polymer ordering. Illustration of modified LB technique is presented in Figure

05-4506832 pustaka.upsi.edu.my Perpustakaan Tuanku Bainun Kampus Sultan Abdul Jalil Shah PustakaTBainun ptbupsi

05-4506832 pustaka.upsi.edu.my Perpustakaan Tuanku Bainun Kampus Sultan Abdul Jalil Shah PustakaTBainun ptbupsi

3.7. Whilst Figure 3.8 shows a region of lack of materials after depositing the first layer of floating polymer onto substrate.

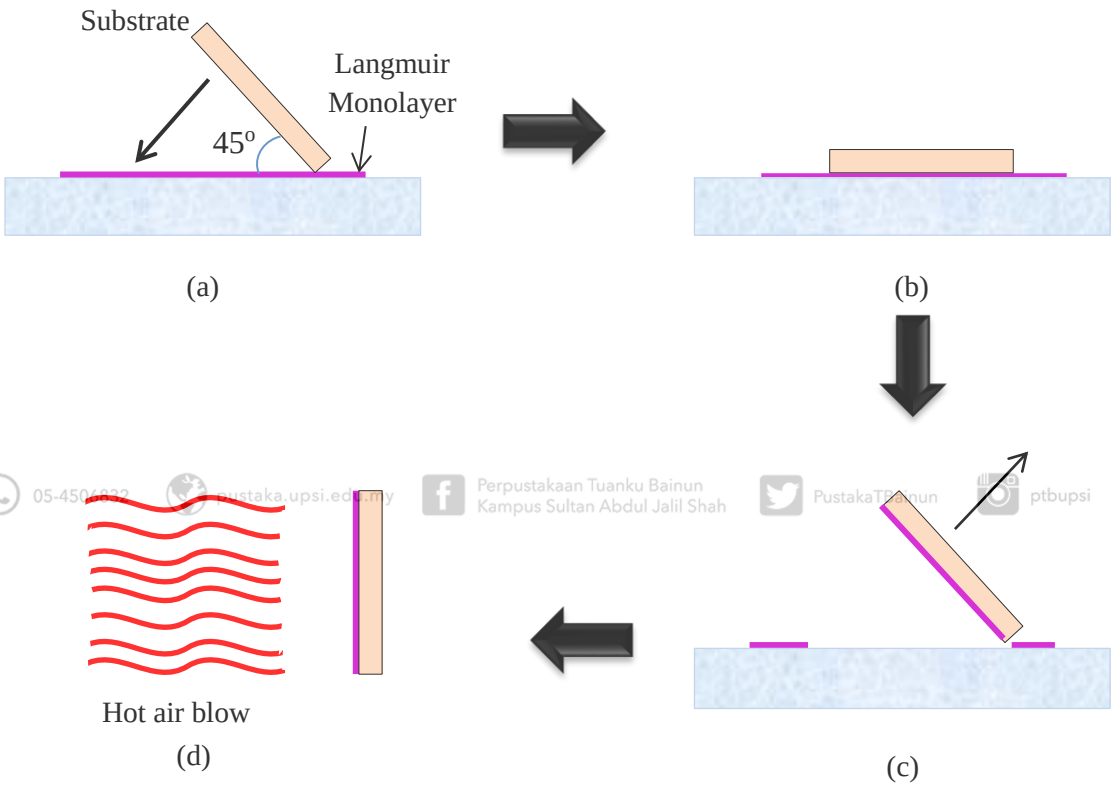


Figure 3.7. Schematic illustration of modified LB technique

05-4506832 pustaka.upsi.edu.my Perpustakaan Tuanku Bainun Kampus Sultan Abdul Jalil Shah PustakaTBainun ptbupsi

05-4506832 pustaka.upsi.edu.my Perpustakaan Tuanku Bainun Kampus Sultan Abdul Jalil Shah PustakaTBainun ptbupsi

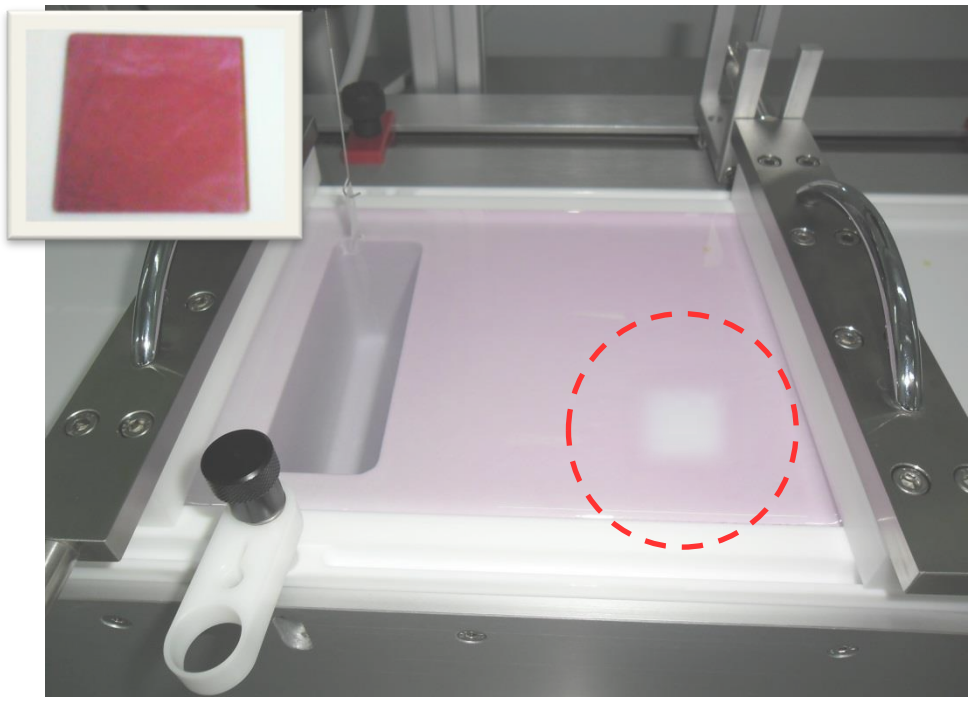


Figure 3.8. Lack of material region of Langmuir film of P3HT at solid phase after first deposition. Insert is the thin films deposited on substrate

05-4506832 pustaka.upsi.edu.my Perpustakaan Tuanku Bainun Kampus Sultan Abdul Jalil Shah PustakaTBainun ptbupsi

After the last deposition, the film was exposed to hydrogen sulfide (H_2S), or hydrogen selenide (H_2Se) gas environment to embed CdS or CdSe nanoparticles in between polymer layers (Figure 3.9).

H_2S and H_2Se gas were produced from acidification of salt process – by adding 20g of iron (II) sulfide (FeS) or iron (II) selenide (FeSe) into 10 ml hydrochloric acid (HCl) in a sealed glass reaction vessel. The reactions are as follow:

$$FeS + 2HCl \rightarrow FeCl_2 + H_2S \quad (3.2)$$

$$FeSe + 2HCl \rightarrow FeCl_2 + H_2Se \quad (3.3)$$

05-4506832 pustaka.upsi.edu.my Perpustakaan Tuanku Bainun Kampus Sultan Abdul Jalil Shah PustakaTBainun ptbupsi

05-4506832 pustaka.upsi.edu.my Perpustakaan Tuanku Bainun Kampus Sultan Abdul Jalil Shah PustakaTBainun ptbupsi



Figure 3.9. Samples are exposed to H_2S or H_2Se gas in a sealed reaction vessel

The exposure time were varied among the samples as to investigate the effect of exposure time to absorbance, luminescence and its electrical properties. Time variation was 0 hour (before gas exposure), 2 hours, 4 hours and 6 hours. After the films were exposed to the said gases, they were annealed at 120^{o}C for 10 minutes. For samples that will be tested for electrical characteristics, 150 nm of aluminum layer serves as electrode was deposited using vacuum thermal evaporator.

3.4.2 *Ex situ* Hybridization

Samples prepared for *ex situ* hybridization still utilizing modified Langmuir-Blodgett method. The difference as compared to *in situ* hybridization is the pre-made quantum dots

05-4506832 pustaka.upsi.edu.my Perpustakaan Tuanku Bainun Kampus Sultan Abdul Jalil Shah PustakaTBainun ptbupsi

05-4506832 pustaka.upsi.edu.my Perpustakaan Tuanku Bainun Kampus Sultan Abdul Jalil Shah PustakaTBainun ptbupsi

are incorporated into the polymer solution instead of producing them. The steps of hybrid nanocomposite thin films for *ex situ* method are explained in the next paragraphs.

The P3HT solutions were prepared by mixing the polymer with chloroform to produce solution of concentration 0.2 mg/ml. Then, CdS or CdSe QDs that have been treated were added into P3HT solution. The QDs were added at 25 wt% or 50 wt% of P3HT, yielding 4 different solutions. QDs was treated to remove ligand that capping it. Similar process was performed by Zhou et. al (2011) to remove ligand from CdSe QD for photovoltaic application. Figure 3.10 (a) – (d) shows the ligand removal process.

The treatment of CdS QDs or CdSe QDs started by adding 432 µl QDs in toluene into 6 ml of hot hexanoic acid (105 ºC) and stirred for 10 minutes. This procedure was done in oil bath placed on a hot plate. Then 12 ml of methanol were added. The hot solution was then centrifuged for 10 minutes at 3000 rpm, causing the QDs to precipitate. The solution was brought back to heat in an oil bath until it reached 90 ºC before adding 1 ml chloroform and 3 ml methanol. After 5 minutes, the mixture was centrifuge at 3000 rpm for 10 minutes to recover the QDs. Then the QDs were dispersed into P3HTsolution. The treatment resulted in 2 mg QDs.

05-4506832 pustaka.upsi.edu.my Perpustakaan Tuanku Bainun Kampus Sultan Abdul Jalil Shah PustakaTBainun ptbupsi

05-4506832 pustaka.upsi.edu.my Perpustakaan Tuanku Bainun Kampus Sultan Abdul Jalil Shah PustakaTBainun ptbupsi

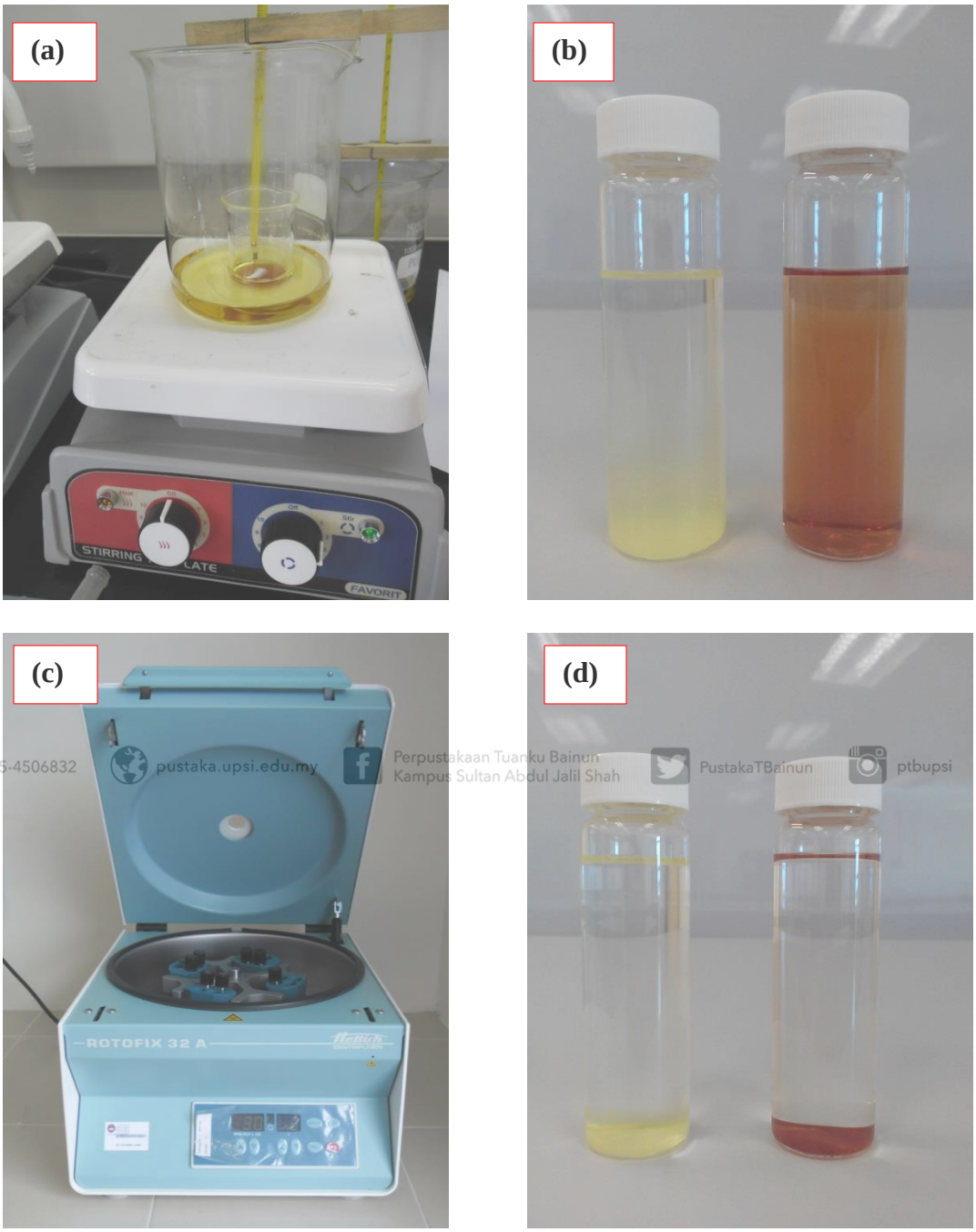


Figure 3.10. The ligand removing process: (a) 432 µl of QDs in toluene was added into 6 ml hexanoic acid in hot oil bath. (b) Hot solution before centrifuge. The yellowish liquid contains CdS QDs while the maroon liquid contains CdSe QDs. (c) Centrifuge at 3000 rpm. (d) Precipitated QDs after centrifuging process

05-4506832 pustaka.upsi.edu.my Perpustakaan Tuanku Bainun Kampus Sultan Abdul Jalil Shah PustakaTBainun ptbupsi

05-4506832 pustaka.upsi.edu.my Perpustakaan Tuanku Bainun Kampus Sultan Abdul Jalil Shah PustakaTBainun ptbupsi

The fabrication still using the same trough, and cleansed using the same method as descirbed in *in situ* hybridization procedure. The subphase is ultra-pure DI water only. 700 µl solution of P3HT mixed with treated QDs dropped onto subphase using glass syringe. Chloroform was allowed to evaporate for 15 minutes, before the barrier started to compress the floating layer.

Once the Langmuir layer reached solid phase at 17 mN/m, the layer were transferred onto substrate using modified LB technique; the same manner described in Section 3.4.1. After every deposition the transferred layers were dried using hot air for 15 s. After thirteen layers of film were deposited, the films were annealed at 120 ^{o}C for 10 minutes.

05-4506832 pustaka.upsi.edu.my Perpustakaan Tuanku Bainun Kampus Sultan Abdul Jalil Shah PustakaTBainun ptbupsi

3.5 Aluminum Thermal Evaporation

Aluminum electrodes were deposited on the samples fabricated on ITO coated glass substrate by using thermal evaporation technique. The size of each aluminum finger is 2.0 cm ×0.2 cm. Figure 3.11 (a) shows the thermal evaporator used and Figure 3.11 (b) shows a sample of thin film coated with aluminum fingers.

05-4506832 pustaka.upsi.edu.my Perpustakaan Tuanku Bainun Kampus Sultan Abdul Jalil Shah PustakaTBainun ptbupsi

05-4506832 pustaka.upsi.edu.my Perpustakaan Tuanku Bainun Kampus Sultan Abdul Jalil Shah PustakaTBainun ptbupsi

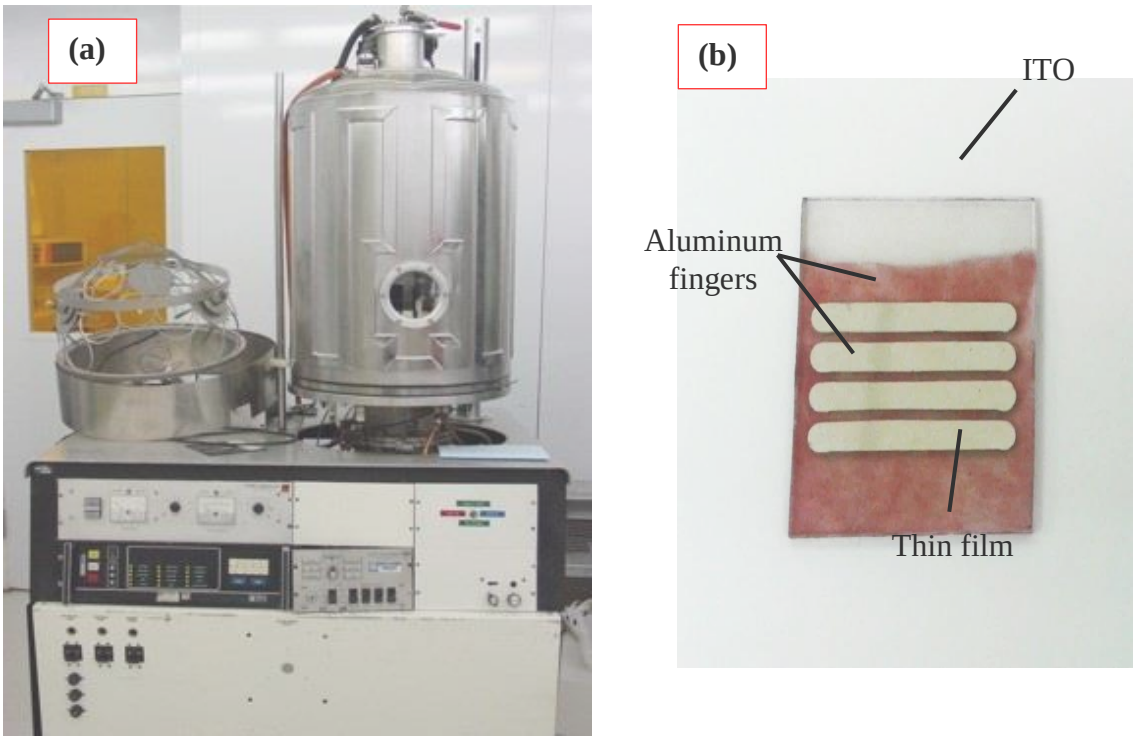


Figure 3.11. (a) Vacuum thermal evaporator used for aluminum coating. (b) Aluminum fingers on thin films deposited on ITO coated glass

05-4506832 pustaka.upsi.edu.my Perpustakaan Tuanku Bainun Kampus Sultan Abdul Jalil Shah PustakaTBainun ptbupsi

3.6 Characterization Methods

3.6.1 Surface Pressure-Area (Π-A) Isotherm

Before thin film is deposited onto substrate, the Langmuir layer was characterized. The information retrieved from the characterization serve as parameters for deposition. Langmuir films were studied by analyzing its surface pressure-area (Π-A) isotherm graph at constant temperature, 25 ^{o}C.

05-4506832 pustaka.upsi.edu.my Perpustakaan Tuanku Bainun Kampus Sultan Abdul Jalil Shah PustakaTBainun ptbupsi

05-4506832 pustaka.upsi.edu.my Perpustakaan Tuanku Bainun Kampus Sultan Abdul Jalil Shah PustakaTBainun ptbupsi

Formation of Langmuir layer was done by spreading pristine P3HT, pristine stearic acid, P3HT mixed with stearic acid, or P3HT mixed with quantum dots solution over the subphase of LB trough. Once the solvent evaporated, the barrier intercepting the subphase surface was moved as to compress the surface film. The compression causing the surface pressure to increase, the layer goes through phase transformation. The transformation is analogous to gas-liquid-solid phase as discussed in Chapter 2. The effect of $CdCl_2$ and solutions' volume toward the layer's phase transformation were recorded. The thin films were deposited at a pressure when the layer reached solid phase. This is the phase where the Langmuir layer is closed-pack and behaves like 2-dimensional solid.

3.6.2 UV-Vis Spectroscopy

05-4506832 pustaka.upsi.edu.my Perpustakaan Tuanku Bainun Kampus Sultan Abdul Jalil Shah PustakaTBainun ptbupsi

Ultraviolet-visible (UV-Vis) spectroscopy is one of the experimental techniques used to investigate the optical and electronic properties of the conjugated system. Generally, it corresponds to electronic excitations between the energy level where electrons are excited from the HOMO to LUMO when the incident photons contain energy that matches electronic transition within the sample, *S*:

$$S + h\nu = S^* \qquad (3.4)$$

where, $h\nu$ is the photon energy and S^* is short-lived electronically excited molecule. The relaxation process of the excited molecules causing it to return to its ground state within 10^{-8} to 10^{-9} s. The relaxation usually converting the excitation energy to heat. The change in electronic energy is accompanied with corresponding changes in vibrational energy and

05-4506832 pustaka.upsi.edu.my Perpustakaan Tuanku Bainun Kampus Sultan Abdul Jalil Shah PustakaTBainun ptbupsi

05-4506832 pustaka.upsi.edu.my Perpustakaan Tuanku Bainun Kampus Sultan Abdul Jalil Shah PustakaTBainun ptbupsi

rotational energy causing the absorption spectrum obtained is broad, smooth and not very sharp.

The electronic transition can be expressed mathematically as below:

$$\Delta E = hv \qquad (3.5)$$

$$\Delta E = h\frac{c}{\lambda} \qquad (3.6)$$

where ΔE is the energy absorbed in electronic transition from HOMO to LUMO, h is Planck's constant, v is frequency, c is velocity of light and λ is wavelength. The position of the absorption peak depends on the energy difference. The larger the energy difference, the higher its absorption frequency, hence the lower the wavelength.

05-4506832 pustaka.upsi.edu.my Perpustakaan Tuanku Bainun Kampus Sultan Abdul Jalil Shah PustakaTBainun ptbupsi

The absorbance (A) at a specific wavelength, λ can be calculated using:

$$A = -log\left(\frac{I}{I_o}\right) \qquad (3.7)$$

where I_o and I are the intensity of the incident and transmitted light, respectively, as illustrated in Figure 3.12.

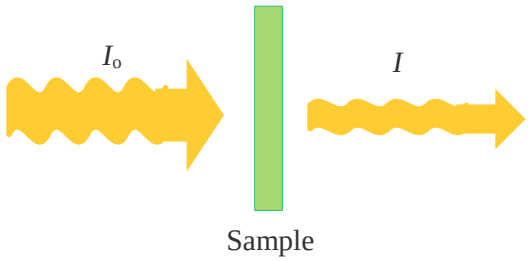


Figure 3.12. Illustration of absorption when light passes through a sample

05-4506832 pustaka.upsi.edu.my Perpustakaan Tuanku Bainun Kampus Sultan Abdul Jalil Shah PustakaTBainun ptbupsi

05-4506832 pustaka.upsi.edu.my Perpustakaan Tuanku Bainun Kampus Sultan Abdul Jalil Shah PustakaTBainun ptbupsi

The spectrophotometer consists of three main components, namely the source, the dispersive system and a detector. The compartment for sample is placed in the optical path, either before or after the dispersive system. Two types of light source are used in the measurement: a medium pressure deuterium arc lamp to measure wavelengths shorter than 350 nm, and an incandescent lamp made from a tungsten filament to measure wavelengths longer than 350 nm. Usually the tungsten lamp has very long life time as compared to the deuterium lamp. The light signal passes the sample to reach the detectors which converts the light signal into an electrical signal.

Two types of detectors commonly used in UV-Vis spectrophotometers are photomultiplier and photodiode array detector. The photomultiplier detector amplifies the signal for low radiant power measurement. It has relatively good sensitivity over the UV-visible spectrum and at low light levels, and has low noise. On the other hand, noise level photodiode array detector is large because the amount of light is small.

Generally, photodiodes array detector is a series of individual diode positioned side by side, detecting light that dispersed by a diffraction grating. The recorded spectra are then treated by using computer algorithm and meaningful data are displayed. The absorption spectral measurements represented in this thesis were performed predominantly using JASCO V570 UV-Vis (Ultraviolet-visible) spectrophotometer operated at a resolution of 1 nm (Figure 3.13).

05-4506832 pustaka.upsi.edu.my Perpustakaan Tuanku Bainun Kampus Sultan Abdul Jalil Shah PustakaTBainun ptbupsi

05-4506832 pustaka.upsi.edu.my Perpustakaan Tuanku Bainun Kampus Sultan Abdul Jalil Shah PustakaTBainun ptbupsi



Figure 3.13. In-house UV-Vis spectrophotometer

05-4506832 pustaka.upsi.edu.my Perpustakaan Tuanku Bainun Kampus Sultan Abdul Jalil Shah PustakaTBainun ptbupsi

3.6.3 Photoluminescence (PL) Measurement

Photoluminescence (PL) in solid is a phenomenon where the electronic states of molecular orbital are excited by light and the excitation energy is also released as light. During the spectroscopy process, monochromatic light that has greater energy than the sample's bandgap is directed onto the sample surface. The photons were absorbed by the sample creating electron-hole pairs called excitons. The electrons are excited to LUMO and then lose part of their energy. It resulted in photons emission, and this spectrum is studied in PL. The spectrum provides information on energy states that are present in the sample.

Photoluminescence is a nondestructive method to measure the effective lifetime of a material by absorbing and re-radiating photons. Hence, we are able to probe the ability

05-4506832 pustaka.upsi.edu.my Perpustakaan Tuanku Bainun Kampus Sultan Abdul Jalil Shah PustakaTBainun ptbupsi

05-4506832 pustaka.upsi.edu.my Perpustakaan Tuanku Bainun Kampus Sultan Abdul Jalil Shah PustakaTBainun ptbupsi

of transferring electrons within the polymer matrix to the nanoparticles or quantum dots (Jain, 2001).

In this study, Perkin Elmer LS 55 Fluorescence Spectroscopy was used to study the PL characteristic of the samples (Figure 3.14). The samples were excited at 430 nm and the excitation slit was set at 10 nm, whilst the laser emission slit was 15 nm. Scan speed was 500 nm/min. The parameters were determined by optimizing the value of a reference sample.

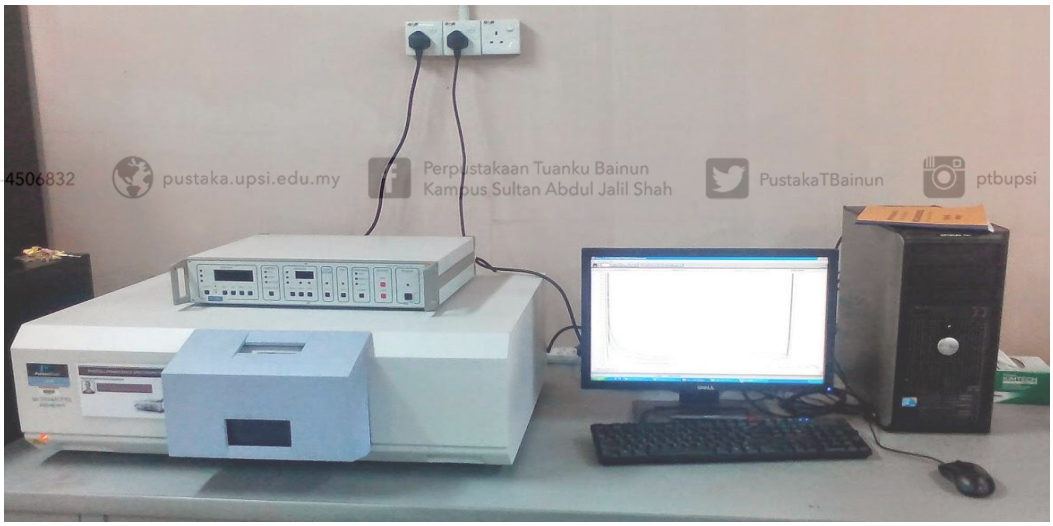


Figure 3.14. Fluorescence Spectroscopy for photoluminescence analysis

3.6.4 Current Density-Voltage (J-V) Measurement

Current density-Voltage (J-V) characteristics measurement was carried out using Keithley 2636A source measure unit (SMU) attached to a 4-point probe and a solar simulator as

05-4506832 pustaka.upsi.edu.my Perpustakaan Tuanku Bainun Kampus Sultan Abdul Jalil Shah PustakaTBainun ptbupsi

05-4506832 pustaka.upsi.edu.my Perpustakaan Tuanku Bainun Kampus Sultan Abdul Jalil Shah PustakaTBainun ptbupsi

shown in Figure 3.15. The Keithley unit is capable of supplying voltage to the device under test (DUT) in the range of 1μV to 200V and simultaneously measures current flowing through it from 1 fA to 50 A. The 4-point probe is used to measure the resistivity or conductivity of any semiconductor materials. It is also attached with special designed 2-point probe.

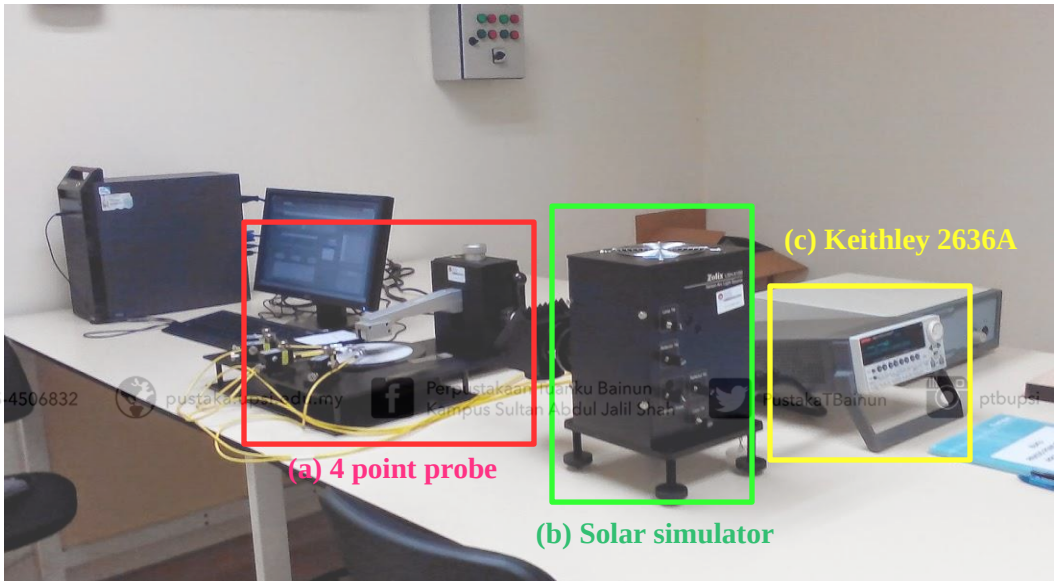


Figure 3.15. In-house computerized J-V measurement equipment consists of (a) four-point probe, (b) solar simulator, (c) Keithley 2636A source measure unit

Solar simulator is a light source that simulates solar radiation. Since solar radiation changes due to several factors such as solar angle at particular time of the year, and atmospheric condition, a standard spectrum have been developed based on the effects. The pathlength of solar radiation through the Earth's atmosphere is called air mass (AM). When the sun is overhead, the solar zenith angle is zero, the global radiation is called "Air Mass 1 Global" (AM 1G) radiation. "Air Mass 0" spectrum is for the radiation passes through no

05-4506832 pustaka.upsi.edu.my Perpustakaan Tuanku Bainun Kampus Sultan Abdul Jalil Shah PustakaTBainun ptbupsi

05-4506832 pustaka.upsi.edu.my Perpustakaan Tuanku Bainun Kampus Sultan Abdul Jalil Shah PustakaTBainun ptbupsi

air mass at extraterrestrial. Solar simulator generally applying AM 1.5 G spectrum, in which the light going through 1.5 atmosphere, corresponding to zenith angle of 48.2°.

Current density-voltage measurement was carried out to investigate the thin films' electrical properties, and to weigh the possibility to adopt it in electronic devices. The measurement was done by connecting Indium Tin Oxide (ITO) to positive electrode and aluminum (Al) to the negative. The schematic of the measurement's connection mimicking photovoltaic device as shown in Figure 3.16. The currents were measure in dark and under solar simulator illumination by continuously sweeping the feed voltage from -1.5 to +1.5 V. The measurements under illumination were done using solar simulator with light density of 100 mW/cm^2 and complies with AM 1.5G spectrum

05-4506832 pustaka.upsi.edu.my Perpustakaan Tuanku Bainun Kampus Sultan Abdul Jalil Shah PustakaTBainun ptbupsi

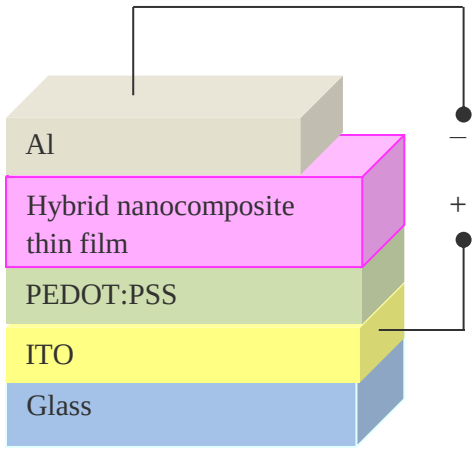


Figure 3.16. Electrical connection schematic of thin film for current J-V measurement where ITO acts as anode and Aluminum layer acts as cathode

05-4506832 pustaka.upsi.edu.my Perpustakaan Tuanku Bainun Kampus Sultan Abdul Jalil Shah PustakaTBainun ptbupsi

05-4506832 pustaka.upsi.edu.my Perpustakaan Tuanku Bainun Kampus Sultan Abdul Jalil Shah PustakaTBainun ptbupsi

3.6.5 Johnson Noise Measurement

There are many types of electrical noise exists in electronic devices such as Johnson noise, generation-combination noise and $1/f$ noise. Johnson noise, also known as thermal noise stems from the random thermal motion of electrons in a material that produce fluctuating electromotive force (emf) at it ends (Darabi, 2015). Every time the electrons are scattered, its velocity is randomized with more electrons moving in a certain direction, causing a small net current flow. This noise increases with resistance and temperature of the material.

The theory of Johnson noise has been explained by Nyquist in 1928 (Johnson, 1928; Nyquist, 1928). The Johnson-Nyquist formula states that

$$S_V(f) = 4RhfN(f,T) \quad (3.8)$$

05-4506832 pustaka.upsi.edu.my Perpustakaan Tuanku Bainun Kampus Sultan Abdul Jalil Shah PustakaTBainun ptbupsi

where $S_V(f)$ is the power spectral density (PSD) of the voltage noise, R is the resistance, h is Planck constant and f is the frequency. $N(f,T)$ is Planck number representing the energy quanta hf, at frequency f and temperature, T. Or mathematically,

$$N(f,T) = kT/hf \quad (3.9)$$

where k is Boltzmann constant. Hence, the noise voltage power spectral density under open-circuit condition is given by

$$S_V(f) = 4kTR \quad (3.10)$$

Alternatively, the noise current power spectral density can be calculated using

$$S_I(f) = 4k\,T/R \quad (3.10)$$

05-4506832 pustaka.upsi.edu.my Perpustakaan Tuanku Bainun Kampus Sultan Abdul Jalil Shah PustakaTBainun ptbupsi

05-4506832 pustaka.upsi.edu.my Perpustakaan Tuanku Bainun Kampus Sultan Abdul Jalil Shah PustakaTBainun ptbupsi

Rocha et al. (2013) has applied the noise measurement to organic materials that has offers insight on degradation mechanism in Organic Light Emitting Diode (OLED). The result is in parallel with earlier study by Carbone research group (Carbone, Kotowska & Kotowski, 2005) and Ke research group (Ke, Zhao, Kumar & Chua, 2008) that reported the low frequency noise relies upon the intrinsic transport mechanism. Johnson noise is analyzed using low-frequency electrical noise measurement (LFeNM). It is a technique often used as a diagnostic tool for determining the reliability of electronic devices (von Haartman & Östling, 2007).

The measurement requires a setup comprise of a low noise biasing circuit, amplifier system (5182 Current Preamplifier, Signal Discovery), 35670A Dynamic Signal Analyzer (DSA, Agilent) and a double metal shield box to shield the measurement from external interference. The experiment setup is as shown in Figure 3.17. The noise measured from DUT was feed to amplifier system, where it will convert the current power (A^2) to voltage power (V^2). The output from amplifier will then become the input of DSA and displayed. The measurement was done from 10 Hz to 1 kHz. The averaging of each measurement is 200.

05-4506832 pustaka.upsi.edu.my Perpustakaan Tuanku Bainun Kampus Sultan Abdul Jalil Shah PustakaTBainun ptbupsi

05-4506832 pustaka.upsi.edu.my Perpustakaan Tuanku Bainun Kampus Sultan Abdul Jalil Shah PustakaTBainun ptbupsi

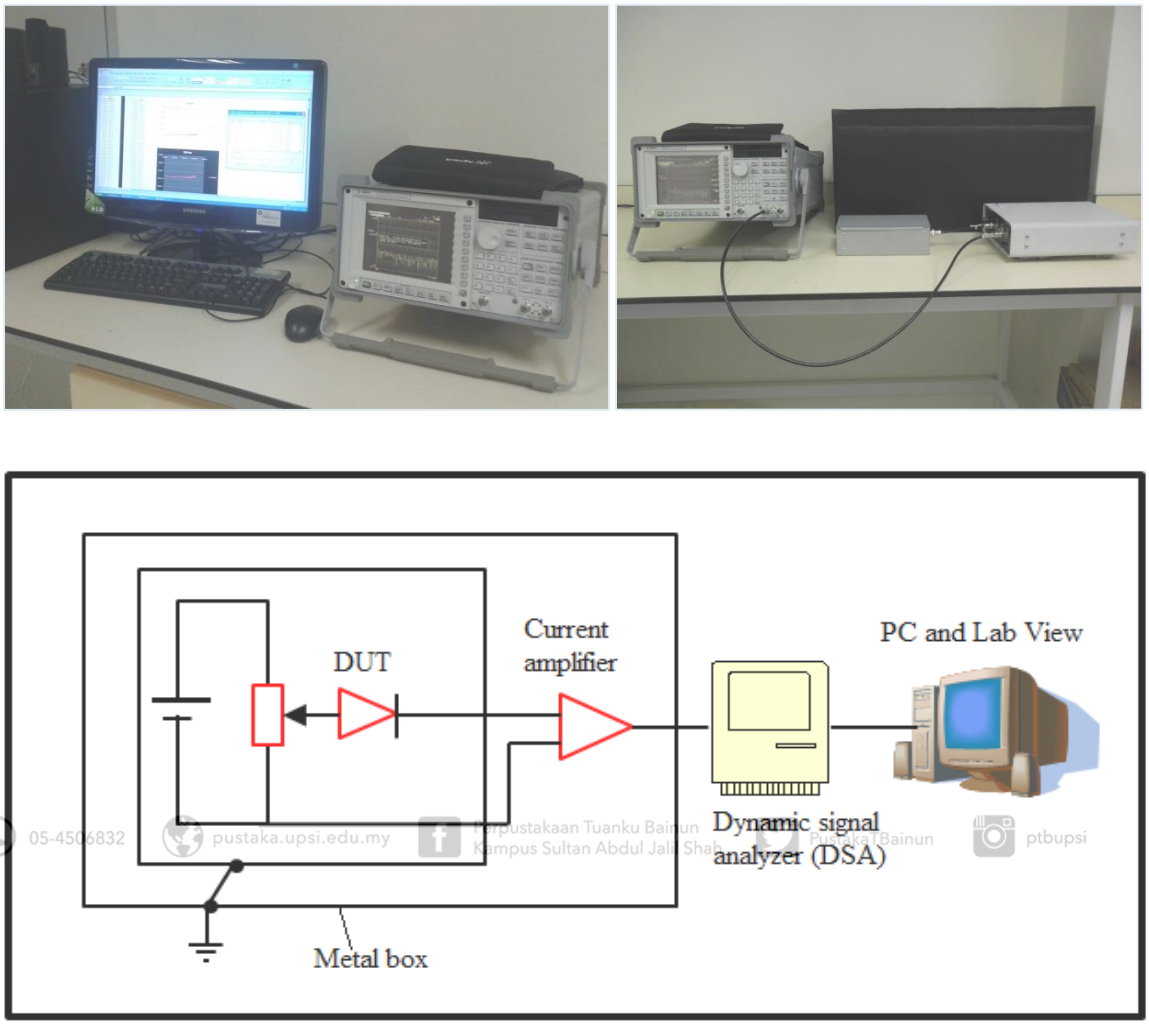


Figure 3.17. LFeNM experimental setup and the schematic diagram

3.7 Conclusion

Chapter 3 discussed the details of experimental design, set up, and process of study for this thesis. The critical parameters used to fabricate the thin films and its characterizations were also declared. The equipment involved is presented, and was operated by author herself. The results for characterization and optimization are discussed in Chapter 4.

05-4506832 pustaka.upsi.edu.my Perpustakaan Tuanku Bainun Kampus Sultan Abdul Jalil Shah PustakaTBainun ptbupsi

05-4506832 pustaka.upsi.edu.my Perpustakaan Tuanku Bainun Kampus Sultan Abdul Jalil Shah PustakaTBainun ptbupsi

CHAPTER 4

RESULTS AND DISCUSSION

05-4506832 pustaka.upsi.edu.my Perpustakaan Tuanku Bainun Kampus Sultan Abdul Jalil Shah PustakaTBainun ptbupsi

4.1 Introduction

This chapter is dedicated to present and discuss the properties of Langmuir layer and the fabricated thin films. The results were presented according to objectives sequence. The surface pressure - area isotherm of Langmuir layers for P3HT, stearic acid, P3HT mixed with stearic acid, and P3HT mixed with quantum dots are explained. The optical properties of nanocomposite thin films were characterized using UV-Vis spectrophotometer and photoluminescence spectroscopy. The effects of nanoparticle formation by gas exposure technique and quantum dots weight percentage towards thin films' electrical properties are clarified. Finally, the Johnson noise of the thin films is discussed.

05-4506832 pustaka.upsi.edu.my Perpustakaan Tuanku Bainun Kampus Sultan Abdul Jalil Shah PustakaTBainun ptbupsi

05-4506832 pustaka.upsi.edu.my Perpustakaan Tuanku Bainun Kampus Sultan Abdul Jalil Shah PustakaTBainun ptbupsi

4.2 Surface Pressure–Area (Π-A) Isotherm

Surface pressure-area (Π-A) isotherm graph provides information on the phase transformation of Langmuir monolayer, and enable us to measure the dependency of surface pressure (Π) on the mean molecular area per molecule (A). It also allows us to comprehend the manner of organic molecules arrangement, structure and their characteristics at the air-water interface (Özbek et al., 2011). In this study, Π-A isotherm graphs were achieved by closing the LB barrier very slowly at a constant horizontal speed of 12 mm/min, at constant temperature of 25 ^{o}C. The barrier closure will decrease the trough area, consequently reorganizing the molecules arrangement on the surface of subphase.

05-4506832 pustaka.upsi.edu.my Perpustakaan Tuanku Bainun Kampus Sultan Abdul Jalil Shah PustakaTBainun ptbupsi

4.2.1 *In situ* Hybridization

The Π-A isotherm graph of pristine stearic acid of concentration 0.14 mg/ml with different spreading volume are shown in Figure 4.1. Throughout this study, 100 µl stearic acid (SA) were spread on water subphase using the technique mentioned in Section 3.41. However, the full phase transformations of the said volume could not be discerned from the isotherm graph due to the limitation of stearic acid molecules' quantity. In order to observe the complete phase transformation of the stearic acid monolayer, the spreading volume was increase to 600 µl.

05-4506832 pustaka.upsi.edu.my Perpustakaan Tuanku Bainun Kampus Sultan Abdul Jalil Shah PustakaTBainun ptbupsi

05-4506832 pustaka.upsi.edu.my Perpustakaan Tuanku Bainun Kampus Sultan Abdul Jalil Shah PustakaTBainun ptbupsi

The monolayer behavior of the pristine stearic acid (600 µl) shows a distinct gas-liquid-solid phase development. The Π-A isotherm graphs are denoted with roman number, where (i) is gas phase, (ii) is liquid phase, (iii) is solid phase and (iv) is collapse phase. Liquid-solid phase transition occurs at a surface pressure 24 mN/m and collapsed at 42 mN/m. By extrapolating the solid phase linear section of the graph, it was found that a stearic acid molecule occupied at a molecular area (A_o) of approximately 20.5 $Å^2$/molecule. This result is comparable to the established data in literatures (Petty, 1996; Sudheesh, Ahmad & Singh, 2012; Gew & Misran, 2014).

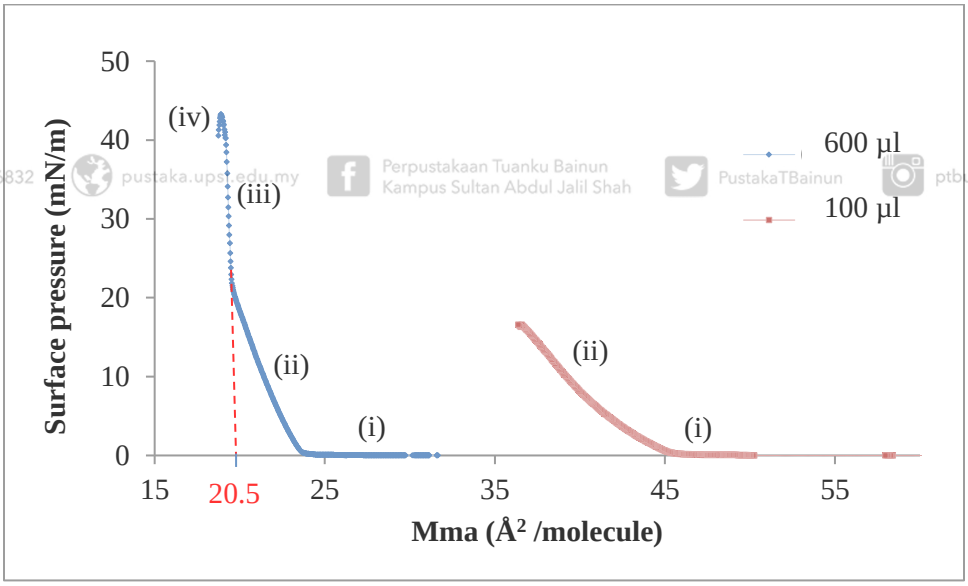


Figure 4.1. Surface pressure versus area (Π-A) isotherm graph displays the phase transformation of pristine stearic acid with different spreading volume, where (i) gas phase, (ii) liquid phase, (iii) solid phase, (iv) collapse phase

Contrariwise, as shown in Figure 4.2, pristine P3HT does not exhibit distinct phase changes. This feature is due to long polymer chains that cause a two-dimensional lattice to form (Petty, 1996). Nonetheless, the steepest part of the graph is the condensed phase of

05-4506832 pustaka.upsi.edu.my Perpustakaan Tuanku Bainun Kampus Sultan Abdul Jalil Shah PustakaTBainun ptbupsi

05-4506832 pustaka.upsi.edu.my Perpustakaan Tuanku Bainun Kampus Sultan Abdul Jalil Shah PustakaTBainun ptbupsi

P3HT, and when a tangent line is computed to this area, the limiting area of the P3HT is around 2600 $Å^2$/molecule.

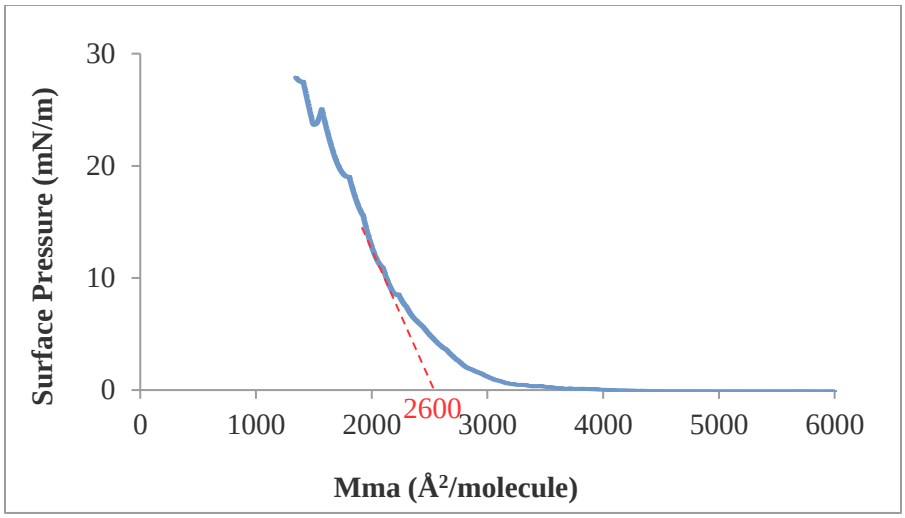


Figure 4.2. Surface pressure versus area (Π-A) isotherm of pristine P3HT at 400 µl

05-4506832 pustaka.upsi.edu.my Perpustakaan Tuanku Bainun Kampus Sultan Abdul Jalil Shah PustakaTBainun ptbupsi

The graph distortion at the solid phase of P3HT profile implies rearrangement of polymer chain during barrier compression. Identical curve has been observed for triblock copolymer of polyisoprene-b-polystyrene-b-poly(3-hexylthiophene) (PI-PS-P3HT), suggesting the phenomena is due to absence of polymer chain relaxation causing the monolayer to be incompressible once formed (Zhao et al., 2013). Apart by extrapolating the solid phase linear section of the graph to get the area per molecule for pristine P3HT and stearic acid, the area can also be calculated using the following equation (R. Çapan, Richardson & Lacey, 2001):

$$A_o = \frac{AM_w}{cN_A V} \qquad (4.1)$$

05-4506832 pustaka.upsi.edu.my Perpustakaan Tuanku Bainun Kampus Sultan Abdul Jalil Shah PustakaTBainun ptbupsi

05-4506832 pustaka.upsi.edu.my Perpustakaan Tuanku Bainun Kampus Sultan Abdul Jalil Shah PustakaTBainun ptbupsi

where, A_o is molecular area, A is area of water surface confined by the barriers, M_w is molecular weight, c is solution concentration, N_A is Avogadro's number, and V is spreading volume. From the calculation, it was found that the difference in area between theoretical and experimental results are small; about 292 $Å^2$/molecule and 2.1 $Å^2$/molecule for P3HT and stearic acid, respectively. The experimental and theoretical values of the mean molecular area are tabulated in Table 4.1.

Table 4.1

Mean molecular area (Mma) of P3HT and stearic acid on DI water subphase

Material	**Experimental Mma at 27 mN/m ($Å^2$/molecule)**	**Theoretical Mma at 27 mN/m ($Å^2$/molecule)**	**Deviation ($Å^2$/molecule)**
P3HT (400 µl)	2600	2892.00	292
Stearic acid (600 µl)	20.5	22.6	2.1

05-4506832 pustaka.upsi.edu.my Perpustakaan Tuanku Bainun Kampus Sultan Abdul Jalil Shah PustakaTBainun ptbupsi

When P3HT, a non-amphiphilic, is mixed with stearic acid, the Π-A isotherm graphs of P3HT/stearic acid show a drastic improvement as shown in Figure 4.3. Even the volume stearic acid added and stearic acid size's is very small compared to P3HT, the curve follows stearic acids monolayer trend. As can be seen from the figure, the graph segments are distinct at ratio 1:1 (100 µl P3HT: 100 µl stearic acid), where the surface pressure and limiting surface area are higher, and phase changes is distinguishable.

05-4506832 pustaka.upsi.edu.my Perpustakaan Tuanku Bainun Kampus Sultan Abdul Jalil Shah PustakaTBainun ptbupsi

05-4506832 pustaka.upsi.edu.my Perpustakaan Tuanku Bainun Kampus Sultan Abdul Jalil Shah PustakaTBainun ptbupsi

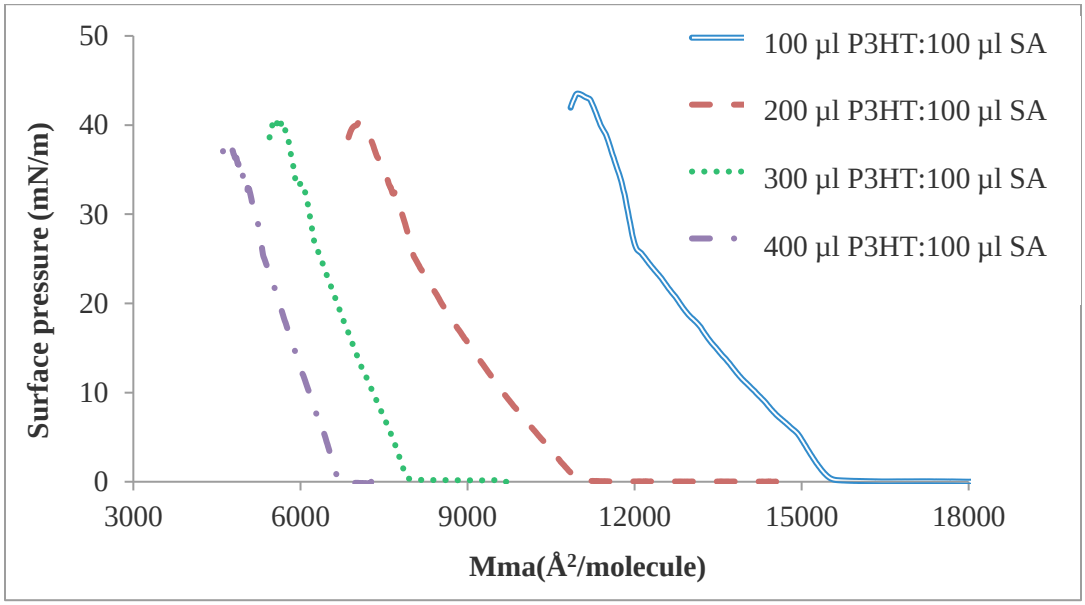


Figure 4.3. Surface pressure versus area (Π-A) isotherms of P3HT mixed with stearic acid (SA) at different volume ratio

05-4506832 pustaka.upsi.edu.my Perpustakaan Tuanku Bainun Kampus Sultan Abdul Jalil Shah PustakaTBainun ptbupsi

This result is consistent with a study by Singhal group, in which the liquid-solid phase transition occurs when the surface pressure reaches 28 mN/m (Singhal et al., 2003). Another research group reported isotherm for P3HT improve drastically when mixed with poly(N-dodecylacrylamide) or pDDA (Aoki & Fukuyama, 2012). Long tail fatty acid (e.g. stearic acid) and inert polymer matrix (e.g. pDDA) act as a stabilizer to P3HT on the air-water interface. Attempts to transfer another polythiophene derivative namely poly(3-alkylthiophenes) (P3ATs) generally failed unless the Langmuir layer were mixed with long chain fatty acids or liquid crystal (Olivati, Gonçalves & Balogh 2012).

The Π-A isotherm measurements of the mixed monolayer were repeated several times by varying the ratio of P3HT toward stearic acid. The floating monolayer phase

05-4506832 pustaka.upsi.edu.my Perpustakaan Tuanku Bainun Kampus Sultan Abdul Jalil Shah PustakaTBainun ptbupsi

05-4506832 pustaka.upsi.edu.my Perpustakaan Tuanku Bainun Kampus Sultan Abdul Jalil Shah PustakaTBainun ptbupsi

transformation was found stable for every P3HT/stearic acid ratio, indicating good constancy and reproducibility. Figure 4.3 also shows the shape of Π-A isotherm gradually changed with increasing ratio of P3HT.

At lower P3HT volume, the graph resembling stearic acid's behavior. It can be seen from the isotherm curves, at ratio 1:1, the Langmuir layer were able to be compressed to a surface pressure as high as 43 mN/m before being collapsed as compared to pristine P3HT, at merely 27 mN/m. At ratio of 4:1 (400 µl P3HT:100 µl stearic acid), the collapse pressure lessens to 37 mN/m. The increment of P3HT quantity causing the profile to morph to pristine P3HT's curve. The same effect has also been observed when stearic acid is mixed with bovine serum albumin, where the profile of bovine serum albumin becoming more dominant when its volume increases (Gew & Misran, 2014). The increasing in P3HT spreading volume also causing tighter packing in the polymeric chain, consequently the molecular occupied area became smaller. Similar trend has also been detected by increasing the volume of fullerenes (Kutner, Noworyta, Marczak & D'Souza, 2001), polystyrene-*b*-poly(acrylic acid) (X. Wang, X. Ma & Zang, 2013) and calixarenes (Razali et al, 2015).

Nevertheless, all Π-A isotherm graphs show a stable gas-liquid-solid transition value, and pressure of 27 mN/m has been selected to deposit the Langmuir film. The pressure signifies the monolayer already reached its solid state, but it yet too rigid to avoid 3D formation of the transferred layer. Throughout the study, the ratio of P3HT towards stearic acid is taken to be 4:1 (400 µl P3HT:100 µl stearic acid). The amount was chosen

05-4506832 pustaka.upsi.edu.my Perpustakaan Tuanku Bainun Kampus Sultan Abdul Jalil Shah PustakaTBainun ptbupsi

05-4506832 pustaka.upsi.edu.my Perpustakaan Tuanku Bainun Kampus Sultan Abdul Jalil Shah PustakaTBainun ptbupsi

to ensure P3HT is dominating the thin film since stearic acid is resistive in nature, but enough stearic acid as to cap Cd^{2+} ions in the subphase. The data extracted from Figure 4.3 are shown in Table 4.2.

Table 4.2

Phase transformation of P3HT:stearic acid (P3HT:SA) at different spreading volume ratio

Material	Gas Phase (mN/m)	Liquid Phase (mN/m)	Solid Phase (mN/m)	Collapse (mN/m)	Mma ($Å^2$/molecule)
P3HT:SA (1:1)	0 - 1	1 - 26	26 - 43	43	12800
P3HT:SA (2:1)	0 - 1	1 - 26	26 - 39	39	9200
P3HT:SA (3:1)	0 - 1	1 - 26	26 - 39	39	7200
P3HT:SA (4:1)	0 - 1	1 - 26	26 - 37	37	6000

05-4506832 pustaka.upsi.edu.my Perpustakaan Tuanku Bainun Kampus Sultan Abdul Jalil Shah PustakaTBainun ptbupsi

Figure 4.4 shows the Π-A isotherms graphs of (a) pristine P3HT, (b) pristine stearic acid and (c) 400µl P3HT:100µl stearic acid, spread on three different subphases – deionized (DI) water, DI water containing 0.5 mM cadmium (II) chloride ($CdCl_2$) or 1.0 mM $CdCl_2$. The addition of $CdCl_2$ into water subphase resulted in smoother P3HT's Π-A graph and larger area per molecule, A_o. The "impurities" in the subphase caused the surface pressure of pristine P3HT to increase earlier than that of DI water. Pristine stearic acid and P3HT:stearic acid isotherms also displayed similar profile. The higher concentration of Cd^{2+} ions in the subphase, the earlier gas-liquid phase transformation occur. The proclivity is apparent for pristine P3HT, even the amount of $CdCl_2$ added were very small.

05-4506832 pustaka.upsi.edu.my Perpustakaan Tuanku Bainun Kampus Sultan Abdul Jalil Shah PustakaTBainun ptbupsi

05-4506832 pustaka.upsi.edu.my Perpustakaan Tuanku Bainun Kampus Sultan Abdul Jalil Shah PustakaTBainun ptbupsi

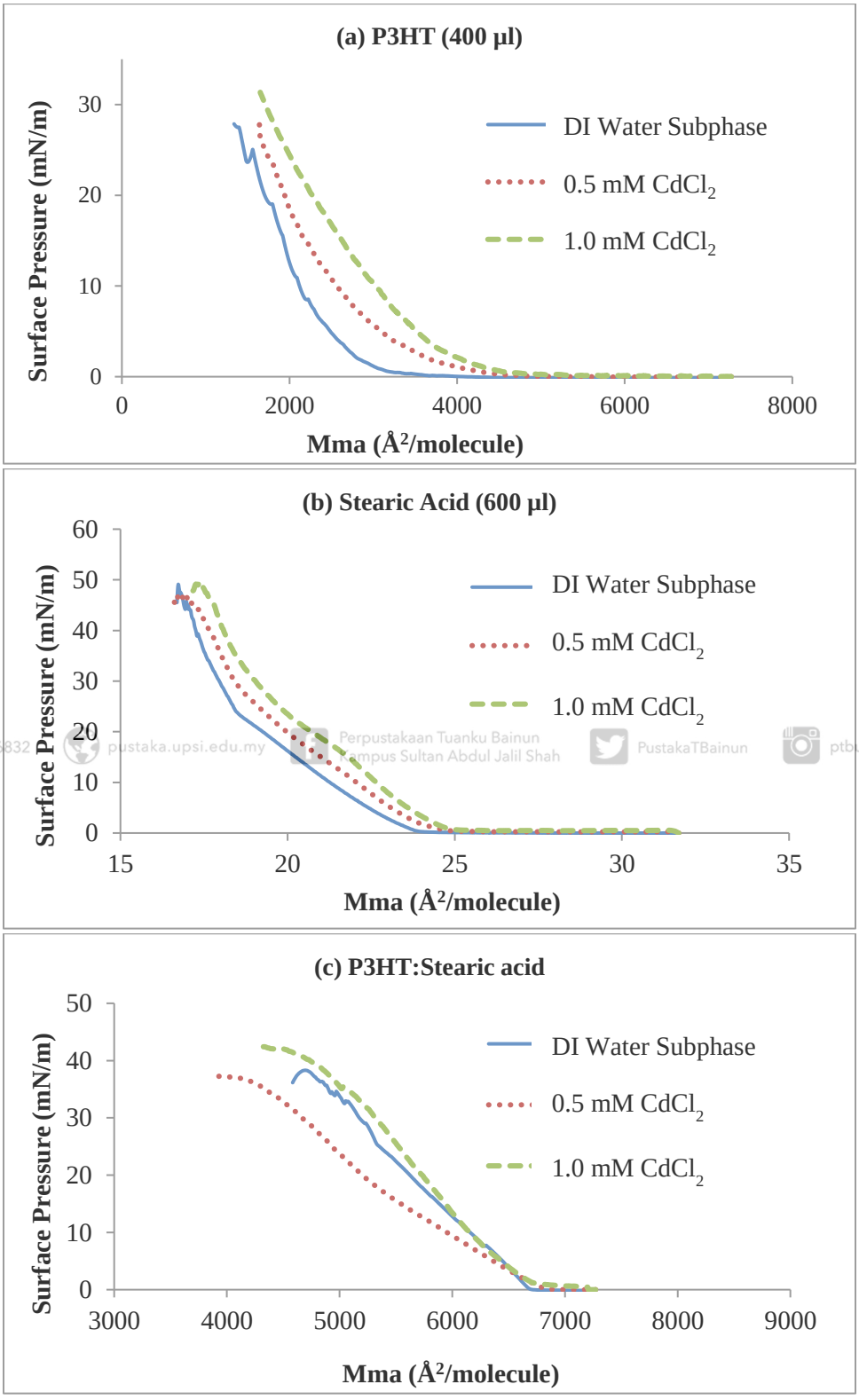


Figure 4.4. The surface pressure versus area (Π-A) isotherm graphs of (a) 400 µl P3HT, (b) 600 µl stearic acid, (c) 400 µl P3HT: 100 µl stearic acid, on different subphases

05-4506832 pustaka.upsi.edu.my Perpustakaan Tuanku Bainun Kampus Sultan Abdul Jalil Shah PustakaTBainun ptbupsi

05-4506832 pustaka.upsi.edu.my Perpustakaan Tuanku Bainun Kampus Sultan Abdul Jalil Shah PustakaTBainun ptbupsi

Such profiles can be observed because when bivalent metal ions, for example Cd^{2+} and Pb^{2+} were added to water subphase, more stable Langmuir layers are formed. Consequently, yielding more ordered LB films. This is because most solid surfaces assume finite surface charge in water, hence interacting with polar or charged organic molecule. The strong electrostatic interaction of bivalent ions acts as glues or immobilizers that stick organic molecules to substrate. Higher multivalent ions also show the same characteristic (Simoni, Bosma, Harms & Zehnder, 2000). On contrary, monovalent ions do not show the same attribute. The effect of $CdCl_2$ addition in water subphase towards the gas-liquid-solid phase transformation is summarized in Table 4.3.

Table 4.3

Summary of gas–liquid–solid phase transformation

Material	Subphase	Gas Phase (mN/m)	Liquid Phase (mN/m)	Solid Phase (mN/m)	Collapse (mN/m)	Mma (Å^2/molecule)
P3HT (100µl)	DI Water	0 – 1	1 – 9	9 – 27	27	2600
	0.5 mM $CdCl_2$	0 – 1	1 – 13	13 – 27	27	3000
	1.0 mM $CdCl_2$	0 – 1	1 – 13	13 – 30	30	3400
Stearic Acid (600 µl)	DI Water	0 – 1	1 – 24	24 – 48	48	20.5
	0.5 mM $CdCl_2$	0 – 1	1 – 30	30 – 47	47	20.7
	1.0 mM $CdCl_2$	0 – 1	1 – 30	30 – 49	49	21.2
P3HT:SA (4:1)	DI Water	0 – 1	1 – 26	26 – 37	37	6000
	0.5 mM $CdCl_2$	0 – 1	1 – 18	18 – 36	36	6250
	1.0 mM $CdCl_2$	0 – 1	1 – 14	14 – 42	42	6300

05-4506832 pustaka.upsi.edu.my Perpustakaan Tuanku Bainun Kampus Sultan Abdul Jalil Shah PustakaTBainun ptbupsi

05-4506832 pustaka.upsi.edu.my Perpustakaan Tuanku Bainun Kampus Sultan Abdul Jalil Shah PustakaTBainun ptbupsi

The deviations in the Π-A isotherm graph in the presence of Cd^{2+} ions is due to structural rearrangement of Langmuir layer molecules. Studies show that the molecules are able to expose the polar head groups to both substrate and subphase (Ye, Noda, Nishida, Morita, & Osawa, 2004; Gosvami et al., 2012). Similar profile changes have also been observed when Cd^{2+} ions were added on graphene oxide monolayer (Narayanam et al. (2012). Interaction of Cd^{2+} ions only occur with the stearic acid due to ions' electronegativity and the acid's affinity towards the ions, forming cadmium stearate $(C_{17}H_{35}COO)_2Cd$.

4.2.2 *Ex situ* Hybridization

05-4506832 pustaka.upsi.edu.my Perpustakaan Tuanku Bainun Kampus Sultan Abdul Jalil Shah PustakaTBainun ptbupsi

The Π-A isotherm curves of CdS or CdSe quantum dots incorporated into P3HT monolayer are shown in Figure 4.5. The quantum dots were treated with hexanoic acid before physically mixed into the P3HT solution at 25 wt% or 50 wt%. The Π-A isotherm graphs of P3HT:CdS and P3HT:CdSe exhibit similar trend as pristine P3HT as shown in Figure 4.2, where no apparent liquid-solid phase transformation can be observed. However, the transition of gas to liquid phase for PHT mixed with QDs happened slightly later than pristine P3HT.

The gaseous phase of physically mixed QDs are started from lift off area, $A_{i,}$ 4155 $Å^2$/molecules, with surface pressure varies from 0.001 to 0.9 mN/m. The gaseous phase of P3HT:QDs monolayers are longer stretched as compared to pristine P3HT, in which the

05-4506832 pustaka.upsi.edu.my Perpustakaan Tuanku Bainun Kampus Sultan Abdul Jalil Shah PustakaTBainun ptbupsi

05-4506832 pustaka.upsi.edu.my Perpustakaan Tuanku Bainun Kampus Sultan Abdul Jalil Shah PustakaTBainun ptbupsi

liquid phase of pristine P3HT started at 3034 Å^2/molecules. The larger amount of materials introduced, the later gas-liquid phase transition occur.

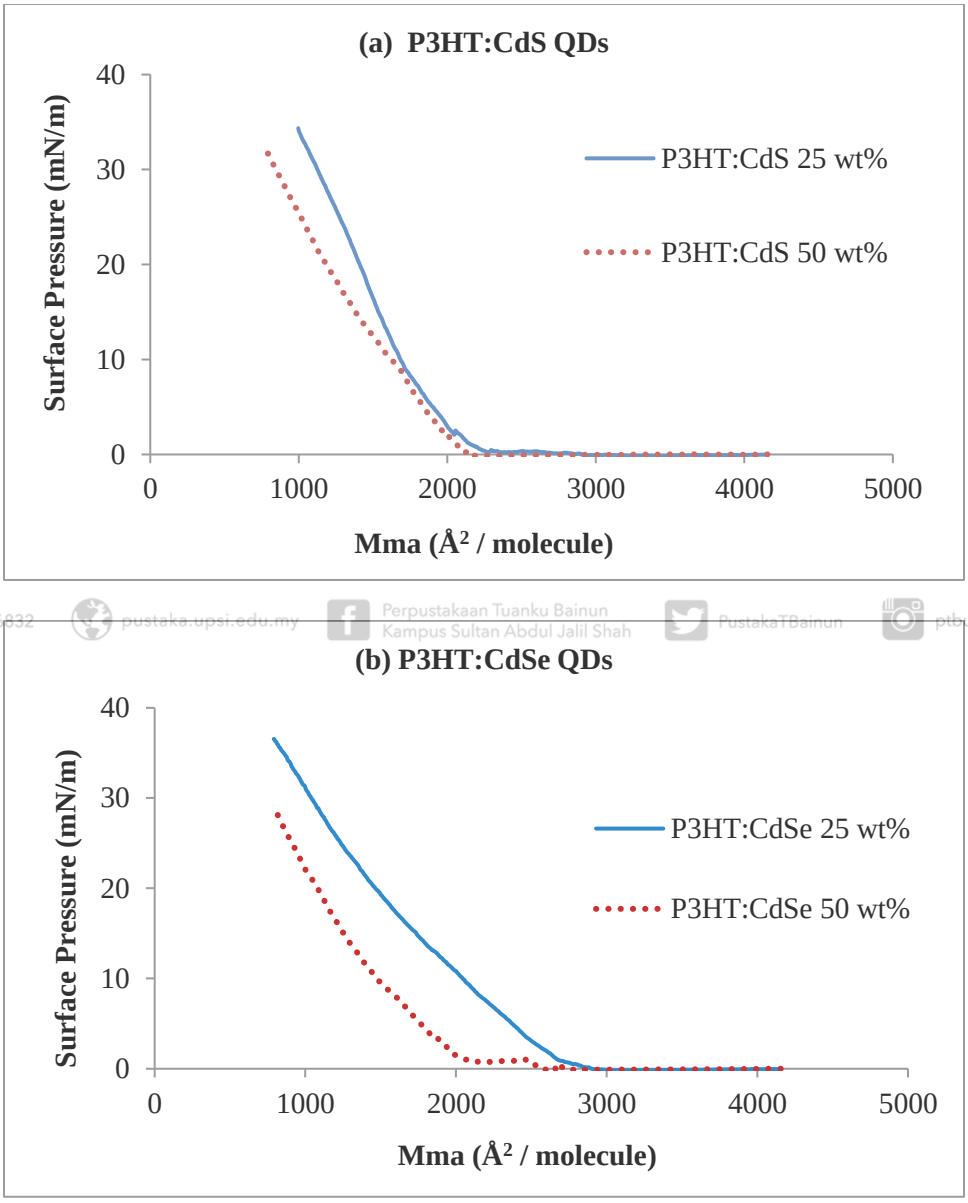


Figure 4.5. The surface pressure versus area (Π-A) isotherm graphs of (a) CdS QDs incorporated into P3HT (b) CdSe QDs incorporated into P3HT, at different weight percentage

05-4506832 pustaka.upsi.edu.my Perpustakaan Tuanku Bainun Kampus Sultan Abdul Jalil Shah PustakaTBainun ptbupsi

05-4506832 pustaka.upsi.edu.my Perpustakaan Tuanku Bainun Kampus Sultan Abdul Jalil Shah PustakaTBainun ptbupsi

The trend is comparable with the outcome in *in situ* hybridization approaches, where the amount of solution spreads and the amount of substance added into subphase influenced the phase transformation. The greater amount of QDs (50 wt%) causing delay in surface pressure rise as compared to that of 25 wt% QDs incorporated into P3HT solution. Similar phenomenon has been recorded when polyaniline-camphorsulphonic acid were doped with CdS (Das, Roy, Clarke, Ganesan & Gupta, 2014). The graph of P3HT:CdS is smoother as compared to pristine P3HT (refer Figure 4.2) owing to quantum dots that adhered in polymer matrix.

4.3 UV-Vis Spectroscopy

05-4506832 pustaka.upsi.edu.my Perpustakaan Tuanku Bainun Kampus Sultan Abdul Jalil Shah PustakaTBainun ptbupsi

Ultraviolet-Visible (UV-Vis) spectroscopy has been used to study the optical properties of hybrid nanocomposite thin films due to its sensitivity to aromatic conjunctions within molecules. The absorption properties of thin films fabricated *in situ* and *ex situ* are described in the next subtopics.

4.3.1 *In situ* Hybridization

The Π-A isotherm graphs offer crucial information on suitable surface pressure for thin films deposition. Materials that made up the Langmuir monolayer coalesced becoming P3HT:SA:Cd^{2+} and transferred onto a substrate. Thirteen layers were transferred using

05-4506832 pustaka.upsi.edu.my Perpustakaan Tuanku Bainun Kampus Sultan Abdul Jalil Shah PustakaTBainun ptbupsi

05-4506832 pustaka.upsi.edu.my Perpustakaan Tuanku Bainun Kampus Sultan Abdul Jalil Shah PustakaTBainun ptbupsi

modified LB method becoming thin film before further treated with gas exposure to impregnate CdS or CdSe nanoparticles in the thin films, yielding of P3HT:SA:CdS or of P3HT:SA:CdSe thin film. The changes in thin films optical absorption properties before and after exposure to gas were studied using UV-Vis spectrophotometer.

Figure 4.6 shows absorption spectra of stearic acid, pristine P3HT, P3HT:SA:Cd^{2+} thin film that has been deposited under same condition. Since stearic acid does not exhibit conjugation in its chemical structure, the optical absorption is relatively very little throughout the entire spectrum. On the other hand, conjugation system in P3HT causes two peaks at 522 and 556 nm and a shoulder at 605 nm to appear in the UV-Vis graph.

05-4506832 pustaka.upsi.edu.my Perpustakaan Tuanku Bainun Kampus Sultan Abdul Jalil Shah PustakaTBainun ptbupsi

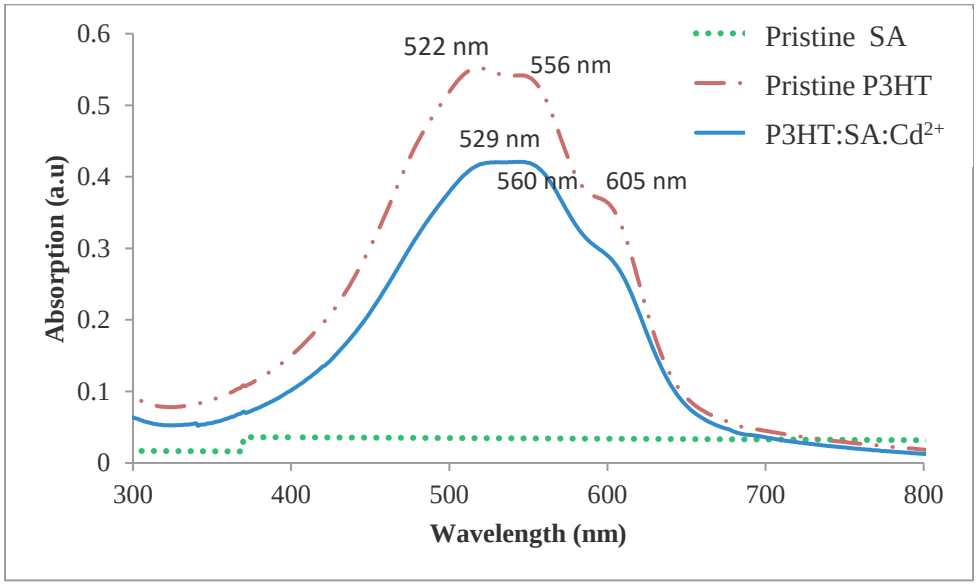


Figure 4.6. UV-Vis absorption spectra of pristine stearic acid, pristine P3HT and P3HT:SA:Cd^{2+} thin films

05-4506832 pustaka.upsi.edu.my Perpustakaan Tuanku Bainun Kampus Sultan Abdul Jalil Shah PustakaTBainun ptbupsi

05-4506832 pustaka.upsi.edu.my Perpustakaan Tuanku Bainun Kampus Sultan Abdul Jalil Shah PustakaTBainun ptbupsi

Similar result has been obtained by Liao research group (Liao et. al, 2011). The peaks attribute to π-π* transition or the order of intermolecular chains of the polymer, whilst the shoulder is due to crystallization of polymer (Farva, Khan & Park, 2008; Brown et al, 2003). When P3HT is mixed with SA on subphase containing Cd^{2+} ions, the absorption spectra is lower than that of pristine P3HT and its peak shifted towards red spectrum at 529 and 560 nm, and the shoulder becoming less distinguishable. The shift suggests the existence of Cd^{2+} ion in the stearic acid matrices and shorter π-conjugation length of P3HT.

Figure 4.7 shows the changes of thin film absorption spectra before and after exposed to H_2S gas. The unexposed thin film has absorption peak at 560 nm, however after the film was exposed to H_2S gas environment for 2, 4 and 6 hours, the peak has shifted to 559, 558 and 556.5 nm respectively. The blue shift of the peaks is an indication of quantum confinement effect from the CdS nanoparticles formed in the thin film (Prabhu & Khadar, 2005; Sonar, Sreenivasan, Madddanimath & Vijayamohanan, 2006). Also can be seen a shoulder at 605 nm that is more distinguishable as compared to unexposed thin film. This shoulder generally attributed to a higher crystallization of intra-chain interactions. When the thin films were exposed to H_2S gas, the absorption intensity becoming less with time. This is due to reaction of cadmium stearate with H_2S gas:

$$(CH_3(CH_{12})_{16}COO)_2Cd + H_2S \rightarrow 2H(CH_3(CH_{12})_{16}COO) + CdS \qquad (4.2)$$

05-4506832 pustaka.upsi.edu.my Perpustakaan Tuanku Bainun Kampus Sultan Abdul Jalil Shah PustakaTBainun ptbupsi

05-4506832 pustaka.upsi.edu.my Perpustakaan Tuanku Bainun Kampus Sultan Abdul Jalil Shah PustakaTBainun ptbupsi

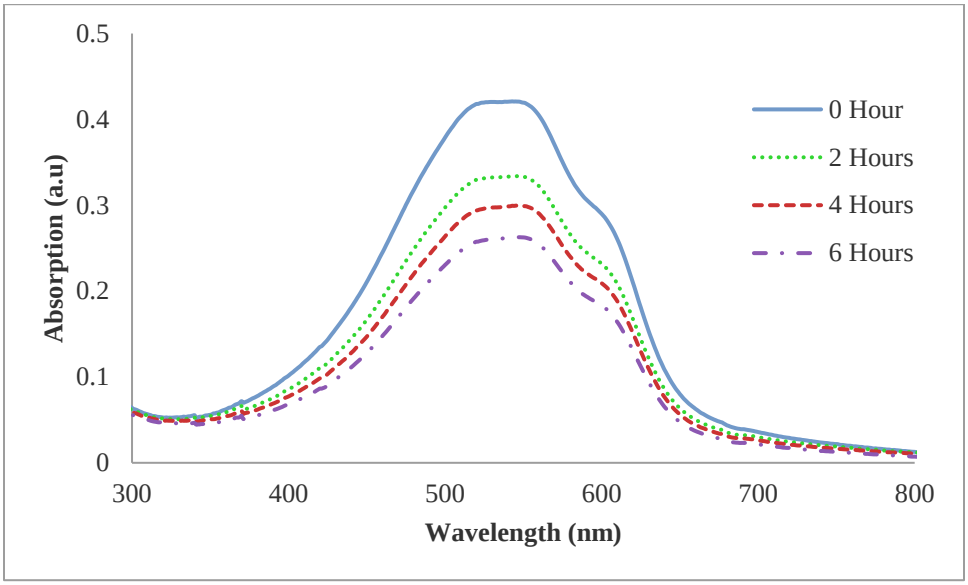


Figure 4.7. UV-Vis absorption spectra of P3HT:SA:Cd^{2+} thin films exposed to H_2S gas

Generally, the absorption of thin film is expectedly increasing with the increasing amount of nanoparticles. However, in this study, the trend shows otherwise. Depreciation in absorption intensity is due to scattering effect by the nanoparticles created in the thin film (Khan, Bhargav, Kaur, Dhawan & Chand, 2010). An identical observation has also been reported for hybrid cadmium tellueride (CdTe) and poly (2-methoxy-5(2'-ethyl) hexoxy-phenylenevinylene) (MEH-PPV) at low weight ratio. However, the study shows increment in absorption intensity when they increased the volume of CdTe in the polymer, as anticipated earlier (Verma, Rao & Dutta, 2009). Likewise, other material such as fullerene demonstrated similar characteristic at lower weight percentage (Shrotriya, Ouyang, Tseng, Li & Yang, 2005). They argue the presence of fullerene molecules lowering the interaction between P3HT chains.

05-4506832 pustaka.upsi.edu.my Perpustakaan Tuanku Bainun Kampus Sultan Abdul Jalil Shah PustakaTBainun ptbupsi

05-4506832 pustaka.upsi.edu.my Perpustakaan Tuanku Bainun Kampus Sultan Abdul Jalil Shah PustakaTBainun ptbupsi

In this study, the amount of CdS nanoparticles generated are very small as verified by Field Emission Scanning Microscopy (FESEM) and Energy Dispersive X-ray (EDX) analysis, around 8% only (refer Appendix A). The small amount of nanoparticles caused the P3HT profile dominating the UV-Vis absorbance spectra graph. From FESEM analysis, the CdS nanoparticles' size range from 13 nm to 18 nm. Apparently, the range of size of the CdS nanoparticles did not increase with increment of the exposure time. This may be due to the long chain high molecular weight polymer restricting the growth of CdS nanoparticles.

On the contrary, Yang research group found that the CdS nanoparticles size increases with increase in reaction time when the thin film consists of stearic acid only (X. M. Yang, G. M. Wang & Lu, 1998). This is because the small size of stearic acid molecules, ~22 $Å^2$, allows the molecules to shift from its original position easily when there is further aggregation of the CdS particles.

Figure 4.8 depicted absorption spectra of thin films exposed to H_2Se gas for 2, 4 and 6 hours. Similar to H_2S gas exposure, the absorption intensity decreased compared to unexposed thin film. Conversely, the absorption is much higher for film that has been exposed for 6 hours, whilst exposure for 2 and 4 hours show similar spectra curve and intensity. One possible reason that contributes to such profile is the shape and amount of CdSe nanoparticles created as shown in FESEM images (Refer Appendix B). The aspect ratio of CdSe nanoparticles when exposed for 6 hours is high, in which it resembles rod like, and some of the nanoparticles agglomerate creating larger cluster.

05-4506832 pustaka.upsi.edu.my Perpustakaan Tuanku Bainun Kampus Sultan Abdul Jalil Shah PustakaTBainun ptbupsi

05-4506832 pustaka.upsi.edu.my Perpustakaan Tuanku Bainun Kampus Sultan Abdul Jalil Shah PustakaTBainun ptbupsi

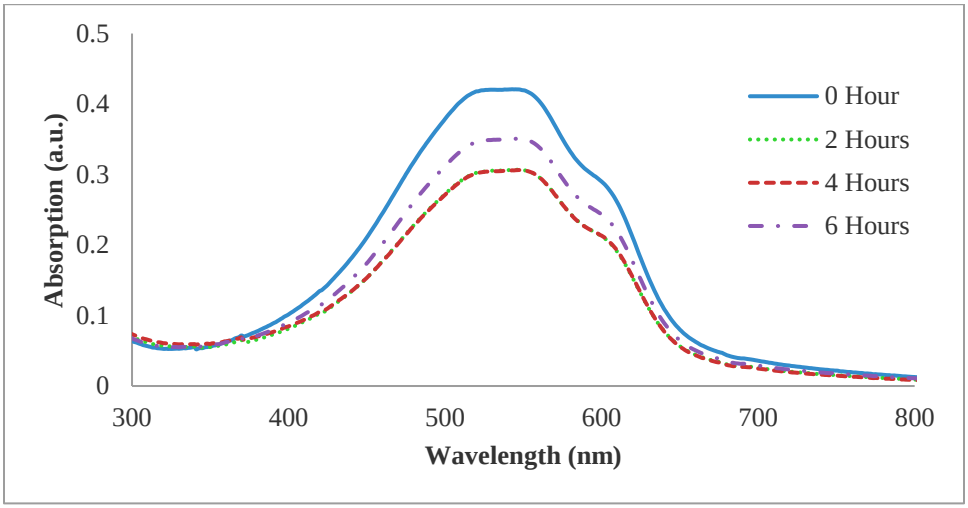


Figure 4.8. UV-Vis absorption spectra of P3HT:SA:Cd^{2+} thin films exposed to H_2Se gas

However, at 4 hour exposure, the nanoparticles size are very small, and almost no evidence of aggregation. This is due to the film's inability to absorb the H_2Se gas because the gas is not yet saturated in the reaction chamber. The absence of Se^{2-} in the thin film was recorded in EDX analysis.

The probable scheme of nanoparticles nucleation in the thin film is illustrated in Figure 4.9 (a) - (e). During thin film deposition, stearic acid molecules capped the Cd^{2+} ions (blue circle), and transferred together onto substrate as cadmium stearate ($CdSt_2$), as depicted in (a). The Cd^{2+} ions act as the nanoparticles' seeds while P3HT chains are represented by pink color only. This is due to its long chain molecule and larger quantity of P3HT as compared to stearic acid. P3HT mers also do not have function in capping the cadmium ion.

05-4506832 pustaka.upsi.edu.my Perpustakaan Tuanku Bainun Kampus Sultan Abdul Jalil Shah PustakaTBainun ptbupsi

05-4506832 pustaka.upsi.edu.my Perpustakaan Tuanku Bainun Kampus Sultan Abdul Jalil Shah PustakaTBainun ptbupsi

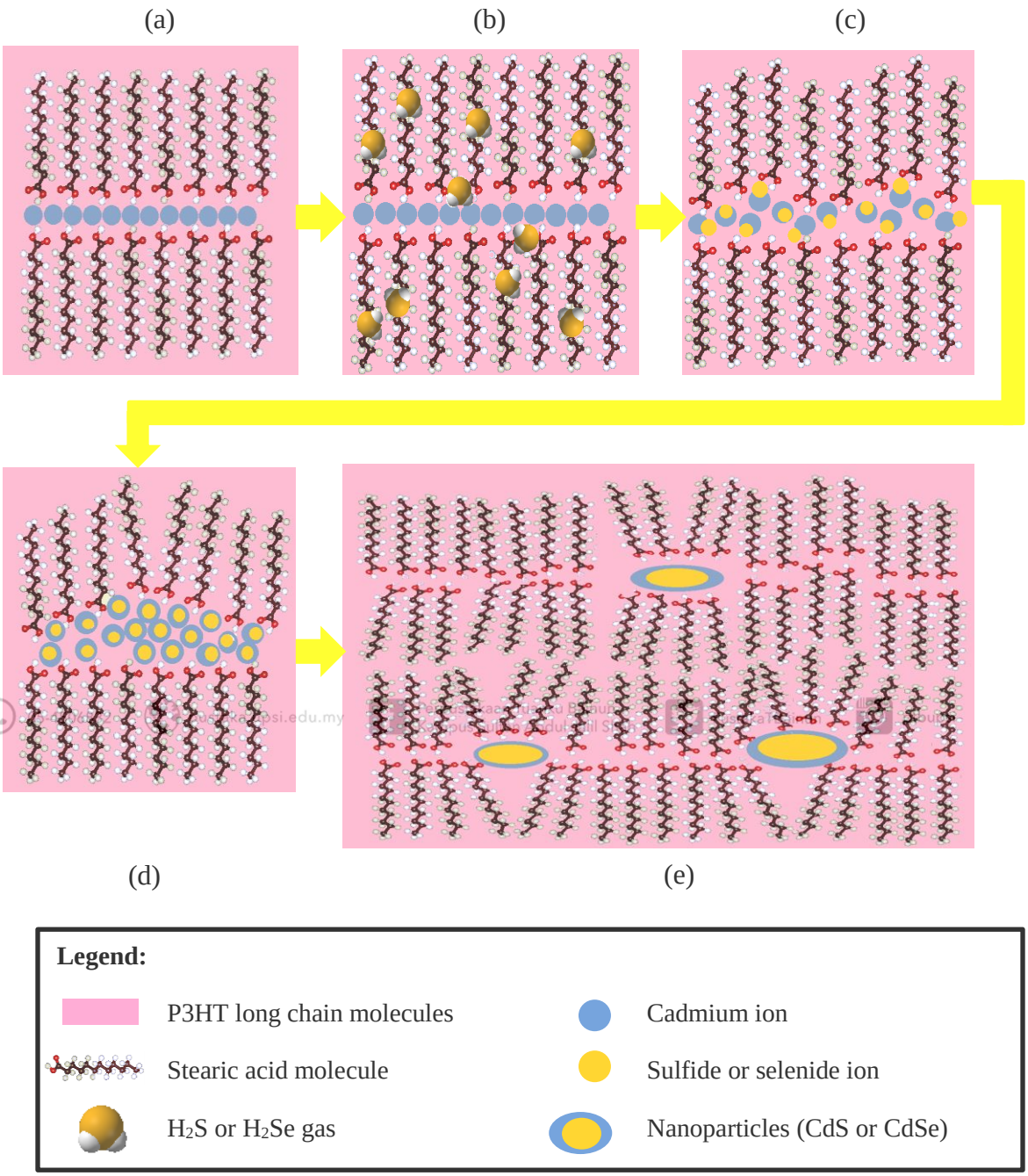


Figure 4.9. The nucleation process of nanoparticles in between the P3HT/SA matrix: (a) $CdSt_2$ after deposition (b) Gas exposure (c) Nucleation of nanoparticles (d) Further nanoparticles formation (e) Aggregation of larger nanoparticles cluster

05-4506832 pustaka.upsi.edu.my Perpustakaan Tuanku Bainun Kampus Sultan Abdul Jalil Shah PustakaTBainun ptbupsi

05-4506832 pustaka.upsi.edu.my Perpustakaan Tuanku Bainun Kampus Sultan Abdul Jalil Shah PustakaTBainun ptbupsi

Figure 4.9 (b) represents the event when the thin film is exposed to H_2S or H_2Se gas. The next stage as in (c), the Cd^{2+} ion will attract the S^{-2} or Se^{-2} ions (yellow dot), nucleating CdS or CdSe nanoparticles. (d) showed further formation of CdS or CdSe nanoparticles, whilst (e) demonstrated the aggregation of the nanoparticles into larger cluster. However, as contrary to nucleation process for nanoparticles in pristine long fatty acid that has been described by Nabok in which the size of nanoparticles grows as exposure time increases (Nabok, 2005), the P3HT chains restricted the growth of nanoparticles. The same effect is shown when calixarene molecules were used to cap the Cd^{2+} ions (Torrent-Burgués, Vocanson, Pérez-González & Errachid, 2012). They suggested calixarenes cavities restrict the aggregation of CdS.

05-4506832 pustaka.upsi.edu.my Perpustakaan Tuanku Bainun Kampus Sultan Abdul Jalil Shah PustakaTBainun ptbupsi

4.3.2 *Ex situ* Hybridization

The UV-Vis spectra when the CdS quantum dots were physically mixed into P3HT polymer is shown in Figure 4.10. The absorption of pristine P3HT is comparable to the thin film with 25 wt% CdS QDs. However, the absorption is lower when the amount of QDs is doubled. The peaks and shoulder remains at the same wavelength as pristine P3HT. It give almost similar trend as in *in situ* hybridization system, where the higher the foreign materials in the polymer, the lower its absorption. The absence of CdS QDs absorption band is likely due to the overlap with the P3HT absorption.

05-4506832 pustaka.upsi.edu.my Perpustakaan Tuanku Bainun Kampus Sultan Abdul Jalil Shah PustakaTBainun ptbupsi

05-4506832 pustaka.upsi.edu.my Perpustakaan Tuanku Bainun Kampus Sultan Abdul Jalil Shah PustakaTBainun ptbupsi

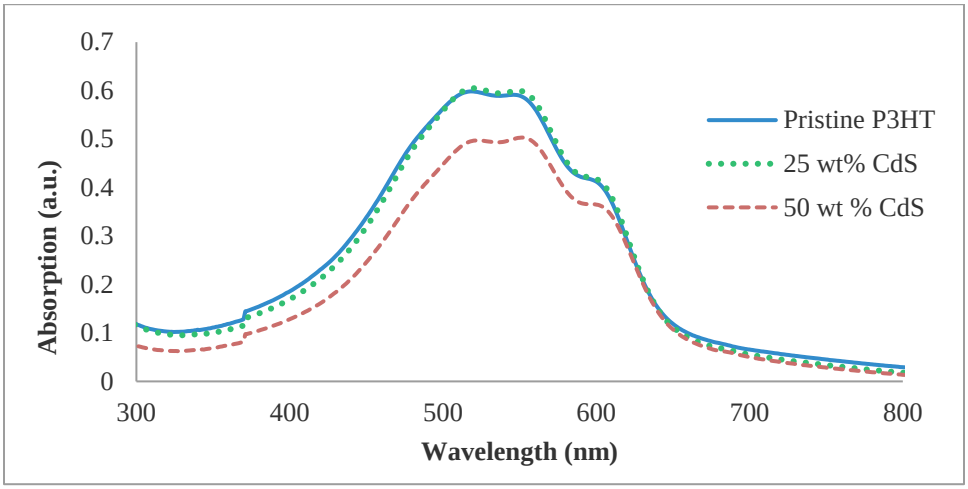


Figure 4.10. UV-Vis absorption spectra of P3HT mixed with CdS quantum dots

Meanwhile, Figure 4.11 demonstrated the spectra of P3HT:CdSe QDs hybrid thin film. Pristine P3HT thin film and thin film with 25 wt% of CdSe QDs exhibit identical spectra. However, at 50 wt% of CdSe, the absorption is higher, and the shoulder is less distinguishable.

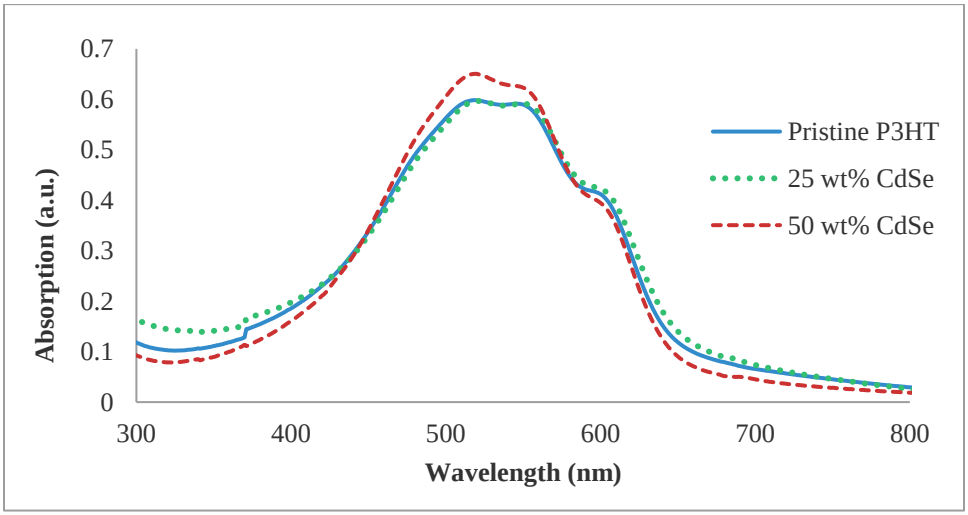


Figure 4.11. UV-Vis absorption spectra of P3HT mixed with CdSe quantum dots

05-4506832 pustaka.upsi.edu.my Perpustakaan Tuanku Bainun Kampus Sultan Abdul Jalil Shah PustakaTBainun ptbupsi

05-4506832 pustaka.upsi.edu.my Perpustakaan Tuanku Bainun Kampus Sultan Abdul Jalil Shah PustakaTBainun ptbupsi

The peaks are poorly shifted to red, 524 and 557.5 nm indicating the polymer chains are less crystallized due to QDs added. Both P3HT: CdS and CdSe show no significant in amplitude variation with the increment of QDs wt%, comparable to the results reported for P3HT:CdSe TBPO-capped at different weight percentage (Loubiri et al., 2015).

4.4 Photoluminescence (PL) Measurement

Optical characterization using photoluminescence (PL) provides information on carrier properties, thus complementary to electrical characterization analysis. Among the advantages of PL measurement are it is a non-destructive technique, does not require any particular sample preparation and only small quantity of materials are needed for the characterization.

4.4.1 *In situ* Hybridization

Photoluminescence (PL) is a process of spontaneous light emission from a material under optical excitation. Ideally, the PL spectrum mirroring the image of the absorption spectrum, hence it clearly can be seen from Figure 4.12 and 4.13 the spectra resemble the UV-Vis absorption spectra as in Figure 4.7 and Figure 4.8 respectively. All thin films were excited at 450 nm. PL measurement is an indicator of excitons (excited electron-hole pair)

05-4506832 pustaka.upsi.edu.my Perpustakaan Tuanku Bainun Kampus Sultan Abdul Jalil Shah PustakaTBainun ptbupsi

05-4506832 pustaka.upsi.edu.my Perpustakaan Tuanku Bainun Kampus Sultan Abdul Jalil Shah PustakaTBainun ptbupsi

dissociation and its efficiency to transfer charge in the composite materials (J. Yu, Hu & Barbara, 2000).

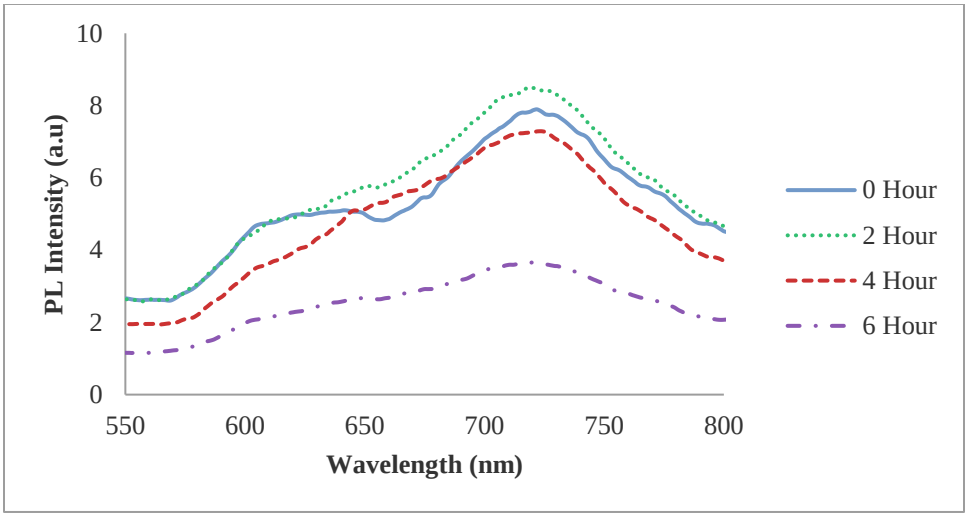


Figure 4.12. Photoluminescence spectra for thin films exposed to H_2S gas

05-4506832 pustaka.upsi.edu.my Perpustakaan Tuanku Bainun Kampus Sultan Abdul Jalil Shah PustakaTBainun ptbupsi

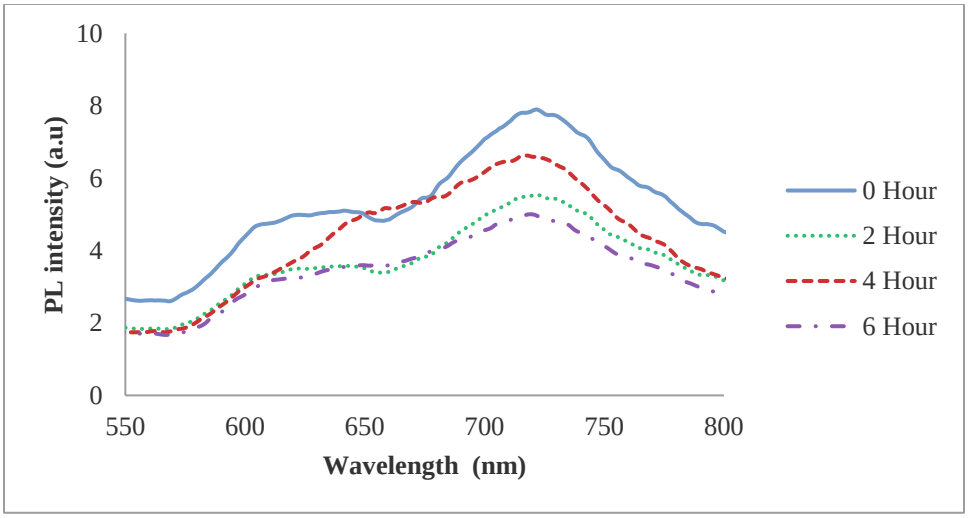


Figure 4.13. Photoluminescence spectra for thin films exposed to H_2Se gas

05-4506832 pustaka.upsi.edu.my Perpustakaan Tuanku Bainun Kampus Sultan Abdul Jalil Shah PustakaTBainun ptbupsi

05-4506832 pustaka.upsi.edu.my Perpustakaan Tuanku Bainun Kampus Sultan Abdul Jalil Shah PustakaTBainun ptbupsi

Unexposed thin film and thin films exposed to H_2S gas for 2 and 4 hours shows unstable PL intensity. The low amount of CdS nanoparticles created might contributed to the phenomena. At higher exposure time (6 hours) in which the percentage of CdS increased, the PL intensity decreased. Similar trend was displayed by thin film exposed to H_2Se gas. Nonetheless, comparing the unexposed thin film with thin films exposed to H_2S or H_2Se gas for 6 hours, the peak for exposed thin film shifted towards blue region, from 720 nm to 718 nm and 714 nm respectively. The shift suggests the reduction in P3HT aggregation (Clark, Silva, Friend & Spano, 2007) causing the PL to quench.

Even P3HT has high hole mobility, it has low charge carrier distance. Hence the span a charge carrier can be transported before exciton recombination occurs is very short. The excitons must reach nanoparticle interface before it decays through radiative or non-radiative process. The polymer/nanoparticle interface also known as donor/acceptor (D/A) interface. The terms are coined from the characteristics of the materials itself, where polymer acts as an electron donor whilst the nanoparticles are electrons acceptor. The interface also widely known as heterojunction or p-n junction.

The occurrence of PL depends on the distance from the excitons' origin to the D/A interface (Freisinger, 2013). If the distance is lesser than the exciton diffusion length, a charge transfer to the nanoparticle is expected and PL is quenched (Ferguson, Kopidakis, Shaheen & Rumbles, 2008). The larger distance caused recombination to take place. From literature, exciton diffusion length for P3HT is around 8 nm (Shaw, Rusecka & Samuel, 2008).

05-4506832 pustaka.upsi.edu.my Perpustakaan Tuanku Bainun Kampus Sultan Abdul Jalil Shah PustakaTBainun ptbupsi

05-4506832 pustaka.upsi.edu.my Perpustakaan Tuanku Bainun Kampus Sultan Abdul Jalil Shah PustakaTBainun ptbupsi

However, as reported in Section 4.3.1, the FESEM images show the distance between nanoparticles are very large, in the range of 100-150 nm. The small amount of nanoparticles impregnated in the thin film causing the exciton that is further from D/A interface to recombine before reaching the interface. This circumstance explains the instability of PL intensity reading for the exposed thin films.

4.4.2 *Ex situ* Hybridization

Photoluminescence spectra for P3HT:CdS QDs and P3HT:CdSe QDs are shown in Figure 4.14 and 4.15 respectively. Both types of thin film displays similar characteristics, in which higher amount of QDs (50 wt%) mixed into P3HT cause the film to quench stronger as compared to films with 25 wt% QDs. The quenching indicates a reduction in domain size of P3HT blended with nanoparticles (MacLachlan et. al., 2015), owing to shorter distance for the excitons to travel to D/A interface when the weight percentage of nanoparticles in the polymer is doubled. The PL quenching also possibly due to π-π interaction of P3HT with the nanoparticles (H. C. Liao, Chen & Liu, 2009), creating extra decaying pathway for excitons (Khan et al., 2010). Higher excitons dissociation can be justified for better device performance.

Nonetheless, the PL intensity of P3HT:CdS QDs is higher and has narrower peak than that of P3HT:CdSe QDs. The P3HT:25 wt% CdS has a peak at 704 nm whilst for P3HT:50 wt% CdS, the peak shifted to longer wavelength, 713.5 nm. The shift also known

05-4506832 pustaka.upsi.edu.my Perpustakaan Tuanku Bainun Kampus Sultan Abdul Jalil Shah PustakaTBainun ptbupsi

05-4506832 pustaka.upsi.edu.my Perpustakaan Tuanku Bainun Kampus Sultan Abdul Jalil Shah PustakaTBainun ptbupsi

as Stokes-shift. The red shift implies the increment in polymer aggregation, which can be induced by incorporation of QDs into the polymer matrix as have also been observed by others (Sharma, Vats, Dhenadhayalan, Ramamurthy & Narula, 2012; Bruevich, 2007).

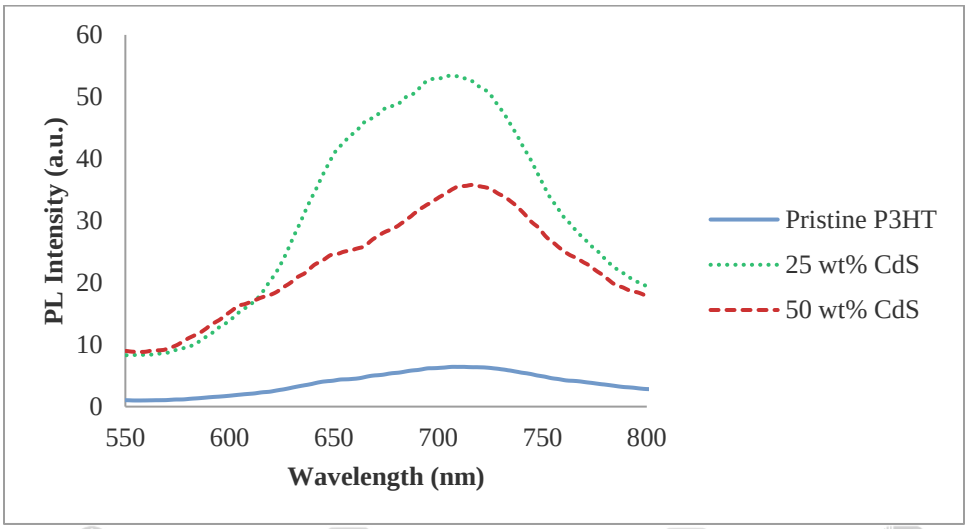


Figure 4.14. Photoluminescence spectra for hybrid P3HT:CdS QDs thin films

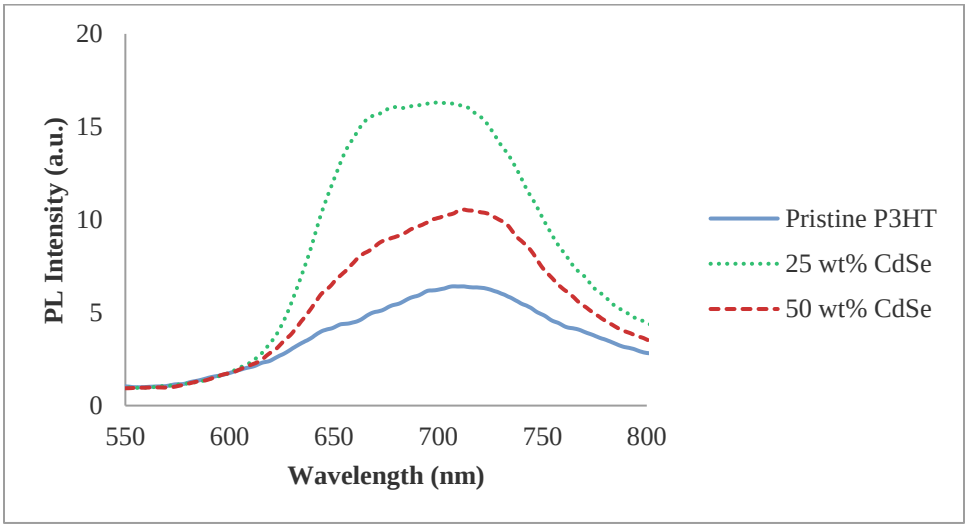


Figure 4.15. Photoluminescence spectra for hybrid P3HT:CdSe QDs thin films

05-4506832 pustaka.upsi.edu.my Perpustakaan Tuanku Bainun Kampus Sultan Abdul Jalil Shah PustakaTBainun ptbupsi

05-4506832 pustaka.upsi.edu.my Perpustakaan Tuanku Bainun Kampus Sultan Abdul Jalil Shah PustakaTBainun ptbupsi

4.5 Current Density-Voltage (J-V) Measurement

The electrical properties of the thin film were characterized using four-point probe assisted with solar simulator and controlled by a computer. For all types of thin film, standard test conditions have been imposed. The conditions are similar size of the thin films (or also called devices under test, DUT), temperature of 25 ^{o}C and the solar simulator irradiance was 100 W/m^2.

4.5.1 *In situ* Hybridization

Current density-voltage (J-V) measurement was carried out to investigate the thin films' electrical properties, and to weigh the possibility to adopt it in electronic devices. The effect of gas exposure time on the thin films' electrical properties was investigated, in which the evaluation were done under dark and illuminated conditions. The measured parameters were open-circuit voltage (V_{oc}), short-circuit current density (J_{sc}), fill factor (FF) and maximum power output (P_{max}).

Figure 4.16 (a), (b), (c) and (d) shows the J-V graphs for samples exposed to H_2S gas for 0, 2, 4 and 6 hours respectively, in dark and under illumination. From the graphs, all thin films show a slight increment in current density when illuminated under solar simulator as compared to in dark condition. The changes indicate thin film absorbed incident photons, consequently generating excitons.

05-4506832 pustaka.upsi.edu.my Perpustakaan Tuanku Bainun Kampus Sultan Abdul Jalil Shah PustakaTBainun ptbupsi

05-4506832 pustaka.upsi.edu.my Perpustakaan Tuanku Bainun Kampus Sultan Abdul Jalil Shah PustakaTBainun ptbupsi

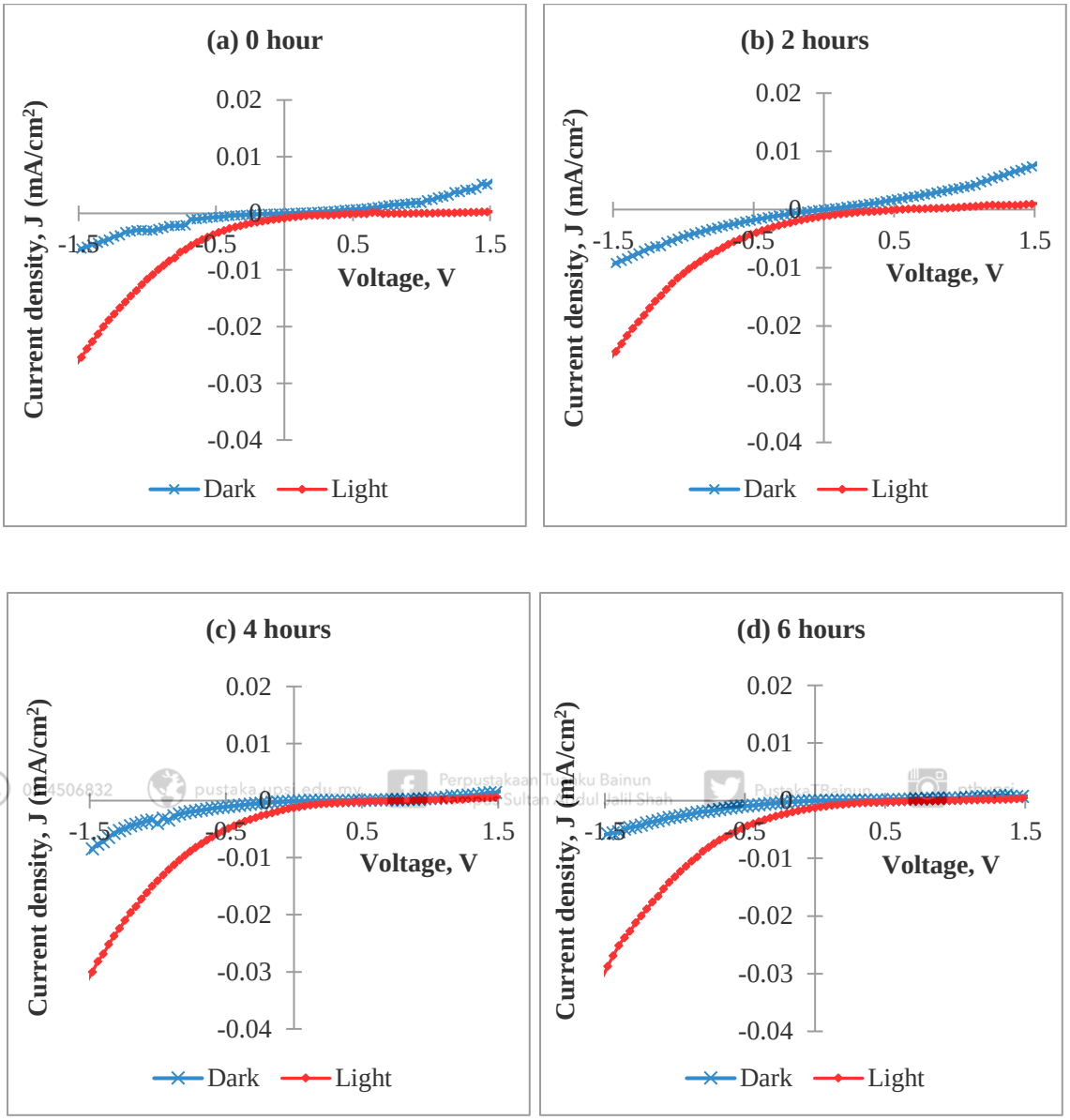


Figure 4.16. Current density versus voltage (J-V) graphs for sample under dark and under illumination of a solar simulator. The thin films were exposed to H_2S gas for (a) 0 hour, (b) 2 hours, (c) 4 hours, (d) 6 hours

Excitons are generated when the photons have energy equal or larger than the polymer band gap (Halls et. al, 1995). The excitons then diffused inside the polymer matrix until they meet polymer/nanoparticles interface and dissociated into an electron and a hole

05-4506832 pustaka.upsi.edu.my Perpustakaan Tuanku Bainun Kampus Sultan Abdul Jalil Shah PustakaTBainun ptbupsi

05-4506832 pustaka.upsi.edu.my Perpustakaan Tuanku Bainun Kampus Sultan Abdul Jalil Shah PustakaTBainun ptbupsi

(Kippelen & Bredas, 2009). This causes an electric field to form at the boundary layer, pushing electrons to one side and holes to the other. The energy of HOMO and LUMO of the nanoparticle is sufficiently lower than that of polymer. The separated charges are then transported to their respective electrodes, i.e. holes to anode and electrons to cathode to produce photocurrent (Sariciftci, Smilowitz, Heeger & Wudl, 1992).

The small current increment for illuminated samples shows the thin films still incompetence for photodetector usage. Among factors contributing to poor thin film performance is the existing of stearic acid in the thin films, where stearic acid is resistor in nature. Another is the P3HT has relatively narrow absorptions band that caused only a small fraction of solar spectrum absorbed (Nicholson & Castro, 2010). Morphology of the thin films also plays some roles because excitons may be trapped in defect or impurity sites that contribute to excitons loss (S. S. Sun & Bonner, 2005).

The J-V graphs were analyzed and parameters mentioned in the earlier paragraphs were excerpted by studying the fourth quardrant of the graphs as shown in Figure 4.17. The graph is obtained by deducting the value of samples' current density in dark and under illumination. The curves indicate the longer hour of gas exposure yield in better short-circuit current density as compared to unexposed film. However, the films exposed for 2 hours shows almost straight line, a metallic behavior.

05-4506832 pustaka.upsi.edu.my Perpustakaan Tuanku Bainun Kampus Sultan Abdul Jalil Shah PustakaTBainun ptbupsi

05-4506832 pustaka.upsi.edu.my Perpustakaan Tuanku Bainun Kampus Sultan Abdul Jalil Shah PustakaTBainun ptbupsi

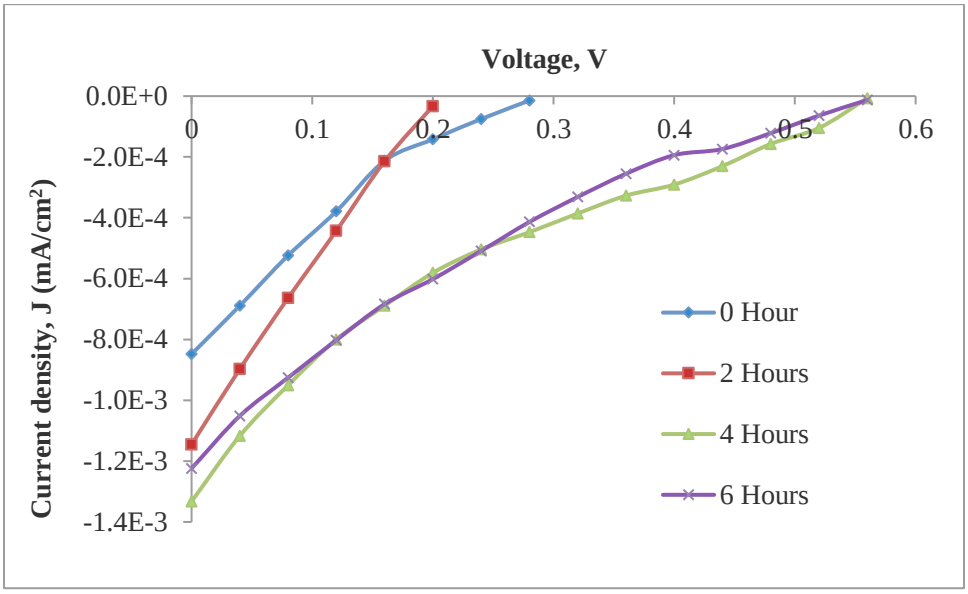


Figure 4.17. The fourth quadrant of current density versus voltage (J-V) curve for thin films exposed to H_2S gas at varying time

05-4506832 pustaka.upsi.edu.my Perpustakaan Tuanku Bainun Kampus Sultan Abdul Jalil Shah PustakaTBainun ptbupsi

The parameters for thin film exposed to H_2S gas environment at various exposure times are compared in Figure 4.18. Open-circuit voltage, V_{oc} is the voltage across the open terminals, that is when J = 0 A. The V_{oc} for the films exposed for 4 and 6 hours are doubled as compared to untreated thin films and thin film exposed to merely 2 hours. The nature of V_{oc} is still not well understood, but Brabec et al. (2001) suggest it is strongly dependent on the donor's ionization potential and acceptor's electron affinity, hence the energy level offset. Recent study (Qi, Zhou & Wang, 2015) also shows V_{oc} is subject to the blend composition even it is not a simple linear relationship. These findings explain the low V_{oc} value for 0 and 2 hours exposure thin films, where the CdS nanoparticles is not yet formed in the polymer matrix.

05-4506832 pustaka.upsi.edu.my Perpustakaan Tuanku Bainun Kampus Sultan Abdul Jalil Shah PustakaTBainun ptbupsi

05-4506832 pustaka.upsi.edu.my Perpustakaan Tuanku Bainun Kampus Sultan Abdul Jalil Shah PustakaTBainun ptbupsi

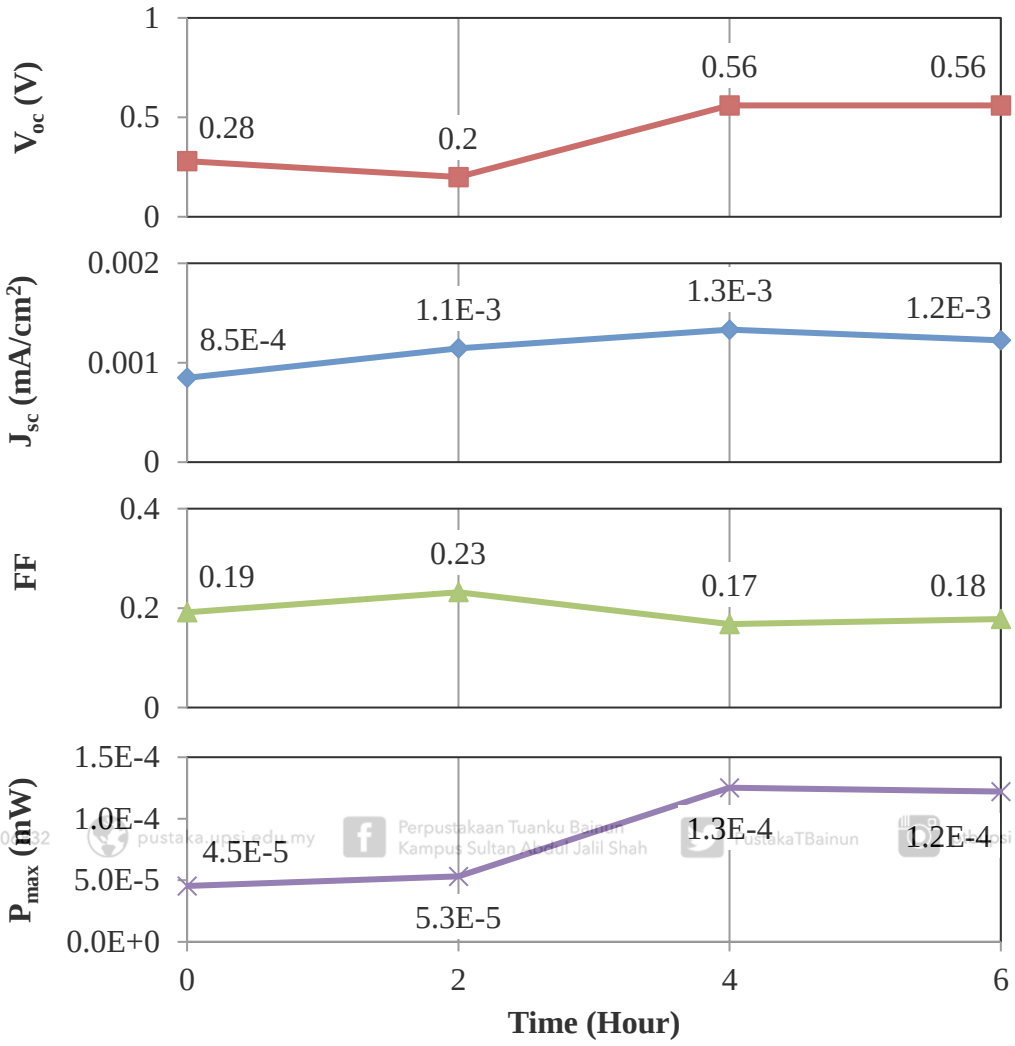


Figure 4.18. Evaluation of open-circuit voltage (V_{oc}), short-circuit current density (J_{sc}), fill factor (FF) and maximum power output (P_{max}) at different H_2S gas exposure time.

Short-circuit current density, J_{sc}, is the maximum current that a thin film is able to produce under a given illumination power without an external voltage source connected, that is when V=0 V. It is used to measure thin film absorption. From the graph, the J_{sc} is very low for all thin films, at the fraction of micrometer Ampere. The J_{sc} is only slightly improved when exposed for 4 and 6 hours, owing to increment in CdS nanoparticles

05-4506832 pustaka.upsi.edu.my Perpustakaan Tuanku Bainun Kampus Sultan Abdul Jalil Shah PustakaTBainun ptbupsi

05-4506832 pustaka.upsi.edu.my Perpustakaan Tuanku Bainun Kampus Sultan Abdul Jalil Shah PustakaTBainun ptbupsi

volume. The raised in amount of nanoparticles created more D/A interface and reduced recombination rate, consequently enhanced the charge transport (Truong, W. K. Kim & C. Park, 2011).

Fill factor or FF is related to charge transport, where it is desired to have high mobility in order to prevent significant loss by recombination (Bartelt, Lam, Burke, Sweetnam & McGehee, 2015; Riedel & Dyakonov, 2004). However, the FF for all thin films are quite small, reflects the high recombination rates occur in the thin film as supported by low J_{sc} value as discussed earlier. Generally, large FF value implies good device efficiency.

Maximum power output, P_{max} is related to FF, in which it implies the point where voltage and current of a device is at maxima, or the "squareness" of the FF. Mathematically,

$$P_{max}=V_{MPP}\times J_{MPP} \quad (4.3)$$

where, V_{MPP} and J_{MPP} are voltage and current density at maximum power point (MPP). Electronic device must be operated at maximum power point in order to generate maximum energy efficiency and minimum losses (Bartesaghi et. al. 2015). All thin films have very low P_{max}, with a slight improvement when the films were exposed for 4 and 6 hour. In general, thin films exposed to H_2S gas for 4 hours give the best electrical performance.

The J-V graphs for thin films exposed to H_2Se gas for 0, 2, 4 and 6 hours are displayed in Figure 4.19 (a), (b), (c) and (d). It can be seen from the graphs, the thin films exposed to H_2Se gas also generated electricity when illuminated with solar simulator.

05-4506832 pustaka.upsi.edu.my Perpustakaan Tuanku Bainun Kampus Sultan Abdul Jalil Shah PustakaTBainun ptbupsi

05-4506832 pustaka.upsi.edu.my Perpustakaan Tuanku Bainun Kampus Sultan Abdul Jalil Shah PustakaTBainun ptbupsi

Similar to the samples exposed to H_2S gas, the current generated were small. The presence of stearic acid and the morphology of thin films are suspected to be the perpetrator.

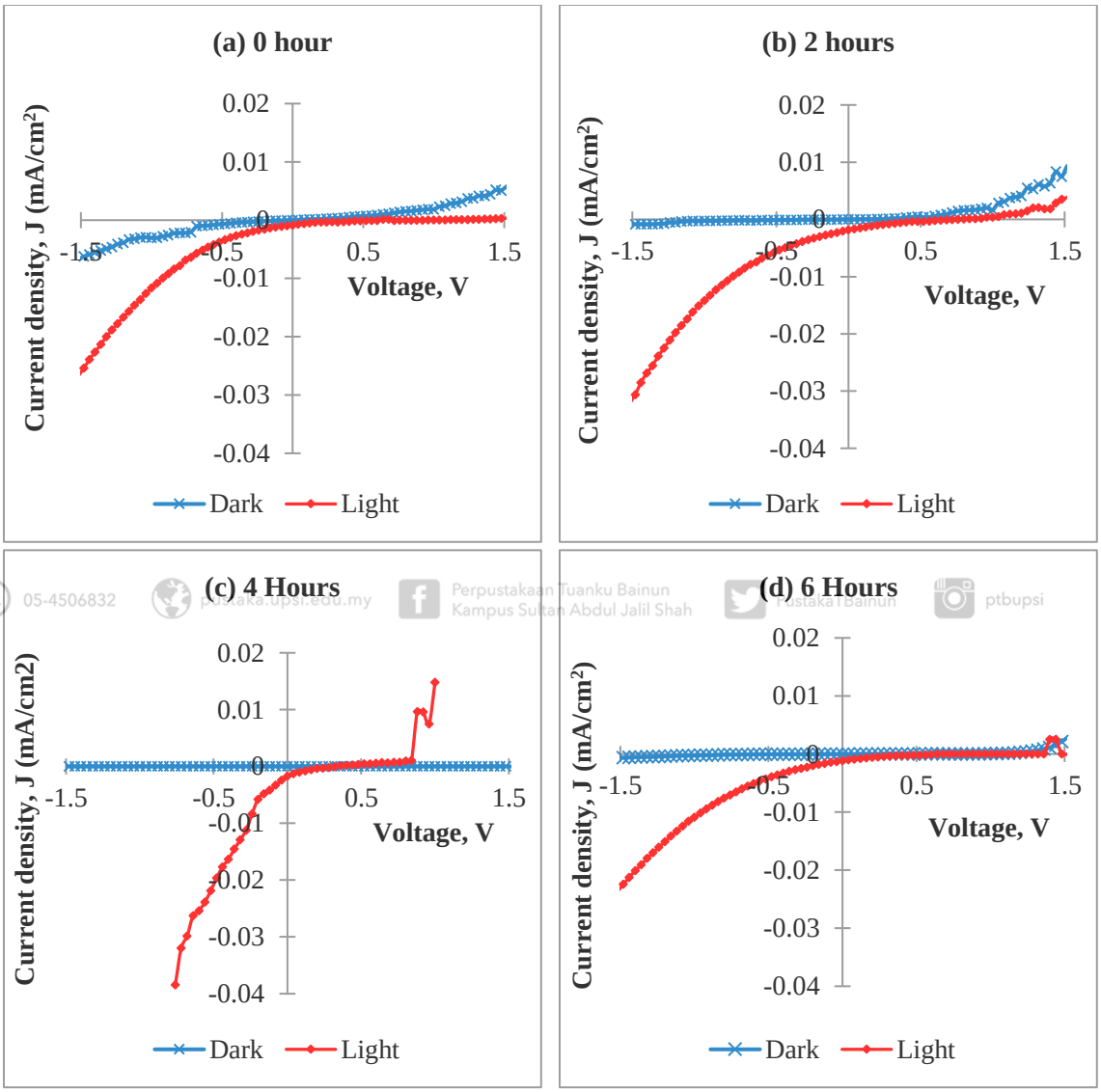


Figure 4.19. Current density versus voltage (J-V) graphs for sample exposed to H_2Se gas for (a) 0 hour, (b) 2 hours, (c) 4 hours, (d) 6 hours

05-4506832 pustaka.upsi.edu.my Perpustakaan Tuanku Bainun Kampus Sultan Abdul Jalil Shah PustakaTBainun ptbupsi

05-4506832 pustaka.upsi.edu.my Perpustakaan Tuanku Bainun Kampus Sultan Abdul Jalil Shah PustakaTBainun ptbupsi

Figure 4.20 shows data extracted from the graphs of Figure 4.19 (a) to (d), by subtracting the current density values in dark and under illumination. Similar to thin films exposed to H_2S gas mentioned earlier, the focus of electrical properties is in the fourth quadrant of the graph only. Thin film exposed to H_2Se gas for 2 hours shows metallic behavior, similar to that of exposed to H_2S gas.

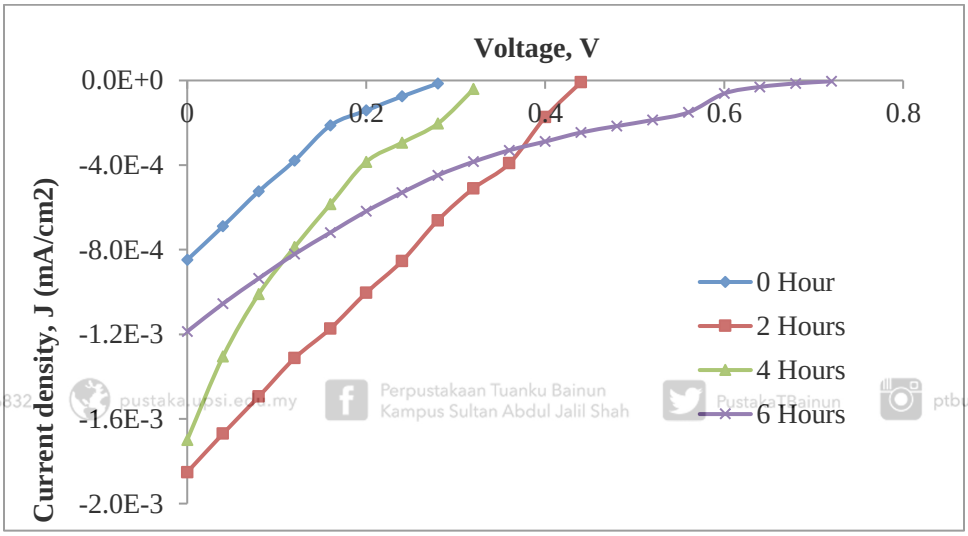


Figure 4.20. The fourth quadrant of current density versus voltage (J-V) curve for thin films exposed to H_2Se gas at varying time

The analyzed electrical parameters of the hybrid nanocomposite thin films exposed to H_2Se gas is shown in Figure 4.21. From the overall parameters measured, the best electrical performance is showed by thin films treated for 2 hours. The comparison graphs also manifest the instability of electrical properties the thin films in all films except for 2 hour exposure, in which they do not follow any profile of increment or

05-4506832 pustaka.upsi.edu.my Perpustakaan Tuanku Bainun Kampus Sultan Abdul Jalil Shah PustakaTBainun ptbupsi

05-4506832 pustaka.upsi.edu.my Perpustakaan Tuanku Bainun Kampus Sultan Abdul Jalil Shah PustakaTBainun ptbupsi

decrease. The same trend of fluctuation has been evidenced in UV-Vis and PL investigation.

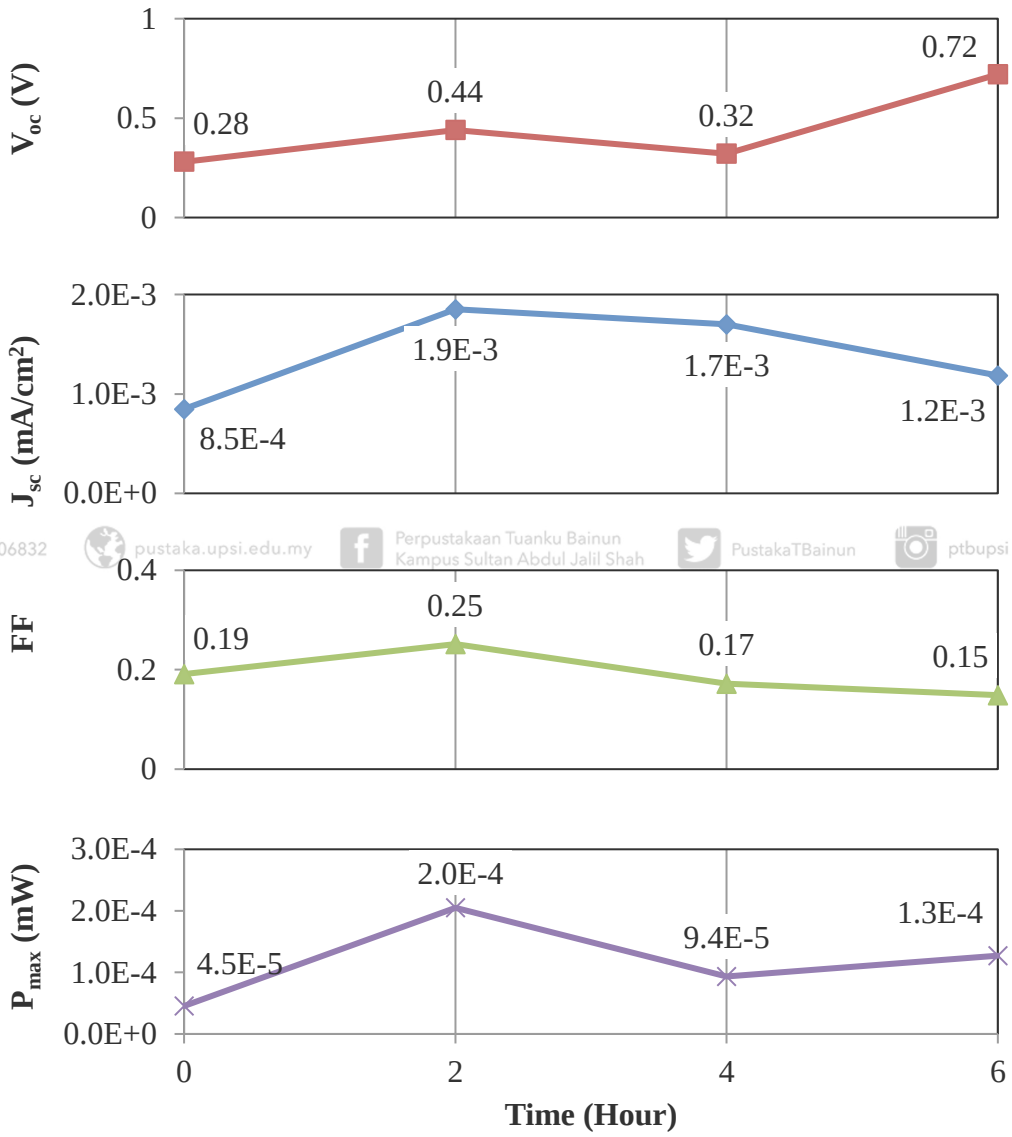


Figure 4.21. Evaluation of open-circuit voltage (V_{oc}), short-circuit current density (J_{sc}), fill factor (FF) and maximum power output (P_{max}) at different H_2Se gas exposure time

05-4506832 pustaka.upsi.edu.my Perpustakaan Tuanku Bainun Kampus Sultan Abdul Jalil Shah PustakaTBainun ptbupsi

05-4506832 pustaka.upsi.edu.my Perpustakaan Tuanku Bainun Kampus Sultan Abdul Jalil Shah PustakaTBainun ptbupsi

The details for samples exposed to H_2S and H_2Se gas is shown in Table 4.4. It can be concluded that all samples have quite low FF. Nonetheless, the P_{max} shows increment as H_2S gas exposure time increase. Samples exposed to H_2Se environment shows fluctuating data. However, after 6 hours of gas exposure, the sample gives high P_{max}, V_{oc} and J_{sc}.

Table 4.4

The electrical properties of thin films exposed to H_2S and H_2Se gas at different exposure time

		V_{oc} (V)	J_{sc} (mA/cm^2)	V_{MPP} (V)	J_{MPP} (mA/cm^2)	FF	P_{max} (mW)
	0 Hour	0.28	8.5×10^{-4}	0.12	3.8×10^{-6}	0.19	4.5×10^{-5}
H_2S	**2 Hours**	0.2	1.1×10^{-3}	0.12	4.4×10^{-6}	0.23	5.3×10^{-5}
	4 Hours	0.32	1.3×10^{-3}	0.28	4.6×10^{-4}	0.17	1.3×10^{-4}
	6 Hours	0.2	1.2×10^{-3}	0.24	5.0×10^{-4}	0.18	1.2×10^{-4}
H_2Se	**2 Hours**	0.44	1.9×10^{-3}	0.24	8.3×10^{-4}	0.25	2.0×10^{-4}
	4 Hours	0.32	1.7×10^{-3}	0.16	5.9×10^{-6}	0.17	9.4×10^{-5}
	6 Hours	0.72	1.2×10^{-3}	0.24	5.5×10^{-4}	0.15	1.3×10^{-4}

4.5.2 *Ex situ* Hybridization

Electrical parameters for thin films made from P3HT:QDs at different weight percentage has been evaluated from J-V graphs presented in Figure 4.22 (a) and (b). The graph for thin films implanted with 25 wt% and 50 wt % of quantum dots almost overlapping for

05-4506832 pustaka.upsi.edu.my Perpustakaan Tuanku Bainun Kampus Sultan Abdul Jalil Shah PustakaTBainun ptbupsi

05-4506832 pustaka.upsi.edu.my Perpustakaan Tuanku Bainun Kampus Sultan Abdul Jalil Shah PustakaTBainun ptbupsi

both in dark and under illumination. The trend is identical for both P3HT:CdS and P3HT:CdSe.

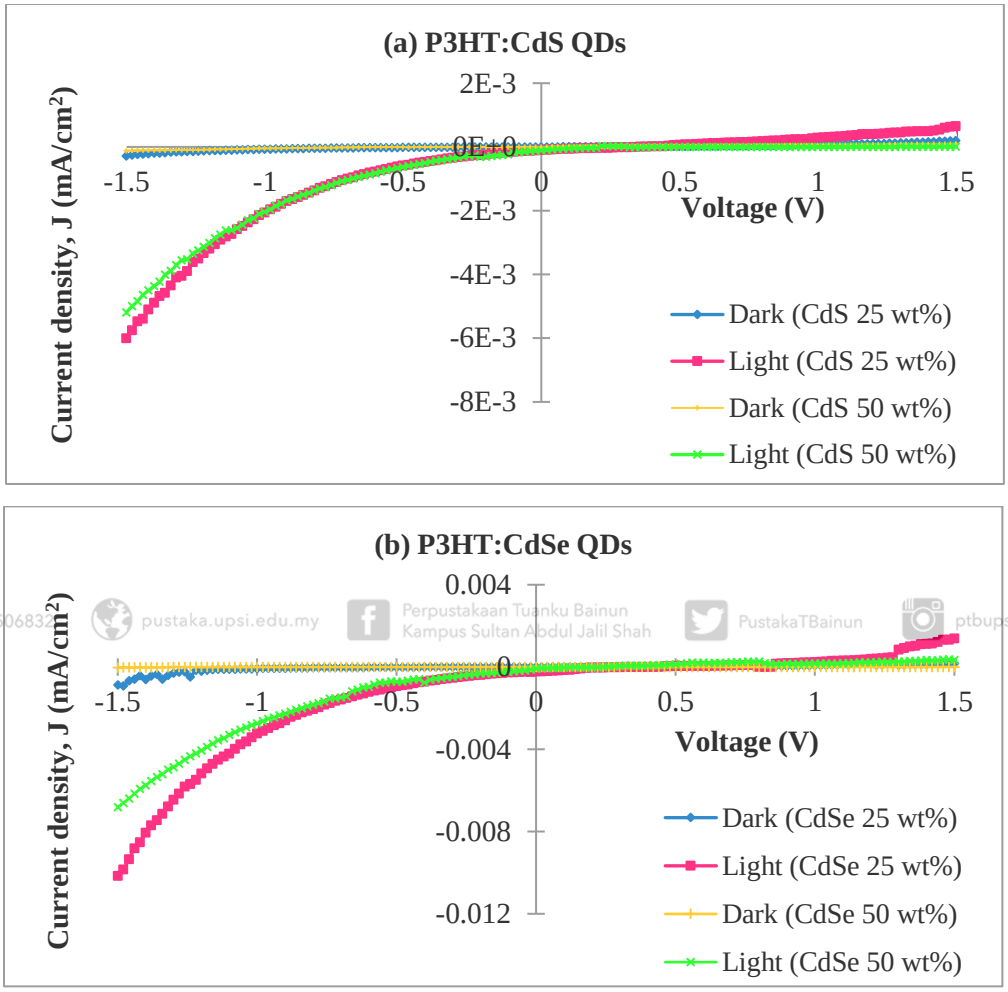


Figure 4.22. Current density versus voltage (J-V) graphs for (a) P3HT:CdS quantum dots thin films, (b) P3HT:CdSe quantum dots thin films

When only the fourth quadrant of the graph is considered in order to study the electrical parameters of the thin film, Figure 4.23 can be extracted. It is obvious that the current density for all thin films is not stable. While the effect of weight percentage is not

05-4506832 pustaka.upsi.edu.my Perpustakaan Tuanku Bainun Kampus Sultan Abdul Jalil Shah PustakaTBainun ptbupsi

05-4506832 pustaka.upsi.edu.my Perpustakaan Tuanku Bainun Kampus Sultan Abdul Jalil Shah PustakaTBainun ptbupsi

apparent for thin films added with CdS quantum dots, doubling the amount of CdSe quantum dots causing the short-circuit current density, J_{sc} and open-circuit voltage, V_{oc} to drop.

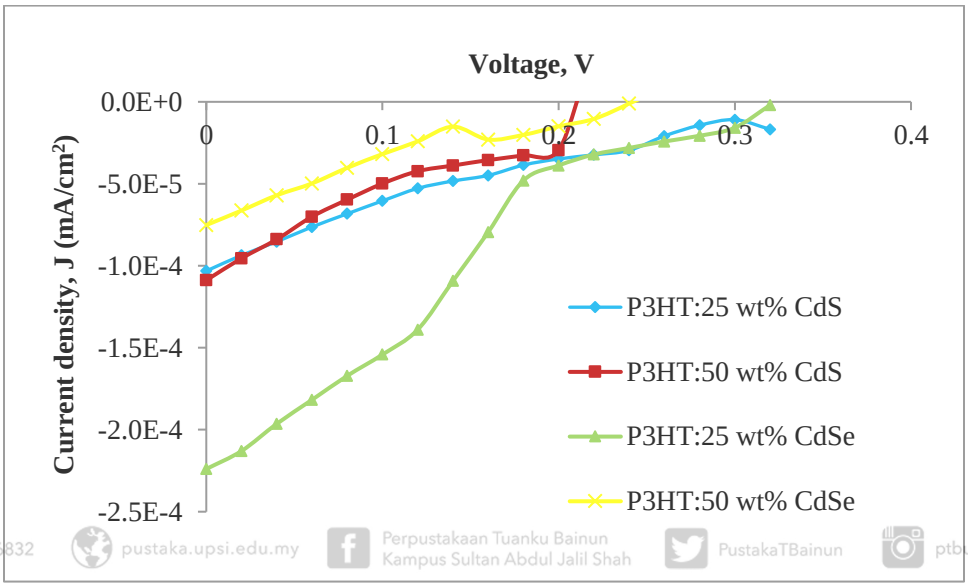


Figure 4.23. The fourth quadrant of current density versus voltage (J-V) curve for thin films fabricated by physically mixing P3HT with quantum dots at different weight percentage

The electrical parameters of the thin films fabricated by physical mixing method are portrayed in Figure 4.24. From the graphs, the polymer hybridized with 50 wt% of CdS quantum dots show very small improvement in terms of currents generated, J_{sc} and open-circuit voltage, V_{oc} even the amount of quantum dots were doubled. Contrary to P3HT:CdSe thin film, where the J_{sc} and V_{oc} decrease when the CdSe quantum dots quantity was increased to 50 wt%.

05-4506832 pustaka.upsi.edu.my Perpustakaan Tuanku Bainun Kampus Sultan Abdul Jalil Shah PustakaTBainun ptbupsi

05-4506832 pustaka.upsi.edu.my Perpustakaan Tuanku Bainun Kampus Sultan Abdul Jalil Shah PustakaTBainun ptbupsi

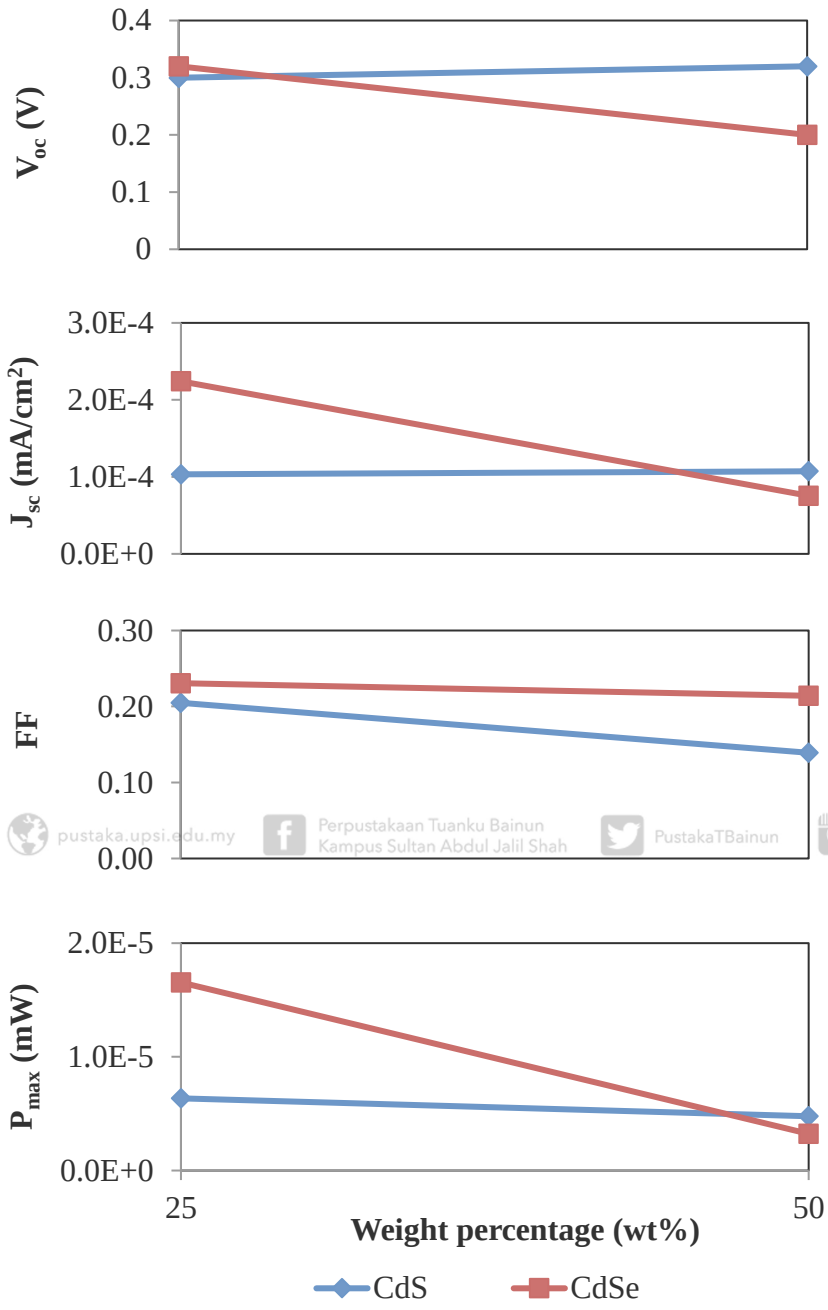


Figure 4.24. Measurement parameters for P3HT:CdS and P3HT:CdSe thin films made from different quantum dots loading amounts

From the graphs, it can be seen that P3HT:25 wt% CdSe QDs gave the best performance in every aspect. The other three thin film samples have comparable low value

05-4506832 pustaka.upsi.edu.my Perpustakaan Tuanku Bainun Kampus Sultan Abdul Jalil Shah PustakaTBainun ptbupsi

05-4506832 pustaka.upsi.edu.my Perpustakaan Tuanku Bainun Kampus Sultan Abdul Jalil Shah PustakaTBainun ptbupsi

for every tested parameter, with P3HT:25% CdS QDs shows better FF and P_{max} than its 50 wt% counterpart. Fill factor and P_{max} are very important parameters in determining the efficiency of a device. The detail figures of the electrical properties is summarized in Table 4.5 below.

Table 4.5

The electrical properties of P3HT:QDs thin films at different weight percentage

	V_{oc} (V)	J_{sc} (mA/cm^2)	V_{MPP} (V)	J_{MPP} (mA/cm^2)	FF	P_{max} (mW)
P3HT:25 wt% CdS	0.3	1.03×10^{-4}	0.16	3.97×10^{-5}	0.20	6.35×10^{-6}
P3HT:50 wt% CdS	0.32	1.07×10^{-4}	0.10	4.77×10^{-5}	0.14	4.77×10^{-6}
P3HT:25 wt% CdSe	0.32	2.24×10^{-4}	0.12	1.25×10^{-4}	0.23	1.65×10^{-5}
P3HT:50 wt% CdSe	0.2	7.54×10^{-05}	0.08	4.04×10^{-5}	0.21	3.23×10^{-6}

05-4506832 pustaka.upsi.edu.my Perpustakaan Tuanku Bainun Kampus Sultan Abdul Jalil Shah PustakaTBainun ptbupsi

The result in this study however is somewhat disagreeing with results that have been reported earlier (Lek, Lam, Niziol & Marzec, 2012). They found by increasing the CdSe weight ratio, the electrical performance increases. On the other hand, the increment in performance will only increase until certain weight percentage (Zhou et al., 2011). Low nanoparticles or quantum dots loading causing inefficient percolation pathways for electron transport. However, when the loading is too high the holes mobility is restricted, causing the decrement in device performance.

Overall, these results show much lower parameter performance compared to hybrid nanocomposite thin films fabricated using *in situ* approach. In *in situ* hybridization, the

05-4506832 pustaka.upsi.edu.my Perpustakaan Tuanku Bainun Kampus Sultan Abdul Jalil Shah PustakaTBainun ptbupsi

05-4506832 pustaka.upsi.edu.my Perpustakaan Tuanku Bainun Kampus Sultan Abdul Jalil Shah PustakaTBainun ptbupsi

nanoparticles created were about 9 % only as shown in EDX results, but the V_{oc} and J_{sc} were greater than that of *ex situ* hybrid thin films with 25 wt% and 50 wt% quantum dots in the polymeric layer.

4.6 Johnson Noise Measurement

Johnson noise originates from random motion of free electrons in the device, causing temporary agglomeration of electrons and fluctuating voltage (Vasilescu, 2005). The noise was measured by analyzing the spectra obtained from low frequency electrical noise measurement. Generally, the technique can be used to study quality and reliability of electronic devices (Vandamme, 1994) by screening out potential failure devices that hold excess noise. This is because the power spectral density (PSD) of noise increases with stress and damage (Chobola, Hasse & Růžička, 2003).

The measurement was carried out by first measuring the Johnson noise of transimpedance amplifier at various gain setting. The noise PSD of the 5182 preamplifier used is shown in Figure 4.25, whilst Table 4.6 shows the data at each sensitivity.

05-4506832 pustaka.upsi.edu.my Perpustakaan Tuanku Bainun Kampus Sultan Abdul Jalil Shah PustakaTBainun ptbupsi

05-4506832 pustaka.upsi.edu.my Perpustakaan Tuanku Bainun Kampus Sultan Abdul Jalil Shah PustakaTBainun ptbupsi

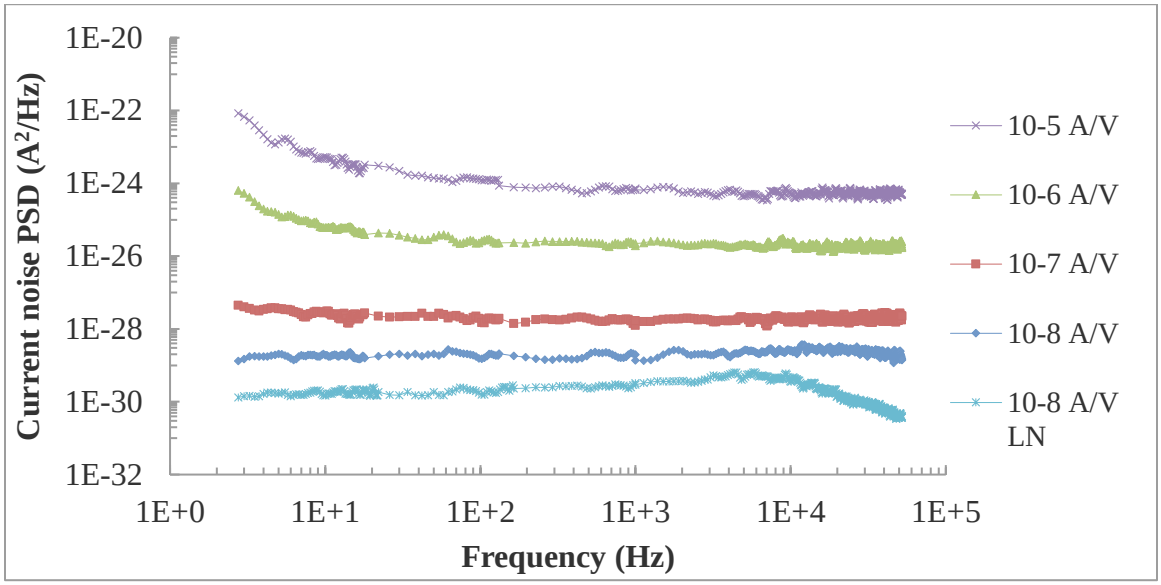


Figure 4.25. Johnson noise of low-noise (LN) current preamplifier 5182 with different gain setting

05-4506832 pustaka.upsi.edu.my Perpustakaan Tuanku Bainun Kampus Sultan Abdul Jalil Shah PustakaTBainun ptbupsi

Table 4.6

The maximum direct current and noise current for every gain setting of 5182 preamplifier

Gain (A/V)	Maximum DC Input Current	Noise Current at 1 kHz
10^{-5}	9 mA	$\frac{10pA}{\sqrt{Hz}}$
10^{-6}	900 μA	$\frac{5pA}{\sqrt{Hz}}$
10^{-7}	9 μA	$\frac{135fA}{\sqrt{Hz}}$
10^{-8}	900 nA	$\frac{45fA}{\sqrt{Hz}}$
10^{-8} , low noise	90 nA	$\frac{15fA}{\sqrt{Hz}}$

05-4506832 pustaka.upsi.edu.my Perpustakaan Tuanku Bainun Kampus Sultan Abdul Jalil Shah PustakaTBainun ptbupsi

05-4506832 pustaka.upsi.edu.my Perpustakaan Tuanku Bainun Kampus Sultan Abdul Jalil Shah PustakaTBainun ptbupsi

The graph shows the lower gain setting that provides more sensitive reading. The lowest gain, 10^{-8} low noise (10^{-8} LN) offers the sensitivity limit of the preamplifier. Noise which is lower than the sensitivity limit will not be able to be recorded by dynamic signal analyzer (DSA). Each gain setting or sensitivity encompasses its own maximum direct current (DC) and noise current. The maximum DC is a safety factor of allowable current to flow through device under test (DUT). On the other hand, maximum noise current is the maximum current noise of the preamplifier at 1 kHz.

The next step was LFNM system set-up validation. The objective of validation is to ensure the experimental set-up measures the correct value of the device noise spectral density. The measurement has been done by measuring Johnson noise of a 5 MΩ resistor. The noise current spectral density under short-circuit condition is then calculated by using Equation 3.11.

Theoretically, the noise is found to be 3.31×10^{-27} A^2/Hz, in which within the same order with the experimental curve portrayed in Figure 4.26. Hence, it can be concluded that the measurement system have been set up properly and are able to record the correct data reading.

05-4506832 pustaka.upsi.edu.my Perpustakaan Tuanku Bainun Kampus Sultan Abdul Jalil Shah PustakaTBainun ptbupsi

05-4506832 pustaka.upsi.edu.my Perpustakaan Tuanku Bainun Kampus Sultan Abdul Jalil Shah PustakaTBainun ptbupsi

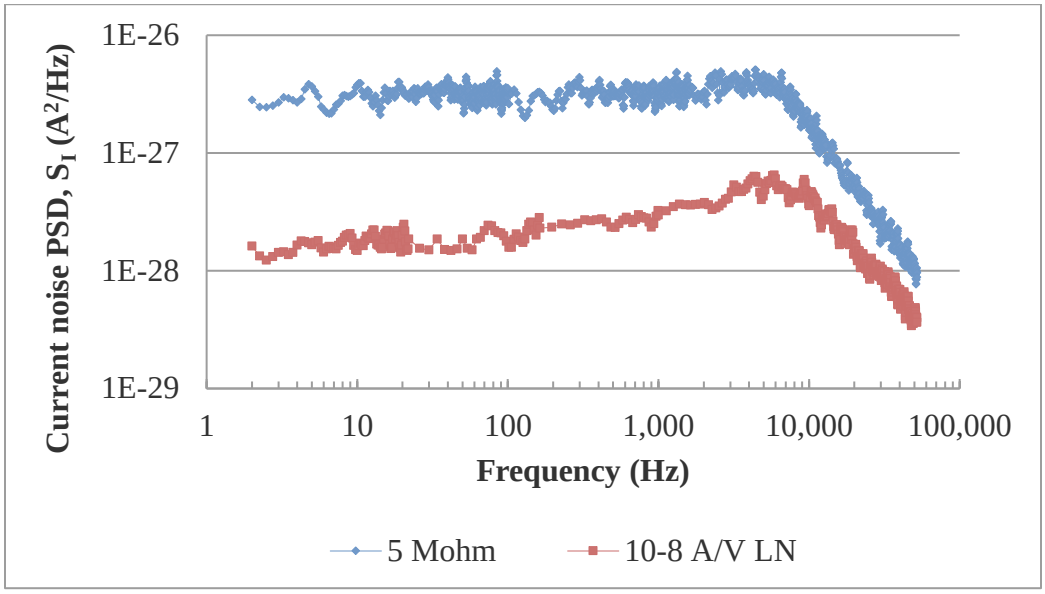


Figure 4.26. Validation of measurement set up using 5 Mohm resistor

05-4506832 pustaka.upsi.edu.my Perpustakaan Tuanku Bainun Kampus Sultan Abdul Jalil Shah PustakaTBainun ptbupsi

4.6.1. *In situ* Hybridization

Once the system set-up validation has been done, the background noise of thin films exposed to H_2S gas was measured as shown in Figure 4.27. The measurement gain has been set at 10^{-8} low noise (LN). The noise current power spectral density, $S_I(f)$ has been measured in the frequency range of 10 Hz to 1000 Hz, in dark room environment. The spectral density of current fluctuation was calculated by averaging 200 of measured traces.

The untreated film has the highest resistance that is conveyed as highest noise spectrum as compared to the treated films. The nature of unexposed film itself, in which comprises of stearic acid is the reason of its high resistivity. Even P3HT is a conjugated

05-4506832 pustaka.upsi.edu.my Perpustakaan Tuanku Bainun Kampus Sultan Abdul Jalil Shah PustakaTBainun ptbupsi

05-4506832 pustaka.upsi.edu.my Perpustakaan Tuanku Bainun Kampus Sultan Abdul Jalil Shah PustakaTBainun ptbupsi

polymer that conducts electrons easily, stearic acid intrinsic property as a resistor thwart electrons movement. Once the films were exposed to H_2S gas, the nucleation of CdS nanoparticles in the polymeric layer aids the electron movement, consequently lowering the noise spectral density. The results compliment J-V measurement discussed in subsection 4.5 in which the higher exposure time, the better the electrical performance.

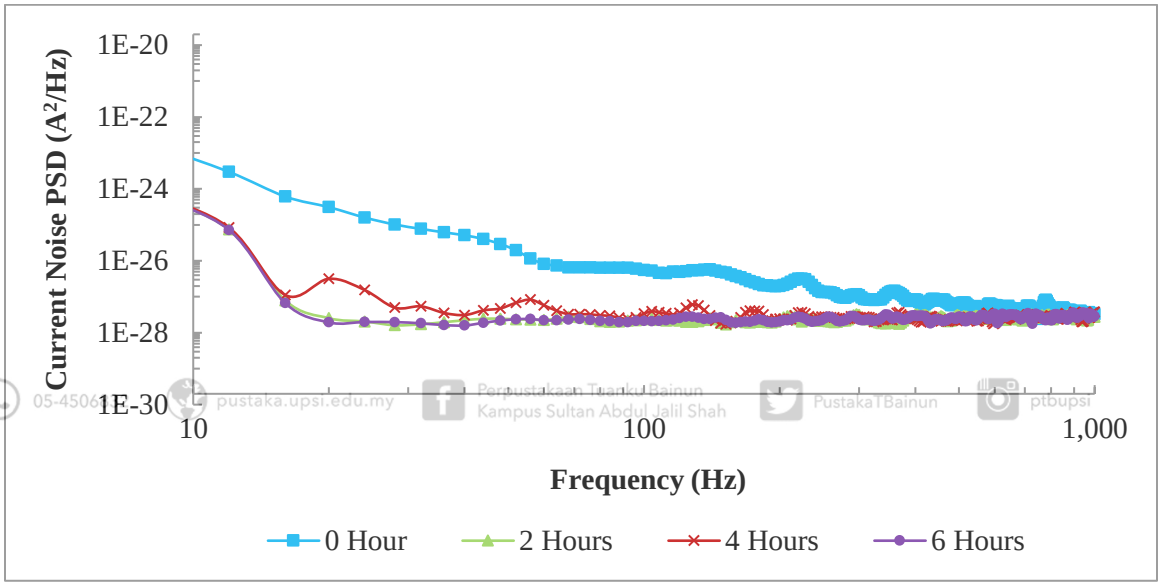


Figure 4.27. Johnson noise current spectral density of thin films exposed to H_2S gas at varying time

On the other hand, for thin films exposed to H_2Se gas, the highest noise spectra is contributed by film exposed for 4 hours, followed by 2 hours and untreated thin film. The film exposed for 6 hours has the lowest noise, implying the nanoparticles created in the film assist in charge mobility. The noise behavior is presented in Figure 4.28. Nonetheless, as demonstrated in other measurement techniques discussed earlier, the thin film exposed to H_2Se gas is bound to less stable as compared to H_2S gas treated film.

05-4506832 pustaka.upsi.edu.my Perpustakaan Tuanku Bainun Kampus Sultan Abdul Jalil Shah PustakaTBainun ptbupsi

05-4506832 pustaka.upsi.edu.my Perpustakaan Tuanku Bainun Kampus Sultan Abdul Jalil Shah PustakaTBainun ptbupsi

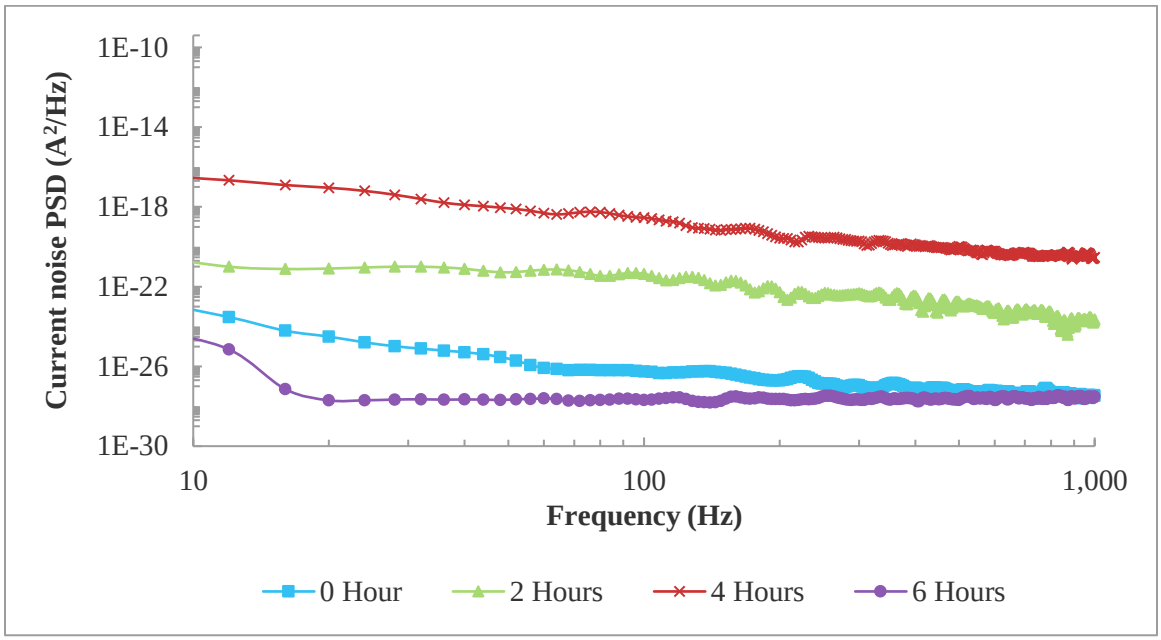


Figure 4.28. Johnson noise current spectral density of thin films exposed to H_2Se gas at varying time

05-4506832 pustaka.upsi.edu.my Perpustakaan Tuanku Bainun Kampus Sultan Abdul Jalil Shah PustakaTBainun ptbupsi

4.6.2 *Ex situ* Hybridization

Thin films made by physically mixing P3HT with CdS or CdSe QDs has very low Johnson noise as compared to thin films fabricated *in situ* approach. One of the advantages of thin film in *ex situ* hybridization is both polymer and QDs are good conductor. Hence the noise for this system in significantly small, regardless of QDs weight percentage or type, as shown in Figure 4.29 and 4.30.

05-4506832 pustaka.upsi.edu.my Perpustakaan Tuanku Bainun Kampus Sultan Abdul Jalil Shah PustakaTBainun ptbupsi

05-4506832 pustaka.upsi.edu.my Perpustakaan Tuanku Bainun Kampus Sultan Abdul Jalil Shah PustakaTBainun ptbupsi

However, at higher frequency, P3HT:CdS thin films showing increasing trend in noise spectra at frequency higher than 100 Hz. This implies the thin film is susceptible to degradation at high frequency.

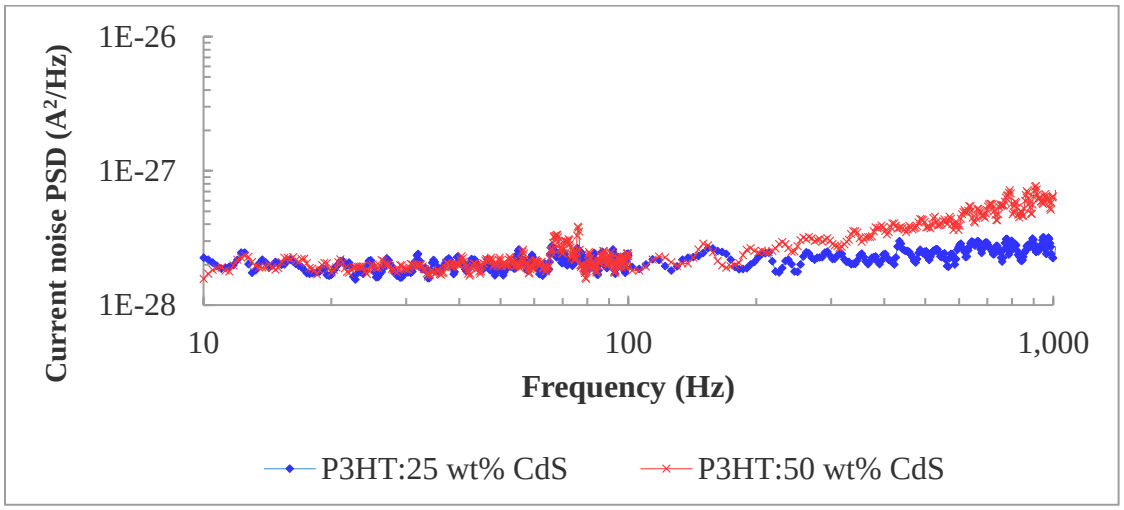


Figure 4.29. Johnson noise current spectral density of P3HT mixed with CdS quantum dot thin films

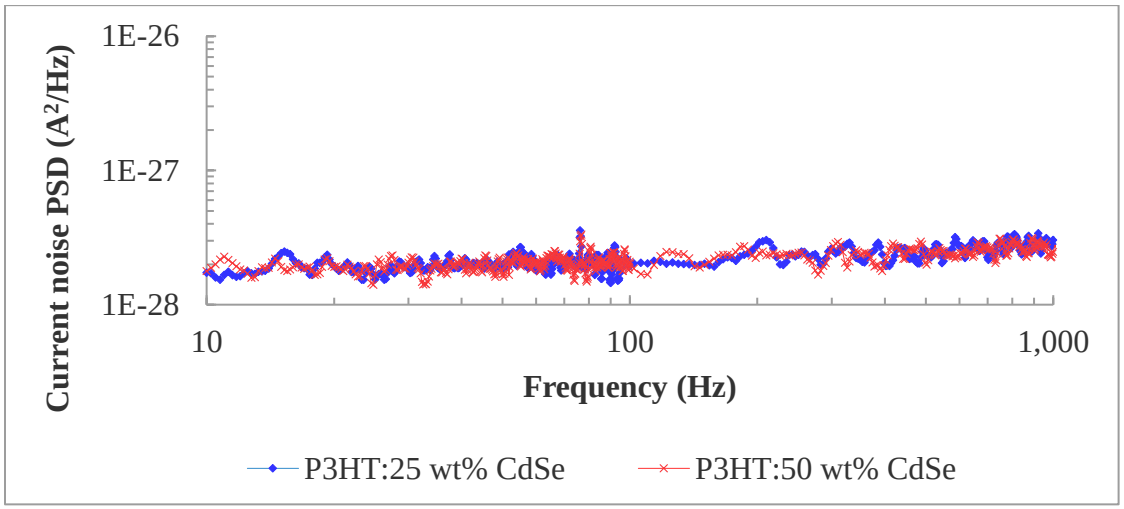


Figure 4.30. Johnson noise current spectral density of P3HT mixed with CdSe quantum dot thin films

05-4506832 pustaka.upsi.edu.my Perpustakaan Tuanku Bainun Kampus Sultan Abdul Jalil Shah PustakaTBainun ptbupsi

05-4506832 pustaka.upsi.edu.my Perpustakaan Tuanku Bainun Kampus Sultan Abdul Jalil Shah PustakaTBainun ptbupsi

4.7 Conclusion

The analysis done on the thin film characterization shows that the nanoparticles embedded in-situ in the polymeric layer has a great potential in electronic device. The gas exposure technique is very simple and cost effective. Nonetheless, nucleation of CdS nanoparticles show more stable results as compared to thin films containing CdSe. The longer exposure time to H_2S gas generally producing better hybrid nanocomposite thin films. Whilst samples exposed to H_2Se gas also shows fluctuating results in all measured characterizations, sample exposed for 6 hours is an exceptional where it starts giving good results.

Thin films fabricated through *ex situ* method do not show significant improvement in optical and electrical properties even when the wt% of quantum dots were doubled. Hence, it can be concluded that even *in situ* method produced nanoparticles less than 10%, the results demonstrated it has better performance than that of *ex situ* method that contain 25 and 50 wt% of QDs.

05-4506832 pustaka.upsi.edu.my Perpustakaan Tuanku Bainun Kampus Sultan Abdul Jalil Shah PustakaTBainun ptbupsi

05-4506832 pustaka.upsi.edu.my Perpustakaan Tuanku Bainun Kampus Sultan Abdul Jalil Shah PustakaTBainun ptbupsi

CHAPTER 5

CONCLUSIONS AND SUGGESTIONS FOR FUTURE WORK

05-4506832 pustaka.upsi.edu.my Perpustakaan Tuanku Bainun Kampus Sultan Abdul Jalil Shah PustakaTBainun ptbupsi

5. 1 Introduction

A thorough investigation of hybrid organic-inorganic nanocomposite thin films deposited using modified Langmuir-Blodgett technique has been conducted. Two fabrication systems have been designed: *in situ* and *ex situ* hybrid nanocomposite thin film fabrication. The focus of study is on *in situ* hybridization where CdS or CdSe nanoparticles were nucleated in the P3HT:stearic acid thin films through gas exposure technique. On the other hand, *ex situ* hybridization thin films were fabricated by physically mixing CdS or CdSe quantum dots into P3HT solution. The surface pressure –area isotherm of Langmuir layer, the optical and electrical properties of the thin films fabricated were characterized. The finding of this

05-4506832 pustaka.upsi.edu.my Perpustakaan Tuanku Bainun Kampus Sultan Abdul Jalil Shah PustakaTBainun ptbupsi

05-4506832 pustaka.upsi.edu.my Perpustakaan Tuanku Bainun Kampus Sultan Abdul Jalil Shah PustakaTBainun ptbupsi

study can be a reference in the future for evaluating the reliability of hybrid nanocomposite thin films prepared through modified Langmuir Blodgett technique.

In this chapter, the general conclusion formulated from the finding of this study is presented. Several recommendations are also highlighted to improve the methodology of the current study and as a continuation of the research in the future.

5.2 Conclusion

This study was motivated by the possibility of exploiting hybrid organic/inorganic nanocomposite thin films as the alternative for optoelectronics devices. Modified Langmuir-Blodgett technique has been employed to deposit the thin film. All research objectives have been met in this research.

Study on surface pressure–area (Π-A) isotherm graphs reveals that Langmuir layer is sensitive towards its environment. The Π-A graphs of P3HT layer shows no distinct phase due to its long chain structure while stearic acid displays distinct gas-liquid-solid phase development. The mixture of the P3HT with stearic acid (P3HT:stearic acid) is dominated by stearic acid profile, until the ratio of 3:1. The changes in subphase purities also affecting the Langmuir profile, even the concentration of $CdCl_2$ were very small, 0.5 mM and 1.0 mM, where the gas-liquid transformation occurs earlier. On the other hand, the higher weight percentage of quantum dots in the P3HT solution caused the lift-off to

05-4506832 pustaka.upsi.edu.my Perpustakaan Tuanku Bainun Kampus Sultan Abdul Jalil Shah PustakaTBainun ptbupsi

05-4506832 pustaka.upsi.edu.my Perpustakaan Tuanku Bainun Kampus Sultan Abdul Jalil Shah PustakaTBainun ptbupsi

start later. Once the Langmuir layer has been studied, the nanocomposite thin films were devised.

Hybrid organic/inorganic nanocomposite thin films were fabricated through *in situ* and *ex situ* approach. *In situ* hybridization is a method where CdS or CdSe nanoparticles were directly growth in the thin films once the Langmuir layers of P3HT:stearic acid have been deposited on the substrate. The nanoparticles were nucleated by exposing the thin films to H_2S or H_2Se gas. The gas exposure time has been varied as to investigate its influence on optical and electrical properties. On the other hand, *ex situ* hybridization were done by mixing CdS or CdSe quantum dots into P3HT solution. The amount of quantum dots was varied as to comprehend its effect.

05-4506832 pustaka.upsi.edu.my Perpustakaan Tuanku Bainun Kampus Sultan Abdul Jalil Shah PustakaTBainun ptbupsi

The optical properties of the thin films were investigated using UV-Vis spectrophotometer and photoluminescence (PL) spectroscopy. The optical absorption of thin films fabricated by *in situ* method shows lower absorbance as gas exposure time increases. The reduction in absorption intensity might due to scattering effect by the nanoparticles. Longer gas exposure time causing higher amount of nanoparticle created, hence higher scattering effect. The thin films fabricated ex situ displays similar spectra profile even when the amount of quantum dots was doubled. Whilst the amount of quantum dots did not affecting the absorbance greatly, the PL intensity decreased with increment of quantum dots' weight percentage.

05-4506832 pustaka.upsi.edu.my Perpustakaan Tuanku Bainun Kampus Sultan Abdul Jalil Shah PustakaTBainun ptbupsi

05-4506832 pustaka.upsi.edu.my Perpustakaan Tuanku Bainun Kampus Sultan Abdul Jalil Shah PustakaTBainun ptbupsi

The electrical performance was investigated through open circuit voltage (V_{oc}), short-circuit current density (J_{sc}), fill factor, maximum power (P_{max}), and Johnson noise. The *in situ* hybrid thin films exhibit greater V_{oc}, J_{sc}, FF and P_{max} than that of *ex situ*. The results also showed for thin films mixed with either CdS or CdSe quantum dots, the performance is even lower when the quantum dots loading were doubled to 50 wt%. *Ex situ* hybrid thin films possess very low Johnson noise. Good conductivity in conjugated polymer P3HT and semiconductor properties of the quantum dots might contribute to this phenomenon.

Generally, the thin film exposed to H_2S gas, hence forming CdS nanoparticles, shows better optical and electrical properties than the thin films exposed to H_2Se gas. Improved performances were attained with longer gas exposure time, 4 and 6 hours. This might be due to higher percentage of nanoparticle nucleated in the film as revealed by FESEM and EDX analysis.

These findings concluded that both *in situ* and *ex situ* hybrid thin films have their own advantages. Whilst the noise of the *ex situ* films were very low, in the other aspect of characterizations it did not give good performance. Hybrid nanocomposite thin films fabricated through *in situ* method show better results in both optical and electrical measurement. The steps in fabricating the thin films also less tedious as compared to *ex situ* method. Therefore this technique can be manipulated in producing high quality hybrid organic-inorganic nanocomposite thin films.

05-4506832 pustaka.upsi.edu.my Perpustakaan Tuanku Bainun Kampus Sultan Abdul Jalil Shah PustakaTBainun ptbupsi

05-4506832 pustaka.upsi.edu.my Perpustakaan Tuanku Bainun Kampus Sultan Abdul Jalil Shah PustakaTBainun ptbupsi

5.4 Suggestions for Future Work

Arising from the results of the work obtained, the study could be further investigated in several aspects as follows:

i) Investigation of different types of salt (such as lead chloride or copper chloride) added into the subphase in order to produce other types of nanoparticles in the thin films.

ii) Study the electron transport mechanism in the hybrid nanocomposite thin films to gain further understanding of their electrical properties.

iii) Design and develop a gas pressure system when exposing the thin films to the H_2S or H_2Se gas to force the gas to penetrate the polymeric thin films deeply.

iv) Thorough analysis on the morphology of the thin films as to relate the optical behavior of the thin films.

05-4506832 pustaka.upsi.edu.my Perpustakaan Tuanku Bainun Kampus Sultan Abdul Jalil Shah PustakaTBainun ptbupsi

05-4506832 pustaka.upsi.edu.my Perpustakaan Tuanku Bainun Kampus Sultan Abdul Jalil Shah PustakaTBainun ptbupsi

REFERENCES

Aberle, A. G. & Widenborg, P. I. (2011). Crystalline silicon thin-film solar cells via high-temperature and intermediate-temperature approaches. In A. Luque & S. Hegedus (Eds.), *Handbook of Photovoltaic Science and Engineering* (pp. 452-486). Chichester, UK: John Wiley & Sons Ltd. doi: 10.1002/9780470974704.ch11

Alam, J., Riaz, U. & Ahmad, S. (2007). Effect of ferrofluid concentration on electrical and magnetic properties of the Fe_3O_4/PANI nanocomposites. *Journal of Magnetism and Magnetic Material 314*(2), 93-99. doi: 10.1016/j.jmmm.2007.02.195

Al-Bat'hi S. A. M. (2015). Electrodeposition of nanostructure materials. In A. Mahmood (Ed.), *Electroplating of nanostructures*. Retrieved from: http://www.intechopen.com/books/electroplating-of-nanostructures/electrodeposition-of-nanostructure-materials

Alhreb, B. M., Almasri, K. & Alhariri, S. (2014). Fabrication and characterization of poly(3-hexylthiophene) (P3HT) sensor in two techniques (dip-coating and spin-coating) and sensitivity compared for various vapors. *International Journal of ChemTech Research, 6*(7), 3690-3696. Retrieved from http://sphinxsai.com/2014/ch_vol_6_7/4/%283690-3696%29O14.pdf

Amin, B. (2011). *Structural, electronic, optical and magnetic properties of metals doped III-V semiconductors* (Doctoral Dissertation). Retrieved from http://prr.hec.gov.pk/ Thesis/ 1364S.pdf

Aminuzzaman, M., Mitsuishi, M. & Miyashita, T. (2010). Fabrication of fluorinated polymer nanosheets using the Langmuir–Blodgett technique: characterization of their surface properties and applications. *Polymer International*, *59*, 583–596. doi: 10.1002/pi.276

Anita, S., Ramachandran, T., Koushik, C. V., Rajendran, R. & Mahalakshmi, M. (2010). Preparation and characterization of zinc oxide nanoparticles and a study of anti-microbial property of cotton fabric treated with the particles. *Journal of Textile and Apparel, Technology and Management, 6*(4), 1-7.

Aoki, A. & Fukuyama, S. (2012). Organic thin film solar cell composed of hetero-deposited Langmuir-Blodgett films. *Electrochemistry*, *78*(2), 178-180. doi: 10.5796/ electrochemistry.78.178

05-4506832 pustaka.upsi.edu.my Perpustakaan Tuanku Bainun Kampus Sultan Abdul Jalil Shah PustakaTBainun ptbupsi

05-4506832 pustaka.upsi.edu.my Perpustakaan Tuanku Bainun Kampus Sultan Abdul Jalil Shah PustakaTBainun ptbupsi

Ariga, K., Yamauchi, Y., Mori, T. & Hill, J. P. (2013). What can be done with the Langmuir-Blodgett method? Recent developments and its critical role in materials science. *Advanced Materials, 25*, 6477–6512. doi: 10.1002/adma.201302283

Atwater, H. A. & Polman, A. (2010). Plasmonics for improved photovoltaic devices. *Nature Materials, 9*, 205–213. doi:10.1038/nmat2629

Bakalova, R., Ohba, H., Zhelev, Z., Ishikawa, M. & Baba, Y. (2004). Quantum dots as photosensitizers? *Nature Biotechnology, 22*(11), 1360–1361. doi: 10.1038/nbt1104-1360

Banerjee, R., Jayakrishnan, R. & Ayyub, P. (2000). Effect of the size-induced structural transformation on the band gap in CdS nanoparticles. *Journal of Physics: Condensed Matter*, *12*, 10647-10654.

Barraud, A., Leloup, J. & Lesieur, P. (1985). Monolayers on a glycerol subphase. *Thin Solid Films*, *133*, 113-116. doi: 10.1016/0040-6090(85)90430-4

Bartelt J. A., Lam D., Burke T. M., Sweetnam S. M. & McGehee M. D. (2015). Charge-carrier mobility requirements for bulk heterojunction solar cells with high fill factor and external quantum efficiency >90%. *Advanced Energy Materials, 5*, 1500577. doi: 10.1002/aenm.201500577

05-4506832 pustaka.upsi.edu.my Perpustakaan Tuanku Bainun Kampus Sultan Abdul Jalil Shah PustakaTBainun ptbupsi

Bartesaghi, D., Pérez, I. D., Kniepert, J., Roland, S., Turbiez, M. & Koster, D. N. L. J. A. (2015). Competition between recombination and extraction of free charges determines the fill factor of organic solar cells. *Nature Communications 6*, Article number 7083. doi:10.1038/ncomms8083

Baschir, L., Fagadar-Cosma, E., Creanga, I., Palade, A., Lascu, A., Birdeanu, M. … Simandan I. D. (2014). UV sensing effect in Langmuir-Blodgett complex films containing a novel synthesized Fe(III) porphyrin. *Digest Journal of Nanomaterials and Biostructures 9*, 847–857.

Bhattacharya, R. & Saha, S. (2008). Growth of CdS nanoparticles by chemical method and its characterization. *Pramana - Journal of Physics*, *71*(1), 187-192. doi: 10.1007/ s12043-008-0152-7

Bicelli, L. P., Bozzini, B., Mele, C. & D'Urzo, L. (2008). A review of nanostructural aspects of metal electrodeposition. *International Journal of Electrochemical Science, 3*, 356 – 408.

Bilewicz, R. & Majda, M. (1991). Monomolecular Langmuir-Blodgett films at electrodes. Formation of passivating monolayers and incorporation of electroactive reagents. *Langmuir*, *7*(11), 2794-2802. doi: 10.1021/la00059a063

05-4506832 pustaka.upsi.edu.my Perpustakaan Tuanku Bainun Kampus Sultan Abdul Jalil Shah PustakaTBainun ptbupsi

05-4506832 pustaka.upsi.edu.my Perpustakaan Tuanku Bainun Kampus Sultan Abdul Jalil Shah PustakaTBainun ptbupsi

Blodgett, K. B. & Langmuir, I. (1937). Built-up films of barium stearate and their optical properties. *Physics Review*, *51*(11), 964-982. doi: 10.1103/PhysRev.51.964

Blodgett, K. B. (1935). Films built by depositing successive monomolecular layers on a solid surface. *Journal of the American Chemical Society, 57*(6), 1007-1022. doi: 10.1021/ja01309a011

Bosi, M. & Pelosi, C. (2007). The potential of III-V semiconductors as terrestrial photovoltaic devices. *Progress in Photovoltaics: Research and Applications, 15*, 51–68. doi: 10.1002/pip.715

Brabec, C. J., Zerza, G., Cerullo, G., De Silvestri, S., Luzzati, S., Hummelen, J. C. & Sariciftci, S. (2001). Tracing photoinduced electron transfer process in conjugated polymer/fullerene bulk heterojunctions in real time. *Chemical Physics Letters 340*(3-4) 232-236 doi: 10.1016/S0009-2614(01)00431-6

Brandão, L., Viana, J., Bucknall, D. G. & Bernardo, G. (2014). Solventless processing of conjugated polymers - A review. *Synthetic Metals, 197*, 23-33 doi:10.1016/ j.synthmet. 2014.08.003.

Brinker, C. J. & Scherer, G. W. (1990). *Sol–gel science: The physics and chemistry of sol–gel processing.* San Diego, CA: Academic Press Limited.

05-4506832 pustaka.upsi.edu.my Perpustakaan Tuanku Bainun Kampus Sultan Abdul Jalil Shah PustakaTBainun ptbupsi

Brown, P. J., Thomas, D. S., Köhler, A., Kim, J. S., Ramsdale, C. M., Sirringhaus, H. & Friend, R. H. (2003). Effect of interchain interactions on the absorption and emission of poly(3-hexylthiophene). *Physics Review B, 67*(6), 064203. doi: 10.1103/PhysRevB. 67.064203

Bruevich, V. V., Sh. T., Makhmutov, S. G., Elizarov, E. M, Nechvolodova, D. & Paraschuk, Y. (2007). Raman spectroscopy of intermolecular charge transfer complex between a conjugated polymer and an organic acceptor molecule. *Journal of Chemical Physics, 127*, 104905–104913. doi: 10.1063/1.2767266

Buthainah. A, Dayang Radiah, A. B, Alnuami. W, Shiva. G., Noor Hazira. H. & Chandima, G. (2013). Review article: applications of nanocomposites in industrial systems. *Journal of Purity, Utility Reaction and Environment*, 2 (5), 92-114.

Cai, W., Gong, X. & Cao, Y. (2010). Polymer solar cells: Recent development and possible routes for improvement in the performance. *Solar Energy Materials and Solar Cells 94*(2), 114–127. doi:10.1016/j.solmat.2009.10.005

Çapan, İ., Uzunoğlu, T., Tarımcı, Ç. & Tanrısever, T. (2008). Electrical characterisation of poly(methyl methacrylate)/arachidic acid Langmuir–Blodgett films. *Thin Solid Films, 516*(24), 8975-8978. doi: 10.1016/j.tsf.2007.11.073

05-4506832 pustaka.upsi.edu.my Perpustakaan Tuanku Bainun Kampus Sultan Abdul Jalil Shah PustakaTBainun ptbupsi

05-4506832 pustaka.upsi.edu.my Perpustakaan Tuanku Bainun Kampus Sultan Abdul Jalil Shah PustakaTBainun ptbupsi

Çapan, R., Richardson, T. H. & Lacey, D. (2001). The Langmuir properties of a mixed copolysiloxane monolayer. *Turkish Journal of Physics, 25*(5), 445-449.

Carbone, A., Kotowska, B. K. & Kotowski, D. D. (2005). Space-charge-limited current fluctuations in organic semiconductors. *Physical Review Letters, 95*, 236601-236605. doi: 10.1103/PhysRevLett.95.236601

Cea, P., Ballesteros, L. M. & Martín, S. (2014). Nanofabrication techniques of highly organized monolayers sandwiched between two electrodes for molecular electronics. *Nanofabrication, 1*, 96–117. doi: 10.2478/nanofab-2014-0010

Cha, S. H., Bae, J. & Lee, K. J. (2015). Enhancement of adhesion between inorganic nanoparticles and polymeric matrix in nanocomposite by introducing polymeric thin film onto nanoparticles. *Polymer Engineering and Science, 55*(8), 1906–1911. doi: 10.1002/pen.24031

Chan, W. C. W, Maxwell, D. J., Gao, X., Bailey, R. E., Han, M. & Nie, S. (2002). Luminescent quantum dots for multiplexed biological detection and imaging. *Current Opinion in Biotechnology, 13*(1), 40–46. doi: 10.1016/S0958-1669(02)00282-3

Chandra, A., Turng, L. S., Gopalan, P., Rowell, R. M. & Gong, S. (2008). Study of utilizing thin polymer surface coating on the nanoparticles for melt compounding of polycarbonate/alumina nanocomposites and their optical properties. *Composite Science Technology, 68*(3-4), 768-776. doi: 10.1016/j.compscitech.2007.08.027

Chapin, D. M., Fuller, C. S. & Pearson, G. L. (1954). A new silicon P-N junction photocell for converting solar radiation into electrical power. *Journal of Applied Physics, 25*, 676–677. doi: 10.1063/1.1721711

Chattopadhyay K. K. & Banerjee A. N. (2009). *Introduction to nanoscience and nanotechnology*. New Delhi, India: PHI Learning Pvt. Ltd.

Chobola, Z., Hasse, L. & Růžička, Z. (2003, June). Measurement of low frequency noise of monocrystalline silicon solar cells. Paper presented at the *XVII IMEKO World Congress,* Croatia.

Choy, K. L. (2003). Chemical vapour deposition of coatings. *Progress in Materials Science, 48*(2), 57-170. doi: 10.1016/S0079-6425(01)00009-3.

Christopher, O. O. & Lerner, M. (2001). Nanocomposites and intercalation compound. In R. Meyers (Ed.), *Encyclopedia of physical science and technology* (pp. 269-283). San Diego, CA: Academic Press. doi: 10.1016/B0-12-227410-5/00468-3

Chung, S. R., Chen, H. S., Chien, C. Y., Bai, M. Y. & Wang, K. W. (2014). The promotion of the efficiency of organic photovoltaic devices by addition of anisotropic CdSe

05-4506832 pustaka.upsi.edu.my Perpustakaan Tuanku Bainun Kampus Sultan Abdul Jalil Shah PustakaTBainun ptbupsi

05-4506832 pustaka.upsi.edu.my Perpustakaan Tuanku Bainun Kampus Sultan Abdul Jalil Shah PustakaTBainun ptbupsi

nanocrystals. *International Journal of Photoenergy, 2014*, 8 pages. doi: 10.1155/ 2014/219123

Chung, W., Park, K., Yu, H. J., Kim, B. & Kim, S. H. (2010). White emission using mixtures of CdSe quantum dots and PMMA as a phosphor. *Optical Materials, 32*(4), 515–521. doi: 10.1016/j.optmat.2009.11.005

Clark , J., Silva, C., Friend, R. H. & Spano, F. C. (2007). Role of intermolecular coupling in the photophysics of disordered organic semiconductors:aggregate emission in regioregular polythiophene. *Physics Review Letter*, *98*, 206406. doi: 10.1103/ PhysRevLett.98.206406

Colvin, V. L., Schlamp, M. C. & Alivisatos, A. P. (1994). Light-emitting diodes made from cadmium selenide nanocrystals and a semiconducting polymer. *Nature*, *370*, 354–357. doi: 10.1038/370354a0

Crisp, D. J. (1946). Surface films of polymers. Part I. Films of the fluid type. *Journal of Colloid Science, 1*(1), 49-70. doi:10.1016/0095-8522(46)90006-2

Czichos, H., Saito, T. & Smith, L. E. (2007). *Springer Handbook of Materials Measurement Methods*. Berlin: Springer Berlin Heidelberg.

Darabi, H. (2015). *Radio frequency integrated circuits and systems*. Cambridge, UK: Cambridge University Press.

Das, N. M., Roy, D., Clarke, N., Ganesan, V. & Gupta, P. S. (2014). Dynamics of roughening and growth kinetics of CdS–polyaniline thin films synthesized by the Langmuir–Blodgett technique. *RSC Advances, 4*, 32490-32503. doi: 10.1039/ C4RA03906H

Dayal, S., Kopidakis, N., Olson, D. C., Ginley, D. S. & Rumbles, G. (2010). Photovoltaic devices with a low band gap polymer and CdSe nanostructures exceeding 3% efficiency. *Nano Letters 10*(1), 239-242. doi: 10.1021/nl903406s

de Freitas, J. N., Grova, I. R., Akcelrud, L. C., Arici, E., Sariciftci, N. S. & Nogueira, A. F. (2010). The effects of CdSe incorporation into bulk heterojunction solar cells. *Journal of Materials Chemistry, 20*(23), 4845-4853. doi: 10.1039/C0JM00191K

Dumbrava, A., Badea, C., Prodan, G. & Ciupina, V. (2010). Synthesis and characterization of cadmium sulfide obtained at room temperature. *Chalcogenide Letters, 7*(2), 111-118.

Durola, F., Sauvage, J. P. & Wenger, O. S. (2010). The magic effect of endocyclic but non sterically hindering biisoquinoline chelates: From fast-moving molecular shuttles to [3]rotaxanes. *Coordination Chemistry Review*, *254*(15-16), 1748-1759. doi: 10.1016/ j.ccr.2009.09.034

05-4506832 pustaka.upsi.edu.my Perpustakaan Tuanku Bainun Kampus Sultan Abdul Jalil Shah PustakaTBainun ptbupsi

05-4506832 pustaka.upsi.edu.my Perpustakaan Tuanku Bainun Kampus Sultan Abdul Jalil Shah PustakaTBainun ptbupsi

Dynarowicz-Latka, P., Dhanabalan, A. & Oliveira, O. N. (2001). Modern physicochemical research on Langmuir monolayers. *Advances in Colloid Interface Science, 91*(2), 221-293. doi: 10.1016/S0001-8686(99)00034-2

El-Bially, A. B., Seoudi, R., Eisa, W., Shabaka, A. A., Soliman, S. I., El-Hamid, R. K. A. & Ramadan, R. A. (2012). Preparation, characterization and physical properties of CdS nanoparticles with different sizes. *Journal of Applied Sciences Research*, *8*, 676-685.

Eloul, S., Batchelor-McAuley, C. & Compton, R. G. (2014). Thin film-modified electrodes: a model for the charge transfer resistance in electrochemical impedance spectroscopy. *Journal of Solid State Electrochemistry 18*(12), 3239-3243. doi: 10.1007/s10008-014-2662-1

Emslie, A. G., Bonner, F. T. & Peek, L. G. (1958). Flow of a viscous liquid on a rotating disk. *Journal of Applied Physics, 29,* 858-862. doi: 10.1063/1.1723300

Erdogan, M., Özbek, Z., Çapan, R. & Yagci, Y. (2012). Characterization of polymeric LB thin films for sensor applications. *Journal of Applied Polymer Science, 123*(4), 2414–2422. doi:10.1002/app.34793

Fang, Z., Wang, X. C., Wu, H. C. & Zhao C. Z. (2011). Achievements and challenges of CdS/CdTe solar cells. *International Journal of Photoenergy, 2011*, 8 pages. doi: 10.1155/2011/297350

Farva, U., Khan, M. A. & Park, C. (2008, May). *Effect of post annealing on the performance of CdSe/P3HT bulk hetero-junction solar cells*. Paper presented at Photovoltaic Specialist Conference, San Diego, CA, USA.

Ferguson, A. J., Kopidakis, N., Shaheen, S. E. & Rumbles, G. (2008). Quenching of excitons by holes in poly(3-hexylthiophene) films. *Journal of Physical Chemistry C, 112*, 9865- 9871. doi: 10.1021/jp7113412

Foest, R., Schmidt, M. & Gargouri, H. (2014). Self-assembling and self-limiting monolayer deposition. *The European Physical Journal D, 68*, 23 pages. doi: 10.1140/epjd/e2013-40420-y

Foubert, A., Beloglazova, N. V., Rajkovic, A., Sas, B., Madder, A., Goryacheva, I. Y. & De Saeger, S. (2016). Bioconjugation of quantum dots: Review and impact on future application. *Trends in Analytical Chemistry*, 83B, 31-48. doi: 10.1016/j.trac.2016.07.008.

Franklin, B. (1774). The stilling of waves by means of oil. *Philosophical Transaction 64,* 445-460. doi: 10.1098/rstl.1774.0044

05-4506832 pustaka.upsi.edu.my Perpustakaan Tuanku Bainun Kampus Sultan Abdul Jalil Shah PustakaTBainun ptbupsi

05-4506832 pustaka.upsi.edu.my Perpustakaan Tuanku Bainun Kampus Sultan Abdul Jalil Shah PustakaTBainun ptbupsi

Freisinger, B. (2013). *Investigation of P3HT/PCBM Particle-Based Solar Cells* (Doctoral Dissertation). Retrieved from https://publications.ub.uni-mainz.de/theses/volltexte/2013/3450/pdf/3450.pdf

Füchsel, K., Schulz, U., Kaiser, N. & Tünnermann, A. (2008). Low temperature deposition of indium tin oxide films by plasma ion-assisted evaporation. *Applied Optics, 47*(13), C297-C302. doi: 10.1364/AO.47.00C297

Gaspera, E. D. & Martucci, A. (2015). Sol-gel thin films for plasmonic gas sensors. *Sensors*, 15, 16910-16928. doi: 10.3390/s150716910

Gaspera, E. D., Gulgielmi, M. & Martucci, A. (2015). Sol-gel for gas sensing applications. In D. Levy, & M. Zayat, (Eds.), *The sol-gel handbook – Synthesis, characterization and applications*: *Synthesis, characterization and applications – 3 Volume set.* (pp. 1173-1206). Weinheim, Germany: Wiley-VCH Verlag GmbH & Co. KGaA. doi: 10.1002/9783527670819.ch38

Gaudiana, R. & Brabec, C. J. (2008). Organic materials – fantastic plastic. *Nature Photonics, 2*, 287–289. doi:10.1038/nphoton.2008.69

Gew, L. T. & Misran, M. (2014). Albumin-fatty acid interactions at monolayer interface. *Nanoscale Research Letters, 9*(1), 218. doi:10.1186/1556-276X-9-218

05-4506832 pustaka.upsi.edu.my Perpustakaan Tuanku Bainun Kampus Sultan Abdul Jalil Shah PustakaTBainun ptbupsi

Giancane, G., Borovkov, V., Inoue, Y., Conoci S. & Valli, L. (2013). Syn–anti conformation switching of a bis-porphyrin derivative at the air–water interface and in the solid state as an effective tool for chemical sensing. *Soft Matter, 9*, 2302-2307. doi: 10.1039/C2SM27141A

Gole, A., Jana, N. R., Selvan, S. T. & Ying, J. Y. (2008). Langmuir−Blodgett thin films of quantum dots: synthesis, surface modification, and Fluorescence Resonance Energy Transfer (FRET) studies. *Langmuir 24*(15), 8181-8186 doi: 10.1021/la8000224

Gomez-Romero, P. (2001). Hybrid organic-inorganic materials – In search of synergic activity. *Advanced Materials 13*(3), 163-174. doi: 10.1002/1521-4095(200102)13: 3<163::AID-ADMA163>3.0.CO;2-U

Gonzalez-Delgado, A. M., Giner-Casares, J. J., Brezesinski, G., Regnouf-de-Vains. J. B. & Camacho. L. (2012). Langmuir monolayers of an inclusion complex formed by a new calixarene derivative and fullerene. *Langmuir*, *28*(33), 12114-12121. doi: 10.1021/la302440g

Gorga, R. E. & Cohen, R. E. (2004). Toughness enhancements in poly(methyl methacrylate) by addition of oriented multiwall carbon nanotube. *Journal of Polymer Science Part B: Polymer Physics*, *42*(14), 2690–2702. doi: 10.1002/polb.20126

05-4506832 pustaka.upsi.edu.my Perpustakaan Tuanku Bainun Kampus Sultan Abdul Jalil Shah PustakaTBainun ptbupsi

05-4506832 pustaka.upsi.edu.my Perpustakaan Tuanku Bainun Kampus Sultan Abdul Jalil Shah PustakaTBainun ptbupsi

Gosnell, J. D., Schreuder, M. A., Rosenthal, S. J. & Weiss S. M. (2007, August). *Efficiency improvements of white-light CdSe nanocrystal-based LEDs*. Paper presented at Seventh International Conference on Solid State Lighting, San Diego, CA.

Gosvami, N. N., Parsons, E., Marcovich, C., Berkowitz, M. L., Hoogenboom, B. W. & Perkin, S. (2012). Resolving the structure of a model hydrophobic surface: DODAB monolayers on mica. *RSC Advances*, *2*(10), 4181-4188. doi: 10.1039/C2RA20108A

Greenham, N. C, Peng, X. & Alivisatos, A. P. (1997). Charge separation and transport in conjugated polymer/cadmium selenide nanocrystal composites studied by photoluminescence quenching and photoconductivity. *Synthetics Metals 84*(1-3), 545-546. doi: 10.1016/S0379-6779(97)80852-1

Günes, S., Fritz, K., Neugebauer, H., Sariciftci, N. S., Kumar, S. & Scholes, G. (2007a). Hybrid solar cells using PbS nanoparticles. *Solar Energy Materials & Solar Cells 91*(5), 420–423. doi: 10.1016/j.solmat.2006.10.016

Günes, S., Neugebauer, H. & Sariciftci, N. S. (2007b). Conjugated polymer-based organic solar cells. *Chemical Reviews, 107*(4), 1324–1338. doi: 10.1021/cr050149z

Guzelturk, B. & Demir, H. V. (2015). Organic−inorganic composites of semiconductor nanocrystals for efficient excitonics. *The Journal of Physical Chemistry Letters, 6*, 2206−2215. doi: 10.1021/acs.jpclett.5b00415

Hagting, J. G. (1999). *Langmuir-Blodgett films of poly(p-henylenevinylene) precursor polymers* (Doctoral Dissertation). Retrieved from http://www.rug.nl/research

Halls J. M., Walsh C. A., Greenham N. C., Marseglia E. A., Friend R. H., Moratti S. C. & Holmes A. B. (1995). Efficient photodiodes from interpenetrating networks. *Nature 376*, 498–500. doi: 10.1038/376498a0

Halls, J. M., Arias, A. C., MacKenzie, J. D., Wu, W., Inbasekaran, M., Woo, E. P. & Friend, R. H. (2000). Photodiodes based on polyfluorene composites: influence of morphology. *Advanced Materials 12*(7), 498–502, doi: 10.1002/(SICI)1521-4095(200004)12:7<498::AID-ADMA498>3.0.CO;2-H

Haridas M., Srivastava S. & Basu J. K. (2008). Tunable variation of optical properties of polymer capped gold nanoparticles. *The European Physics Journal D 49*, 93–100, doi:10.1140/epjd/e2008-00135-x

Hector, A.L. (2007). Materials synthesis using oxide free sol-gel systems. *Chemical Society Review, 36*(11), 1745-1753. doi: 10.1039/B608838B

Ho, C. S., Huang, E. L., Hsu, W. C., Lee, C. S., Lai, Y. N. & Lai, W. H. (2011). Effects of annealing on polymer solar cells with high polythiophene–fullerene concentrations.

05-4506832 pustaka.upsi.edu.my Perpustakaan Tuanku Bainun Kampus Sultan Abdul Jalil Shah PustakaTBainun ptbupsi

05-4506832 pustaka.upsi.edu.my Perpustakaan Tuanku Bainun Kampus Sultan Abdul Jalil Shah PustakaTBainun ptbupsi

Japanese Journal of Applied Physics, 50, 04DK21-1-04DK21-3. doi: 10.1143/JJAP. 50.04DK21

Hoppe, H. (2004). *Nanomorphology – efficiency Relationship in Organic Bulk Heterojunction Plastic Solar Cells* (Doctoral Dissertation). Retrieved from http://www.jku.at/ipc/content/e166717/e180430/e180447/e80468/thesishoppe.pdf

Hou, J. & Guo, X. (2012). Active layer materials for organic solar cells. In W. C. H. Choy (Ed.), *Organic solar cells: Materials and device physics* (pp.17-42). London: Springer-Verlag. doi: 10.1007/978-1-4471-4823-4

Huang, C. C., Al-Saab, F., Wang, Y., Ou, J. Y., Walker, J. C., Wang, S. … Hewak, D. W. (2014). Scalable high-mobility MoS_2 thin films fabricated by an atmospheric pressure chemical vapor deposition process at ambient temperature. *Nanoscale, 6,* 12792-12797. doi: 10.1039/C4NR04228J

Hunt, L. B. (1973).The early history of gold plating. *Gold Bulletin, 6,* 16–27. doi: 10.1007/BF03215178

Hussain, F., Hojjati, M., Okamoto, M. & Gorga, R. E. (2006). Polymer-matrix nanocomposites, processing, manufacturing, and application: An overview. *Journal of Composite Materials, 40,* 1511-1575. doi:10.1177/0021998306067321

05-4506832 pustaka.upsi.edu.my Perpustakaan Tuanku Bainun Kampus Sultan Abdul Jalil Shah PustakaTBainun ptbupsi

Huynh W. U., Dittmer J. J. & Alivisatos A. P. (2002). Hybrid nanorod-polymer solar cells. *Science, 295*(5564), 2425-2427. doi:10.1126/science.1069156

Jain, S. (2001). *Photoluminescence study of cadmium zinc telluride* (Master Dissertation). Retrieved from http://citeseerx.ist.psu.edu/viewdoc/download?doi=10.1.1.502.2707&rep=rep1&type=pdf

Jayaraman, S. (2012). *Organic/inorganic hybrid structures by molecular assembly* (Doctoral Dissertation). Retrieved from http://www.academia.edu/24273241/Organic_Inorganic_Hybrid_Structures_by_Molecular_Assembly

Jeon, I. Y. & Baek, J. B. (2010). Nanocomposites derived from polymers and inorganic nanoparticles. *Materials, 3*(6), 3654-3674. doi: 10.3390/ma3063654

Johnson, J. B. (1928). Thermal agitation of electricity in conductors. *Physics Review, 32,* 97-109. doi: 10.1103/PhysRev.32.97

Justo, Y., Moreels, I., Lambert K. & Hens, Z. (2010). Langmuir–Blodgett monolayers of colloidal lead chalcogenide quantum dots: morphology and photoluminescence. *Nanotechnology, 21*(29), 295606 doi: 10.1088/0957-4484/21/29/295606

05-4506832 pustaka.upsi.edu.my Perpustakaan Tuanku Bainun Kampus Sultan Abdul Jalil Shah PustakaTBainun ptbupsi

05-4506832 pustaka.upsi.edu.my Perpustakaan Tuanku Bainun Kampus Sultan Abdul Jalil Shah PustakaTBainun ptbupsi

Kappert, E. J., Pavlenko, D., Malzbender, J., Nijmeijer, A., Benes N. E. & Tsai P. A. (2015). Formation and prevention of fractures in sol–gel-derived thin films. *Soft Matter, 11,* 882-888. doi: 10.1039/C4SM02085E

Karabıyık, U. (2003). *Optical and thermal characteristics of thin polymer and polyehedral oligomeric silsequioxane (POSS) filled polymer films* (Doctoral Dissertation). Retrieved from https://theses.lib.vt.edu/theses/available/etd-05142008-181528/

Kärber, E., Katerski, A., Acik, I. O., Mikli, V., Mere, A., Sildos, I., & Krunks, M. (2014). Low-cost plasmonic solar cells prepared by chemical spray pyrolysis. *Beilstein Journal of Nanotechnology, 5,* 2398–2402. doi: 10.3762/bjnano.5.249

Kawaharamura, T. (2014). Physics on development of open-air atmospheric pressure thin film fabrication technique using mist droplets: Control of precursor flow. *Japanese Journal of Applied Physics, 53,* 05FF08-1-05FF08-7. doi: 10.7567/JJAP.53.05FF08

Ke, L., Zhao, X. Y., Kumar, R. S. & Chua, S. J. (2008). Low frequency optical noise from organic light emitting diode. *Solid-State Electonics*. *52*(1), 7-10. doi: 10.1016/j.sse. 2007.07.004

Kekuda, D., Lin, H. S., Wu, M. C., Huang, J. S., Ho, K. C. & Chu, C. W. (2011). The effect of solvent induced crystallinity of polymer layer on poly(3-hexylthiophene)/C70 bilayer solar cells. *Solar Energy Materials and Solar Cells 95*(2), *419-422*. doi: 10.1016/j.solmat.2010.05.055

Khan, M. T., Bhargav, R., Kaur, A., Dhawan, S. K. & Chand, S. (2010). Effect of cadmium sulphide quantum dot processing and post thermal annealing on P3HT/PCBM photovoltaic device. *Thin Solid Films, 519*(3), 1007-1011. doi: 10.1016/j.tsf. 2010.08.032.

Kim, Y., Ballantyne, A. M., Nelson, J. & Bradley, D. D. C. (2009). Effects of thickness and thermal annealing of the PEDOT:PSS layer on the performance of polymer solar cells. *Organic Electronics, 10*(1), 205-209. doi: 10.1016/j.orgel.2008.10.003

Kippelen B. & Bredas J. L. (2009). Organic photovoltaics. *Energy and Environmental Science 2*, 251–261. doi: 10.1039/B812502N

Kippler, M. (2009). *Interaction between Cadmium and Micronutrients in Pregnant and Lactating Women* (Master Dissertation). Retrieved from https://openarchive.ki.se/ xmlui/handle/10616/39066

Kittel, C. (1995). *Introduction to solid state physics- 7th Edition*. New York: John Wiley & Sons.

05-4506832 pustaka.upsi.edu.my Perpustakaan Tuanku Bainun Kampus Sultan Abdul Jalil Shah PustakaTBainun ptbupsi

05-4506832 pustaka.upsi.edu.my Perpustakaan Tuanku Bainun Kampus Sultan Abdul Jalil Shah PustakaTBainun ptbupsi

Klimov, V. I. (2007). Spectral and dynamical properties of multiexcitons in semiconductor nanocrystals. *Annual Review of Physical Chemistry 58*, 635–673. doi: 10.1146/annurev.physchem.58.032806.104537

Knapp C. E. (2010). *Synthesis, chemical vapour deposition and structural studies of group 13 alkoxide* (Doctoral Dissertation). Retrieved from http://discovery.ucl.ac.uk/20176/

Kraack, H., Deutsch, M., Ocko, B. M. & Pershan, P. S. (2003). The structure of organic langmuir films on liquid metal surfaces. *Nuclear Instruments and Methods in Physics Research B 200*, 363–370. doi: 10.1016/S0168-583X(02)01724-X

Kraack, H., Ocko, B. M., Pershan, P. S., Sloutskin, E., Tamam, L. & Deutsch, M. (2004). Fatty Acid Langmuir Films on Liquid Mercury: X-ray and Surface Tension Studies**.** *Langmuir*, *20*(13), 5375-5385. doi: 10.1021/la049977y

Kumaki, J., Kajitani, T., Nagai, K., Okoshi, K. & Yashima, E. (2010). Visualization of polymer chain conformations in amorphous polyisocyanide Langmuir−Blodgett films by atomic force microscopy. *Journal of the American Chemical Society 132*(16), 5604-5606. doi: 10.1021/ja908426u

Kumar, N., Wang, L., Siretanu, I., Duits, M. & Mugele, F. (2013). Salt dependent stability of stearic acid Langmuir–Blodgett films exposed to aqueous electrolytes. *Langmuir, 29*(17), 5150–5159. doi: 10.1021/la400615j

Kutner, W., Noworyta, K., Marczak, R. & D'Souza, F. (2001). Electrochemical and ECQM characterization of molecular and of thin-solid of higher fullerenes: C_{76}, C_{78} and C_{84}, *Proceedings of the International Symposium on Fullerenes, Nanotube, and Carbon Nanocluster, 11*, 19-26.

Lai, C. Y., Groth, A., Gray S. & Duke, M. (2014). Nanocomposites for improved physical durability of porous PVDF membranes. *Membranes*, *4*(1), 55-78. doi: 10.3390/membranes4010055

Lane P. A. & Kafafi Z. H. (2005). Solid-state organic: A review of molecular and polymeric devices. In S. S. Sun & N. S. Sariciftci (Eds.), *Organic Photovoltaics* (pp 49 – 1040). Boca Raton, FL: Taylor & Francis Group

Langmuir, I. & Schaefer, V. J. (1938). Activities of urease and pepsin monolayers. *Journal of the American Chemical Society, 60*(6), 1351-1360. doi: 10.1021/ja01273a023

Langmuir, I. (1920). The mechanism of the surface phenomena of flotation. *Transactions of Faraday Society, 15*, 62-74. doi: 10.1039/TF9201500062

Lazar, M. A., Tadvani, J. K., Tung, W. S., Lopez, L. & Daoud, W. A. (2010). Nanostructured thin films as functional coatings. 2010 *IOP Conference Series:*

05-4506832 pustaka.upsi.edu.my Perpustakaan Tuanku Bainun Kampus Sultan Abdul Jalil Shah PustakaTBainun ptbupsi

05-4506832 pustaka.upsi.edu.my Perpustakaan Tuanku Bainun Kampus Sultan Abdul Jalil Shah PustakaTBainun ptbupsi

Material Science and Engineering 12(1), 012017. doi: 10.1088/1757-899X/12/1/012017

Lee, H. J., Yum, J. H., Leventis, H. C., Zakeeruddin, S. M., Haque, S. A., Chen, P. & Nazeeruddin M. K. (2008). CdSe quantum dot-sensitized solar cells exceeding efficiency 1% at full-sun intensity. *Journal of Physical Chemistry C 112*(30), 11600–11608. doi: 10.1021/jp802572b

Lee, K. R., Hsu, Y. P., Chang, J. K., Lee, S. W., Tseng, C. J. & Jang, J. S. C. (2014). Effects of spin speed on the photoelectrochemical properties of Fe_2O_3 thin films. *International Journal of Electrochemical Science, 9*, 7680-7692.

Lee, K. S., Kim, I., Gullapalli, S., Wong, M. S. & Jabbour, G. E. (2011). Enhanced performance of hybrid solar cells using longer arms of quantum cadmium selenide tetrapods, *Applied Physics Letters, 99*, 223515-1 – 223515-3. doi: 10.1063/1.3662839

Lek, J. Y., Lam, Y. M., Niziol, J. & Marzec, M. (2012). Understanding polycarbazole-based polymer:CdSe hybrid solar cells. *Nanotechnology, 23*(31), 315401. doi: 10.1088/0957-4484/23/31/315401.

Levell, J. W., Giardini, M. E. & Samuel, I. D. W. (2010). A hybrid organic semiconductor / silicon photodiode for efficient ultraviolet photodetection. *Optic Express, 18*(4), 3219 – 3225. doi: 10.1364/OE.18.003219

Li, F., Chen, C., Tan, F., Li, C., Yue, G., Shen, L., & Zhang, W. (2014). Semitransparent inverted polymer solar cells employing a sol-gel-derived TiO_2 electron-selective layer on FTO and MoO_3/Ag/MoO_3 transparent electrode. *Nanoscale Research Letters*, *9*(579), 1-5. doi: 10.1186/1556-276X-9-579

Li, G., Yao, Y., Yang, H., Shrotriya, V., Yang, G. & Yang Y. (2007). Solvent annealing effect in polymer solar cells based on poly(3-hexylthiophene) and methanofullerenes. *Advanced Functional Materials, 17*(10), 1636-1644. doi: 10.1002/adfm.200600624

Li, J. & Wu, Y. (2014). Lubricants in pharmaceutical solid dosage forms. *Lubricants 2*(1), 21-43. doi: 10.3390/lubricants2010021

Li, S., Qin, J., Fornara, A., Toprak, M., Muhammed, M. & Kim D. K. (2009). Synthesis and magnetic properties of bulk transparent PMMA/ Fe-oxide nanocomposites. *Nanotechnology, 20*(18), 6-11. doi: 10.1088/0957-4484/20/18/185607

Li, W., Guo, J., Sun, X. & Zhou, B. (2010). Effect of solvents on the performance of P3HT:PCBM solar cells, *Proceedings of the SPIE, 7847*, 784709-784709-6. doi: 10.1117/12.868374

05-4506832 pustaka.upsi.edu.my Perpustakaan Tuanku Bainun Kampus Sultan Abdul Jalil Shah PustakaTBainun ptbupsi

05-4506832 pustaka.upsi.edu.my Perpustakaan Tuanku Bainun Kampus Sultan Abdul Jalil Shah PustakaTBainun ptbupsi

Liao Z., Hsieh W. T., Baumgart T. & Dmochowski I. J. (2013). Measuring interactions between polydimethylsiloxane and serum proteins at the air-water interface. *Langmuir, 29*(30), 9420-9427. doi: 10.1021/la401619s

Liao, H. C., Chantarat, N., Chen, S. Y. & Peng, C. H. (2011). Annealing effect on photovoltaic performance of hybrid P3HT/In-situ grown CdS nanocrystal solar cells. *Journal of Electrochemical Society, 158*(7), 5251-5455. doi: 10.1149/1.3585668

Liao, H. C., Chen, S. Y. & Liu, D. M. (2009). In-situ growing CdS single-crystal nanorods via P3HT polymer as a soft template for enhancing photovoltaic performance. *Macromolecules, 42*(17), 6558-6563. doi: 10.1021/ma900924y

Litzov I. & Brabec, C. J. (2013). Development of efficient and stable inverted bulk heterojunction (BHJ) solar cells using different metal oxide interfaces. *Materials*, *6*, 5796-5820; doi: 10.3390/ma6125796

Liu, J., Tanaka, T., Sivula, K., Alivisatos, A. P. & Fréchet, J. M. J. (2004). Employing end-functional polythiophene to control the morphology of nanocrystal—polymer composites in hybrid solar cells. *Journal of the American Chemical Society, 126*(21), 6550–6551. doi: 10.1021/ja0489184

Liu, X., Adachi, Y., Tomita, Y., Oshima, J., Nakashima, T. & Kawai, T. (2012). High-order nonlinear optical response of a polymer nanocomposite film incorporating semiconducotor CdSe quantum dots. *Optics Express* 20, 13457-13469. doi: 10.1364/OE.20.013457

Liu, Y., Lam J. W. Y. & Tang, B. Z. (2015). Conjugated polymers developed from alkynes. *National Science Review, 2*(4), 493-509. doi: 10.1093/nsr/nwv047

Loubiri, D., Ben Hamed, Z., Ilahi, S., Sanhoury, M. A., Kouki, F. & Yacoubi, N. (2015). Effect of TBPO-capped CdSe nanoparticles concentration on sub-bandgap absorption in poly(3-hexylthiophene) thin films studied by photothermal deflection spectroscopy. *Synthetic Metals, 206*, 1-7. doi: 10.1016/j.synthmet.2015.04.018.

Lu, X., Lu, N., Gao, J., Jin, X. & Lu, C. (2007). Synthesis and properties of ZnS/ polyimide nanocomposite films. *Polymer International*, *56*(5), 601-605. doi: 10.1002/pi.2170

Luo, J. J. & Daniel, I. M. (2003). Characterization and modeling of mechanical behavior of polymer/clay nanocomposites. *Composites Science and Technology, 63*(11): 1607–1616. doi: 10.1016/S0266-3538(03)00060-5

Ma, C. C. M., Chen, Y. J. & Kuan, H. C. (2006). Polystyrene nanocomposite materials - preparation, mechanical, electrical and thermal properties, and morphology. *Journal of Applied Polymer Science*, *100*(1), 508-515. doi: 10.1002/app.23221

05-4506832 pustaka.upsi.edu.my Perpustakaan Tuanku Bainun Kampus Sultan Abdul Jalil Shah PustakaTBainun ptbupsi

05-4506832 pustaka.upsi.edu.my Perpustakaan Tuanku Bainun Kampus Sultan Abdul Jalil Shah PustakaTBainun ptbupsi

MacLachlan, A. J., Rath, T., Cappel, U. B., Dowland, S. A., Amenitsch, H., Knall, A. C. … Haque, S. A. (2015). Polymer/nanocrystal hybrid solar cells: influence of molecular precursor design on film nanomorphology, charge generation and device performance. *Advanced Functional Materials, 25*, 409–420. doi: 10.1002/ adfm.201403108

Maestro, A., Bonales, L. J., Ritacco, H., Fischer, T. M., Rubio R. G. & Ortega F. (2011). Surface rheology: macro- and microrheology of poly(tert-butyl acrylate) monolayers. *Soft Matter, 7*, 7761-7771. doi: 10.1039/C1SM05225J

Mallik, A. &. Ray, B. C. (2011). Evolution of principle and practice of electrodeposited thin film: A review on effect of temperature and sonication. *International Journal of Electrochemistry, 2011*, 16 pages. doi:10.4061/2011/568023

Mangadlao, D., Santos, C. M., Felipe, M. J. L., de Leon, A. C. C., Rodrigues D. F. & Advincula, R. C. (2015). On the antibacterial mechanism of graphene oxide (GO) Langmuir–Blodgett films. *Chemical Communication, 51*, 2886-2889. doi: 10.1039/C4CC07836E

Mark, J. E. (1996). Ceramic-reinforced polymers and polymer-modified ceramics. *Polymer Engineering and Science, 36*(24), 2905-2920. doi: 10.1002/pen.10692

Markley, K. S. (1960) Isomerism. In K. S. Markley (Ed.), *Fatty acids: Their chemistry, properties, production and uses* (pp. 251-283). New York: Interscience Publishers.

Martín-García, B., Paulo, P. M. R., Costa, S. M. B. & Velázquez, M. M. (2013). Photoluminescence dynamics of CdSe QD/polymer Langmuir–Blodgett thin films: morphology effects. *The Journal of Physical Chemistry C 117*(28), 14787-14795. doi: 10.1021/jp311492z

Mo, T. C., Wang, H. W., Chen, S. Y. & Yeh, Y. C. (2008). Synthesis and dielectric properties of polyaniline/titanium dioxide nanocomposites. *Ceramic International, 34*(7), 1767-1771. doi: 10.1016/j.ceramint.2007.06.002

Moffat, T. P. & Josell, D. (2010). Superconformal electrodeposition for 3-dimensional interconnects. *Israel Journal of Chemistry 50*(3), 312–320. doi: 10.1002/ijch. 201000029

Mori, T., Sakakibara, K., Endo, H., Akada, M., Okamoto, K., Shundo, A., … Ariga, K. (2012). One-touch nanofabrication of regular-sized disks through interfacial dewetting and weak molecular interaction. *Chemistry Letters, 41*(2), 170-172. doi: 10.1246/ cl.2012.170

05-4506832 pustaka.upsi.edu.my Perpustakaan Tuanku Bainun Kampus Sultan Abdul Jalil Shah PustakaTBainun ptbupsi

05-4506832 pustaka.upsi.edu.my Perpustakaan Tuanku Bainun Kampus Sultan Abdul Jalil Shah PustakaTBainun ptbupsi

Morsi, I., Nasser, A. A. A., Ali, I., Hassan, H. S., & Kashyout, A. B. (2015). Fabrication of ZnO gas sensor for detection of LPG Gas. *ETRI Journal, 37*(2), 1-7. doi: 10.4218/etrij.15.0114.0851

Muhibbullah, M. (2011). *Deposition of copper oxide thin films by chemical techniques* (Doctoral Dissertation). Retrieved from http://repo.lib.nitech.ac.jp/handle/ 123456789/ 6200.

Müller-Buschbaum, P., Gutmann, J. S. & Stamm, M. (2000). Influence of blend composition on phase separation and dewetting of thin polymer blend films. *Macromolecules, 33*(13), 4886–4895, doi: 10.1021/ma991073+

Nabok, A. (2005). Organic and inorganic nanostructures, Norwood: Artech House.

Nam, M., Lee, S., Park, J., Kim S. W. & Lee K. K. (2011). Development of hybrid photovoltaic cells by incorporating $CuInS_2$ quantum dots into organic photoactive layers. *Japanese Journal of Applied Physics, 50,* 06GF02-1 – 06GF02-5. doi: 10.1143/ JJAP.50.06GF02

Narayanam, P. K., Singh, G., Botcha, V. D., Sutar, D. S., Talwar, S.S., Srinivasa R. S. & Majo, S. S. (2012). Growth of CdS nanocrystallites on graphene oxide Langmuir–Blodgett monolayers. *Nanotechnology, 23*(32), 325605. doi: 10.1088/0957-4484/23/ 32/325605

05-4506832 pustaka.upsi.edu.my Perpustakaan Tuanku Bainun Kampus Sultan Abdul Jalil Shah PustakaTBainun ptbupsi

Nicholson P. G. & Castro F. A. (2010). Organic photovoltaics: Principles and techniques for nanometer scale characterization. *Nanotechnology, 21*(49), 492001-492026. doi: 10.1088/0957-4484/21/49/492001

Norris, D. J. & Bawendi, M. G. (1996). Measurement and assignment of the size dependent optical spectrum in CdSe quantum dots. *Physical Review B 53*(24), 16338-16346. doi: 10.1103/PhysRevB.53.16338

Norris, D. J., Efros, A. L., Rosen, M. & Bawendi, M. G. (1996). Size dependence of exciton fine structure in CdSe quantum dots. *Physical Review B 53*(24), 16347- 16354. doi: 10.1103/PhysRevB.53.16347

Norris, D. J., Sacra, A., Murray, C. B. & Bawendi, M. G. (1994). Measurement of the size dependent hole spectrum in CdSe quantum dots. *Physical Review Letters, 72*(16), 2612-2615. doi: 10.1103/PhysRevLett.72.2612

Nyquist, H. (1928). Thermal agitation of electric charge in conductors. *Physics Review, 32,* 110-113. doi: 10.1103/PhysRev.32.110

Olivati, C. A., Gonçalves, V. C. & Balogh, D. T. (2012). Optically anisotropic and photoconducting Langmuir–Blodgett films of neat poly(3-hexylthiophene). *Thin Solid Films 520,* 2208–2210, doi:10.1016/j.tsf.2011.10.032

05-4506832 pustaka.upsi.edu.my Perpustakaan Tuanku Bainun Kampus Sultan Abdul Jalil Shah PustakaTBainun ptbupsi

05-4506832 pustaka.upsi.edu.my Perpustakaan Tuanku Bainun Kampus Sultan Abdul Jalil Shah PustakaTBainun ptbupsi

Onah, E. J. (2006). Nanofilms and the emerging nanotechnology. *Polymeric Nanofibers, 918,* 384–398. doi:10.1021/bk-2006-0918.ch027

Osuntokun J. & Ajibade, P. A. (2016). Structural and thermal studies of ZnS and CdS nanoparticles in polymer matrices. *Journal of Nanomaterials, 2016,* Article ID 3296071, 14 pages. doi:10.1155/2016/3296071

Özbek, Z., Çapan, R., Göktaş, H., Şen, S., İnce, F. G., Özel, M. E. & Davis, F. (2011). Optical parameters of calix[4]arene films and their response to volatile organic vapors. *Sensors and Actuators B: Chemical, 158*(1), 235-240. doi: 10.1016/j.snb.2011.06.011

Panahandeh-Fard, M., Yin, J., Kurniawan, M., Wang, Z., Leung, G., Sum, T. C. & Soci, C. (2014). Ambipolar charge photogeneration and transfer at GaAs/P3HT heterointerfaces. *Journal of Physical Chemistry Letter, 5*(7), 1144−1150. doi: 10.1021/jz500332z

Pandey, R. K., Yadav, S. K., Upadhyay, C., Prakash, R. & Mishra, H. (2015). Surface plasmon coupled metal enhanced spectral and charge transport properties of poly(3,3‴-dialkylquarterthiophene) Langmuir Schaefer films. *Nanoscale, 7*, 6083-6092. doi: 10.1039/C5NR00682A

05-4506832 pustaka.upsi.edu.my Perpustakaan Tuanku Bainun Kampus Sultan Abdul Jalil Shah PustakaTBainun ptbupsi

Park, S. M., Ikegami, T., Ebihara, K. & Shin, P. K. (2006). Structure and properties of transparent conductive doped ZnO films by pulsed laser deposition. *Applied Surface Science, 253*(3), 1522-1527. doi: 10.1016/j.apsusc.2006.02.046

Patel, J., Mighri, F., Ajji, A., Tiwari, D. & Chaudhuri, T. K. (2014). Spin-coating deposition of PbS and CdS thin films for solar cell application. *Applied Physics A, 117*(4), 1791-1799. doi: 10.1007/s00339-014-8659-x

Pawlowski, L. (November 2014). *Review of solution precursor spray techniques applied to obtain ceramic films and coatings*. Paper presented at the Asian Thermal Spray Conference, Hyderabad, India.

Pearson, C., Gibson, J. E., Petty, M. C., Moore, A. J. & Bryce, M. R. (1993). Field-effect transistor based on organometallic Langmuir-Blodgett film. *Electronics Letters, 29*(15), 1377–1378. doi: 10.1049/el:19930922

Peet, J., Kim, J. Y., Coates, N. E., Ma, W. L., Moses, D., Heeger, A. J. & Bazan, G. C. (2007). Efficiency enhancement in low-bandgap polymer solar cells by processing with alkane dithiols. *Natural Materials 6*(7), 497–500. doi: 10.1038/nmat1928

Perednis, D. & Gauckler, L. J. (2005). Thin film deposition using spray pyrolysis. *Journal of Electroceramics, 14,* 103–111. doi: 10.1007/s10832-005-0870-x

05-4506832 pustaka.upsi.edu.my Perpustakaan Tuanku Bainun Kampus Sultan Abdul Jalil Shah PustakaTBainun ptbupsi

05-4506832 pustaka.upsi.edu.my Perpustakaan Tuanku Bainun Kampus Sultan Abdul Jalil Shah PustakaTBainun ptbupsi

Petiraksakul P. (2000). *Effect of stearate/stearic acid coating on filled high density polyethylene properties* (Doctoral Dissertation). Retrieved from https://dspace.lboro.ac.uk/dspace-jspui/handle/2134/11166

Petty, M. C. (1996). *Langmuir-Blodgett Film: An Introduction*. Cambridge, UK: Cambridge University Press.

Pichumani M., Bagheri, P., Poduska, K. M., González-Viñas W. & Yethiraj, A. (2013). Dynamics, crystallization and structures in colloid spin coating. *Soft Matter***,** *9*, 3220-3229. doi: 10.1039/C3SM27455A

Pier, A. C. (1998). *Introduction to sol-gel processing*. Norwell, Massachusetts: Kluwer.

Pisanic, T. R., Zhang, Y., & Wang, T. H. (2014). Quantum dots in diagnostics and detection: principles and paradigms. *Analyst, 39*, 2968-298. doi: 10.1039/C4AN00294F

Pockels, A. (1891). Surface tension. *Nature, 43*, 437-439. doi: 10.1038/043437c0

Polivtseva, S., Acik, I. O., Katerski, A., Mere, A., Mikli, V. & Krunks, M. (2014). Spray pyrolysis deposition of Sn_xS_y thin films. *Energy Procedia, 60*, 156-165, doi: 10.1016/j.egypro.2014.12.358

05-4506832 pustaka.upsi.edu.my Perpustakaan Tuanku Bainun Kampus Sultan Abdul Jalil Shah PustakaTBainun ptbupsi

Prabhu, R. R. & Khadar, M. A. (2005). Characterization of chemically synthesized CdS nanoparticles. *Pramana*: *Journal of Physics, 65*, 801-807. doi: 10.1007/BF02704078

Pulker, H. K. (1999). Optical coatings deposited by ion and plasma PVD processes. *Surface and Coatings Technology***,** *112*(1-3), 250-256. doi: 10.1016/S0257-8972(98)00764-6

Qi, B., Zhou, Q. & Wang, J. (2015). Exploring the open-circuit voltage of organic solar cells under low temperature. *Scientific Reports 5*, Article number 11363. doi:10.1038/srep11363

Qian, F., Peng, S., Yu-Kun, L., Kai, D., Qiang, W., Qing, F. & Yue, H. (2014). Hybrid solar cell based on polythiophene and GaN nanoparticles composite. *Journals of Chinese Physics B, 23*(2), 028802. doi: 10.1088/1674-1056/23/2/028802

Rao, C. N. R. & Cheetham A. K. (2006). Materials science at nanoscale (1-12). In. Y. Gogotsi, *Nanomaterials Handbook*. Boca Raton, FL: CRC Taylor & Francis Group.

Ratnesh, R. K. & Mehata, M. S. (2015). Controlled synthesis and optical properties of tunable CdSe quantum dots and effect of pH. *AIP Advances, 5*, 097114. doi: 10.1063/1.4930586

05-4506832 pustaka.upsi.edu.my Perpustakaan Tuanku Bainun Kampus Sultan Abdul Jalil Shah PustakaTBainun ptbupsi

05-4506832 pustaka.upsi.edu.my Perpustakaan Tuanku Bainun Kampus Sultan Abdul Jalil Shah PustakaTBainun ptbupsi

Razali, A. S., Supian, F. L., Bakar, S. A., Richardson, T. H. & Azahari, N. A. (2015). The properties of carbon nanotube on novel calixarene thin film. *International Journal of Nanoelectrics and Materials 8*(1), 39-45.

Riedel I. & Dyakonov V. (2004). Influence of electronic transport properties of polymer-fullerene blends on the performance of bulk heterojunction photovoltaic devices. *Physica status solidi (a), 201 (6),* 1332–1341. doi: 10.1002/pssa.20040433

Rocha, P. R. F., Gomes, H. L., Vandamme, L. K. J., De Leeuw, D. M., Meskers, S. C. J. & van de Weijer, P. (2013). Low-frequency noise as a diagnostic tool for OLED reliability. *Proceeding of 22nd International Conference on Noise and Fluctuations, 1*(4), 24-28. doi: 10.1109/ICNF.2013.6578947

Roh, K. M., Jo, E. H., Chang, H., Han, T. H. & Jang, H. D. (2015). High performance dye-sensitized solar cells using grapheme modified fluorine-doped tin oxide glass by Langmuir-Blodgett technique. *Journal of Solid State Chemistry, 224*, 71-75, doi:10.1016/j.jssc.2014.04.022

Roy, D., Das, N. M. & Gupta, P. S. (2013). Structural morphology study of Cd^{2+} induced Langmuir Blodgett multilayer films of arachidic acid. *Applied Surface Science, 271*, 394-401. doi:10.1016/j.apsusc.2013.01.212

Sachse, S., Gendre, L., Silva, F., Zhu, H., Leszczyska, A., Pielichowski, K. … Njuguna, J. (2013). On nanoparticles release from polymer nanocomposites for applications in lightweight automotive components. *Journal of Physics: Conference Series, 429*(1), 012046. doi: 10.1088/1742-6596/429/1/012046

Sahu, N., Parija, B. & Panigrahi, S. (2009). Fundamental understanding and modeling of spin coating process: A review. *Indian Journal of Physics, 83*(4), 493-502. doi: 10.1007/s12648-009-0009-z

Sajeesh, T. H., Cherian, A. S., Kartha, C. S. & Vijayakumar, K. P. (2012). Engineering structural and opto-electronic properties of SnS films deposited using chemical spray pyrolysis technique by controlling pH of the precursor solution. *Energy Procedia*, *15*, 325-332. doi: 10.1016/j.egypro.2012.02.039

Sako, E. O., Kondoh, H., Nakai, I., Nambu, A., Nakamura, T., and Ohta, T. (2005). Reactive adsorption of thiophene on Au(111) from solution. *Chemical Physics Letters, 413*(4-6), 267-71. doi: 10.1016/j.cplett.2005.07.086

Sariciftci N. S., Smilowitz L., Heeger A. J. & Wudl F. (1992). Photoinduced electron transfer from a conducting polymer to buckminsterfullerene. *Science 258,* 1474-1476 doi: 10.1126/science.258.5087.1474

Schreiber, F. (2000). Structure and growth of self-assembling monolayers. *Progress in Surface Science*, *65*(5-8), 151-256. doi: 10.1016/S0079-6816(00)00024-1

05-4506832 pustaka.upsi.edu.my Perpustakaan Tuanku Bainun Kampus Sultan Abdul Jalil Shah PustakaTBainun ptbupsi

05-4506832 pustaka.upsi.edu.my Perpustakaan Tuanku Bainun Kampus Sultan Abdul Jalil Shah PustakaTBainun ptbupsi

Schubert, U. (2015) Chemistry and Fundamentals of the Sol–Gel Process. In D. Levy, & M. Zayat, (Eds.), *The sol-gel handbook – Synthesis, characterization and applications*: *Synthesis, characterization and applications – 3 Volume set.* (pp. 1-28). Weinheim, Germany: Wiley-VCH Verlag GmbH & Co. KGaA. doi: 10.1002/9783527670819.ch01

Shahidi, S., Moazzenchi, B. & Ghoranneviss, M. (2015). A review-application of physical vapor deposition (PVD) and related methods in the textile industry. *The European Physics Journal - Applied Physics, 71*(3), 31302-31315. doi: 10.1051/epjap/2015140439

Sharma, S. N., Vats, T., Dhenadhayalan, N., Ramamurthy, P. & Narula, A. K. (2012). Ligand-dependent transient absorption studies of hybrid polymer:CdSe quantum dot composites. *Solar Energy Materials and Solar Cells, 100*, 6–15. doi: 10.1016/j.solmat.2011.10.020

Shaw, P. E., Rusecka, A. & Samuel, I. D. W. (2008). Exciton diffusion measurements in poly(3-hexylthiophene). *Advanced Materials, 20*(18), 3516-3520. doi: 10.1002/adma.200800982

Shrotriya, V., Ouyang, J., Tseng, R. J., Li, G. & Yang, Y. (2005). Absorption spectra modification in poly(3-hexylthiophene):methanofullerene blend thin films. *Chemical Physics Letters, 411*, 138–143. doi: 10.1016/j.cplett.2005.06.027

Simoni, S. F., Bosma, T. N. P., Harms, H. & Zehnder, A. J. B. (2000). Bivalent cations increase both the subpopulation of adhering bacteria and their adhesion efficiency in sand columns. *Environmental Science and Technology, 34*(6), 1011-1017. doi:10.1021/es990476m

Singh J. & Wolfe D. E. (2005). Review nano and macro-structured component fabrication by electron beam physical vapor deposition (EB-PVD). *Journal of Material Science, 40*(1), 1-26. doi: 10.1007/s10853-005-5682-5

Singhal, R., Chaubey, A., Srikhirin, T., Aphiwantrakul, S., Pandey, S. S. & Malhotra, B. D. (2003). Immobilization of glucose oxidase onto Langmuir–Blodgett films of poly-3-hexylthiophene. *Current Applied Physics, 3*(2–3), 275–279. doi: 10.1016/S1567-1739(02)00215-8

Somesree G. M, Diercks, D. R., Mills, N. C., Hynds, D. L. & Ghosh, S. (2011). Excellent biocompatibility of semiconductor quantum dots encased in multifunctional poly(N-isopropylacrylamide) nanoreservoirs and nuclear specific labeling of growing neurons. *Applied Physics Letter 98*(10), 103702–103703. doi: 10.1063/1.3562036

Sonar, P., Sreenivasan, K. P., Madddanimath, T. & Vijayamohanan, K. (2006). Comparative behavior of CdS and CdSe quantum dots in poly(3-hexylthiophene)

05-4506832 pustaka.upsi.edu.my Perpustakaan Tuanku Bainun Kampus Sultan Abdul Jalil Shah PustakaTBainun ptbupsi

05-4506832 pustaka.upsi.edu.my Perpustakaan Tuanku Bainun Kampus Sultan Abdul Jalil Shah PustakaTBainun ptbupsi

based nanocomposites. *Materials Research Bulletin, 41*(1), 198-208. doi: 10.1016/j.materresbull.2005.07.032.

Sorokin, A.V., Bai, M., Ducharme, S. & Poulsen, M. (2002). Langmuir-Blodgett films of polyethylene. *Journal of Applied Physics, 92*(10), 5977-5981. doi: 10.1063/1.1513201

Stagon, S. P. (2013). *Physical vapor deposition of nanorods from science to technology* (Doctoral Dissertation). Retrieved from http://digitalcommons.uconn.edu/dissertations/189/

Staikov, G. & Milchev, A. (2007). The impact of electrocrystallization on nanotechnology. In G. Staikov (Ed.), *Electrocrystallization in Nanotechnology* (pp. 1-29). Weinheim, Germany: Wiley-VCH Verlag GmbH & Co. KGaA. doi: 10.1002/9783527610198.ch1

Su, S. J. & Kuramoto, N. (2000). Processable polyaniline-titanium dioxide nanocomposites: effect of titanium dioxide on the conductivity. *Synthetic Metals*, *114*(2), 147-153. doi: 10.1016/S0379-6779(00)00238-1

Sudheesh, S., Ahmad, J. & Singh, G. S. (2012). Hysteresis of isotherms of mixed monolayers of n-octadecyl-n′-phenylthiourea and stearic acid at air/water interface. *ISRN Physical Chemistry*, *2012*, Article ID 835397, 6 pages. doi:10.5402/2012/835397

Sun S. S & Bonner C. E. (2005). Optimization of organic solar cells. In S. S. Sun & N. S. Sariciftci (Eds.), *Organic Photovoltaic* (pp. 183 – 214). Boca Raton, Fl.: Taylor & Francis Group.

Sun, B., Marx, E. & Greenham, N. C. (2003). Photovoltaic devices using blends of branched CdSe nanoparticles and conjugated polymers. *Nano Letters*, *3*(7), 961–963. doi: 10.1021/nl0342895

Swain, S. K. & Jena, I. (2010), Polymer/carbon nanotube nanocomposites: A novel material, *Asian Journal of Chemistry, 22*(1), 1-15.

Swalen, J. D., Allara, D. L., Andrade, J. D., Chandross, E. A., Garoff, S., Israelachvili, J., … Yu, H. (1987). Molecular Monolayers and Films. *Langmuir*, *3*(6), 932-950. doi: 10.1021/la00078a011

Tang, H., Zhao, F. & Zhang, F. (2011). Investigation on an optically-controlled phase-shifter based organic semiconductor poly-(3-hexylthiophene) (P3HT). *Journal of Physics: Conference Series*, *276*(1), 012092. doi: 10.1088/1742-6596/276/1/012092

05-4506832 pustaka.upsi.edu.my Perpustakaan Tuanku Bainun Kampus Sultan Abdul Jalil Shah PustakaTBainun ptbupsi

05-4506832 pustaka.upsi.edu.my Perpustakaan Tuanku Bainun Kampus Sultan Abdul Jalil Shah PustakaTBainun ptbupsi

Taniguchi, T., Yokoyama, Y. & Miyashita, T. (1997). Spreading behavior of short-branched n-alkylacrylamide polymers and the formation of Langmuir−Blodgett films, *Macromolecules*, *30*(12), 3646-3649. doi: 10.1021/ma961371w

Tao, A., Kim, F., Hess, C., Goldberger, J., He, R., Sun, Y., Xia, Y. & Yang, P. (2003). Langmuir-Blodgett silver nanowire monolayers for molecular sensing using surface-enhanced raman spectroscopy. *Nano Letter 3*(9), 1229–1233. doi: 10.1021/nl0344209

Thostenson, E., Li, C. & Chou, T. (2005). Nanocomposites in context. *Composites Science and Technology, 65*(3-4), 491–516. doi: 10.1016/j.compscitech.2004.11.003

Tolbert, S. H. & Alivisatos, A. P. (1994). Size dependence of a first order solid–solid phase transition: the wurtzite to rock salt transformation in CdSe nanocrystals. *Scienc*e, *265*(5170), 373-376.

Torrent-Burgués, J., Vocanson, F., Pérez-González, J. J & Errachid, A. (2012). Synthesis, Langmuir and Langmuir–Blodgett films of a calix[7]arene ethyl ester. *Colloids and Surfaces A: Physicochemical and Engineering Aspects, 401*, 137-147. doi: 10.1016/j.colsurfa.2012.03.040.

Truong, N. T. N., Kim, W. K. & Park, C. (2011). Effect of CdSe/P3HT composition on electrical and structural properties of bulk hetero-junction solar cell active layer. *Solar Energy Materials and Solar Cells*, *95*(1), 167-170. doi: 10.1016/j.solmat.2010.05.017

Turina, A. V., Clop, P. D. & Perillo, M. A. (2015). Synaptosomal membrane-based Langmuir–Blodgett films: A platform for studies on γ-aminobutyric acid type A receptor binding properties. *Langmuir 31*(5), 1792-1801. doi: 10.1021/la5042986

Ulman, A. (1991). *An introduction to ultrathin organic films: from Langmuir-Blodgett to self-assembly*. San Diego, CA: Academic Press, Inc.

Vandamme, L. K. J. (1994). Noise as a diagnostic tool for quality and reliability of electronic devices. *IEEE Transaction on Electron Device, 41*(11), 2176 – 2187. doi: 10.1109/16.333839

Vasilescu, G. (2005). *Electronic noise and interfering signals: Principles and application*. doi: 10.1007/b137720

Verma, D., Rao, A. R. & Dutta, V. (2009). Surfactant-free CdTe nanoparticles mixed MEH-PPV hybrid solar cell deposited by spin coating technique. *Solar Energy Materials and Solar Cells, 93*(9), 1482-1487. doi: 10.1016/j.solmat.2009.03.030

Vilarinho, P. M. (2005). Functional materials: Properties, processing and applications. In P. M. Vilarinho, Y. Rosenwaks & A. Kingon (Eds.), *Scanning probe microscopy:*

05-4506832 pustaka.upsi.edu.my Perpustakaan Tuanku Bainun Kampus Sultan Abdul Jalil Shah PustakaTBainun ptbupsi

05-4506832 pustaka.upsi.edu.my Perpustakaan Tuanku Bainun Kampus Sultan Abdul Jalil Shah PustakaTBainun ptbupsi

Characterization, nanofabrication and device application of functional materials, Volume 186 of the series NATO Science Series II: Mathematics, Physics and Chemistry (pp 3-33). The Netherlands: Kluwer Academic Publisher.

von Haartman, M. & Östling, M. (2007). *Low-frequency noise in advanced MOS devices*. The Netherland: Springer Science & Business Media.

Vukmirovic, M. B., Bliznakov, S. T., Sasaki, K., Wang, J. X. & Adzic, R. R. (2011). Electrodeposition of metals in catalyst synthesis: The case of platinum monolayer electrocatalysts. *The Electrochemical Society, Interface, 20*(2), 33–40.

Walther, T. (2015). Electron microscopy of quantum dots. *Journal of Microscopy, 257*(3), 171-178. doi: 10 .1111/jmi.12196

Wang, H. J., Chen, C. P. & Jeng, R. J. (2014). Polythiophenes comprising conjugated pendants for polymer solar cells: A review. *Materials 7*(4), 2411-2439. doi: 10.3390/ma7042411

Wang, J. & Isshiki, M. (2007a). Wide-bandgap II–VI semiconductors: Growth and properties. In S. Kasap & P. Capper (Eds.), *Springer Handbook of Electronic and Photonic Materials* (pp. 325-342). New York: Springer US.

Wang, L., Liu, Y. S., Jiang, X., Qin, D. H. & Cao, Y. (2007b). Enhancement of photovoltaic characteristics using a suitable solvent in hybrid polymer/multiarmed CdS nanorods solar cells. *Journal of Physical Chemistry C 111*(26), 9538–9542. doi: 10.1021/jp0715777

Wang, X., Ma, X. & Zang, D. (2013). Aggregation behavior of polystyrene-*b*-poly(acrylic acid) at the air–water interface. *Soft Matter*, *9*, 443-453. doi:10.1039/C2SM26797G

Watanabe, R., Eguchi, Y., Yamada, T. & Saito, Y. (2015). Optical properties of spin-coated TiO_2 antireflection films on textured single-crystalline silicon substrates. *International Journal of Photoenergy, 2015*, 8 pages. doi:10.1155/2015/147836

Wen, J., Jiang, Y., Yang, Y. & Li, S. (2014). Conducting polymer and reduced graphene oxide Langmuir–Blodgett films: a hybrid nanostructure for high performance electrode applications. *Journal of Materials Science: Materials in Electronics 25*(2), 1063-1071. doi: 10.1007/s10854-013-1687-z

West A. R. (2003). *Solid State Chemistry.* Singapore: John Willey & Sons.

Wright M. & Uddin, A. (2012). Organic-inorganic hybrid solar cells: A comparative review. *Solar Energy Materials and Solar Cells, 107*, 87-111. doi: 10.1016/j.solmat. 2012.07.006.

05-4506832 pustaka.upsi.edu.my Perpustakaan Tuanku Bainun Kampus Sultan Abdul Jalil Shah PustakaTBainun ptbupsi

05-4506832 pustaka.upsi.edu.my Perpustakaan Tuanku Bainun Kampus Sultan Abdul Jalil Shah PustakaTBainun ptbupsi

Wu, C. L., Zhang, Q., Rong, M. Z. & Friedrich, K. (2002). Tensile performance improvement of low nanoparticles filled-polypropylene nanocomposites. *Composite Science and Technology, 62*(10-11), 1327-1340. doi: 10.1016/S0266-3538(02)00079-9

Wuu, D. S., Wu, C. C. & Horng, R. H. (2013). Metaloorganic vapor deposition and characterization of ZnO-based nanostructures and thin film. In Z. C. Feng (Ed.), Handbook of zinc oxide and related materials (pp. 3-58). Florida, US: CRC Press, Taylor & Francis Group.

Xu, J., Ji, X., Gattás-Asfura, K. M., Wang, C. & Leblanc, R. M. (2006). Langmuir and Langmuir–Blodgett films of quantum dots, *Colloids and Surfaces A: Physicochemical and Engineering Aspects, 284–285*, 35-42. doi: 10.1016/j.colsurfa.2005.11.046

Yang, J., Lee, S., Lee, H., Lee, J., Kim, H. K., Lee, S. U. & Sohn, D. (2011). Metal ion coordination with an asymmetric fan-shaped dendrimer at the air–water interface. *Langmuir 27*(14), 8898-8904. doi: 10.1021/la200259s

Yang, X. M., Wang, G. M. & Lu, Z. H. (1998). Characterization of CdS nanoparticles formed and aggregated in stearic acid Langmuir-Blodgett films by atomic force microscopy. *Supramolecular Science, 5*, 549–552. doi: 10.1016/S0968-5677(98)00072-8

05-4506832 pustaka.upsi.edu.my Perpustakaan Tuanku Bainun Kampus Sultan Abdul Jalil Shah PustakaTBainun ptbupsi

Yang, X. N., Loos, J., Veenstra, S. C., Verhees, W. J. H., Wienk, M. M., Kroon, J. M., ... Janssen, R. A. J. (2005). Nanoscale morphology of high-performance polymer solar cells. *Nano Letters 5*(4), 579–583. doi: 10.1021/nl048120i

Ye, S., Noda, H., Nishida, T., Morita, S. & Osawa, M. (2004). Cd^{2+}-induced interfacial structural changes of Langmuir-Blodgett films of stearic acid on solid substrates: A sum frequency generation study. *Langmuir*, *20* (2), 357-365. doi:10.1021/la036008e

Yoo, D., Kim, J. & Kim, J. H. (2014). Direct synthesis of highly conductive poly (3,4-ethylenedioxythiophene): poly(4-styrenesulfonate) (PEDOT:PSS)/graphene composites and their applications in energy harvesting systems. *Nano Research, 7*(5), 717-730. doi: 10.1007/s12274-014-0433-z

Yu, H., Chung, W. & Kim, S. H. (2010). White light emission from blue InGaN LED with hybrid phosphor. *Proceedings of the 10th IEEE Conference on Nanotechnology (IEEE-NANO)*, 958–961. doi: 10.1109/NANO.2010.5697998

Yu, J., Hu, D. H. & Barbara, P. F. (2000). Unmasking electronic energy transfer of conjugated polymers by suppression of O_2 quenching. *Science 289*(5483), 1327-1330. doi: 10.1126/science.289.5483.1327

05-4506832 pustaka.upsi.edu.my Perpustakaan Tuanku Bainun Kampus Sultan Abdul Jalil Shah PustakaTBainun ptbupsi

05-4506832 pustaka.upsi.edu.my Perpustakaan Tuanku Bainun Kampus Sultan Abdul Jalil Shah PustakaTBainun ptbupsi

Yu, Q., Shi, M., Cheng, Y., Wang, M. & Chen, H. (2008). Fe_3O_4 @ Au/polyaniline multifunctional nanocomposites: their preparation and optical, electrical and magnetic properties. *Nanotechnology, 19*, 265702. doi: 10.1088/0957-4484/19/26/265702

Zangari, G. (2015). Electrodeposition of alloys and compounds in the era of microelectronics and energy conversion technology. *Coatings*, *5*(2), 195-218. doi: 10.3390/coatings5020195

Zekry, J. E. E. (2014). *Microsystems encapsulation using nanoporous alumina* (Doctoral Dissertation). Retrieved from https://lirias.kuleuven.be/handle/123456789/447633

Zhao, L., Feng, C., Pang, X., Jung, J., Stefan, M. C., Sista, P. … Lin, Z. (2013). Self-assembly of a conjugated triblock copolymer at the air-water interface. *Soft Matter, 3*(9), 8050-8056. doi: 10.1039/C3SM51488A

Zhavnerko, G. K., Agabekov, V. E., Gallyamov, M. O., Yaminsky, I. V. & Rogach, A. L. (2002). Composite Langmuir–Blodgett films of behenic acid and CdTe nanoparticles: the structure and reorganization on solid surfaces. *Colloids and Surfaces A: Physicochemical and Engineering Aspects, 202*(2–3) 233-241. doi: 10.1016/S0927-7757(01)01085-8

Zhou, Y., Eck, M. & Krüger, M. (2011a). Organic-inorganic hybrid solar cells: State of the art, challenges and perspectives. In L. A. Kosyachenko (Ed.), Solar cells - New aspects and solutions. Retrieved from: http://www.intechopen.com/books/solar-cells-new-aspects-and-solutions/organic-inorganic-hybrid-solar-cells-state-of-the-art-challenges-and-perspectives.

Zhou, Y., Eck, M., Men, C., Rauscher, F., Niyamakom, P., Yilmaz, S. … Krüger, M. (2011b). Efficient polymer nanocrystal hybrid solar cells by improved nanocrystal composition, *Solar Energy Materials and Solar Cells, 95*(12), 3227-3232. doi: 10.1016/ j.solmat.2011.07.015

Zhou, Y., Li, Y., Zhong, H., Hou, J., Ding, Y., Yang C. & Li, Y. (2006). Hybrid nanocrystal/polymer solar cells based on tetrapod-shaped $CdSe_xTe_{1-x}$ nanocrystals. *Nanotechnology*, *17*(16) 4041–4047. doi: 10.1088/0957-4484/17/16/008

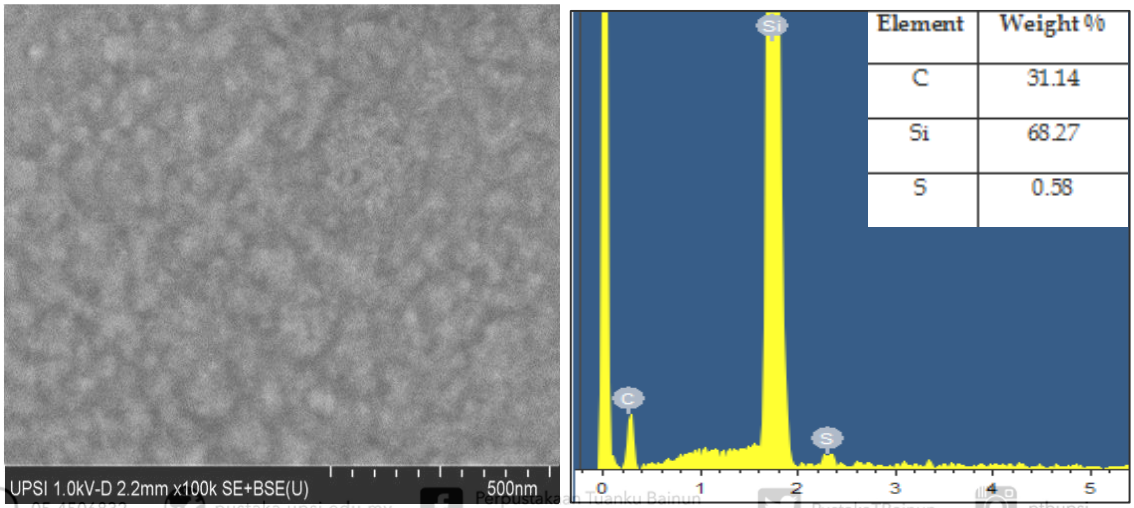
Zhu, D., Zhu, C., Xu, Y., Long, C., Liu, Y., Han, M., Yao, Y., Zhao, X. & Xia, X. (1996). Langmuir-Blodgett films of fullerene derivatives. *Thin Solid Films, 284–285*, 102-105. doi: 10.1016/S0040-6090(95)08281-6

05-4506832 pustaka.upsi.edu.my Perpustakaan Tuanku Bainun Kampus Sultan Abdul Jalil Shah PustakaTBainun ptbupsi

05-4506832 pustaka.upsi.edu.my Perpustakaan Tuanku Bainun Kampus Sultan Abdul Jalil Shah PustakaTBainun ptbupsi

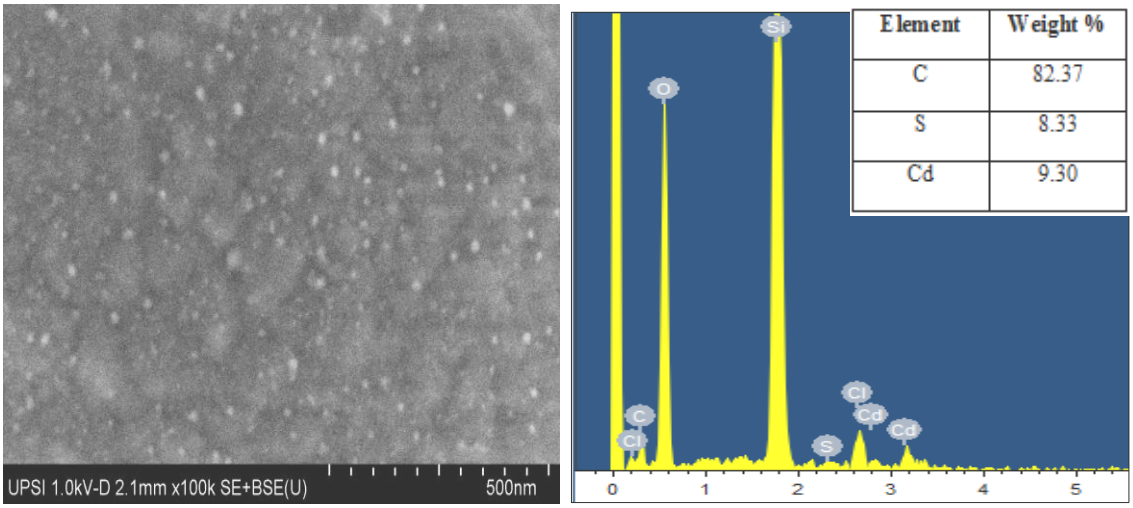
Appendix A

FESEM and EDX result for P3HT:SA:Cd^{2+} thin films before gas exposure.



Element	Weight %
C	31.14
Si	68.27
S	0.58

FESEM and EDX result for P3HT:SA:Cd^{2+} thin films after exposure to H_2S gas for 6 hours.



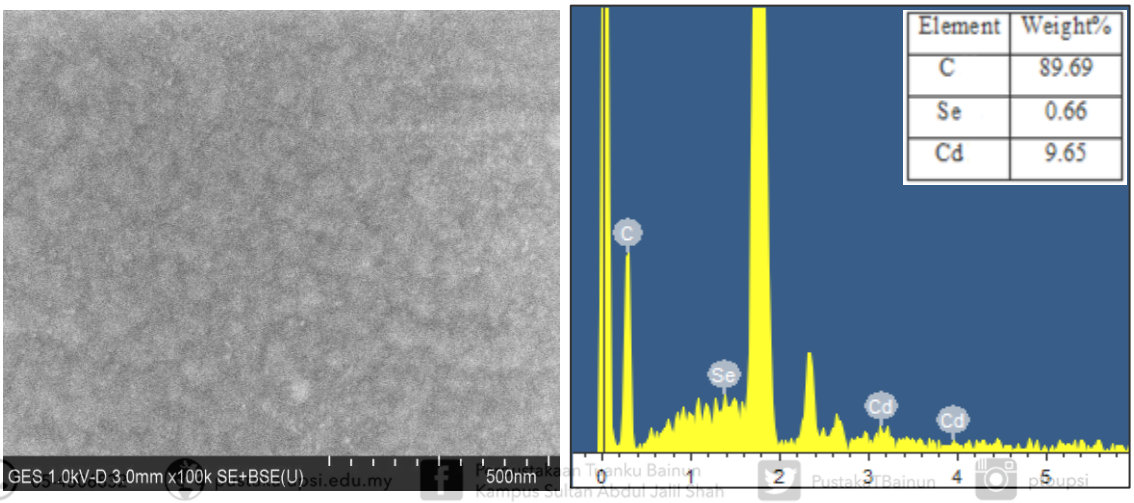
Element	Weight %
C	82.37
S	8.33
Cd	9.30

05-4506832 pustaka.upsi.edu.my Perpustakaan Tuanku Bainun Kampus Sultan Abdul Jalil Shah PustakaTBainun ptbupsi

05-4506832 pustaka.upsi.edu.my Perpustakaan Tuanku Bainun Kampus Sultan Abdul Jalil Shah PustakaTBainun ptbupsi

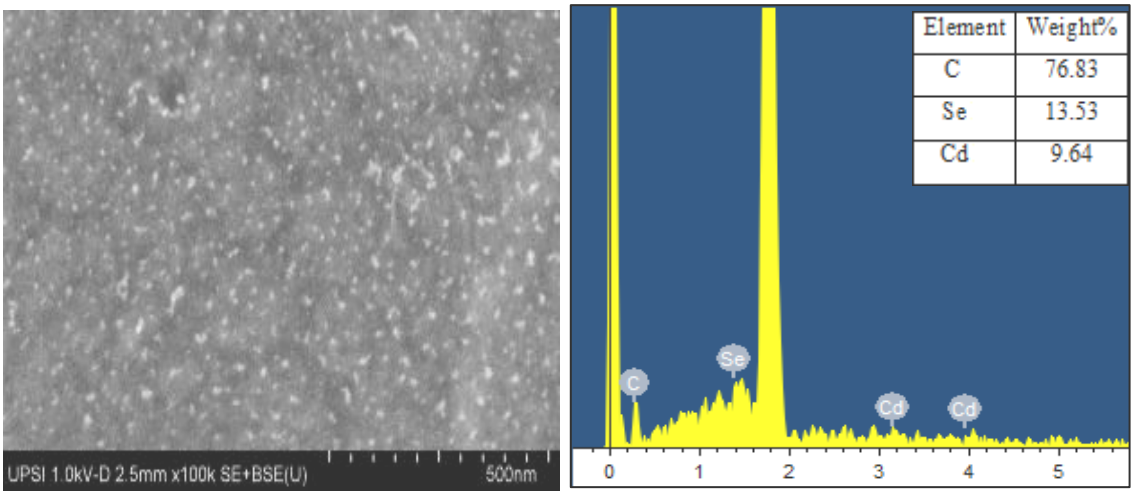
Appendix B

FESEM and EDX result for P3HT:SA:Cd^{2+} thin films after exposure to H_2Se gas for 4 hours



Element	Weight%
C	89.69
Se	0.66
Cd	9.65

FESEM and EDX result for P3HT:SA:Cd^{2+} thin films after exposure to H_2Se gas for 6 hours



Element	Weight%
C	76.83
Se	13.53
Cd	9.64

05-4506832 pustaka.upsi.edu.my Perpustakaan Tuanku Bainun Kampus Sultan Abdul Jalil Shah PustakaTBainun ptbupsi

05-4506832 pustaka.upsi.edu.my Perpustakaan Tuanku Bainun Kampus Sultan Abdul Jalil Shah PustakaTBainun ptbupsi

LIST OF PUBLICATIONS

1. S. Malik, Fatin Hana Naning & Azyuni Aziz (2016). Isotherm and morphology of nanocomposite thin films deposited using modified Langmuir-Schaefer technique. *Jurnal Teknologi*, 78 (5-10). doi: 10.11113/jt.v78.8846

2. Fatin Hana Naning, S. Malik & Zanuldin Ahmad (2015). In-situ cadmium sulfide synthesis in polymer thin film for solar cells application. *Advanced Materials Research*, 1107, 625-630. doi: 10.4028/www.scientific.net/AMR.1107.625

3. Fatin Hana Naning, S. Malik, Zanuldin Ahmad, Azmi Zakaria & Azyuni Aziz (2015). Synthesis and deposition of CdSe:P3HT:SA nanocomposite thin film. *International Journal of Advances in Science, Engineering and Technology, 3*(1), 1-4.

4. Fatin Hana Naning, S. Malik & Zanuldin Ahmad (2014). In-situ CdS nanoparticles synthesis in polymeric thin film. Proceeding of *2014 International Conference on Materials Science and Engineering*, Chennai, India.

05-4506832 pustaka.upsi.edu.my Perpustakaan Tuanku Bainun Kampus Sultan Abdul Jalil Shah PustakaTBainun ptbupsi

5. Fatin Hana Naning, S. Malik, Azmi Zakaria, Reza Zamiri, Syarifah Nadzirah S.A.A., Uda Hashim, Adel Iskandar, Norani Muti Mohamed & Zanuldin Ahmad (2013). Effect of active layer deposition method on solar cells efficiency. Presented at *International Postgraduate Conference on Science and Mathematics*, Tanjong Malim, Perak.

6. S. Malik & Fatin Hana Naning (2013). Cadmium selenide nanoparticles synthesis in polymer matrices for solar cells application. Proceeding of *International Conference on Innovation Challenges in Multidisciplinary Research and Practice*, Kuala Lumpur.

7. Fatin Hana Naning, A.N Falina, Azyuni Aziz & S. Malik (2013). CdS synthesis in photovoltaic active layer. Poster presentation at *Nanomalaysia 2013*, Melaka.

8. Fatin Hana Naning, Syed A. Malik & Faridah Lisa Supian (2012). Hybrid conjugated polymer / quantum dots thin films for electronics application. Proceeding of *2012 IEEE International Conference on Electronics Design, Systems and Applications*, Kuala Lumpur.

9. Fatin Hana Naning, Syed A. Malik, Faridah Lisa Supian, Ismail Zainol, Mustaffa Ahmad (2010). Solar Cell Technology: A Review. Presented at *Kolokium Kebangsaan Pasca Siswazah Sains & Matematik 2010*.

05-4506832 pustaka.upsi.edu.my Perpustakaan Tuanku Bainun Kampus Sultan Abdul Jalil Shah PustakaTBainun ptbupsi